TECHNISCHE UNIVERSITÄT
KAISERSLAUTERN

Mathematical Modeling and Numerical Simulation of Magnetoelastic Coupling

Vom Fachbereich Mathematik
der Technischen Universität Kaiserslautern
zur Verleihung des akademischen Grades
Doktor der Naturwissenschaften
(Doctor rerum naturalium, Dr. rer. nat.)
genehmigte Dissertation.

Mané Harutyunyan

1. Gutachter: Prof. Dr. Bernd Simeon, Techische Universität Kaiserslautern
2. Gutachter: Prof. Dr. Sebastian Schöps, Technische Universität Darmstadt

Disputation: 18. Mai 2018

D 386

In the memory of my grandfather Romen Mkrtchyan

Acknowledgements

I would like to thank my thesis advisor Prof. Dr. Bernd Simeon for his constant motivation, encouragement and guidance throughout my studies.
I also express my gratitude to Prof. Dr. Sebastian Schöps for the great assistance, the elaborate discussions, for his enthusiasm and his patience.
Moreover, I would like to acknowledge Prof. Dr. Herbert De Gersem and Prof. Dr. Martin Grothaus for providing me with ideas and for the fruitful discussions we had. I also thank Dr. Alain Bossavit for the opportunity to discuss with him and for his useful comments regarding this thesis.

To my colleagues Felix Dietrich, Clarissa Arioli, Alexander Shamanskiy, Michael Gfrerer and Dennis Merkert, to my former colleagues Daniela Fußeder and Anmol Goyal I express my gratitude for their help and encouragement and for the great time we spent together. I would like to thank Alexander Hunt for releasing me from my teaching duty during the last days of my submission and Felix Dietrich and Philipp Korell for proof-reading.

Finally, I must express my profound gratitude to my big family. To my parents Lilit and Arthur for their continuous guidance and advice, for always being there for me as mentors, role models and friends. To my husband Gevorg for his support and patience, for proof-reading, commenting and helping me with the thesis. To my dear sister Elen, my aunt Armine and grandma Klara as well as to my mother-in-law Gayane for their great support during the stressful periods of my life. To my father-in-law Razmik for reading and commenting on my thesis and for the nice discussions we had. To my brother-in-law Geram for cheering me up when I needed it. To Neo and Luka for bringing me so much joy and comfort.
And to my daughter Lia: Sweetie, thanks for being so patient and understanding, even if I couldn't spend much time with you. I promise I'll be better.

Contents

1 Introduction **9**

1.1 Magnetoelastic coupling: an overview 9

1.1.1 Classes of magnetic materials 11

1.1.2 The magnetostrictive effect 12

1.1.3 Magnetostrictive vs. piezomagnetic materials 13

1.2 Current state of research 14

1.3 Scope and outline of the thesis 15

2 Fundamentals **19**

2.1 Linear elasticity 19

2.1.1 General framework 19

2.1.2 Derivation of the elastic boundary value problem 23

2.1.3 Function spaces 26

2.1.4 The trace space 28

2.1.5 Existence and uniqueness of the solution 29

2.1.6 Influence of perturbations 30

2.2 Classical electrodynamics 31

2.2.1 Maxwell's equations 31

2.2.2 Integral relations in Lipschitz domains 39

2.2.3 Energy of electromagnetic fields 40

2.2.4 Weak formulation of Maxwell's equations 43

2.2.5 Function spaces and weak differential operators 44

2.2.6 Differential operators on surfaces 46

2.2.7 Traces of $H(\mathrm{div})$ and $H(\mathrm{curl})$ 47

2.2.8 Existence and uniqueness of the solution 48

2.2.9 Influence of perturbations 53

3 The Coupled Model: Magnetic Scalar Potential Formulation 55

3.1 Derivation of the coupled model 55

3.1.1 Constitutive equations 56

3.1.2 Strong and weak formulations 57

3.2 Existence and uniqueness of the solution 63

3.3 Influence of perturbations 69

3.4 Numerical treatment 70

3.4.1 Magneto-elastic coupling properties of polycrystals 71

3.4.2 Reduction to 2D 74

3.4.3 Solvability in the discrete case 75

3.4.4 Algebraic approach 77

4 The Coupled Model: Magnetic Vector Potential Formulation 80

4.1 The energy - coenergy approach 81

4.2 The magnetic vector potential model 86

4.2.1 Derivation of the coupled model 86

4.2.2 The uniqueness issue 91

4.2.3 The coupled problem in the magnetostatic case 92

4.2.4 The coupled problem for the eddy current setting 94

4.2.5 The coupled problem for the full Maxwell system 96

4.3 Existence and uniqueness of the solution 97

4.3.1 The coupled problem for $\kappa_{ij} \in \mathbb{R}_+$ 97

4.3.2 The coupled problem in the magnetostatic case 102

4.4 Reduction to 2D 104

5 Numerical Simulations 106

5.1 1D model: the Euler-Bernoulli beam 106

5.2 2D model: the plane stress - plate 109

6 Summary and Outlook 113

Chapter 1

Introduction

1.1 Magnetoelastic coupling: an overview

Nowadays, nearly all modern shops use special tags fixed on merchandise to prevent shoplifting. A common type of these tags are the so-called *acoustomagnetic* or *magnetostrictive* tags that are often used in clothes shops and cause, if active, a penetrant, periodic sound produced by the detectors at the exit of the shop. These tags take advantage of the *magnetoelastic coupling*, an effect that makes it possible for them to convert magnetic energy into mechanical energy. They usually consist of a thin, magnetostrictive amorphous metal strip that reacts to an external magnetic field in form of vibrations and of a semi-hard magnet strip that works as a biasing magnet in order to increase the strength of the produced signal and to activate or deactivate the tag [65] (see Figure 1.1). The magnetic signal emitted by the detectors meets the resonance frequency of the amorphous metal strip in the tag and causes a vibration of the strip, which in turn involves a change of its magnetization. The detectors, on the other hand, react to this change with an AC voltage, which finally activates the alarm.

This prominent example shows one of the numerous applications of magnetostrictive materials and the magnetoelastic coupling. Magnetostrictive materials belong to the class of *smart materials* that experience a change in their shape, dimensions, stiffness or viscosity due to the influence of an external field, such as a temperature or pressure field, an electric field or, as in the case of magnetostrictive materials, the magnetic field. The term "smartness" may refer to different characteristics like self-adaptibility, self-sensing, memory and multiple functionalities [77]. Among prominent smart materials are *piezoelectric*

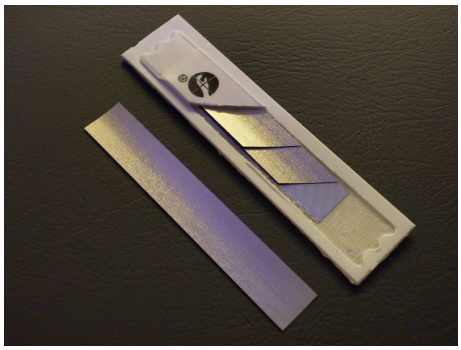

Figure 1.1: Cut-away view of a typical acousto-magnetic tag (distributed under a CC0 1.0 license).

Material	$\Delta l/l_0$ [10^{-6}]	T [°C]	E [GPa]	ρ [g/cm^3]
Fe	-14	770	285	7.88
Ni	-50	358	210	8.9
Co	-93	1120	210	8.9
Tb	3000 (-196°C)	-48	55.7	8.33
Dy	6000 (-196°C)	-184	61.4	8.56
$TbFe_2$	1753	424		9.06
Terfenol-D	1620	380	25-35	9.25
$SmFe_2$	-1560	403		8.53
Samfenol-D	-1125			
$CoFe_2O_4$ (single-crystal)	600-900	520	141.6	
$CoFe_2O_4$ (polycrystalline)	230	520	141.6	
Metglass 2605SC	60	370	25-200	7.32

Table 1.1: Common magnetostrictive materials and their characteristic properties (after [46, 108]).

materials that induce a voltage due to an elastic deformation (applied e.g. in headphones or speakers), *photo- or thermochrome* materials, that change their colors due to temperature or ultraviolet light (used in sunglasses or thermometers with colored scale), *shape memory alloys*, which "remember" their original shape after the deformation (applied in modern medicine) and *piezomagnetic* materials, which generate a magnetic field in consequence of an applied mechanical field.
Magnetostrictive materials react to a magnetic field with a change in their dimensions, which is sometimes referred to as *magnetostriction*, and vice versa. Magnetostriction can be detected in most ferromagnetic materials like iron, cobalt and nickel, as long as they are affected by a sufficiently strong magnetic field. The magnetostriction they experience is measurable, yet of rather small magnitude. However, it can be increased by alloying different materials. Certain alloys such as Terfenol-D, a terbium-disposium-iron-mix (denoted by $Tb_xDy_{1-x}Fe_2$) developed in the 1980s under a program funded by the U.S. Navy, can exhibit several thousand times greater magnitudes and are thus called *giant magnetostrictive* materials [41, 56]. Another common magnetostrictive material is *Metglass*, an amorphous metallic glass developed by the companies *AlliedSignal* from New Jersey and *Vakuumschmelze* in Hanau. In contrast to common metals, it has a non-crystalline structure and combines unique physical and magnetic properties. Its effective Young's modulus (characterizing the stiffness of the material), for example, can be considerably reduced due to magnetization, a phenomenon characterized as the so-called ΔE*-effect*, which will be described in the next subsection.
Table 1.1 provides some typical values of properties like magnetostriction (measured as the ratio of change in length Δl and the initial length l_0 of the specimen), temperature T, elastic modulus E and density ρ of the most common magnetostrictive materials. Although the experienced strains merely reach values of up to 0.1%, they are sufficient to be applied as oscillators in sonar systems, as energy converters or, for example, as actors that transfer electric signals to mechanical motion. Potential applications also include vibration control and hydraulics. Moreover, magnetostrictive materials come into operation as variable-stiffness-devices, transducers (see Figure 1.2) and high-strain-actuators in mechanical systems, as artificial muscles as well as sensors and actuators in robotics. The magnetostrictive effect is also responsible for the "electric hum", the special noise that can be heard in the vicinity of high-power electrical devices and machines such as transformers. A thorough discussion of industrial applications can be found e.g. in Farshad and Le Roux [57] or Jolly et al. [74].

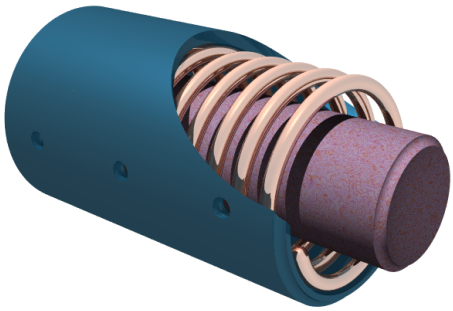

Figure 1.2: Sketch of a transducer with a magnetostrictive core surrounded by a magnetizing coil and magnetic enclosure (distributed under a CC0 1.0 license).

In the following sections, we will give a brief overview of the different types of magnetism, as well as a discussion of the cause and effect of magnetostriction and magnetomechanical coupling.

1.1.1 Classes of magnetic materials

In this section, we characterize and classify the magnetic properties of different materials. While describing the different magnetic phenomena, we will use notions and terms such as magnetization, magnetic susceptibility, current and magnetic field without a detailed explanation of what they represent in the context of electromagnetic theory. An elaborate characterization of most notions that are of importance within the scope of the thesis will be given in Chapter 2, while a few concepts will only be mentioned with a reference to suitable literature.
The magnetic properties of materials are strongly influenced by their crystalline structure and microstructure [82]. Depending on how materials respond to a magnetic field, they can be classified into five groups: *diamagnets, paramagnets, ferromagnets, ferrimagnets* and *antiferromagnets*.
Although rather weak in its nature, the property of *diamagnetism* can be ascribed to all materials. In contrast to paramagnetic or ferromagnetic materials, diamagnets are repelled rather than attracted by an externally applied magnetic field. Their characteristics are a negative magnetization (as long as the applied magnetic field is non-zero) and a negative magnetic susceptibility. This class of materials includes, among others, copper, gold, silver, quartz and water.
Paramagnetic materials have the interesting property that, in the presence of an external magnetic field, their atomic magnetic moments are partially aligned in the direction of the field, which implies a positive value of susceptibility and magnetization. Iron-bearing materials like aluminium, titanium, iron oxyde, as well as magnesium, calcium and platinum belong to the paramagnetic class. In contrast to ferromagnetic materials, paramagnets have a zero magnetization in the absence of an external magnetic field.
In *ferromagnetic* materials, the magnetic moments show a parallel alignment and thus have a great magnitude of magnetization, even when the external magnetic field is removed. Only few materials occuring in the nature are ferromagnetic, among which are iron, nickel, cobalt, as well as most of their alloys. Ferromagnetic materials and their alloys are widely used in industrial and technical applications and are essential components of electromagnetic and electromechanical devices. Most of the typical permanent magnets we use in our everyday life are ferromagnets or ferrimagnets [62]. An important property of ferromagnetic materials is their hysteresis behavior, the ability to retain a "memory" of the external magnetic field, even after it is removed. Figure 1.3 shows an example

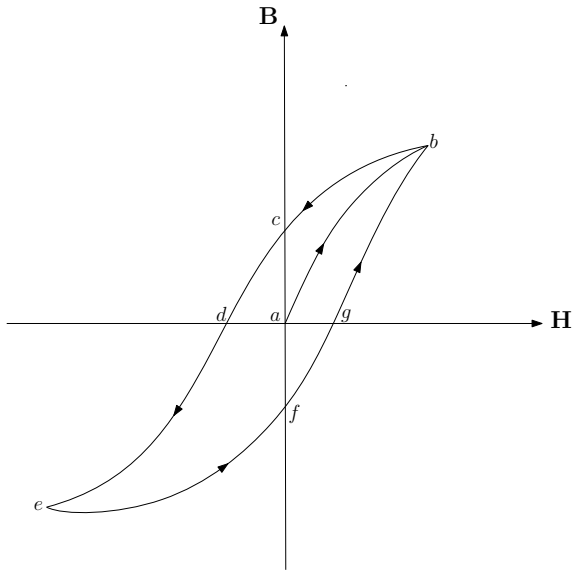

Figure 1.3: Magnetic hysteresis loop (after [62]).

of a *hysteresis loop* of a ferromagnetic material, a plot of the magnetic flux density $\boldsymbol{B}$ over the magnetic field $\boldsymbol{H}$. Starting from point a, the magnetic field is increased, which results in an increase of the magnetic flux density until it reaches the so-called *saturation point* b. Now, all magnetic dipoles are aligned and a further increase of the magnetic field would not affect the flux density any more. Reducing the magnetic field, we would expect to follow the same trace back until the flux density reaches the value zero. Instead, the flux density (and thus the magnetization) decreases only up to a certain point, leaving a residual value when the magnetic field is zero (point c). At this point, we can only get rid of the remaining magnetization through a negative value of $\boldsymbol{H}$ (i.e. the magnetic field has to change its direction). As the negative field increases, the flux density tends to zero (point d) and reaches its (negative) saturation point e. Note that, although the magnetic field is zero in the points a, c and f, the flux density takes different values. Thus, we can conclude that the magnetic flux density and the magnetization of the material depend on the applied field as well as on the "magnetic history" [62].
Ferrimagnetic and *antiferromagnetic* materials are related to each other in that both material types exhibit an anti-parallel alignment of the magnetic moments. These opposing moments are however not equal in ferrimagnetic materials and they retain a certain amount of *spontaneous magnetization*, a magnetization on the microscopic scale which has a magnitude that is independent of position but a direction that varies in different points of the structure [25]. Moreover, a certain analogy with ferromagnets has been observed. For a detailed description of the similarities and differences of these material classes, refer to [82] and [103]. Common ferrimagnetic materials are ferrits, while antiferomagnetic properties were detected in some salts of metals such as manganoxide. The giant magnetostrictive material Terfenol-D mentioned in the previous section is also classified into the group of ferrimagnets. Figure 1.4 depicts the orientations of the magnetic moments of different classes of materials.

1.1.2 The magnetostrictive effect

Having been introduced to the different classes of magnetic materials, we now want to throw a glance to coupling effects that can be observed in some of them.
The first insight into the coupling that occurs between the magnetic and mechanical fields

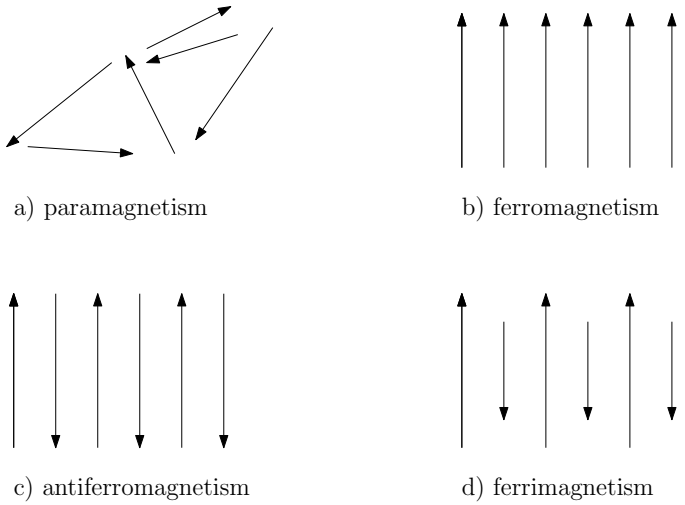

Figure 1.4: Magnetic moments of paramagnetic, ferromagnetic, antiferromagnetic and ferrimagnetic materials (after [82]).

was gained from James Joule's observations in 1842 [75]. Joule found out that a sample of iron experienced a change of length under the influence of a magnetic field. This effect, which is also called *Joule magnetostriction*, is volume-preserving and occurs in all ferro- and ferrimagnetic materials. As explained in the previous section, a parallel alignment of the magnetic moments of these materials can be observed. Their crystalline structure is divided into regions of uniform magnetization, called domains, which experience a rotation and migration of domain walls once an external magnetic field is applied to the material (see Figure 1.5). This is due to the property of the anisotropic crystalline material to minimize its free energy by changing its structure in such a way that the magnetic domains are aligned in the direction of the magnetic field. The deformation that arises from the Joule magnetostriction is independent of the sign (the direction) of the magnetic field.
When a magnetic field is acting on magnetic matter, the sample is magnetized. The *Villari effect* [111] or *inverse magnetostriction* describes the change of this magnetization as a result of a mechanical stress that is imposed on the sample. This reversible effect is mostly used in sonar applications [89].
The change of the material's modulus of elasticity (Young's modulus) is characterized by the ΔE-*effect*. This effect is particularly present in giant magnetostrictive materials such as Terfenol-D or Metglass and is utilized e.g. in broadband sonar systems [45].
The *Wiedemann effect* is comparable to the Joule effect but related to the appearance of shear strain (rather than tensile or compressive strain) under magnetic influence. The *inverse Wiedemann effect* or *Mateucci effect*, on the other hand, occurs e.g. in amorphous wires with a helical domain structure resulting from twisting the wire, which induces a change in its magnetization.
The Joule effect and the Villari effect are the most widely used magnetostrictive effects. The above phenomena and other typical phenomena linked to the magnetostrictive effect are described in detail in [19] or [89].

1.1.3 Magnetostrictive vs. piezomagnetic materials

The magnetomechanical coupling effects that can be observed in piezomagnetic and magnetostrictive materials have certain parallels. Yet, there is a fundamental difference between them: While the piezomagnetic effect refers to the magnetic field arising in the matter from an applied deformation, the inverse magnetostrictive effect cannot generate

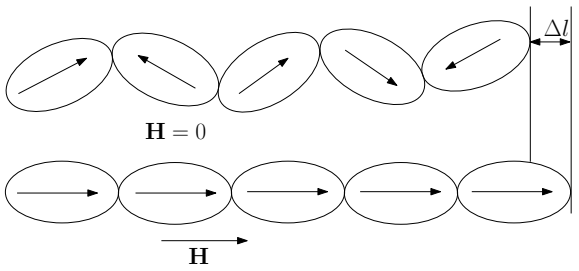

Figure 1.5: Sketch of the rotation of magnetic domains (represented by magnetic dipoles) in direction of the magnetic field $\boldsymbol{H}$

.

a magnetic field purely from applying mechanical stress - it merely characterizes a *change* in the magnetization of the material. Moreover, the relationship between the magnetic influence and the induced strain is linear in piezomagnetic materials, while magnetostrictive materials in general show a non-linear behavior. Piezomagnetism is a rather rare effect that only occurs in centro-symmetric crystals [112] with certain crystallographic and magnetic symmetry relations (see also Chapter 3).
However, in most applications, magnetostrictive materials are *biased*: A magnetic bias is applied in form of a magnetic field that magnetizes the material [5, 40], and a mechanical bias is used in form of a (compressive) pre-stress. The benefit of biasing is the characterization of the behavior of the underlying magnetostrictive material by the linear piezomagnetic coupling equations, which are in analogy with the linear relations of piezoelectricity. This procedure is very common in literature linked with the modeling of magnetoelastic coupling phenomena, see e.g. [56, 70] and will be discussed in detail in the Chapters 3 and 4.

1.2 Current state of research

Due to their distinctive features such as high controllability, self-sensing and self-adaptability, magnetostrictive materials have attracted considerable interest in the recent years, see e.g. the works of Dorfmann et al. [49, 50, 51], Kankanala and Tryantifyllidis [78] and Steigmann [104].
The theoretical background for the magnetoelastic coupling provide, among others, Brown [25], Hutter and van den Veen [69], Pao [90], as well as Truesdell and Toupin [109]. Kankanala and Tryantifyllidis [78] classified the modeling approaches used in literature into two categories: While models based on the so-called "direct" method use conservation laws of continuum mechanics [83, 90, 106, 109], models based on the "energy method" aim at the minimization of a suitable (potential) energy function [25, 83, 107]. Those using a direct approach are based on the Eulerian description referring to the current configuration, whereas energy formulations exploit the Lagrangian formalism related to the reference configuration (the latter ansatz is also used for the derivation of the equations of motion of (linear) elasticity, presented in Section 2.1). Kankanala and Tryantifyllidis [78] use both approaches to derive constitutive equations for magnetoelastic coupling and show that they lead to the same results.
More recent models also include micromechanical approaches that establish a link between the material's microstructure and its effective macroscopic properties (see e.g. [13]). Micromechanical models of magnetostrictive materials are usually based on the approach of Jiles and Atherton [72, 73] that focuses on modeling the migration process of the magnetic domain walls. Such models on the micro-scale are in general able to give a precise

prediction of the material behavior but have the big drawback of involving high numerical computation costs [82]. Models like the Preisach approach [94] operate on the macro scale and are thus more efficient. This approach can be modified to incorporate different types of magnetic hysteresis behavior, see e.g. [1, 105].
Another modeling technique is based on thermodynamical principles, describing the behavior of the material by a suitable free-energy function depending on the magnetization and the strain [114, 116, 117]. These models capture the hysteresis behavior of the material by splitting the independent variables into reversible and irreversible parts, where the irreversible parts characterize the internal state of magnetization. Linnemann [82] sets up a constitutive model in the same manner, focusing on the splitting of the magnetic field and mechanical strains as independent variables, thus enabling a facilitated implementation of the constitutive equations into the Finite Element formulation.
Obtaining an exact solution of the coupled magnetoelastic equations has been proven to be rather difficult. The computation of exact solutions suggested in the publications of Pucci and Saccomandi [96], as well as Dorfmann and Ogden [47, 48, 52, 53] relied on the assumption of infinite geometries such as cylinders or slabs of infinite length (but finite radius). This assumption is strongly connected with the incorporation of continuity conditions on the interfaces of two different materials (such as the magnetoelastic material and the surrounding vacuum or air region) described by Kovetz [80], for example. Thus, finding the exact solution of coupled magnetoelastic boundary problems in finite regions constitutes a considerable challenge, even in case of limiting to simple geometries, which increases the need for suitable numerical methods.
For the numerical treatment of coupled piezomagnetic and magnetoelastic problems, different variational formulations and numerical solutions schemes have been introduced in the recent years. Bustamante et al. [28] use a finite-difference method to solve a nonlinear magnetoelastic problem with a simple geometry, while the work of Barham et al. [8] studies the deformation of a magnetoelastic membrane. One of the first variational principles suggested for the magnetoelastic coupling was due to Brown [25] who used the magnetization and the elastic deformation function as independent variables. This partial variational formulation was supplemented with a third variable, the magnetic vector potential and developed into a full variational principle by Kankanala and Tryantifyllidis [78], whereas Steigmann [104] introduced a similar formulation based on the magnetic field rather than the magnetization. The work of Bustamante et al. [28] focuses on a purely phenomenological approach using the magnetic field and the magnetic induction instead of the magnetization to develop variational principles for non-linear magnetoelasticity under static conditions. The authors present different variational and energy formulations based on the magnetic scalar and vector potentials. Due to the numerous analogies between the magnetoelastic and electroelastic concepts, these formulations can be directly transferred to the electro-elastostatic case [29]. In a recent paper, Salas and Bustamante [99] study the influence of the magnetic field on a cylinder of finite length surrounded by free space and present numerical simulations based on the Finite Element method, while another publication treats a finite strain problem involving the deformation of a slab surrounded by vacuum under the influence of a magnetic field applied far away [30].

1.3 Scope and outline of the thesis

This thesis draws attention to the mathematical aspects of the modeling of magnetoelastic coupling. As depicted in the last section, a considerable amount of work has been done so far to characterize magnetoelastic coupling and magnetostrictive materials, as well as magnetosensitive and magnetorheological elastomers. Early publications mostly focus on

deriving appropriate constitutive equations for the description of various material classes. They utilize different approaches based on changing independent quantities, including material properties such as non-linear and hysteresic behavior, geometric peculiarities and micromechanical considerations. More recent works are concerned with variational formulations and numerical solutions of different coupled magnetoelastic boundary value problems. However, none of the works found so far in the literature deals with fundamental aspects like the structure of the obtained coupled system of partial differential equations and the questions of existence, uniqueness and stability of the corresponding solution. The present thesis is therefore aimed to fill this gap and to establish ties between the fields of mathematics and (mechanical) engineering by examining the coupled multi-field problem within the framework of the theory and numerics of partial differential equations and functional analysis.
On the one hand, the thesis intends to set up a basic, comprehensible and clearly-arranged model for the linear magnetoelastic coupling in magnetostrictive materials. It offers a profound analysis of the problem starting from the derivation of the coupled system using a special case of Hamilton's principle in analogy to the approaches of the elasticity theory. Although this basic model requires a strongly simplified setting such as the assumptions of linearity (considering only small strains and neglecting magnetic hysteresis) and stationarity of the elastic field, it provides a thorough insight into the concept of magnetoelasticity and gives a better understanding of the coupling. After setting the foundation, the model can then be extended to cover more complex settings such as geometric and material non-linearities and time-dependence of both elastic and electromagnetic fields.

On the other hand, the thesis deals with the question of how the use of different approaches in the characterization of the magnetic and elastic fields and their constitutive equations affects the structure and solvability of the resulting problem. Making use of two common techniques for solving Maxwell's equations that describe the behavior of the magnetic field, the *(total) magnetic scalar potential* and *magnetic vector potential formulations*, as well as the concepts of energy and co-energy treating dualities of notions in elasticity and electromagnetism (described e.g. by Bossavit [15, 17] and Preumont [95]), we show that the magnetic scalar potential approach results in a coupled penalized saddle point problem, while the vector potential approach yields a symmetric system of partial differential equations for the magneto-quasistatic setting as well as for the full Maxwell system in the frequency domain.
For the scalar potential setting, the existence and uniqueness of the problem can be shown using the theory of mixed problems developed by Brezzi [24]. In particular, we prove an inf-sup condition for the continuous and discrete problems and obtain unique solvability as well as suitable estimates for the influence of perturbations of the given data on the solution. In the second case, the coupled magnetostatic and magnetoquasi-static electromagnetic problems are treated separately, since both problems are of different nature: As the magnetic vector potential is not unique, the coupled problems based on the vector potential as independent variable need additional gauging. In the time-varying case, the gauging can be directly incorporated into a system through the addition of a penalization term, which yields the unique solvability for both strong and weak (variational) forms. In the magnetostatic case, the uniqueness of the variational problem can be achieved by casting the problem into a mixed setting with the help of a Lagrange multiplier. These differences are also incorporated in the coupled case, which leads to interesting structures of the resulting systems. After a thorough analysis of the coupled problem in various settings, numerical simulations are carried out that show the mutual influence of the magnetic and elastic fields for an Euler-Bernoulli beam and for a thin plate in the state of plane stress. While many simulations of the magnetoelastic coupling presented in the literature are carried out by codes like COMSOL (e.g. the works of Bustamante [99]), where pro-

gramming steps including the definition of the geometry, the meshing, the implementation of the finite element functions, etc. are automatized, the coupled models presented in this thesis are implemented into the software MATLAB, which enables an active intervention and control over each step of the numerical analysis.

The thesis consists of four main chapters. Chapter 2 provides a detailed insight into the theories of linear elasticity and linear magnetostatics. In Section 2.1, the governing equations of linear elasticity and their derivation based on a minimum energy principle are presented and the equations of motion are characterized in their strong and variational form. Moreover, appropriate function spaces for the elastic field quantities are introduced and the existence, uniqueness and stability (influence of perturbations) of the solution to the boundary value problem of linear elasticity is discussed.
In Section 2.2, we follow the same procedure by presenting and discussing various forms of Maxwell's equations, setting up electromagnetic boundary value problems in the stationary and time-dependent cases and considering their solvability in strong and weak forms. Suitable potential formulation based on the magnetic scalar potential and the magnetic vector potential are established that enable the solution of Maxwell's equations in a more convenient way than their original formulation in terms of the magnetic field and magnetic flux density. As in the case of linear elasticity, appropriate function spaces are identified that are of particular importance for the vector potential formulation, where, in contrast to the scalar case, the governing equation is given in a "curl-curl"-form and entails a thorough analysis of function properties and boundary conditions. The distinct treatment of the static and time-varying cases for the vector potential formulation is due to the structure of the resulting system of equations: While in the magnetostatic case, the problem is brought into a mixed form to guarantee its unique solvability, the eddy current and full Maxwell settings in the frequency domain yield a symmetric problem.
This chapter lays the foundation for the subsequent analysis of the magnetoelastic coupling carried out in Chapter 3 and Chapter 4, which offer two approaches into coupled magnetoelasticity based on the two different potential formulations pictured in Chapter 2. Although magnetostrictive materials, which we focus on, have in general a non-linear behavior, we can enforce linearity by assuming only small strains and neglecting magnetic hysteresis. This simplification can be justified by using biased magnetostrictive materials, as depicted in Section 3. The initial biased state is incorporated into the linear equations through the constant material and coupling parameters in tensor form. On the basis of these constitutive equations, the coupled system of partial differential equations is derived using Hamilton's principle. In their structure and organization, Chapters 3 and 4 are in accordance with the introductory Chapter 2, which enables to draw direct parallels between the coupled and uncoupled cases. However, there are significant differences between the problems derived on the basis of the two potential formulations. First of all, a formulation relying purely on a magnetic scalar potential can only be used in current-free regions, as an irrotational magnetic field is required to enable the existence of a magnetic scalar potential. Second, the constitutive equations and the energy approach chosen in Chapter 3 lead to a coupled magnetoelastic saddle point problem with a penalty term. On the contrary, the reformulation of the coupled constitutive equations in terms of the magnetic flux density and elastic stress rather than the magnetic field and the elastic strain results in a symmetric coupled system of partial differential equations in Chapter 4. The approach used for the constitutive equations thus strongly influences the structure of the resulting problem. This phenomenon can be ascribed to the duality of formalisms in elasticity and electromagnetic theory and the notions of energy and co-energy: While in Chapter 3, the Lagrangian used in the variational principle is a combination of an elastic energy and a magnetic co-energy function, whose different signs lead to a mixed problem,

reformulating the constitutive equations results in a Lagrangian consisting of two energy functions (having the same sign) and thus yielding a symmetric problem in Chapter 4. This aspect can also be visualized by considering the coupled free-energy (density) function of the system. In order to reformulate the coupled free energy function in terms of the pairing "elastic strain and magnetic flux density" instead of "elastic strain and magnetic field", we need a Lagrange-Fenchel transformation of the energy function, which results in a change of signs of the different terms within the function.
Independent of the chosen formulation, the existence and uniqueness of the resulting problems can be proven by setting up an appropriate framework for the coupled problem, as shown in Chapters 3 and 4. Corresponding numerical simulations for different 1D and 2D-settings carried out with MATLAB can be found in Chapter 5. Finally, a brief summary and outlook are given in Chapter 6.

Chapter 2

Fundamentals

This chapter gives a thorough insight into the theories of linear elasticity and electrodynamics and lays the foundations for the analysis of the coupled magnetoelastic models presented in Chapters 3 and 4.
In the course of this chapter, as well as in all following chapters, we will use a bold notation to refer to vector-valued or tensor-valued quantities and a non-bold notation for scalars.

2.1 Linear elasticity

In this section, we briefly outline the basic concepts and notions of linear elasticity, including elastic material laws, the equations of motion in strong and weak forms, as well as their derivation based on Hamilton's principle, following Atkinson and Han [4] and Simeon [102]. Appropriate function spaces are presented and the existence, uniqueness and continuous dependence of the solution to a linear elastic boundary value problem on the given data are discussed.

2.1.1 General framework

Consider an elastic body subjected to volume forces such as gravitation and surface tractions such as tensile or compressive forces. Assuming that the body undergoes only small strains and deformations, the setting can be described by a linear elastic boundary value problem. In order to set up and examine such a boundary value problem, we need to define the quantities that describe the mechanical behavior and the deformation of the material in the first instance.
Let Ω be an open, connected and bounded subset of $\mathbb{R}^3$, i.e. a bounded domain in $\mathbb{R}^3$. We assume that Ω has a connected Lipschitz boundary $\partial\Omega$ with an outer unit normal vector $\boldsymbol{n} \in \mathbb{R}^3$.
Moreover, let $\partial\Omega = \overline{\Gamma}_D \cup \overline{\Gamma}_N$ be a non-overlapping decomposition of the boundary, i.e. $\Gamma_D \cap \Gamma_N = \varnothing$ with open, connected subsets Γ_D and Γ_N. On the Dirichlet boundary Γ_D, we prescribe the motion, while on the Neumann boundary Γ_N we specify the surface traction.
Let T denote a time interval. Due to the impact of external forces on the material, the body undergoes a deformation characterized by the time-dependent *displacement field*

$$\boldsymbol{u} : \Omega \times T \to \mathbb{R}^3, \quad \boldsymbol{u}(\boldsymbol{x}, t) = (u_1(\boldsymbol{x}, t), u_2(\boldsymbol{x}, t), u_3(\boldsymbol{x}, t))^T.$$

As a result, every point $\boldsymbol{x} \in \Omega$ in the undeformed body (the so-called *reference configuration*) moves to the position $\boldsymbol{x} + \boldsymbol{u}(\boldsymbol{x}, t)$ (see Figure 2.1). Note that we assume an or-

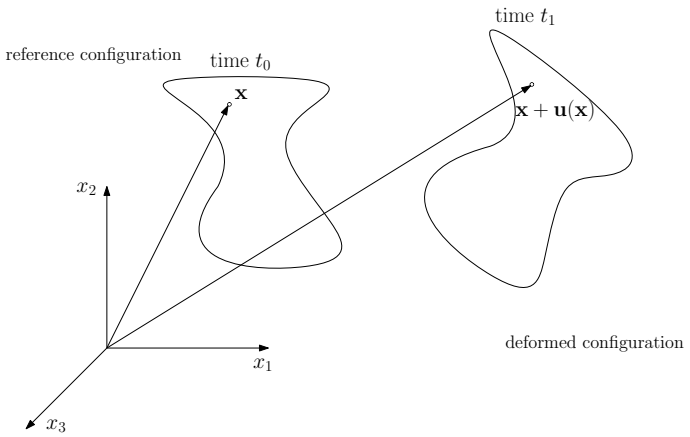

Figure 2.1: Sketch of the body in the deformed and reference configurations.

thonormal reference frame that does not change in time. The *deformation* $\boldsymbol{F} : \Omega \to \mathbb{R}^3 \times T$ then assigns to each material point $\boldsymbol{x} \in \Omega$ in the reference configuration its deformed state $\boldsymbol{F}(\boldsymbol{x}, t)$ at time t. In terms of $\boldsymbol{u}$, the deformation $\boldsymbol{F}$ can be expressed as

$$\boldsymbol{F}(\boldsymbol{x}, t) = \boldsymbol{x} + \boldsymbol{u}(\boldsymbol{x}, t).$$

We assume that the deformation is orientations-preserving, i.e.

$$\det \nabla \boldsymbol{F} > 0.$$

The gradient $\nabla \boldsymbol{F}$ with respect to the space variable $\boldsymbol{x}$ is the 3×3-Jacobian of the function $\boldsymbol{F}$, defined as

$$\nabla \boldsymbol{F}(\boldsymbol{x}, t) := \left(\frac{\partial F_i(\boldsymbol{x}, t)}{\partial x_j} \right)_{i,j=1,2,3}.$$

Using the displacement field $\boldsymbol{u}$, we can express the Dirichlet boundary condition as

$$\boldsymbol{u}(\boldsymbol{x}, t) = \boldsymbol{u}_0(\boldsymbol{x}, t) \quad \text{on } \Gamma_D, \tag{2.1}$$

where $\boldsymbol{u}_0$ is a given function that characterizes the displacement on the boundary segment Γ_D. Another deformation measure is the *strain*, given e.g. by the second order *Green Lagrange strain tensor* (neglecting the arguments $\boldsymbol{x}$ and t).

$$\boldsymbol{E} = \frac{1}{2}(\nabla \boldsymbol{u} + \nabla \boldsymbol{u}^T + \nabla \boldsymbol{u}^T \boldsymbol{u}).$$

In terms of the deformation $\boldsymbol{F}$, the tensor $\boldsymbol{E}$ can be expressed as

$$\boldsymbol{E} = \frac{1}{2}(\nabla \boldsymbol{F}^T \nabla \boldsymbol{F} - \boldsymbol{I}),$$

where $\nabla \boldsymbol{F}^T \nabla \boldsymbol{F}$ is the *right Cauchy-Green deformation tensor* and $\boldsymbol{I}$ is the identity tensor. Note that $\nabla \boldsymbol{F}$ alone is not suitable as a strain measure since in contrast to the Green-Lagrange tensor, it is not invariant under translations and rotations. As the name suggests, the Green-Lagrange strain tensor is based on the Lagrangian description referring to the coordinates of the undeformed body, which is more suitable for expressing constitutive relations than the Eulerian description. The corresponding linearized strain tensor is a symmetric tensor denoted by $\boldsymbol{\epsilon} \in \mathbb{R}^{3\times3}$,

$$\boldsymbol{\epsilon}(\boldsymbol{u}) = \frac{1}{2}(\nabla \boldsymbol{u} + \nabla \boldsymbol{u}^T). \tag{2.2}$$

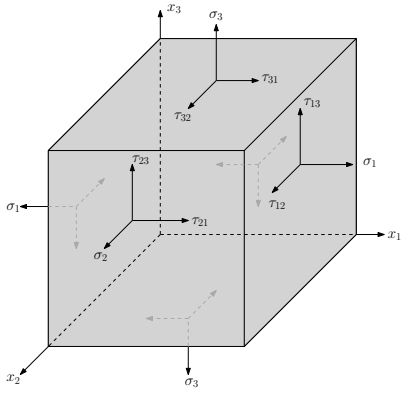

Figure 2.2: Components of the Cauchy stress tensor acting on a cubic element.

To describe the behavior of the material, we need a *constitutive relation*, a material law linking two specific material quantities. The linear elastic constitutive law relates the strain $\boldsymbol{\epsilon}$ with the mechanical *stress* $\boldsymbol{\sigma}$, describing the pressure that arises from inner forces on the surface of an infinitesimal volume element in the deformed state of the body. Like the strain, the stress $\boldsymbol{\sigma}$ is a symmetric tensor (proven, along with the existence and uniqueness of the tensor, by Cauchy (e.g. in [35]), which is the reason why $\boldsymbol{\sigma}$ is often called the *Cauchy stress tensor*) having the form

$$\boldsymbol{\sigma} = \begin{pmatrix} \sigma_{11} & \tau_{12} & \tau_{13} \\ \tau_{21} & \sigma_{22} & \tau_{23} \\ \tau_{31} & \tau_{32} & \sigma_{33} \end{pmatrix}.$$

The Cauchy stress tensor is used for stress analysis of materials undergoing small deformations and thus having a uniform stress distribution. For large deformations, other measures of stress such as the Piola-Kirchhoff stress tensor [18] are useful. Figure 2.2 illustrates the stress tensor on a cubic element. The normal stresses $\sigma_1, \sigma_2, \sigma_3$ are defined to be positive for tensile stress and negative for compressive stress. The first subscript of the shear stresses σ_{ij} (often denoted by τ_{ij}) $i \neq j$, characterizes the direction of the normal to the surface where the stress acts, while the second subscript specifies the direction of the stress. The sign convention of shear stresses is displayed in Figure 2.3. Due to its reference to the deformed system, the Cauchy stress tensor is sometimes also called a *true stress tensor*.
Strains are regarded to be positive (negative) if they are caused by positive (negative) stresses. There are two types of notations for the components of the strain tensor, the notation using the *engineering shear strains* γ_{ij} and the *tensor shear strain* notation ϵ_{ij}, which are linked by the relation

$$\gamma_{ij} = 2\epsilon_{ij}, \quad i \neq j.$$

Referring to an originally square element, engineering shear strain induces a rotation of the element in addition to the deformation, whereas the tensor shear strain merely represents extension and distortion of angles. The material's response to external forces is described by *Hooke's law*

$$\boldsymbol{\sigma}(\boldsymbol{u}) = \boldsymbol{C} : \boldsymbol{\epsilon}(\boldsymbol{u}), \tag{2.3}$$

a linear constitutive relation between stress and strain. Here, $\boldsymbol{C} \in \mathbb{R}^{3\times3\times3\times3}$ is the so-called *mechanical stiffness tensor*, a constant material tensor of order four. Note that the double dot notation (:) is used to describe the double inner product of tensors. In componentwise

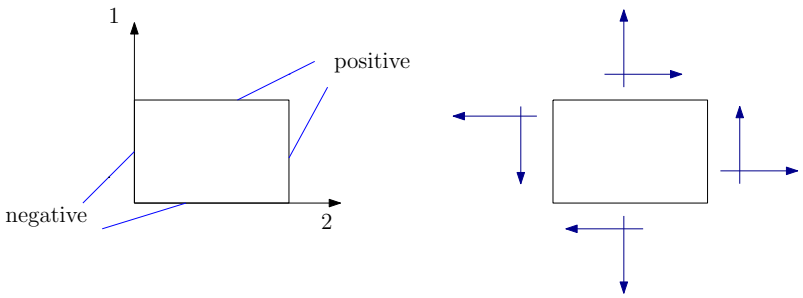

Figure 2.3: Sign convention for shear stresses.

notation, Hooke's law (2.3) reads

$$\sigma_{ij} = \sum_{k,l=1}^{3} C_{ijkl}\epsilon_{kl} \quad \text{for } i,j = 1,..,3. \tag{2.4}$$

The fourth order tensor $\boldsymbol{C}$ has in general 36 components. Using the symmetries of the stress and strain tensors, as well as examining the characteristics of the strain energy, however, one can show that $\boldsymbol{C}$ is symmetric [4], i.e.

$$C_{ijkl} = C_{jikl} = C_{klij} = C_{ijlk}. \tag{2.5}$$

Furthermore, we can assume that $\boldsymbol{C}$ is bounded,

$$C_{ijkl} \in L^{\infty}(\Omega) \quad \text{for all } i,j,k,l \in \{1,..,3\}, \tag{2.6}$$

and pointwise stable [4, 97], i.e.

$$\boldsymbol{\epsilon} : \boldsymbol{C} : \boldsymbol{\epsilon} \geq \alpha|\boldsymbol{\epsilon}|^2, \tag{2.7}$$

where $\alpha > 0$ is a constant and $|\cdot|$ denotes the matrix norm

$$|\boldsymbol{\epsilon}|^2 = \sum_{i,j=1}^{3} \epsilon_{ij}\epsilon_{ij}.$$

The property of pointwise stability of tensors corresponds to the positive definiteness of matrices. Note that for two second order tensors, calculating the double inner product corresponds to computing the trace of their product.
Exploiting the symmetries of $\boldsymbol{C}$, $\boldsymbol{\sigma}$ and $\boldsymbol{\epsilon}$, it is possible to rewrite the constitutive relation (2.4) in a more compact form in terms of vectors and matrices. Following the scheme

Tensor-subscription	11	22	33	23 or 32	13 or 31	12 or 21
Matrix-subscription	1	2	3	4	5	6,

the elasticity tensor turns into a matrix $\boldsymbol{C} \in \mathbb{R}^{6\times 6}$. Using the *Voigt notation* [113], the stress and strain tensors are represented as vectors,

$$\boldsymbol{\sigma} := (\sigma_1, \sigma_2, \sigma_3, \sigma_4, \sigma_5, \sigma_6)^T = (\sigma_{11}, \sigma_{22}, \sigma_{33}, \tau_{23}, \tau_{31}, \tau_{12})^T, \tag{2.8}$$

$$\boldsymbol{\epsilon} := (\epsilon_1, \epsilon_2, \epsilon_3, \epsilon_4, \epsilon_5, \epsilon_6)^T = (\epsilon_{11}, \epsilon_{22}, \epsilon_{33}, \gamma_{23}, \gamma_{31}, \gamma_{12})^T. \tag{2.9}$$

In this chapter, we will retain the tensorial notation of $\boldsymbol{\sigma}$ and $\boldsymbol{\epsilon}$, especially for the derivation of the equations of motion. The vector notation will come into play in Chapters 3 and 4 within the context of the coupling of the elastic and magnetic fields. To avoid the introduction of additional variables, we will use the same notations for the vector and matrix forms of stress and strain, as well as for the matrix and tensor forms of the elasticity

matrix.
For general anisotropic materials having no material symmetry planes, $\boldsymbol{C}$ has 21 independent material constants. This number can be reduced for material classes having certain symmetry properties, such as orthotropic, transversely isotropic or isotropic materials [18]. In the most simple, homogeneous and isotropic case, the matrix $\boldsymbol{C}$ has the form

$$\boldsymbol{C} = \frac{E}{(1+\nu)(1-2\nu)} \begin{pmatrix} 1-\nu & \nu & \nu & 0 & 0 & 0 \\ \nu & 1-\nu & \nu & 0 & 0 & 0 \\ \nu & \nu & 1-\nu & 0 & 0 & 0 \\ 0 & 0 & 0 & (1-2\nu)/2 & 0 & 0 \\ 0 & 0 & 0 & 0 & (1-2\nu)/2 & 0 \\ 0 & 0 & 0 & 0 & 0 & (1-2\nu)/2 \end{pmatrix}, \tag{2.10}$$

with 2 independent material constants, *Young's modulus* E and *Poisson's ratio* ν. Isotropic materials have the same material properties in all axial directions. Transversely isotropic materials, in contrast, have the same material properties in a symmetry plane (isotropy plane) and different properties in the direction perpendicular (transverse) to it. Their elasticity matrix has the same structure as the matrix above, however, it has 5 independent material constants depending on the axial directions (see Chapter 3). The isotropic material constants E and ν can be expressed using the *Lamé moduli* $\hat{\lambda}$ and $\hat{\mu}$ (e.g. in [4]),

$$\nu = \frac{\hat{\lambda}}{2(\hat{\lambda}+\hat{\mu})}, \quad E = \frac{\hat{\mu}(3\hat{\lambda}+2\hat{\mu})}{\hat{\lambda}+\hat{\mu}},$$

and the linear elastic isotropic Hooke's law then reads [34]

$$\boldsymbol{\sigma} = \hat{\lambda}(\operatorname{trace}\boldsymbol{\epsilon})\boldsymbol{I} + 2\hat{\mu}\boldsymbol{\epsilon}.$$

In the next section, we will use the quantities introduced here to set up an energy principle and derive the strong and weak (variational) formulations of the linear elastic boundary value problem.

2.1.2 Derivation of the elastic boundary value problem

We aim at deriving a boundary value problem by using Hamilton's principle, a principle of least action requiring the motion of a conservative system to be such that the integral

$$I = \int_{t_0}^{t_1} (T-U)\mathrm{d}t \tag{2.11}$$

is stationary [9], where T now denotes the kinetic energy and U the potential energy of the system. The equations of motion can be deduced from this principle as necessary conditions. In his original work [63], Hamilton formulated the principle in an equivalent form, stating that in a conservative system, the actual motion is conform to the equation

$$\int_{t_0}^{t_1} \delta(T-U)\mathrm{d}t = 0, \tag{2.12}$$

for all admissible motions, i.e. the *variation* of expression (2.11) vanishes. If a displacement field $\boldsymbol{u}$ satisfies the requirement (2.12), then its perturbation $\boldsymbol{u}+\theta\boldsymbol{v}$ with the variation $\theta\boldsymbol{v}$ for $\theta \in \mathbb{R}$ satisfies Equation (2.12) as well. Furthermore, we require that $\boldsymbol{u}-\theta\boldsymbol{v}$ fulfills the Dirichlet boundary condition (2.1), implying that

$$\boldsymbol{v}(\boldsymbol{x},t) = \boldsymbol{0} \quad \forall \boldsymbol{x} \in \Gamma_D, \tag{2.13}$$

for admissible functions $\boldsymbol{v} = \boldsymbol{v}(\boldsymbol{x}, t)$ at any fixed time $t_0 \le t \le t_1$. Additionally, the variation should not affect the starting point t_0 and the end point t_1 of the deformation path, i.e.

$$\boldsymbol{v}(\boldsymbol{x}, t_0) = \boldsymbol{v}(\boldsymbol{x}, t_1) = \boldsymbol{0} \quad \forall \boldsymbol{x} \in \Omega, \tag{2.14}$$

for arbitrary but fixed time points t_0 and t_1. Now we can express Hamilton's principle in the form

$$\frac{\mathrm{d}}{\mathrm{d}\theta} J(\theta)|_{\theta=0} = 0, \tag{2.15}$$

with the function $J(\theta)$ defined as

$$J(\theta) = \int_{t_0}^{t_1} T(\boldsymbol{u} + \theta\boldsymbol{v}) - U(\boldsymbol{u} + \theta\boldsymbol{v}) \mathrm{d}t. \tag{2.16}$$

The kinetic energy T is of the form

$$T(\boldsymbol{u}) = \frac{1}{2} \int_{\Omega} \rho \dot{\boldsymbol{u}} \cdot \dot{\boldsymbol{u}} \, \mathrm{d}x, \tag{2.17}$$

with ρ being the constant mass density of the material and $\dot{\boldsymbol{u}}$ denoting the partial derivative of $\boldsymbol{u}$ with respect to time t. Note that we use the dot notation $(\cdot)$ to denote the scalar product of vectors.
The total potential energy $U = W - W_{ext}$ is composed of the *strain energy*, i.e. the energy stored in the linear elastic material due to the deformation, given by

$$W(\boldsymbol{u}) = \frac{1}{2} \int_{\Omega} \boldsymbol{\sigma}(\boldsymbol{u}) : \boldsymbol{\epsilon}(\boldsymbol{u}) \, \mathrm{d}x, \tag{2.18}$$

as well as the potential energy of the exterior forces [35, 102],

$$W_{ext}(\boldsymbol{u}) = -\int_{\Omega} \boldsymbol{u} \cdot \boldsymbol{\beta} \, \mathrm{d}x - \int_{\Gamma_N} \boldsymbol{u} \cdot \boldsymbol{\tau} \, \mathrm{d}s, \tag{2.19}$$

where $\boldsymbol{\beta}(\boldsymbol{x}, t) \in \mathbb{R}^3$ is the density of volume forces such as gravity, and $\boldsymbol{\tau}(\boldsymbol{x}, t) \in \mathbb{R}^3$ describe the (given) surface tractions on the Neumann boundary Γ_N. Assuming sufficient smoothness, Equation (2.15) now yields

$$\int_{t_0}^{t_1} \left[\int_{\Omega} \rho \dot{\boldsymbol{v}} \cdot \dot{\boldsymbol{u}} \, \mathrm{d}x - \int_{\Omega} \boldsymbol{\sigma}(\boldsymbol{u}) : \boldsymbol{\epsilon}(\boldsymbol{v}) \, \mathrm{d}x + \int_{\Omega} \boldsymbol{v} \cdot \boldsymbol{\beta} \, \mathrm{d}x + \int_{\Gamma_N} \boldsymbol{v} \cdot \boldsymbol{\tau} \, \mathrm{d}s \right] \mathrm{d}t = 0. \tag{2.20}$$

In order to get rid of the time derivative of the function $\boldsymbol{v}$ in Equation (2.20), we perform integration by parts with respect to t and obtain

$$\int_{t_0}^{t_1} \int_{\Omega} \rho \dot{\boldsymbol{v}} \cdot \dot{\boldsymbol{u}} \, \mathrm{d}x \, \mathrm{d}t = \left[\int_{\Omega} \rho \boldsymbol{v} \cdot \dot{\boldsymbol{u}} \, \mathrm{d}x \right]_{t_0}^{t_1} - \int_{t_0}^{t_1} \int_{\Omega} \rho \boldsymbol{v} \cdot \ddot{\boldsymbol{u}} \, \mathrm{d}x \, \mathrm{d}t.$$

Due to Equation (2.14), both integrals on the right hand side are zero and we get the relation

$$\int_{t_0}^{t_1} \left(\int_{\Omega} \rho \boldsymbol{v} \cdot \ddot{\boldsymbol{u}} + \boldsymbol{\sigma}(\boldsymbol{u}) : \boldsymbol{\epsilon}(\boldsymbol{v}) - \boldsymbol{v} \cdot \boldsymbol{\beta} \, \mathrm{d}x - \int_{\Gamma_N} \boldsymbol{v} \cdot \boldsymbol{\tau} \, \mathrm{d}s \right) \mathrm{d}t = 0, \tag{2.21}$$

for all admissible $\boldsymbol{v}$. Due to the definition (2.2) of the strain tensor, we can rewrite the expression

$$\int_\Omega \boldsymbol{\sigma}(\boldsymbol{u}) : \boldsymbol{\epsilon}(\boldsymbol{v}) \, \mathrm{d}x = \int_\Omega \boldsymbol{\sigma}(\boldsymbol{u}) : \nabla \boldsymbol{v} \, \mathrm{d}x,$$

and apply Gauss' divergence theorem to the product $\boldsymbol{\sigma}(\boldsymbol{u}(\boldsymbol{x},\cdot))\boldsymbol{v}(\boldsymbol{x},\cdot)$, which yields an integral identity that will be again presented, among other integral relations for Lipschitz domains, in the second part of this chapter (Equation (2.102)). To apply the divergence operator on the tensor $\boldsymbol{\sigma}$, we defined the *vector divergence* componentwise as

$$(\mathbf{div}\, \boldsymbol{\sigma})_i := \sum_{j=1}^{3} \frac{\partial \sigma_{ij}}{\partial x_j}, \tag{2.22}$$

i.e. the i-th component of the vector divergence of $\boldsymbol{\sigma}$ is the divergence of the i-th row of $\boldsymbol{\sigma}$. Using this definition, we obtain

$$\int_\Omega \boldsymbol{\sigma}(\boldsymbol{u}) : \boldsymbol{\epsilon}(\boldsymbol{v}) \, \mathrm{d}x = -\int_\Omega \boldsymbol{v} \cdot (\mathbf{div}\, \boldsymbol{\sigma}(\boldsymbol{u})) \, \mathrm{d}x + \int_{\Gamma_N} \boldsymbol{v} \cdot (\boldsymbol{\sigma}\boldsymbol{n}) \, \mathrm{d}s,$$

with $\boldsymbol{n} = \boldsymbol{n}(\boldsymbol{x})$ denoting the outer unit normal vector of Γ_N. Inserting the above equation into (2.21) results in the variational formulation

$$\int_{t_0}^{t_1} \int_\Omega \boldsymbol{v} \cdot (\rho \ddot{\boldsymbol{u}} - \mathbf{div}\, \boldsymbol{\sigma}(\boldsymbol{u}) - \boldsymbol{\beta}) \, \mathrm{d}x \, \mathrm{d}t + \int_{t_0}^{t_1} \int_{\Gamma_N} \boldsymbol{v} \cdot (\boldsymbol{\sigma}(\boldsymbol{u})\boldsymbol{n} - \boldsymbol{\tau}) \, \mathrm{d}s \, \mathrm{d}t = 0. \tag{2.23}$$

The relation (2.23) holds for all admissible $\boldsymbol{v}$, i.e. all fields $\boldsymbol{v}$ satisfying the requirements (2.13) and (2.14). In particular, if $\boldsymbol{v}(\boldsymbol{x},t) = \mathbf{0}$ is true for all $\boldsymbol{x} \in \Gamma_N$, the boundary integral in Equation (2.23) is zero. Applying the Fundamental Lemma of Calculus of Variations (e.g. in [36]), we conclude that

$$\boldsymbol{v} \cdot (\rho \ddot{\boldsymbol{u}} - \mathbf{div}\, \boldsymbol{\sigma} - \boldsymbol{\beta}) = 0$$

for all admissible $\boldsymbol{v}$. This, in turn, implies that

$$\boldsymbol{v} \cdot (\boldsymbol{\sigma}\boldsymbol{n} - \boldsymbol{\tau}) = 0,$$

also in case that $\boldsymbol{v}(\boldsymbol{x},t) \neq \mathbf{0}$ on the Neumann boundary Γ_N. These two equations represent the strong form of the linear elastic hyperbolic problem:

Problem (LE): For each $t \in [t_0, t_1]$ find $\boldsymbol{u}(\cdot,t) \in C^2(\Omega)$ such that

$$\rho \ddot{\boldsymbol{u}}(\boldsymbol{x},t) = \mathbf{div}\, \boldsymbol{\sigma}(\boldsymbol{u}(\boldsymbol{x},t)) + \boldsymbol{\beta}(\boldsymbol{x},t) \quad \text{in } \Omega, \tag{2.24}$$

with the initial conditions

$$\boldsymbol{u}(\boldsymbol{x},t_0) = \boldsymbol{u}_{t_0}(\boldsymbol{x}),$$
$$\dot{\boldsymbol{u}}(\boldsymbol{x},t_0) = \dot{\boldsymbol{u}}_{t_0}(\boldsymbol{x}),$$

the Dirichlet boundary condition

$$\boldsymbol{u}(\boldsymbol{x},t) = \boldsymbol{u}_0(\boldsymbol{x},t) \quad \text{on } \Gamma_D,$$

and the Neumann boundary condition

$$\boldsymbol{\sigma}(\boldsymbol{u}(\boldsymbol{x},t))\boldsymbol{n}(\boldsymbol{x}) = \boldsymbol{\tau}(\boldsymbol{x},t) \quad \text{on } \Gamma_N.$$

To establish a relation between $\boldsymbol{\sigma}$ and $\boldsymbol{u}$, the above system of equations is supplemented with the constitutive equation (2.3).

The weak form of the linear elastic boundary value problem can be obtained by multiplication of Equation (2.24) with now time-independent test functions $\boldsymbol{v}(\boldsymbol{x})$ satisfying the Dirichlet condition (2.13). Integrating over Ω, we then obtain the so-called *principle of virtual work* (in [102]),

$$\int_\Omega \rho \boldsymbol{v} \cdot \ddot{\boldsymbol{u}} \, \mathrm{d}x + \int_\Omega \boldsymbol{\sigma}(\boldsymbol{u}) : \boldsymbol{\epsilon}(\boldsymbol{u}) \, \mathrm{d}x = \int_\Omega \boldsymbol{v} \cdot \boldsymbol{\beta} \, \mathrm{d}x + \int_{\Gamma_N} \boldsymbol{v} \cdot \boldsymbol{\tau} \, \mathrm{d}s,$$

for all $\boldsymbol{v}$ that vanish on the Dirichlet boundary Γ_D. In order to state the complete weak form of the problem, in the last step, we need to define the appropriate function spaces for $\boldsymbol{u}$ and $\boldsymbol{v}$.

2.1.3 Function spaces

Let the (Lebesgue-measurable) domain Ω be a subset of $\mathbb{R}^3$. For a real-valued function $f : \Omega \to \mathbb{R}$, we define the norm

$$\|f\|_{L^p(\Omega)} := \left(\int_\Omega |f(\boldsymbol{x})|^p \, \mathrm{d}x \right)^{\frac{1}{p}} \tag{2.25}$$

and the corresponding Lebesgue spaces

$$L^p(\Omega) := \{ f \mid \|f\|_{L^p(\Omega)} < \infty \}.$$

In the following, we focus on the cases $p = 1$ and $p = 2$. For two functions $f, g : \Omega \to \mathbb{R}$ we define their inner product in $L^2(\Omega)$ by

$$(f, g)_{L^2(\Omega)} := \int_\Omega f(\boldsymbol{x}) g(\boldsymbol{x}) \, \mathrm{d}x. \tag{2.26}$$

Then, the norm (2.25) can be expressed as

$$\|f\|_{L^2(\Omega)} = \sqrt{(f, f)_{L^2(\Omega)}}.$$

Finally, we say that the functions f and g are identical in $L^2(\Omega)$ if

$$\|f - g\|_{L^2(\Omega)} = 0,$$

i.e. if the functions are only different on sets of measure zero. In the following, we will denote the inner product and the norm in $L^2(\Omega)$ with the subscript 0 to simplify the notation, i.e.

$$(f, g)_0 := (f, g)_{L^2(\Omega)}, \quad \|f\|_0 := \|f\|_{L^2(\Omega)}.$$

The space $L^2(\Omega)$ is complete with respect to the metric induced by the norm defined in (2.25) and a Hilbert space with the scalar product defined in (2.26) (for a proof, refer e.g. to [22]). For $f, g \in L^2(\Omega)$, the *Cauchy-Schwarz inequality*

$$\int_\Omega |f(\boldsymbol{x}) g(\boldsymbol{x})| \, \mathrm{d}x \leq \|f\|_{L^2(\Omega)} \, \|g\|_{L^2(\Omega)} \tag{2.27}$$

holds. It is a special case of the *Hölder inequality* [22] which gives a general estimate for the norm $\|fg\|_{L^1(\Omega)}$ of functions $f \in L^p(\Omega)$ and $g \in L^q(\Omega)$ for $p, q \geq 1$ and $1 = 1/p + 1/q$. For $\Phi \in C_0^\infty(\Omega)$, where

$$C_0^\infty(\Omega) := \{\Phi \in C^\infty(\Omega) \mid \text{supp } \Phi \text{ is compact}\},$$

and the support of Φ is given by

$$\text{supp } \Phi := \{\boldsymbol{x} \in \Omega \mid \Phi(\boldsymbol{x}) \neq 0\},$$

we define the partial derivatives

$$D^\alpha \Phi := \frac{\partial^{|\alpha|}\Phi}{\partial x_1^{\alpha_1} ... \partial x_n^{\alpha_n}},$$

with the multi-index $\alpha = (\alpha_1, ..., \alpha_n)$, $|\alpha| = \sum_{i=1}^n \alpha_i$. Then, the weak derivative of a function $f \in L^2(\Omega)$ is a function $g \in L^2(\Omega)$ that satisfies the relation

$$\int_\Omega g(\boldsymbol{x})\Phi(\boldsymbol{x})\,\mathrm{d}x = (-1)^{|\alpha|} \int_\Omega f(\boldsymbol{x}) D^\alpha \Phi(\boldsymbol{x})\,\mathrm{d}x \tag{2.28}$$

for all $\Phi \in C_0^\infty(\Omega)$. If a function $g \in L^2(\Omega)$ with the above property exists, we set $g = D_w^\alpha f$. Furthermore, the set of *locally integrable functions* of the domain Ω is described by

$$L^1_{\text{loc}} := \{f \mid f \in L^1(K) \text{ for all compact subsets } K \subset \Omega\}.$$

With the above definitions, we can finally introduce the function spaces that are essential for the characterization of the solutions to the weak linear elastic boundary value problem. We define the *Sobolev norm* of a function $f \in L^1_{loc}(\Omega)$ for which the weak derivatives $D_w^\alpha f \in L^2(\Omega)$ exist for all $|\alpha| \leq m$, $m \in \mathbb{N}$ as

$$\|f\|_{H^m(\Omega)} := \left(\sum_{|\alpha| \leq m} \|D_w^\alpha f\|^2_{L^2(\Omega)} \right)^{\frac{1}{2}}. \tag{2.29}$$

The corresponding semi-norm is obtained by setting $|\alpha| = m$ in the above definition. The *Sobolev space*

$$H^m(\Omega) := \{f \in L^1_{loc}(\Omega) \mid \|f\|_{H^m(\Omega)} < \infty\} \tag{2.30}$$

is a Hilbert space [22] with the inner product of two functions $f, g \in H^m(\Omega)$ defined as

$$(f, g)_{H^m(\Omega)} := \sum_{|\alpha| \leq m} (D_w^\alpha f, D_w^\alpha g)_0.$$

The norm can be expressed in terms of the inner product as

$$\|f\|_{H^m(\Omega)} := \sqrt{(f, f)_{H^m(\Omega)}}.$$

We are particularly interested in the space $H^1(\Omega)$ or its vector counterpart $H^1(\Omega)^3$, which is defined as the space of all vector-valued functions $\boldsymbol{v} : \Omega \to \mathbb{R}^3$ whose components are elements of $H^1(\Omega)$. As in the case of the space $L^2(\Omega)$, we will denote the inner product, norm and semi-norm in $H^1(\Omega)$ by the subscript 1, i.e.

$$(f, g)_1 := (f, g)_{H^1(\Omega)}, \quad \|f\|_1 := \|f\|_{H^1(\Omega)}, \quad |f|_1 := |f|_{H^1(\Omega)}.$$

For the linear elastic problem, we define the function spaces

$$\mathcal{V} := H^1(\Omega)^3 = \{\boldsymbol{v} = (v_1, v_2, v_3)^T \mid v_i \in H^1(\Omega) \text{ for } i = 1, 2, 3\}, \tag{2.31}$$

$$\mathcal{V}_0 := \{\boldsymbol{v} \in \mathcal{V} \mid v_i = 0,\ i = 1, 2, 3,\ \text{on } \Gamma_D\}. \tag{2.32}$$

The space $\mathcal{V}$, as well as its subspace $\mathcal{V}_0$ are Hilbert spaces with the inner product

$$(\boldsymbol{u}, \boldsymbol{v})_{\mathcal{V}} := \sum_{i=1}^{3} (u_i, v_i)_1 = \int_\Omega \boldsymbol{u} \cdot \boldsymbol{v} \, \mathrm{d}x.$$

With these preliminaries, we are finally able to state the weak or variational form of the problem of linear elasticity [54, 102]:

Problem $(LE)_t^w$: For each $t \in [t_0, t_1]$, find $\boldsymbol{u}(\cdot, t) \in \mathcal{V}$ that satisfies the Dirichlet boundary condition

$$\boldsymbol{u}(\boldsymbol{x}, t) = \boldsymbol{u}_0(\boldsymbol{x}, t) \quad \text{on } \Gamma_D \tag{2.33}$$

and the equation

$$(\rho \ddot{\boldsymbol{u}}, \boldsymbol{v})_{\mathcal{V}} + a(\boldsymbol{u}, \boldsymbol{v}) = l(\boldsymbol{v}) \quad \forall \boldsymbol{v} \in \mathcal{V}_0 \tag{2.34}$$

with the initial conditions

$$(\boldsymbol{u}(\boldsymbol{x}, t_0), \boldsymbol{v})_{\mathcal{V}} = (\boldsymbol{u}_{t_0}, \boldsymbol{v})_{\mathcal{V}} \quad \forall \boldsymbol{v} \in \mathcal{V}_0 \tag{2.35}$$

$$(\dot{\boldsymbol{u}}(\boldsymbol{x}, t_0), \boldsymbol{v})_{\mathcal{V}} = (\dot{\boldsymbol{u}}_{t_0}, \boldsymbol{v})_{\mathcal{V}} \quad \forall \boldsymbol{v} \in L^2(\Omega)^3, \tag{2.36}$$

specifying the initial displacement and initial velocity of a material point $\boldsymbol{x} \in \Omega$. The initial data $\boldsymbol{u}_{t_0}$ and $\dot{\boldsymbol{u}}_{t_0}$ are functions of the space coordinate $\boldsymbol{x}$. In this formulation, $a : \mathcal{V} \times \mathcal{V}_0 \to \mathbb{R}$ is a bilinear form defined as

$$a(\boldsymbol{u}, \boldsymbol{v}) := \int_\Omega \boldsymbol{\sigma}(\boldsymbol{u}) : \boldsymbol{\epsilon}(\boldsymbol{v}) \, \mathrm{d}x, \tag{2.37}$$

while $l : \mathcal{V}_0 \to \mathbb{R}$ is a linear form given by

$$l(\boldsymbol{v}) := \int_\Omega \boldsymbol{v} \cdot \boldsymbol{\beta} \, \mathrm{d}x + \int_{\Gamma_N} \boldsymbol{v} \cdot \boldsymbol{\tau} \, \mathrm{d}s. \tag{2.38}$$

2.1.4 The trace space

The Dirichlet boundary condition (2.33) is not directly incorporated into the weak formulation $(LE)^w$ or into the definition of the function space $\mathcal{V}$ but rather remains in the strong form. This is due to the fact that in $H^1(\Omega)$, $\Omega \subset \mathbb{R}^n$, the pointwise evaluation of a function is not defined for $n \geq 2$, as in this case, singularities may arise and the restriction of the function $\boldsymbol{u}$ to the boundary may not make sense. Thus, we cannot require that $\boldsymbol{u}_0 \in \mathcal{V}$.

The above consideration is the result of the *Sobolev inequality theorem* (e.g. in [22]) which states that for a positive integer m with $m > n/2$, all functions $u \in H^m(\Omega)$, $\Omega \subset \mathbb{R}^n$ are continuous and bounded. The suitable framework for defining this type of boundary conditions is given by so-called *trace spaces*. The idea behind trace spaces is the interpretation of the boundary of a domain Ω as an $(n-1)$–dimensional *manifold* and the restriction of functions in n-dimensional Sobolev spaces to $(n-1)$–dimensional functions. This concept is explained in detail in [22]. To define the trace space, we make use of the following inequality for functions over Lipschitz domains ([22], Section 1.6),

$$\|v\|_0 \leq C \, \|v\|_0^{\frac{1}{2}} \, \|v\|_1^{\frac{1}{2}} \quad \forall v \in H^1(\Omega),$$

with a constant $C > 0$. The bounded linear *trace* operator $\gamma : H^1(\Omega) \to L^2(\partial\Omega)$ can now be defined such that

$$\gamma f = f|_{\partial\Omega} \quad \text{for } f \in H^1(\Omega) \cap C^1(\overline{\Omega}),$$

i.e. γf is the restriction of the function f to the boundary $\partial\Omega$. and

$$\|\gamma f\|_0 \leq C \|f\|_1 \quad \text{for } f \in H^1(\Omega).$$

Note that the extension of the above inequality from functions $f \in H^1(\Omega) \cap C^1(\overline{\Omega})$ to functions $f \in H^1(\Omega)$ is valid due to the completeness of $L^2(\Omega)$ [102]. The mapping γ is in general not surjective and the image of γ constitutes the *trace space*

$$H^{\frac{1}{2}}(\partial\Omega) \subset L^2(\partial\Omega).$$

Alternatively, $\partial\Omega$ can be restricted to the Dirichlet boundary Γ_D and the corresponding space is given by $H^{\frac{1}{2}}(\Gamma_D)$. Moreover, it is possible to extend these definitions to three-dimensional spaces, i.e. $H^{\frac{1}{2}}(\Gamma_D)^3$ and we can finally conclude that the boundary function $\boldsymbol{u}_0$ is an element of the space $H^{\frac{1}{2}}(\Gamma_D)^3$.

2.1.5 Existence and uniqueness of the solution

A possibility to incorporate the Dirichlet boundary condition into the weak problem discussed in the previous sections is to include it as an additional constraint with the help of Lagrange multipliers. This leads to the transient saddle point problem of linear elasticity, which is elaborately discussed e.g. in [102] and which will not be the focus of our attention. As the models presented in this work involve either stationary or quasi-static elastic fields, we draw our focus to the stationary problem of linear elasticity with homogeneous Dirichlet boundary conditions. In this case, the term $\rho\ddot{\boldsymbol{u}}(\boldsymbol{x}, t)$ vanishes and the strong form reads

Problem (LE): Find $\boldsymbol{u}(\boldsymbol{x}) \in C^2(\Omega)^3$ such that

$$\mathbf{div}\, \boldsymbol{\sigma}(\boldsymbol{u}(\boldsymbol{x})) = -\boldsymbol{\beta}(\boldsymbol{x}) \quad \text{in } \Omega, \tag{2.39}$$

holds, together with the Dirichlet boundary condition

$$\boldsymbol{u}(\boldsymbol{x}) = \mathbf{0} \quad \text{on } \Gamma_D, \tag{2.40}$$

and the Neumann boundary condition

$$\boldsymbol{\sigma}(\boldsymbol{u}(\boldsymbol{x}))\boldsymbol{n}(\boldsymbol{x}) = \boldsymbol{\tau}(\boldsymbol{x}) \quad \text{on } \Gamma_N. \tag{2.41}$$

The above strong system represents an elliptic boundary value problem. Using the function space $\mathcal{V}_0$ defined in (2.32), the corresponding weak forms is

Problem $(LE)^w$: Find $\boldsymbol{u} \in \mathcal{V}_0$ such that

$$a(\boldsymbol{u}, \boldsymbol{v}) = l(\boldsymbol{v}) \qquad \text{for all } \boldsymbol{v} \in \mathcal{V}_0, \tag{2.42}$$

with the bilinear form $a(\cdot,\cdot)$ and the linear functional $l(\cdot)$ as defined in (2.37) and (2.38).

Note that $l \in \mathcal{V}_0'$, where $\mathcal{V}_0'$ is the dual space of $\mathcal{V}_0$. We say that $a(\cdot,\cdot)$ is *bounded* (or, equivalently, *continuous*) if there is a constant $c_1 > 0$ such that

$$|a(\boldsymbol{u}, \boldsymbol{v})| \leq c_1 \|\boldsymbol{u}\|_{\mathcal{V}} \|\boldsymbol{v}\|_{\mathcal{V}} \tag{2.43}$$

holds for all $\boldsymbol{u}, \boldsymbol{v} \in \mathcal{V}_0$. Similarly, the linear functional is said to be continuous if

$$|l(\boldsymbol{v})| \leq c_2 \|l\|_{\mathcal{V}_0'} \|v\|_{\mathcal{V}}$$

for a constant $c_2 > 0$. Here, $||l||_{\mathcal{V}_0'} = \sup_{0 \neq \boldsymbol{v} \in \mathcal{V}_0} \frac{|l(\boldsymbol{v})|}{||\boldsymbol{v}||_{\mathcal{V}_0}}$ is the operator norm.
Moreover, $a(\cdot,\cdot)$ is called *coercive* if $\exists\ \alpha > 0$ such that the inequality

$$a(\boldsymbol{u}, \boldsymbol{u}) \geq \alpha \, ||\boldsymbol{u}||_{\mathcal{V}}^2 \tag{2.44}$$

is true for all $\boldsymbol{u} \in \mathcal{V}_0$.
If $a(\cdot,\cdot)$ and $l(\cdot)$ are continuous and $a(\cdot,\cdot)$ is coercive, the Lax-Milgram lemma (e.g. in [4] or [22]) guarantees the existence and uniqueness of the solution to Equation (2.42).
While the continuity is straightforward, the coercivity of $a(\cdot,\cdot)$ can be shown on the basis of Korn's inequality [22, 34], which states that there is a constant $C = C(\Omega)$ such that for all $\boldsymbol{v} \in \mathcal{V}_0$,

$$||\boldsymbol{v}||_{\mathcal{V}} \leq C(\Omega) \left(\sum_{i,j=1}^{3} |\epsilon_{ij}(\boldsymbol{v})|_0^2 + \sum_{i=1}^{3} |v_i|_0^2 \right)^{\frac{1}{2}}.$$

For a proof, refer e.g. to [54] or [58].

2.1.6 Influence of perturbations

Finally, we focus on the question of how perturbations of the given right-hand side data, i.e. of the linear functional $l \in \mathcal{V}_0'$ involving the known volume and surface force terms, influence the solution of the problem. A boundary value problem such as $(LE)^w$ is called *well-posed* if it can be uniquely solved and, additionally, the solution depends continuously on the given data. The property of continuous dependence on the right-hand side is sometimes referred to as *stability* of the solution in the literature (see e.g. [14]). Although this term is a bit misleading, we will adopt the expression *stability estimate* when referring to an estimate for the norm of the solution depending on the norm of the given data.
The question of finding a suitable stability estimate for the solution $\boldsymbol{u}$ of the problem $(LE)^w$ is again answered by the Lax-Milgram lemma. Exploiting the continuity and coercivity properties presented in the previous section, we obtain the inequality chain

$$||\boldsymbol{u}||_{\mathcal{V}}^2 \leq \frac{1}{\alpha} |a(\boldsymbol{u}, \boldsymbol{u})| = \frac{1}{\alpha} \alpha |l(\boldsymbol{u})| \leq \frac{c_2}{\alpha} \, ||l||_{\mathcal{V}'} \, ||u||_{\mathcal{V}},$$

where α is the coercivity constant of $a(\cdot,\cdot)$ and c_2 is the continuity constant of $l(\cdot)$.
Concluding, we obtain the estimate

$$||\boldsymbol{u}||_{\mathcal{V}} \leq \frac{c_2}{\alpha} \, ||l||_{\mathcal{V}'}, \tag{2.45}$$

indicating that the boundary value problem $(LE)^w$ is indeed well-posed.

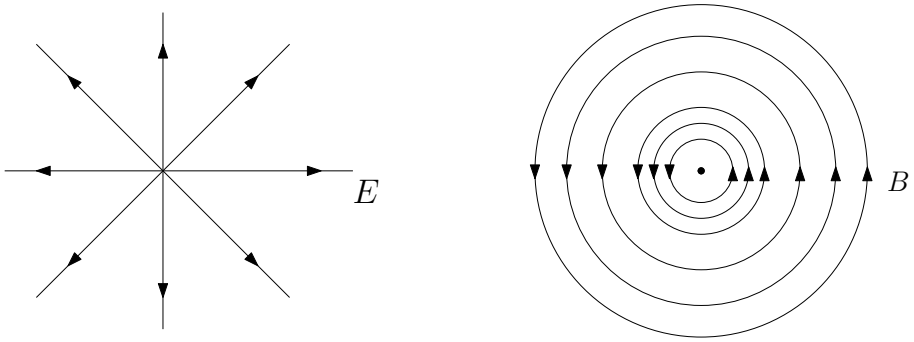

Figure 2.4: (a) Electrostatic field of a point charge and (b) magnetostatic field of a long wire, pointing out of the plane (after [62]).

2.2 Classical electrodynamics

This section follows the outline of Section 2.1: After introducing the basics of electromagnetic theory and various formulations of Maxwell's equations, we focus on their solution. Strong and weak formulations are presented, function spaces are introduced and the existence and uniqueness of the solutions is discussed for different settings. The section concludes with the derivation of suitable stability estimates for the solution.

2.2.1 Maxwell's equations

In his publication "A Dynamical Theory of the Electromagnetic Field" from 1865 [84], James Clerk Maxwell introduced a set of equations that form the foundation of classical electrodynamics. These equations were based on experimental observations of phenomena of electricity and magnetism, primarily made by Coulomb, Gauss, Biot and Savart, as well as Ampère and Faraday. Maxwell recapitulated their laws, which at first glance seemed rather disparate, and merged them into a mutual context, creating one of the most significant accumulations of empirical facts in physics. Maxwell's laws form a set of partial differential equations which, in their original form, were written componentwise, since the short hand notations for the curl and div operators were not yet introduced at that time. His laws were later reformulated in terms of vector calculus, which gave them a more compact and precise form. Thus, a total of four partial differential equations (in space and time) were created, describing the behavior of the electric and magnetic fields in vacuum:

$$\operatorname{div} \boldsymbol{E} = \frac{1}{\epsilon_0}\rho \qquad \textit{Gauss' law}, \tag{2.46}$$

$$\operatorname{div} \boldsymbol{B} = 0 \tag{2.47}$$

$$\operatorname{curl} \boldsymbol{E} = -\frac{\partial B}{\partial t} \qquad \textit{Faraday's law}, \tag{2.48}$$

$$\operatorname{curl} \boldsymbol{B} = \mu_0 \boldsymbol{j} + \mu_0 \epsilon_0 \frac{\partial \boldsymbol{E}}{\partial t}, \qquad \textit{Ampère's law}, \tag{2.49}$$

where $\boldsymbol{E}\left[\frac{V}{m}\right]$ is the *electric field intensity*, $\rho\left[\frac{A}{m^3}\right]$ the *charge density*, $\epsilon_0\left[\frac{A^2 s^4}{kgm^3}\right]$ the *permittivity of free space*, $\boldsymbol{B}\left[\frac{Vs}{m^2}\right]$ the *magnetic flux density*, $\mu_0\left[\frac{N}{A^2}\right]$ the *magnetic permeability of free space* and $\boldsymbol{j}\left[\frac{A}{m^2}\right]$ the *electric current density*.

Maxwell's laws describe the nature of the electric and magnetic fields: While the electric field "diverges away from a positive charge", the magnetic field "curls around a current"

[62], see Figure 2.4. Together with the *Lorentz force* law

$$\boldsymbol{F} = q(\boldsymbol{E} + \boldsymbol{v} \times \boldsymbol{B}), \tag{2.50}$$

which describes the force acting on a particle of charge q and velocity $\boldsymbol{v}$ in the presence of an electric field $\boldsymbol{E}$ and a magnetic field $\boldsymbol{B}$, as well as Newton's second law, Maxwell's equations constitute the basis of classical electrodynamic theory.
Note that the equations stated above are valid in vacuum with the constants ϵ_0 and μ_0. Inside polarized matter, one has to distinguish between so-called *free* and *bound* charges and currents. Following Griffiths [62], we divide the total charge density ρ into a free part ρ_f and a bound part

$$\rho_b := -\operatorname{div} \boldsymbol{P},$$

which is generated by an *electric polarization* $\boldsymbol{P}$

$$\rho = \rho_f - \operatorname{div} \boldsymbol{P}.$$

The total current density $\boldsymbol{j}$ consists of the free current density $\boldsymbol{j}_f$, a bound current density

$$\boldsymbol{j}_b := \operatorname{curl} \boldsymbol{M},$$

resulting from the *magnetization* $\boldsymbol{M}$, and a polarization current density

$$\boldsymbol{j}_p := \frac{\partial \boldsymbol{P}}{\partial t},$$

which is generated by a change in the electric polarization, i.e.

$$\boldsymbol{j} = \boldsymbol{j}_f + \operatorname{curl} \boldsymbol{M} + \frac{\partial \boldsymbol{P}}{\partial t}.$$

These changes imply that Gauss' law can be written as

$$\operatorname{div} \boldsymbol{D} = \rho_f,$$

where

$$\boldsymbol{D} = \epsilon_0 \boldsymbol{E} + \boldsymbol{P} \tag{2.51}$$

denotes the *electric displacement* $\left[\frac{A}{m^2}\right]$ and Ampère's law is transformed to

$$\operatorname{curl} \boldsymbol{B} = \mu_0 \left(\boldsymbol{j}_f + \operatorname{curl} \boldsymbol{M} + \frac{\partial \boldsymbol{P}}{\partial t} \right) + \mu_0 \epsilon_0 \frac{\partial \boldsymbol{E}}{\partial t}.$$

Introducing the magnetic field intensity $\boldsymbol{H}$ $\left[\frac{A}{m}\right]$, defined as

$$\boldsymbol{H} = \frac{1}{\mu_0} \boldsymbol{B} - \boldsymbol{M}, \tag{2.52}$$

Ampère's law turns into

$$\operatorname{curl} \boldsymbol{H} = \boldsymbol{j}_f + \frac{\partial \boldsymbol{D}}{\partial t}.$$

Summing up, the new form of Maxwell's equations in terms of free charges and currents is

$$\operatorname{div} \boldsymbol{D} = \rho_f, \tag{2.53}$$

$$\operatorname{div} \boldsymbol{B} = 0, \tag{2.54}$$

$$\operatorname{curl} \boldsymbol{E} = -\frac{\partial \boldsymbol{B}}{\partial t}, \tag{2.55}$$

$$\operatorname{curl} \boldsymbol{H} = \boldsymbol{j}_f + \frac{\partial \boldsymbol{D}}{\partial t}. \tag{2.56}$$

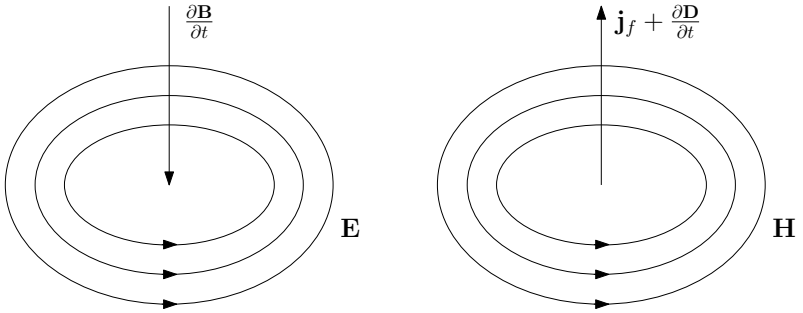

Figure 2.5: (a) Faraday's law: A time-varying magnetic field generates an electric field. (b) Ampère's law: The electric current density and the displacement current induce a magnetic field (after [81]).

Equations (2.53) and (2.54) describe the electric and magnetic Gauss laws. Faraday's law (2.55) states that the electric field is generated by a time-varying magnetic field (see Figure 2.5(a)). Ampère's law (2.56) indicates that the magnetic field is induced by currents in coils as well as by time-varying electric fields (Figure 2.5(b)). The expression

$$\frac{\partial \boldsymbol{D}}{\partial t} =: \boldsymbol{j}_D$$

is characterized by the term *displacement current*.
To complete these equations, we need the constitutive equations relating the magnetic flux density $\boldsymbol{B}$ and the magnetic field $\boldsymbol{H}$, as well as the electric field $\boldsymbol{E}$ and the electric displacement $\boldsymbol{D}$. For linear materials, the polarization $\boldsymbol{P}$ and the magnetization $\boldsymbol{M}$ are proportional to the electric field $\boldsymbol{E}$ and the magnetic field $\boldsymbol{H}$, respectively,

$$\boldsymbol{P} = \hat{\epsilon_0}\boldsymbol{\chi}_l \boldsymbol{E}, \tag{2.57}$$

$$\boldsymbol{M} = \boldsymbol{\chi}_m \boldsymbol{H}, \tag{2.58}$$

where $\boldsymbol{\chi}_l$ and $\boldsymbol{\chi}_m$ are the electric and magnetic *susceptibilities* (dimensionless) and

$$\hat{\boldsymbol{\epsilon}} = \hat{\epsilon_0}(\boldsymbol{I} + \boldsymbol{\chi}_l)$$

is the *permittivity* of the material. In vacuum, the electric susceptibility $\boldsymbol{\chi}_l$ vanishes and thus $\hat{\boldsymbol{\epsilon}} = \boldsymbol{\epsilon}_0 = \epsilon_0 \boldsymbol{I}$, with $\boldsymbol{I}$ denoting the 3×3 identity matrix. One can also define the dimensionless *relative permittivity*

$$\hat{\boldsymbol{\epsilon}_r} := I + \boldsymbol{\chi}_l = \frac{1}{\epsilon_0}\hat{\boldsymbol{\epsilon}}.$$

Similarly,

$$\boldsymbol{\mu} = \mu_0(I + \boldsymbol{\chi}_m)$$

is the *permeability* of the material. In vacuum, $\boldsymbol{\mu} = \boldsymbol{\mu}_0 = \mu_0 \boldsymbol{I}$. The dimensionless *relative permeability* is defined via

$$\boldsymbol{\mu}_r := I + \boldsymbol{\chi}_m = \frac{1}{\mu_0}\boldsymbol{\mu}.$$

Note that for homogeneous anisotropic materials, the above defined material parameters are tensor-valued, i.e. the (relative) permeability $\boldsymbol{\mu}$ and the (relative) permittivity $\hat{\boldsymbol{\epsilon}}$ are symmetric and uniformly positive definite matrices [2]. The susceptibilities $\boldsymbol{\chi}_l$ and $\boldsymbol{\chi}_m$ are second order tensors as well.

With this generalization, the linear constitutive equations relating the electric and magnetic field quantities read

$$\boldsymbol{B} = \boldsymbol{\mu}\boldsymbol{H}, \tag{2.59}$$
$$\boldsymbol{D} = \hat{\boldsymbol{\epsilon}}\boldsymbol{E}, \tag{2.60}$$
$$\boldsymbol{j}_f = \hat{\boldsymbol{\sigma}}\boldsymbol{E}. \tag{2.61}$$

The last equation is *Ohm's law* with $\hat{\boldsymbol{\sigma}}$ characterizing the electric conductivity (tensor) of the material. In regions containing conducting materials, the current density $\boldsymbol{j}_f$ is often expressed as the sum $\boldsymbol{j}_f = \hat{\boldsymbol{\sigma}}\boldsymbol{E} + \boldsymbol{j}_I$, where $\boldsymbol{j}_I$ denotes the *impressed* or *source* current density (see e.g. [79]).

Magnetoquasistatic fields

Current loops appearing in a conductor as a consequence of a time-varying magnetic field are generally referred to as *eddy currents*. Problems involving only eddy currents can be regarded as quasistatic field problems based on the assumption that in the usual low frequency operation range, the displacement current can be neglected, since

$$\|\boldsymbol{j}_f\| >> \left\|\frac{\partial \boldsymbol{D}}{\partial t}\right\|$$

for a norm $\|\cdot\|$ in $\mathbb{R}^3$. This approximation is applicable in the modeling of devices working at power frequencies, e.g. for the analysis of power losses or the prediction of transient problems [2, 3]. Eddy currents also provide a possibility of detecting flaws in conductive materials by using a coil with an alternating current. The coil generates eddy currents in the medium, which leads to different amplitudes of the impedance in regions with flaws. Ammari and Buffa [3] showed that the eddy current model is a first-order approximation of the general Maxwell equations and, with an additional condition on the current density, can even yield a second-order approximation in the frequency.
The eddy current approximation of Maxwell's equations is

$$\operatorname{div}\boldsymbol{D} = \rho_f, \tag{2.62}$$
$$\operatorname{div}\boldsymbol{B} = 0, \tag{2.63}$$
$$\operatorname{curl}\boldsymbol{E} = -\frac{\partial \boldsymbol{B}}{\partial t}, \tag{2.64}$$
$$\operatorname{curl}\boldsymbol{H} = \boldsymbol{j}_f. \tag{2.65}$$

Since $\operatorname{div}\operatorname{curl}\boldsymbol{H} = \operatorname{div}\boldsymbol{j}_f = \operatorname{div}(\hat{\boldsymbol{\sigma}}\boldsymbol{E} + \boldsymbol{j}_I) = 0$, the impressed current density $\boldsymbol{j}_I$ has to fulfill the condition $\operatorname{div}\boldsymbol{j}_f = 0$ in non-conducting regions (where $\hat{\boldsymbol{\sigma}} = \boldsymbol{0}$).

Boundary and interface conditions

Maxwell's differential equations must be supplemented by appropriate boundary and interface conditions. Discontinuities of the fields $\boldsymbol{E}$, $\boldsymbol{D}$, $\boldsymbol{B}$ and $\boldsymbol{H}$ arise at interfaces of two different materials, as well as at (boundary) surfaces carrying a charge density or a current density. The corresponding conditions can be derived from the integral form of Maxwell's equations. Consider a domain $\Omega \subset \mathbb{R}^3$ with boundary surface $\partial\Omega$ (and outer unit normal $\boldsymbol{n}$), which is itself bounded by a closed loop $\mathcal{L}$. Then, applying Gauss and Stokes' integral

laws to Equations (2.53)–(2.56), we get

$$\int_{\partial\Omega} \boldsymbol{D}\cdot\boldsymbol{n}\,\mathrm{d}s = \int_{\Omega} \operatorname{div}\boldsymbol{D}\,\mathrm{d}x = \int_{\Omega} \rho_f\,\mathrm{d}x, \tag{2.66}$$

$$\int_{\partial\Omega} \boldsymbol{B}\cdot\boldsymbol{n}\,\mathrm{d}s = \int_{\Omega} \operatorname{div}\boldsymbol{B}\,\mathrm{d}x = 0, \tag{2.67}$$

$$\int_{\mathcal{L}} \boldsymbol{E}\cdot\mathrm{d}\boldsymbol{l} = \int_{\partial\Omega} (\operatorname{curl}\boldsymbol{E})\cdot\boldsymbol{n}\,\mathrm{d}s = -\int_{\partial\Omega} \frac{\partial\boldsymbol{B}}{\partial t}\cdot\boldsymbol{n}\,\mathrm{d}s, \tag{2.68}$$

$$\int_{\mathcal{L}} \boldsymbol{H}\cdot\mathrm{d}\boldsymbol{l} = \int_{\partial\Omega} (\operatorname{curl}\boldsymbol{H})\cdot\boldsymbol{n}\,\mathrm{d}s = \int_{\partial\Omega} \left(\boldsymbol{j}_f + \frac{\partial\boldsymbol{D}}{\partial t}\right)\cdot\boldsymbol{n}\,\mathrm{d}s. \tag{2.69}$$

While the electric flux lines start and close at electric charges (Equation (2.66)), magnetic charges do not exist (Equation (2.67)). Equation (2.68) shows that the integral of the electric field along any closed loop $\mathcal{L}$ equals to the integral of the time variation of the magnetic flux density over the surface $\partial\Omega$ enclosed by the loop. Similarly, Equation (2.69) states that the integral of the magnetic field along any closed loop $\mathcal{L}$ is equal to the integral of the current densities flowing across the area $\partial\Omega$ bounded by the loop $\mathcal{L}$. The boundary and interface conditions can now be directly deduced from the above integral relations. On the interface of two dielectric materials with $\boldsymbol{D}_1$ and $\boldsymbol{D}_2$, the normal component of the electric displacement is discontinuous,

$$\boldsymbol{n}_I\cdot(\boldsymbol{D}_2-\boldsymbol{D}_1) = \rho_f, \tag{2.70}$$

where $\boldsymbol{n}_I$ denotes the outer unit normal of the interface. On the interface of two materials having the magnetic flux densities $\boldsymbol{B}_1$ and $\boldsymbol{B}_2$,

$$\boldsymbol{n}_I\cdot(\boldsymbol{B}_2-\boldsymbol{B}_2) = 0. \tag{2.71}$$

Similarly,

$$\boldsymbol{n}_I\cdot(\boldsymbol{j}_2-\boldsymbol{j}_1) = \boldsymbol{n}_I\left(\frac{\partial\boldsymbol{D}_1}{\partial t}-\frac{\partial\boldsymbol{D}_2}{\partial t}\right) \tag{2.72}$$

holds on the interface of two magnetic materials, where we have suppressed the subscript "f" for the current density. In case that only magnetoquasistatic fields are present, the normal component of the current density is continuous (charge conservation law),

$$\boldsymbol{n}_I\cdot(\boldsymbol{j}_2-\boldsymbol{j}_1) = 0. \tag{2.73}$$

On the interface of two materials having different electric field intensities $\boldsymbol{E}_1$ and $\boldsymbol{E}_2$, we have

$$\boldsymbol{n}_I\times(\boldsymbol{E}_2-\boldsymbol{E}_1) = \boldsymbol{0}, \tag{2.74}$$

i.e. the tangential component of the electric field intensity is continuous. Similarly,

$$\boldsymbol{n}_I\times(\boldsymbol{H}_2-\boldsymbol{H}_1) = \boldsymbol{K}_I, \tag{2.75}$$

where $\boldsymbol{K}_I$ denotes the current density on the interface.
The corresponding conditions on the boundary $\partial\Omega$ with outer unit normal vector $\boldsymbol{n}$ read

$$\boldsymbol{D}\cdot\boldsymbol{n} = -\rho_f, \tag{2.76}$$

$$\boldsymbol{B}\cdot\boldsymbol{n} = 0, \tag{2.77}$$

$$\boldsymbol{j}_f\cdot\boldsymbol{n} = -\frac{\partial\boldsymbol{D}}{\partial t}\cdot\boldsymbol{n}, \tag{2.78}$$

$$\boldsymbol{E}\times\boldsymbol{n} = \boldsymbol{0}, \tag{2.79}$$

$$\boldsymbol{H}\times\boldsymbol{n} = \boldsymbol{K}. \tag{2.80}$$

The condition (2.77) can be generalized to

$$\boldsymbol{B} \cdot \boldsymbol{n} = -\tilde{B}, \tag{2.81}$$

where $\tilde{B} = \tilde{B}(\boldsymbol{x}, t)$ is a fictitious magnetic surface charge density, and the negative sign indicates that positive surface charges are associated with positive values of $\tilde{B}$ [11, 81].

Potential formulations

Maxwell's equations (2.53) – (2.56), together with suitable boundary and interface conditions as well as the corresponding constitutive equations, represent a uniquely solvable system of partial differential equations for the magnetic and electric fields [87]. However, as the derivatives occur in form of the divergence or curl of these fields, solving the resulting system can be rather challenging. Hence, the choice of a suitable independent variable is essential for reducing the complexity of the problem.
According to the *Helmholtz decomposition* (e.g. in [87]), in simply-connected domains $\Omega \subset \mathbb{R}^3$ with a connected boundary every field $\boldsymbol{u} \in L^2(\Omega)^3$ can be written as

$$\boldsymbol{u} = \nabla p + \operatorname{curl} \boldsymbol{a}, \tag{2.82}$$

with uniquely defined scalar and vector potentials p and $\boldsymbol{a}$ (whose function spaces will not yet be specified at this point). Ampère's law (2.56) suggests that in current-free regions, i.e. $\boldsymbol{j}_f = \boldsymbol{0}$, the curl of the magnetic field vanishes in the static case, enabling the introduction of a *total magnetic scalar potential* Ψ with

$$\boldsymbol{H} = -\nabla \Psi. \tag{2.83}$$

Similarly, Equation (2.55) gives rise to an *electric scalar potential* V with

$$\boldsymbol{E} = -\nabla V \tag{2.84}$$

in the static case. Note that the negative sign in (2.84) is a direct consequence of Coulomb's law on point charges, and the sign convention for the magnetic scalar potential was determined on the basis of its electrostatic analogue [71, 110].
Using scalar potentials, Maxwell's equations can be reduced to a single elliptic second-order partial differential equation in the magnetostatic, as well as the electrostatic case. Inserting Equation (2.83) into Equation (2.54) and using the constitutive equation (2.52) and the linear relation (2.58), we obtain the magnetostatic Laplace-type equation

$$-\operatorname{div}(\boldsymbol{\mu} \nabla \Psi) = 0. \tag{2.85}$$

Alternatively, defining the *effective magnetic charge density* [59]

$$\rho_m = -\operatorname{div} \boldsymbol{M},$$

we obtain the Poisson equation

$$\mu_0 \Delta \Psi = -\rho_m.$$

Boundary conditions (2.77) and (2.80) suggest that

$$\begin{aligned} (\boldsymbol{\mu} \nabla \Psi) \cdot \boldsymbol{n} = 0 \quad \text{or} \quad (\boldsymbol{\mu} \nabla \Psi) \cdot \boldsymbol{n} = -\tilde{B} \qquad & \text{on } \Gamma_H \\ -\nabla \Psi \times \boldsymbol{n} = \boldsymbol{K} \qquad & \text{on } \Gamma_B. \end{aligned}$$

Analogously, Equations (2.84) and (2.53) along with (2.51) result in

$$-\epsilon_0 \Delta V = \rho_f - \operatorname{div} \boldsymbol{P} = \rho \tag{2.86}$$

Another possibility is the usage of the *magnetic vector potential*, which can be introduced for all regions where a current density $\boldsymbol{j}$ is defined. The more general concept of the magnetic vector potential suffers the disadvantage of an increasing number of unknowns for 3D problems. Therefore, a combination of the scalar potential in current-free regions and the vector potential in other parts proves to be rather efficient. A collection of different potential formulations and their combination can be found in [81].
The introduction of the magnetic vector potential $\boldsymbol{A}$ in simply-connected regions is enabled by Equation (2.54),

$$\boldsymbol{B} = \operatorname{curl} \boldsymbol{A}. \tag{2.87}$$

In this way, (2.54) is automatically satisfied and Ampère's law (2.56) turns into

$$\operatorname{curl}(\boldsymbol{\mu}^{-1} \operatorname{curl} \boldsymbol{A}) = \boldsymbol{j}_f + \hat{\boldsymbol{\epsilon}} \frac{\partial \boldsymbol{E}}{\partial t}. \tag{2.88}$$

Using equation (2.55), we can choose $\boldsymbol{A}$ such that [2]

$$\boldsymbol{E} = -\frac{\partial \boldsymbol{A}}{\partial t}.$$

The above formulation often includes an electric scalar potential, V as well [2, 71], i.e.

$$\boldsymbol{E} = -\frac{\partial \boldsymbol{A}}{\partial t} - \nabla V.$$

In the course of the thesis, however, we use formulations solely based on the magnetic vector potential $\boldsymbol{A}$, neglecting V, e.g. by using a modified vector potential [55].
In summary, we obtain

$$\operatorname{curl}(\boldsymbol{\mu}^{-1} \operatorname{curl} \boldsymbol{A}) + \hat{\boldsymbol{\epsilon}} \frac{\partial^2 \boldsymbol{A}}{\partial t^2} = \boldsymbol{j}_f. \tag{2.89}$$

As described in the previous section, the total free current density may contain the impressed current density $\boldsymbol{j}_I$ (see e.g. [2]),

$$\boldsymbol{j}_f = \hat{\boldsymbol{\sigma}} \boldsymbol{E} + \boldsymbol{j}_I = -\hat{\boldsymbol{\sigma}} \frac{\partial \boldsymbol{A}}{\partial t} + \boldsymbol{j}_I,$$

so that Ampere's law in terms of the magnetic vector potential reads

$$\operatorname{curl}(\boldsymbol{\mu}^{-1} \operatorname{curl} \boldsymbol{A}) + \hat{\boldsymbol{\epsilon}} \frac{\partial^2 \boldsymbol{A}}{\partial t^2} + \hat{\boldsymbol{\sigma}} \frac{\partial \boldsymbol{A}}{\partial t} = \boldsymbol{j}_I, \tag{2.90}$$

and is referred to as the *full Maxwell* system in A-formulation. The corresponding boundary conditions for $\boldsymbol{A}$ are

$$(\boldsymbol{\mu}^{-1} \operatorname{curl} \boldsymbol{A}) \times \boldsymbol{n} = \boldsymbol{K} \qquad \text{on } \Gamma_H, \tag{2.91}$$

$$(\operatorname{curl} \boldsymbol{A}) \cdot \boldsymbol{n} = 0 \quad \text{or} \quad (\operatorname{curl} \boldsymbol{A}) \cdot \boldsymbol{n} = -\tilde{B} \qquad \text{on } \Gamma_B. \tag{2.92}$$

Conditions (2.92) imply that

$$\operatorname{div}(\boldsymbol{A} \times \boldsymbol{n}) = -\tilde{B}$$

and we can define a function $\boldsymbol{a} = \boldsymbol{a}(\boldsymbol{x}, t)$ such that

$$\operatorname{div} \boldsymbol{a} = \tilde{B},$$

and

$$\boldsymbol{n} \times \boldsymbol{A} = \boldsymbol{a}. \tag{2.93}$$

In the time-harmonic case, assuming

$$\begin{aligned} \boldsymbol{j}_I(\boldsymbol{x},t) &= Re(\boldsymbol{j}_I(\boldsymbol{x})e^{i\omega t}), \\ \boldsymbol{A}(\boldsymbol{x},t) &= Re(\boldsymbol{A}(\boldsymbol{x})e^{i\omega t}), \end{aligned}$$

with frequencies ω, the time derivatives in Equation (2.90) can be written as

$$\frac{\partial \boldsymbol{A}}{\partial t} = i\omega \boldsymbol{A} \quad \text{and} \quad \frac{\partial^2 \boldsymbol{A}}{\partial t^2} = -\omega^2 \boldsymbol{A},$$

thus yielding the *full Maxwell system in the frequency domain*,

$$\operatorname{curl}(\boldsymbol{\mu}^{-1} \operatorname{curl} \boldsymbol{A}) + (i\omega\hat{\boldsymbol{\sigma}} - \omega^2\hat{\boldsymbol{\epsilon}})\boldsymbol{A} = \boldsymbol{j}_I. \tag{2.94}$$

Summarizing, this type of problems can be written in the form

$$\operatorname{curl}(\boldsymbol{\mu}^{-1} \operatorname{curl} \boldsymbol{A}) + \boldsymbol{\kappa}\boldsymbol{A} = \boldsymbol{j}_I. \tag{2.95}$$

with $\boldsymbol{\kappa} \in \mathbb{C}^{3\times 3}$. As we have seen before, the case $\omega = 0$, i.e. $\kappa_{ij} = 0$ for all $i, j = 1, ..., 3$, corresponds to the magnetostatic setting and

$$\boldsymbol{\kappa} = i\omega\hat{\boldsymbol{\sigma}} - \omega^2\hat{\boldsymbol{\epsilon}} \tag{2.96}$$

describes the time-harmonic case. For low frequencies ω, the second term in the definition of $\boldsymbol{\kappa}$ can be neglected and we obtain the eddy current or magnetoquasistatic system in the frequency domain,

$$\operatorname{curl}(\boldsymbol{\mu}^{-1}(\operatorname{curl} \boldsymbol{A})) + i\omega\hat{\boldsymbol{\sigma}}\boldsymbol{A} = \boldsymbol{j}_I. \tag{2.97}$$

which is a widely used approximation of the full Maxwell system (see e.g. [3]). Schmidt et al. [100] derived estimates for the modeling error made by choosing the eddy current approximation and showed that the error is strongly influenced by the geometry of the model.
Furthermore, we introduce a third formulation of Ampére's law that can be obtained by applying implicit time stepping methods on Equation (2.90). Depending on the time step τ, the matrix $\boldsymbol{\kappa} \in \mathbb{R}^{3\times 3}_+$ can be approximated by

$$\boldsymbol{\kappa} \approx \frac{1}{\tau}\hat{\boldsymbol{\sigma}} + \frac{1}{\tau^2}\hat{\boldsymbol{\epsilon}}.$$

Summarizing these three cases in a single formulation with $\boldsymbol{\kappa} \in \mathbb{C}^{3\times 3}$ or $\boldsymbol{\kappa} \in \mathbb{R}^{3\times 3}$ and choosing appropriate boundary conditions, the strong form of the electromagnetic problem can be written as

Problem (EM): Find $\boldsymbol{A} : \Omega \to \mathbb{R}^3$ or $\boldsymbol{A} : \Omega \to \mathbb{C}^3$ such that

$$\operatorname{curl}(\boldsymbol{\mu}^{-1} \operatorname{curl} \boldsymbol{A}) + \boldsymbol{\kappa}\boldsymbol{A} = \boldsymbol{j}_I \quad \text{in } \Omega \tag{2.98}$$

holds, together with the Dirichlet boundary condition

$$\boldsymbol{A} \times \boldsymbol{n} = \boldsymbol{0} \quad \text{on } \Gamma_D,$$

and the Neumann boundary condition

$$(\boldsymbol{\mu}^{-1} \operatorname{curl} \boldsymbol{A}) \times \boldsymbol{n} = \boldsymbol{K} \quad \text{on } \Gamma_N.$$

If the domain Ω consists of regions with different materials, additional interface conditions have to specified. Note that the material parameter matrices $\boldsymbol{\mu}$, $\boldsymbol{\sigma}$ and $\hat{\boldsymbol{\epsilon}}$ have different values in different material regions.

In the magnetostatic or eddy current case involving a non-conducting region ($\hat{\boldsymbol{\sigma}} = \mathbf{0}$), the magnetic vector potential is not unique, since

$$\nabla \times (\boldsymbol{A} + \nabla\phi) = \boldsymbol{B}$$

for every scalar field ϕ. The lack of uniqueness can be cured by additionally defining the divergence of $\boldsymbol{A}$, i.e. by setting

$$\nu \operatorname{div} \boldsymbol{A} = 0,$$

according to the *Coulomb gauge*. Ampère's law is then modified through an additional penalization term, e.g. in the quasi-static case [32, 43, 88],

$$\operatorname{curl}(\boldsymbol{\mu}^{-1}(\operatorname{curl} \boldsymbol{A})) - \nabla(\nu \operatorname{div} \boldsymbol{A}) = \boldsymbol{j}_I, \tag{2.99}$$

where ν is a suitable average of the entries of $\boldsymbol{\mu}^{-1}$ [2], and supplemented with the boundary conditions

$$\boldsymbol{A} \cdot \boldsymbol{n} = 0 \quad \text{on } \Gamma_D, \tag{2.100}$$

$$\operatorname{div} \cdot \boldsymbol{A} = 0 \quad \text{on } \Gamma_N. \tag{2.101}$$

Note that in electromagnetic literature, the boundary of the domain Ω is usually decomposed into non-overlapping parts Γ_{PMC} and Γ_{PEC} referring to perfect magnetic conductors and perfect electric conductors, rather than into Γ_D and Γ_N known from the continuum mechanics. In this respect, the boundary condition (2.100) should be prescribed on Γ_H and the condition (2.101) on Γ_B. Yet, in this work, we will keep the usual convention of decomposing into Dirichlet and Neumann boundaries since its usage is more convenient within the framework of magnetoelastic coupling.
Although the gauged formulation of Ampère's law yields a unique solution, the numerical approximation of the equation, of course, involves certain errors in the satisfaction of the Coulomb gauge, especially in regions where the values of the magnetic reluctivity $\boldsymbol{\nu} = \boldsymbol{\mu}^{-1}$ are rather low (e.g. in ferromagnetic regions) [11]. This, in turn, results in errors in fulfilling the equation, which makes the gauged formulation not always suitable for numerical implementation. Alonso Rodriguez and Valli [2] showed that their formulation of an eddy current problem with the above penalization term yields good convergence results using nodal finite elements if the domain Ω is a convex polyhedron (which is mostly satisfied in real-life applications). However, it is worth mentioning that the eddy current model used by these authors involves a modification of the solution by assuming the satisfaction of the Coulomb gauge on the whole problem region containing both conducting and non-conducting domains. We will come back to this issue in Chapter 4, where we adopt the approach offered by Alonso Rodriguez and Valli for the coupled eddy current problem.

On the discrete level, gauging can be avoided by using an alternative formulation based on edge elements, which was introduced, among others, by Bíró [31] and Ren and Ida [98]. Although in this case, the resulting system is singular, one can still obtain satisfactory convergence results with iterative solvers for compatible right-hand sides $\boldsymbol{j}_I$ with $\operatorname{div} \boldsymbol{j}_I = 0$ [2]. In our further considerations of Maxwell's equations, especially for their variational treatment, we will adopt the ungauged formulation and postpone the discussion of the gauged approach to Chapter 4 within the setting of magnetoelastic coupling.

2.2.2 Integral relations in Lipschitz domains

Before deriving the weak formulation of Maxwell's equations, we need to introduce certain integral identities that are valid in Lipschitz domains. This section gives an overview of the important integral relations [87] which follow from Gauss' divergence theorem for

Lipschitz domains (e.g. in [86, 87]).
Let $\Omega \in \mathbb{R}^3$ be a bounded Lipschitz domain with boundary $\partial\Omega$ and its unit outer normal vector $\boldsymbol{n}$. Then, the following identities hold.

(a) For functions $\boldsymbol{u} \in C^1(\Omega)^3$ and $\phi \in C^1(\Omega)$,

$$\int_\Omega \phi \operatorname{div} \boldsymbol{u} \,\mathrm{d}x = -\int_\Omega \nabla\phi \cdot \boldsymbol{u} \,\mathrm{d}x + \int_{\partial\Omega} \phi(\boldsymbol{u}\cdot\boldsymbol{n}) \,\mathrm{d}s. \tag{2.102}$$

(b) *(Green's first identity)* For functions $\phi \in C^1(\Omega)$ and $\psi \in C^2(\Omega)$,

$$\int_\Omega \phi\Delta\psi \,\mathrm{d}x = -\int_\Omega \nabla\psi\nabla\phi \,\mathrm{d}x + \int_{\partial\Omega} \phi(\nabla\psi\cdot\boldsymbol{n}) \,\mathrm{d}s. \tag{2.103}$$

(c) *(Green's second identity)* For functions $f, g \in C^2(\Omega)$,

$$\int_\Omega f\Delta g - g\Delta f \,\mathrm{d}x = \int_{\partial\Omega} f(\nabla g\cdot\boldsymbol{n}) - g(\nabla f\cdot\boldsymbol{n}) \,\mathrm{d}s. \tag{2.104}$$

(d) For functions $\boldsymbol{u}, \boldsymbol{v} \in C^1(\Omega)^3$,

$$\int_\Omega \boldsymbol{v}\cdot(\operatorname{curl}\boldsymbol{u}) \,\mathrm{d}x = \int_\Omega \boldsymbol{u}\cdot(\operatorname{curl}\boldsymbol{v}) \,\mathrm{d}x + \int_{\partial\Omega} \boldsymbol{v}\cdot(\boldsymbol{u}\times\boldsymbol{n}) \,\mathrm{d}s. \tag{2.105}$$

Equations (2.102) and (2.105) can be extended to cover functions in Sobolev spaces using appropriate density arguments [87].

2.2.3 Energy of electromagnetic fields

In this section, we briefly introduce the concept of energy in electromagnetic systems. Consider a coil flown with the line current I (charge per unit time passing through the wire) generating a magnetic field with flux density $\boldsymbol{B}$. The flux of the magnetic field through a surface $\mathcal{S}$ with outer normal vector $\boldsymbol{n}$ is given by

$$\Phi = \int_{\mathcal{S}} \boldsymbol{B}\cdot\boldsymbol{n} \,\mathrm{d}x, \tag{2.106}$$

and is proportional to the current,

$$\Phi = LI. \tag{2.107}$$

The proportionality constant L (depending on the geometry of the loop of wire) is the *self-inductance* of the wire. The so-called *electromotive force* induced in the coil is given by

$$\mathrm{E} = -L\frac{\mathrm{d}I}{\mathrm{d}t},$$

so the *total work* per unit time (against this force) can be expressed as

$$\frac{\partial W_m}{\partial t} = -\mathrm{E}I = LI\frac{\mathrm{d}I}{dt}.$$

Hence,

$$W_m = \frac{1}{2}LI^2. \tag{2.108}$$

The magnetic flux (2.106) through a surface $\mathcal{S}$ bounded by the curve $\mathcal{L}$ can also be expressed in terms of the magnetic vector potential $\boldsymbol{A}$ as

$$\Phi = \int_{\mathcal{S}} \boldsymbol{B} \cdot \boldsymbol{n} \, \mathrm{d}s = \int_{\mathcal{S}} (\operatorname{curl} \boldsymbol{A}) \cdot \boldsymbol{n} \, \mathrm{d}s = \int_{\mathcal{L}} \boldsymbol{A} \cdot \mathrm{d}\boldsymbol{l}.$$

Using now Equation (2.107), the total work has the form

$$W_m = \frac{1}{2} \int_{\mathcal{L}} (\boldsymbol{A} I) \cdot \mathrm{d}\boldsymbol{l}.$$

Passing on from line currents I to volume currents $\boldsymbol{j}$ for the magnetic domain Ω, we obtain

$$W_m = \frac{1}{2} \int_{\Omega} (\boldsymbol{A} \cdot \boldsymbol{j}) \, \mathrm{d}x. \tag{2.109}$$

Inserting Ampère's law (2.56) yields in the static case

$$W_m = \frac{1}{2\mu_0} \int_{\Omega} \boldsymbol{A} \cdot (\operatorname{curl} \boldsymbol{B}) \, \mathrm{d}x.$$

Using the identity

$$\operatorname{div}(\boldsymbol{A} \times \boldsymbol{B}) = \boldsymbol{B} \cdot (\operatorname{curl} \boldsymbol{A}) - \boldsymbol{A} \cdot (\operatorname{curl} \boldsymbol{B}),$$

and integration by parts, the total energy can be written as

$$W_m = \frac{1}{2\mu_0} \left[\int_{\Omega} \boldsymbol{B} \cdot \boldsymbol{B} \, \mathrm{d}x - \int_{\partial\Omega} \boldsymbol{A} \cdot (\boldsymbol{B} \times \boldsymbol{n}) \, \mathrm{d}s \right], \tag{2.110}$$

where $\partial\Omega$, as usual, denotes the boundary of Ω with normal vector $\boldsymbol{n}$.
Choosing a larger domain of integration in (2.109) does not change the value of W_m as the current density $\boldsymbol{j}$ is zero outside Ω. Yet, increasing the integration domain in (2.110) should result in a larger volume integral as the integrand is positive. In order for W_m to stay constant, this would imply a decreasing boundary integral. In the limit, this consideration yields

$$W_m = \frac{1}{2\mu_0} \int_{\Omega} \boldsymbol{B} \cdot \boldsymbol{B} \, \mathrm{d}x,$$

which is the amount of energy *stored in a magnetic field*. In materials with a magnetization $\boldsymbol{M}$, the constitutive relation

$$\frac{1}{\mu_0} \boldsymbol{B} = \boldsymbol{H} + \boldsymbol{M},$$

can be used to express the stored energy in terms of $\boldsymbol{B}$, $\boldsymbol{H}$ and $\boldsymbol{M}$ as

$$W_m = \frac{1}{2} \int_{\Omega} \boldsymbol{H} \cdot \boldsymbol{B} \, \mathrm{d}x + \frac{1}{2} \int_{\Omega} \boldsymbol{M} \cdot \boldsymbol{B} \, \mathrm{d}x.$$

Since in linear materials, the magnetization is proportional to the magnetic field, i.e.

$$\boldsymbol{M} = \boldsymbol{\chi}_m \boldsymbol{H},$$

we obtain

$$W_m = \frac{1}{2} \int_{\Omega} (\boldsymbol{\mu}_r \boldsymbol{H}) \cdot \boldsymbol{B} \, \mathrm{d}x.$$

A similar approach can be used for the electrostatic energy [62], yielding

$$W_e = \frac{1}{2}\int_\Omega \boldsymbol{D}\cdot\boldsymbol{E}\,\mathrm{d}x + \frac{1}{2}\int_\Omega \boldsymbol{P}\cdot\boldsymbol{E}\,\mathrm{d}x,$$

where $\boldsymbol{P}$ is the electric polarization. Again, for linear media, the energy stored in a static electric field can be written as

$$W_e = \frac{1}{2}\int_\Omega (\boldsymbol{\epsilon}_r^{-1}\boldsymbol{D})\cdot\boldsymbol{E}\,\mathrm{d}x.$$

Hence, the total (potential) energy stored in an electromagnetic field in the absence of magnetization and electric polarization is

$$W_{em} = \frac{1}{2}\int_\Omega (\boldsymbol{H}\cdot\boldsymbol{B} + \boldsymbol{D}\cdot\boldsymbol{E})\,\mathrm{d}x.$$

In the electrodynamic case we have to consider the work done by the electromagnetic forces on moving charges q. For a charge q moving an amount $\mathrm{d}\boldsymbol{l} = \boldsymbol{v}\mathrm{d}t$ with velocity $\boldsymbol{v}$, Lorentz' force law (2.50) yields

$$\mathrm{d}W = dW_e + dW_m = \boldsymbol{F}\cdot\mathrm{d}\boldsymbol{l} = q(\boldsymbol{E}+\boldsymbol{v}\times\boldsymbol{B})\cdot\boldsymbol{v}\,\mathrm{d}t = q\boldsymbol{E}\cdot\boldsymbol{v}. \tag{2.111}$$

Note that

$$\mathrm{d}W_m = \boldsymbol{F}_m\cdot\mathrm{d}\boldsymbol{l} = q(\boldsymbol{v}\times\boldsymbol{B})\cdot\boldsymbol{v}\,\mathrm{d}t = 0,$$

implying that magnetic forces do no work. Now inserting the relations $q = \rho\,\mathrm{d}x$ and $\rho\boldsymbol{v} = \boldsymbol{j}$ into Equation (2.111), we conclude that

$$\frac{\mathrm{d}W}{\mathrm{d}t} = \int_\Omega \boldsymbol{E}\cdot\boldsymbol{j}\,\mathrm{d}x.$$

Ampère's law (2.49),

$$\boldsymbol{E}\cdot(\operatorname{curl}\boldsymbol{B}) = \mu_0\left(\boldsymbol{E}\cdot\boldsymbol{j} + \epsilon_0\boldsymbol{E}\cdot\frac{\partial\boldsymbol{E}}{\partial t}\right),$$

together with the identity

$$\boldsymbol{E}\cdot(\operatorname{curl}\boldsymbol{B}) = \boldsymbol{B}\cdot(\operatorname{curl}\boldsymbol{E}) - \operatorname{div}(\boldsymbol{E}\times\boldsymbol{B}),$$

turn Faraday's law (2.55) into

$$\int_\Omega \boldsymbol{E}\cdot\boldsymbol{j}\,\mathrm{d}x = \int_\Omega \frac{1}{\mu_0}\boldsymbol{B}\left(-\frac{\partial\boldsymbol{B}}{\partial t}\right)\mathrm{d}x - \int_\Omega \frac{1}{\mu_0}\nabla\cdot(\boldsymbol{E}\times\boldsymbol{B})\,\mathrm{d}x - \int_\Omega \epsilon_0\boldsymbol{E}\frac{\partial\boldsymbol{E}}{\partial t}\,\mathrm{d}x.$$

In a final step, we apply Gauss' integral formula and the product rule,

$$\frac{\mathrm{d}W}{\mathrm{d}t} = -\frac{1}{2}\frac{\partial}{\partial t}\left[\int_\Omega \frac{1}{\mu_0}\boldsymbol{B}\cdot\boldsymbol{B}\,\mathrm{d}x + \int_\Omega \epsilon_0\boldsymbol{E}\cdot\boldsymbol{E}\,\mathrm{d}x\right] - \frac{1}{\mu_0}\int_{\partial\Omega}\boldsymbol{E}\cdot(\boldsymbol{B}\times\boldsymbol{n})\,\mathrm{d}s.$$

Inserting the following relations for linear media,

$$\begin{aligned}\frac{1}{\mu_0}\boldsymbol{B} &= \boldsymbol{\mu}_r\boldsymbol{H},\\ \epsilon_0\boldsymbol{E} &= \boldsymbol{\epsilon}_r^{-1}\boldsymbol{D},\end{aligned}$$

the energy conservation equation can be derived,

$$\frac{\mathrm{d}W}{\mathrm{d}t} = -\frac{\mathrm{d}}{\mathrm{d}t}\int_\Omega \frac{1}{2}\left((\boldsymbol{\mu}_r\boldsymbol{H})\cdot\boldsymbol{B} + (\boldsymbol{\epsilon}_r^{-1}\boldsymbol{D})\cdot\boldsymbol{E}\right)\,\mathrm{d}x - \frac{1}{\mu_0}\int_{\partial\Omega}\boldsymbol{E}\cdot(\boldsymbol{B}\times\boldsymbol{n})\,\mathrm{d}s. \tag{2.112}$$

The first integral characterizes the total energy stored in the electromagnetic field, while the surface integral gives the amount of energy flowing through the bounding surface $\partial\Omega$ of Ω with normal vector $\boldsymbol{n}$. Note that the integrand is reformulated into

$$\boldsymbol{E}\cdot(\boldsymbol{B}\times\boldsymbol{n}) = (\boldsymbol{E}\times\boldsymbol{B})\cdot\mathrm{d}\boldsymbol{s},$$

where $\boldsymbol{S} := \boldsymbol{E}\times\boldsymbol{B}$ is the *Poynting vector* describing the energy flux density [62].

2.2.4 Weak formulation of Maxwell's equations

As we have seen in Section 2.2.1, the usage of a potential approach reduces the set of Maxwell's equations to a single partial differential equation with a convenient structure. On the one hand, the scalar potential approach leads to a Poisson equation which is well-known and thus not of particular interest for numerical investigation. On the other hand, the usage of such a potential is limited to static problems in current-free regions, which is why the vector potential approach is more common in electromagnetic literature. In this section, we will deal with weak formulations of Equation (2.95) for different settings depending on the parameter matrix $\boldsymbol{\kappa}$, following [101]. In this context, the existence and uniqueness of the weak solution will be discussed and appropriate function spaces will be introduced.

Consider now a bounded domain $\Omega \subset \mathbb{R}^3$ with a Lipschitz boundary $\partial\Omega = \overline{\Gamma}_D \cup \overline{\Gamma}_N$, $\Gamma_D \cap \Gamma_N = \varnothing$ with outer (unit) normal vector $\boldsymbol{n}$ and the equation

$$\operatorname{curl}(\boldsymbol{\mu}^{-1}\operatorname{curl}\boldsymbol{A}) + \boldsymbol{\kappa}\boldsymbol{A} = \boldsymbol{j}_I. \tag{2.113}$$

for $\boldsymbol{\kappa} \in \mathbb{C}^{3\times3}$. Multiplying this equation with appropriate test functions $\tilde{\boldsymbol{A}}$ (the corresponding function spaces will be discussed after the derivation of the weak form) and integrating over Ω yields for all $\tilde{\boldsymbol{A}}$,

$$\int_\Omega \operatorname{curl}(\boldsymbol{\mu}^{-1}\operatorname{curl}\boldsymbol{A})\cdot\tilde{\boldsymbol{A}} + \boldsymbol{\kappa}\boldsymbol{A}\cdot\tilde{\boldsymbol{A}}\,\mathrm{d}x = \int_\Omega \boldsymbol{j}_I\cdot\tilde{\boldsymbol{A}}\,\mathrm{d}x.$$

Using integration by parts,

$$\int_\Omega \operatorname{curl}(\boldsymbol{\mu}^{-1}\operatorname{curl}\boldsymbol{A})\cdot\tilde{\boldsymbol{A}}\,\mathrm{d}x = \int_\Omega (\boldsymbol{\mu}^{-1}\operatorname{curl}\boldsymbol{A})\cdot(\operatorname{curl}\tilde{\boldsymbol{A}})\,\mathrm{d}x - \int_{\partial\Omega}\left((\boldsymbol{\mu}^{-1}\operatorname{curl}\boldsymbol{A})\times\boldsymbol{n}\right)\cdot\tilde{\boldsymbol{A}}\,\mathrm{d}s,$$

we obtain

$$\int_\Omega (\boldsymbol{\mu}^{-1}\operatorname{curl}\boldsymbol{A})\cdot(\operatorname{curl}\tilde{\boldsymbol{A}}) + \boldsymbol{\kappa}\boldsymbol{A}\cdot\tilde{\boldsymbol{A}}\,\mathrm{d}x - \int_{\partial\Omega}\left(\boldsymbol{\mu}^{-1}\operatorname{curl}\boldsymbol{A}\times\boldsymbol{n}\right)\cdot\tilde{\boldsymbol{A}}\,\mathrm{d}s = \int_\Omega \boldsymbol{j}_I\cdot\tilde{\boldsymbol{A}}\,\mathrm{d}x \tag{2.114}$$

The boundary integral corresponds to the condition

$$(\boldsymbol{\mu}^{-1}\operatorname{curl}\boldsymbol{A})\times\boldsymbol{n} = \boldsymbol{K} \quad \text{on } \Gamma_N \tag{2.115}$$

i.e. the tangential component of the magnetic field $\boldsymbol{H} = \boldsymbol{\mu}^{-1}\operatorname{curl}\boldsymbol{A}$ is known on the Neumann boundary. Possible Dirichlet boundary conditions for $\boldsymbol{A}$ and its test functions $\tilde{\boldsymbol{A}}$ are

$$\boldsymbol{A}\times\boldsymbol{n} = \boldsymbol{0}, \qquad \tilde{\boldsymbol{A}}\times\boldsymbol{n} = \boldsymbol{0} \quad \text{on } \Gamma_D, \tag{2.116}$$

and thus $\boldsymbol{B} \cdot \boldsymbol{n} = \operatorname{curl} \boldsymbol{A} \cdot \boldsymbol{n} = 0$. Summing up, the weak formulation of the problem is

Problem $(EM)^w$: Find $\boldsymbol{A}$ with $\boldsymbol{A} \times \boldsymbol{n} = \boldsymbol{0}$ on Γ_D such that

$$\int_\Omega (\boldsymbol{\mu}^{-1} \operatorname{curl} \boldsymbol{A}) \cdot (\operatorname{curl} \tilde{\boldsymbol{A}}) + \boldsymbol{\kappa} \boldsymbol{A} \cdot \tilde{\boldsymbol{A}} \, \mathrm{d}x = \int_{\partial\Omega} \boldsymbol{K} \cdot \tilde{\boldsymbol{A}} \, \mathrm{d}s + \int_\Omega \boldsymbol{j}_I \cdot \tilde{\boldsymbol{A}} \, \mathrm{d}x \tag{2.117}$$

holds for all $\tilde{\boldsymbol{A}}$ with $\tilde{\boldsymbol{A}} \times \boldsymbol{n} = \boldsymbol{0}$ on Γ_D. Note that as $\boldsymbol{K} = (\boldsymbol{\mu}^{-1} \nabla \times \boldsymbol{A}) \times \boldsymbol{n}$ is orthogonal to the normal vector $\boldsymbol{n}$, the integrand of the surface integral can also be written as

$$\tilde{\boldsymbol{A}} \cdot ((\boldsymbol{\mu}^{-1} \operatorname{curl} \boldsymbol{A}) \times \boldsymbol{n}) = \tilde{\boldsymbol{A}}_t \cdot ((\boldsymbol{\mu}^{-1} \operatorname{curl} \boldsymbol{A}) \times \boldsymbol{n}),$$

i.e. only the tangential component $\tilde{\boldsymbol{A}}_t = \boldsymbol{n} \times \tilde{\boldsymbol{A}} \times \boldsymbol{n}$ of $\tilde{\boldsymbol{A}}$ affects the Neumann integral.

2.2.5 Function spaces and weak differential operators

So far, the function space of $\boldsymbol{A}$ and $\tilde{\boldsymbol{A}}$ has not been specified for the above problem. For this purpose, we need the definition of weak differential operators with distributional derivatives.
Consider functions $w \in L^2(\Omega)$ and $\boldsymbol{u}, \boldsymbol{v} \in L^2(\Omega)^3$. Then, $\nabla w \in L^2(\Omega)^3$ is called the *weak gradient*, $\operatorname{div} \boldsymbol{v} \in L^2(\Omega)$ is called the *weak divergence* and $\operatorname{curl} \boldsymbol{u} \in L^2(\Omega)^3$ the *weak curl* if the following relations hold for all $\boldsymbol{f} \in (C_0^\infty(\Omega))^3$ and $g \in C_0^\infty(\Omega)$,

$$\int_\Omega \nabla w \cdot \boldsymbol{f} \, \mathrm{d}x = -\int_\Omega w \operatorname{div} \boldsymbol{f} \, \mathrm{d}x, \tag{2.118}$$

$$\int_\Omega (\operatorname{div} \boldsymbol{v}) g \, \mathrm{d}x = -\int_\Omega \boldsymbol{v} \cdot \nabla g \, \mathrm{d}x, \tag{2.119}$$

$$\int_\Omega \operatorname{curl} \boldsymbol{u} \cdot \boldsymbol{f} \, \mathrm{d}x = \int_\Omega \boldsymbol{u} \cdot \operatorname{curl} \boldsymbol{f} \, \mathrm{d}x. \tag{2.120}$$

On the basis of the above definitions, we are now able to introduce the following function spaces. The function space

$$H(\operatorname{div}, \Omega) := \{\boldsymbol{w} \in (L^2(\Omega))^3 \mid \operatorname{div} \boldsymbol{w} \in L^2(\Omega)\}$$

is the completion of $C^\infty(\Omega)^3$ with respect to the norm

$$\|\boldsymbol{w}\|_{H(\operatorname{div},\Omega)} := \left(\|\boldsymbol{w}\|_{\boldsymbol{0}}^2 + \|\operatorname{div} \boldsymbol{w}\|_0^2\right)^{\frac{1}{2}},$$

where $\|\cdot\|_0$ and $\|\cdot\|_{\boldsymbol{0}}$ denotes the norms in L^2 and $L^2(\Omega)^3$, respectively. $H(\operatorname{div}, \Omega)$ is a Hilbert space itself and obviously

$$H^1(\Omega)^3 \subset H(\operatorname{div}, \Omega) \subset L^2(\Omega)^3.$$

In addition, we define the space

$$H_0(\operatorname{div}, \Omega) := \{\boldsymbol{w} \in H(\operatorname{div}, \Omega) \mid \boldsymbol{w} \cdot \boldsymbol{n} = 0 \text{ on } \partial\Omega\}$$

as the space of all functions in $H(\operatorname{div}, \Omega)$ whose normal component vanishes on the boundary $\partial\Omega$. The space $H_0(\operatorname{div}, \Omega)$ is the closure of $C_0^\infty(\Omega)^3$ under the $\|\cdot\|_{H(\operatorname{div},\Omega)}$ - norm (see e.g. [87]). If Dirichlet boundary conditions are prescribed on a part of the boundary, the corresponding space can be defined as

$$H_\Gamma(\operatorname{div}, \Omega) := \{\boldsymbol{w} \in H(\operatorname{div}, \Omega) \mid \boldsymbol{w} \cdot \boldsymbol{n} = 0 \text{ on } \Gamma_D\},$$

with $\boldsymbol{n}$, as usual, denoting the outer normal on the boundary Γ_D. If we define the space

$$X^{\mathrm{div}} := \{\boldsymbol{w} \in C^\infty(\Omega)^3 \mid \boldsymbol{w} \cdot \boldsymbol{n} = 0 \text{ on } \Gamma_D\},$$

then $H_\Gamma(\mathrm{div}, \Omega)$ is the closure of X^{div} with respect to the $\|\cdot\|_{H(\mathrm{div},\Omega)}$-norm. For a proof, refer e.g. to [87].
Similarly, we can define the closure of the space

$$X^{\mathrm{curl}} := \{\boldsymbol{w} \in C^\infty(\Omega)^3 \mid \boldsymbol{w} \times \boldsymbol{n} = \boldsymbol{0} \text{ on } \Gamma_D\},$$

with respect to the $\|\cdot\|_{H(\mathrm{curl},\Omega)}$-norm, which yields the Hilbert space

$$H(\mathrm{curl}, \Omega) := \{\boldsymbol{w} \in (L^2(\Omega))^3 \mid \mathrm{curl}\, \boldsymbol{w} \in L^2(\Omega)^3\},$$

equipped with the norm

$$\|\boldsymbol{w}\|_{H(\mathrm{curl},\Omega)} := \left(\|\boldsymbol{w}\|_{\boldsymbol{0}}^2 + \|\mathrm{curl}\, \boldsymbol{w}\|_{\boldsymbol{0}}^2\right)^{\frac{1}{2}}.$$

This space is of particular importance as it corresponds to the space of finite energy solutions to Maxwell's equations. We can limit the space so that the Dirichlet boundary condition $\boldsymbol{A} \times \boldsymbol{n} = \boldsymbol{0}$ is satisfied, obtaining the Hilbert space

$$H_\Gamma(\mathrm{curl}, \Omega) := \{\boldsymbol{w} \in H(\mathrm{curl}, \Omega) \mid \boldsymbol{w} \times \boldsymbol{n} = \boldsymbol{0} \text{ on } \Gamma_D\}.$$

Note that we assume the existence of the partial derivatives in the distributional sense in the above definitions.
So far, we are only concerned with the function spaces $H(\mathrm{curl}, \Omega)$ and $H_\Gamma(\mathrm{curl}, \Omega)$. The function space $H(\mathrm{div}, \Omega)$ and its subspaces will come into play when using the gauged formulation, see Chapter 4.

An important connection between the spaces $H(\mathrm{div}, \Omega)$ and $H(\mathrm{curl}, \Omega)$ is given by the following exact sequence for a simply connected domain $\Omega \subset \mathbb{R}^3$, which is called *De Rham - complex* (see e.g. [12] or [101]):

$$\mathbb{R} \hookrightarrow H^1(\Omega) \xrightarrow{\nabla} H(\mathrm{curl}, \Omega) \xrightarrow{\mathrm{curl}} H(\mathrm{div}, \Omega) \xrightarrow{\mathrm{div}} L^2(\Omega) \to 0.$$

Hence, every divergence-free vector field in the space $H(\mathrm{div}, \Omega)$ can be considered as the curl of another vector field in $H(\mathrm{curl}, \Omega)$. The corresponding De Rham complex for homogeneous boundary conditions is

$$0 \hookrightarrow H_0^1(\Omega) \xrightarrow{\nabla} H_0(\mathrm{curl}, \Omega) \xrightarrow{\mathrm{curl}} H_0(\mathrm{div}, \Omega) \xrightarrow{\mathrm{div}} L^2(\Omega) \to \mathbb{R}\,.$$

Note that the hook arrow $\hookrightarrow$ indicates a monomorphism.

Returning to the (ungauged) Ampère's law, we can now state the complete weak formulation of the problem including the appropriate function spaces:

Problem $(EM)^w$: Find $\boldsymbol{A} \in H_\Gamma(\mathrm{curl}, \Omega)$, such that

$$\int_\Omega (\boldsymbol{\mu}^{-1} \mathrm{curl}\, \boldsymbol{A}) \cdot \mathrm{curl}\, \tilde{\boldsymbol{A}} + \boldsymbol{\kappa} \boldsymbol{A} \cdot \tilde{\boldsymbol{A}}\, \mathrm{d}x - \int_{\partial\Omega} \boldsymbol{K} \cdot \tilde{\boldsymbol{A}}\, \mathrm{d}s = \int_\Omega \boldsymbol{j}_I \cdot \tilde{\boldsymbol{A}}\, \mathrm{d}x \tag{2.121}$$

holds for all $\tilde{\boldsymbol{A}} \in H_\Gamma(\mathrm{curl}, \Omega)$.
Note that, depending on the setting, the vector potential is real-valued, $\boldsymbol{A} : \Omega \to \mathbb{R}^3$ (magnetostatic case or system obtained from implicit time stepping methods) or complex-valued, $\boldsymbol{A} : \Omega \to \mathbb{C}^3$ (eddy current system or full Maxwell system in the frequency domain). Thus, the above-defined function spaces refer to the $L^2(\Omega)^3$ space over the fields $\mathbb{R}^3$ or $\mathbb{C}^3$. However, as it is not common to specify the field in the definition of these spaces, we will use the same notation for the real and complex cases, assuming that the choice of the corresponding space is clear from the context of the problem.

2.2.6 Differential operators on surfaces

To define tangential boundary conditions for elements of the space $H(\mathrm{curl}, \Omega)$, we have to set up some general preliminaries concerning differential operators on a surface. The following definitions hold for a bounded domain Ω with a C^2-boundary $\Gamma = \partial\Omega$ but can be extended to cover the case of a Lipschitz domain [26]. Instead of considering the whole boundary Γ, it is possible to reduce it to a C^2-surface or a Lipschitz continuous surface $\Sigma \subset \Gamma$. Let

$$L_t^2(\Gamma) := \{\boldsymbol{u} \in (L^2(\Gamma))^3 \mid \boldsymbol{u} \cdot \boldsymbol{n} = 0\}$$

denote the space of surface tangential vector fields in $L^2(\Gamma)$ together with the standard $L^2(\Gamma)$-norm. The surface gradient of a function $f \in H^1(\Gamma)$ can be defined by a parametric representation of Γ [87]. Writing $\boldsymbol{x} \in \Gamma$ as

$$\boldsymbol{x} = (x_1(u_1, u_2), x_2(u_1, u_2), x_3(u_1, u_2)),^T$$

the surface gradient $\nabla_\Gamma : H^{\frac{1}{2}}(\Gamma) \to L_t^2(\Gamma)$ can be defined by

$$\nabla_\Gamma f = \sum_{i,j=1}^{2} g_{ij} \frac{\partial f}{\partial u_i} \frac{\partial x}{\partial u_j},$$

with g_{ij} being the entries of the inverse of the matrix G given by

$$G_{ij} = \frac{\partial x}{\partial u_i} \frac{\partial x}{\partial u_j}$$

for $i, j = 1, 2$. Furthermore, by duality, we can introduce the adjoint operators

$$\mathrm{div}_\Gamma : L_t^2(\Gamma) \to H^{-\frac{1}{2}}(\Gamma)$$

and

$$\mathrm{curl}_\Gamma : L_t^2(\Gamma) \to H^{-\frac{1}{2}}(\Gamma),$$

as well as

$$\mathbf{curl}_\Gamma : H^{\frac{1}{2}}(\Gamma) \to L_t^2(\Gamma).$$

Note that the negative superscript characterizes the dual space of $H^{\frac{1}{2}}(\Gamma)$.
For a function $\boldsymbol{u} \in L_t^2(\Gamma)$, the *surface divergence* $\mathrm{div}_\Gamma \boldsymbol{u}$ satisfies

$$\int_\Gamma (\mathrm{div}_\Gamma \boldsymbol{u}) f \, \mathrm{d}s = -\int_\Gamma \nabla_\Gamma f \, \mathrm{d}s,$$

for all $f \in H^{\frac{1}{2}}(\Gamma)$ and the *surface vector curl* of a function $f \in H^{\frac{1}{2}}(\Gamma)$ is defined by

$$\mathbf{curl}_\Gamma f := \nabla_\Gamma f \times \boldsymbol{u} \quad \text{for} \quad \boldsymbol{u} \in L_t^2(\Gamma)$$

(hence it is just the rotated gradient of the function f). The *surface scalar curl* can be defined using Stokes' theorem,

$$\int_\Gamma (\mathrm{curl}_\Gamma \boldsymbol{u}) f \, \mathrm{d}s = \int_\Gamma \boldsymbol{u} \cdot (\mathbf{curl}_\Gamma f) \, \mathrm{d}s \quad \forall f \in H^{\frac{1}{2}}(\Gamma).$$

Note that the integrals are meant as duality pairings. For the above-defined operators, the following relations hold for a function $\boldsymbol{u} \in L_t^2(\Gamma)$:

$$\begin{aligned} \mathrm{curl}_\Gamma \boldsymbol{u} &= -\mathrm{div}_\Gamma(\boldsymbol{u} \times \boldsymbol{u}), \\ \mathrm{div}_\Gamma \boldsymbol{u} &= \mathrm{curl}_\Gamma(\boldsymbol{u} \times \boldsymbol{u}). \end{aligned}$$

Finally, the *surface Laplacian*

$$\Delta_\Gamma : H^{\frac{1}{2}}(\Gamma) \to H^{-\frac{1}{2}}(\Gamma)$$

of a function $f \in H^{\frac{1}{2}}(\Gamma)$ is defined by

$$\Delta_\Gamma f := \mathrm{div}_\Gamma(\nabla_\Gamma f) = -\mathrm{curl}_\Gamma(\mathbf{curl}_\Gamma f).$$

2.2.7 Traces of $H(\mathrm{div})$ and $H(\mathrm{curl})$

In this section, we briefly present appropriate function spaces for the generalized boundary values $\tilde{\boldsymbol{A}}\times\boldsymbol{n}$ and $\tilde{\boldsymbol{A}}\cdot\boldsymbol{n}$. As we have seen in Section 2.1.4, the elastic Dirichlet boundary data $\boldsymbol{u}_0$ were elements of the trace space $H^{\frac{1}{2}}(\Gamma_D)^3$ corresponding to the Sobolev spaces $H^1(\Omega)^3$. Similar traces can be defined for functions in $C(\overline{\Omega})^3 \cap H(\mathrm{div},\Omega)$ and $C(\overline{\Omega})^3 \cap H(\mathrm{curl},\Omega)$ for a bounded Lipschitz domain Ω. The *trace theorems* (e.g. in [87, 101]) state that

(a) For a function $\boldsymbol{u} \in C(\overline{\Omega})^3 \cap H(\mathrm{div},\Omega)$ there exists a unique continuous operator $\gamma_n : H(\mathrm{div},\Omega) \to H^{-\frac{1}{2}}(\Gamma)$ with the property

$$\gamma_n \boldsymbol{u}(\boldsymbol{x}) = \boldsymbol{u}(\boldsymbol{x}) \cdot \boldsymbol{n}(\boldsymbol{x}) \quad \forall \boldsymbol{x} \in \Gamma.$$

(b) For a function $\boldsymbol{u} \in C(\overline{\Omega})^3 \cap H(\mathrm{curl},\Omega)$ there exists a unique continuous operator $\boldsymbol{\gamma_t} : H(\mathrm{curl},\Omega) \to H^{-\frac{1}{2}}(\Gamma)^3$ satisfying

$$\boldsymbol{\gamma_t} \boldsymbol{u}(\boldsymbol{x}) = \boldsymbol{u}(\boldsymbol{x}) \times \boldsymbol{n}(\boldsymbol{x}) \quad \forall \boldsymbol{x} \in \Gamma.$$

In contrast to γ_n, the trace operator $\boldsymbol{\gamma_t}$ for $H(\mathrm{curl},\Omega)$ is not surjective. Since $(\boldsymbol{A}\times\boldsymbol{n})\cdot\boldsymbol{n} = 0$, the functions $\boldsymbol{\gamma_t}\boldsymbol{A}$ are elements of the space

$$H_t^{-\frac{1}{2}}(\Gamma)^3 := \{\boldsymbol{s} \in H^{-\frac{1}{2}}(\Gamma)^3 \mid \boldsymbol{s}\cdot\boldsymbol{n} = 0 \text{ on } \Gamma\}.$$

Hence, not all elements of $H^{-\frac{1}{2}}(\Gamma)^3$ are tangential to Γ, as the trace map $\boldsymbol{\gamma_t}$ requires. A way out of this problem is to reduce the codomain of the tangential trace map to the space of tangential traces $\boldsymbol{v}\times\boldsymbol{n}|_\Gamma$ on Γ for a function $\boldsymbol{v} \in H(\mathrm{curl},\Omega)$,

$$H^{-\frac{1}{2}}(\mathrm{div},\Gamma) := \{\boldsymbol{u} \in H_t^{-\frac{1}{2}}(\Gamma)^3 \mid \mathrm{div}_\Gamma \boldsymbol{u} \in H^{-\frac{1}{2}}(\Gamma)\},$$

where div_Γ denotes the surface divergence on Γ defined in Section 2.2.6. This space is a Hilbert space with the graph norm

$$\|\boldsymbol{u}\|_{H^{-\frac{1}{2}}(\mathrm{div},\Gamma)} := \left(\|\boldsymbol{u}\|^2_{H_t^{-\frac{1}{2}}(\Gamma)^3} + \|\mathrm{div}_\Gamma \boldsymbol{u}\|^2_{H^{-\frac{1}{2}}(\Gamma)}\right)^2$$

and the trace map

$$\boldsymbol{\gamma_t^*} : H(\mathrm{curl},\Omega) \to H^{-\frac{1}{2}}(\mathrm{div},\Gamma)$$

is surjective. For details and a proof, refer to [87]. Note that for a smooth boundary Γ (or a smooth surface $\Sigma \subset \Gamma$), the space $H_t^{-\frac{1}{2}}(\Gamma)^3$ is equal to the space [2]

$$H_x^{\frac{1}{2}}(\Gamma)^3 := \{(\boldsymbol{v}\times\boldsymbol{n})|_\Gamma \mid \boldsymbol{v} \in H^1(\Omega)^3\},$$

as well as to

$$H_T^{-\frac{1}{2}}(\Gamma)^3 := \{(\boldsymbol{n}\times\boldsymbol{v}\times\boldsymbol{n})|_\Gamma \mid \boldsymbol{v} \in H^1(\Omega)^3\}.$$

The dual space of $H^{-\frac{1}{2}}(\mathrm{div},\Gamma)$ is the space of all tangential components $(\boldsymbol{n}\times\boldsymbol{v}\times\boldsymbol{n})|_\Gamma$ for a vector $\boldsymbol{v} \in H(\mathrm{curl},\Omega)$ given by

$$H^{-\frac{1}{2}}(\mathrm{curl},\Gamma) := \{\boldsymbol{u} \in H_x^{-\frac{1}{2}}(\Gamma)^3 \mid \mathrm{curl}_\Gamma \boldsymbol{u} \in H^{-\frac{1}{2}}(\Gamma)\},$$

with the graph norm

$$\|\boldsymbol{u}\|_{H^{-\frac{1}{2}}(\mathrm{curl},\Gamma)} := \left(\|\boldsymbol{u}\|^2_{H_x^{-\frac{1}{2}}(\Gamma)^3} + \|\mathrm{curl}_\Gamma \boldsymbol{u}\|^2_{H^{-\frac{1}{2}}(\Gamma)}\right)^{\frac{1}{2}}.$$

The spaces $H^{-\frac{1}{2}}(\mathrm{div},\Gamma)$ and $H^{-\frac{1}{2}}(\mathrm{curl},\Gamma)$ are Hilbert spaces [87]. Moreover, the trace map

$$\boldsymbol{\gamma_T} : H(\mathrm{curl},\Omega) \to H^{-\frac{1}{2}}(\mathrm{curl},\Gamma),$$

is well-defined. Notice that $\boldsymbol{u} \in H^{-\frac{1}{2}}(\mathrm{curl},\Gamma)$ holds if and only if $(\boldsymbol{u}\times\boldsymbol{n}) \in H^{-\frac{1}{2}}(\mathrm{div},\Gamma)$, and

$$\mathrm{div}_\Gamma(\boldsymbol{u}\times\boldsymbol{n}) = \mathrm{curl}_\Gamma \boldsymbol{u} \quad \forall \boldsymbol{u} \in H^{-\frac{1}{2}}(\mathrm{div},\Gamma).$$

This setting allows to extend the definitions of the operators ∇_Γ and $\mathbf{curl}_\Gamma$ for $f \in H^{\frac{1}{2}}(\Gamma)$ using duality via

$$\begin{aligned}\int_\Gamma (\nabla_\Gamma f)\cdot\boldsymbol{u}\,\mathrm{d}s &= -\int_\Gamma (\mathrm{div}_\Gamma \boldsymbol{u}) f\,\mathrm{d}s \quad \forall \boldsymbol{u} \in H^{-\frac{1}{2}}(\mathrm{div},\Gamma),\\ \int_\Gamma (\mathbf{curl}_\Gamma f)\cdot\boldsymbol{u}\,\mathrm{d}s &= \int_\Gamma (\mathrm{curl}_\Gamma \boldsymbol{u}) f\,\mathrm{d}s \quad \forall \boldsymbol{u} \in H^{-\frac{1}{2}}(\mathrm{curl},\Gamma),\end{aligned}$$

which yields $\nabla_\Gamma f \in H^{-\frac{1}{2}}(\mathrm{curl},\Gamma)$ and $\mathbf{curl}_\Gamma f \in H^{-\frac{1}{2}}(\mathrm{div},\Gamma)$ [2].
With the results from above, we can characterize the boundary values $\boldsymbol{A}\cdot\boldsymbol{n}$ and $\boldsymbol{A}\times\boldsymbol{n}$ as elements of the trace spaces $H^{-\frac{1}{2}}(\Gamma)$ and $H^{-\frac{1}{2}}(\mathrm{div},\Gamma)$, respectively.

2.2.8 Existence and uniqueness of the solution

In this section, we aim to prove the existence and uniqueness of a solution to the problem $(EM)^w$ defined in Section 2.2.4. For this purpose, we will treat the cases $\kappa_{ij} \in \mathbb{R}_+$, $\kappa_{ij} = 0$ and $\kappa_{ij} \in \mathbb{C}$ for all $i,j = 1,..,3$ separately, following [101].

For $\mathcal{K} \in \{\mathbb{R},\mathbb{C}\}$, define the bilinear form

$$\hat{b} : H_\Gamma(\mathrm{curl},\Omega)\times H_\Gamma(\mathrm{curl},\Omega) \to \mathcal{K}$$

with

$$\hat{b}(\boldsymbol{A},\tilde{\boldsymbol{A}}) = \int_\Omega (\boldsymbol{\mu}^{-1}\,\mathrm{curl}\,\boldsymbol{A})\cdot\mathrm{curl}\,\tilde{\boldsymbol{A}} + \boldsymbol{\kappa}\boldsymbol{A}\cdot\tilde{\boldsymbol{A}}\,\mathrm{d}x, \tag{2.122}$$

as well as the linear form $\hat{l} : H_\Gamma(\mathrm{curl},\Omega) \to \mathcal{K}$,

$$l(\tilde{\boldsymbol{A}}) = \int_\Omega \boldsymbol{j}_I\cdot\tilde{\boldsymbol{A}}\,\mathrm{d}x + \int_{\Gamma_N} \boldsymbol{K}\cdot\tilde{\boldsymbol{A}}_t\,\mathrm{d}s, \tag{2.123}$$

with $\tilde{\boldsymbol{A}}_t = \boldsymbol{n}\times\tilde{\boldsymbol{A}}\times\boldsymbol{n}$. The weak form of the problem can then be written as

Problem $(EM)^w$: Find $\boldsymbol{A} \in H_\Gamma(\mathrm{curl},\Omega)$, such that

$$\hat{b}(\boldsymbol{A},\tilde{\boldsymbol{A}}) = \hat{l}(\tilde{\boldsymbol{A}}) \tag{2.124}$$

holds for all $\tilde{\boldsymbol{A}} \in H_\Gamma(\mathrm{curl},\Omega)$.

The case $\kappa_{ij} \in \mathbb{R}_+$

In order to apply the Lax-Milgram lemma to the problem $(EM)^w$, we have to show the continuity of $\hat{b}(\cdot,\cdot)$ and $\hat{l}(\cdot)$ in a first step. The linear form $l(\cdot)$ can be splitted into the linear functionals L_1 and L_2, with

$$\hat{l}(\tilde{\boldsymbol{A}}) = L_1(\tilde{\boldsymbol{A}}) + L_2(\tilde{\boldsymbol{A}}) = \int_\Omega \boldsymbol{j}_I\cdot\tilde{\boldsymbol{A}}\,\mathrm{d}x + \int_{\Gamma_N} \boldsymbol{K}\cdot\tilde{\boldsymbol{A}}_t\,\mathrm{d}s.$$

The linear functional L_1 is obviously continuous,

$$|L_1(\tilde{\boldsymbol{A}})| \leq \|\boldsymbol{j}_I\|_{\mathbf{0}} \left\|\tilde{\boldsymbol{A}}\right\|_{\mathbf{0}} \leq \|\boldsymbol{j}_I\|_{\mathbf{0}} \left\|\tilde{\boldsymbol{A}}\right\|_{H(\mathrm{curl},\Omega)},$$

where $\|\cdot\|_{\mathbf{0}}$ denotes the norm in $L^2(\Omega)^3$. The tangential trace $\boldsymbol{\gamma_t}$ with $\boldsymbol{\gamma_t}\tilde{\boldsymbol{A}} = \tilde{\boldsymbol{A}} \times \boldsymbol{n}$ is a continuous operator on $H(\mathrm{curl},\Omega)$, i.e.

$$\left\|\boldsymbol{\gamma_t}\tilde{\boldsymbol{A}}\right\|_{H^{-\frac{1}{2}}(\Gamma_N)^3} \leq c \left\|\tilde{\boldsymbol{A}}\right\|_{H(\mathrm{curl},\Omega)}$$

for a constant c. Furthermore, from the surjectivity of $\boldsymbol{\gamma_t^*}$ we can deduce that for $\boldsymbol{K} \in H^{-\frac{1}{2}}(\mathrm{div},\Gamma)$ there exists an $\hat{\boldsymbol{A}} \in H(\mathrm{curl},\Omega)$ such that

$$\boldsymbol{\gamma_t^*}\hat{\boldsymbol{A}} = \boldsymbol{K}.$$

The *trace theorem* [87] for the trace operators $\boldsymbol{\gamma_t^*}$ and $\boldsymbol{\gamma_T}$ implies that for all $\tilde{\boldsymbol{A}} \in H(\mathrm{curl},\Omega)$

$$[\boldsymbol{K}, \boldsymbol{\gamma_T}\tilde{\boldsymbol{A}}]_\Gamma = (\mathrm{curl}\,\hat{\boldsymbol{A}}, \tilde{\boldsymbol{A}})_{\mathbf{0}} - (\hat{\boldsymbol{A}}, \mathrm{curl}\,\tilde{\boldsymbol{A}})_{\mathbf{0}},$$

where $(\cdot,\cdot)$ is the inner product in $L^2(\Omega)^3$ and $[\cdot]_\Gamma$ describes the duality product in the space $H^{-\frac{1}{2}}(\mathrm{div},\Omega)$. Thus, we can conclude that for a fixed $\boldsymbol{K} \in H^{-\frac{1}{2}}(\mathrm{div},\Gamma)$, the linear functional $L_2 : H(\mathrm{curl},\Omega) \to \mathbb{R}$ defined as

$$L_2(\tilde{\boldsymbol{A}}) = [\boldsymbol{K}, \boldsymbol{\gamma_T}\tilde{\boldsymbol{A}}]_\Gamma = \int_\Gamma \boldsymbol{K} \cdot \boldsymbol{\gamma_T}\tilde{\boldsymbol{A}}\,\mathrm{d}s = (\mathrm{curl}\,\hat{\boldsymbol{A}}, \tilde{\boldsymbol{A}})_{\mathbf{0}} - (\hat{\boldsymbol{A}}, \mathrm{curl}\,\tilde{\boldsymbol{A}})_{\mathbf{0}}$$

is continuous since

$$|L_2(\tilde{\boldsymbol{A}})| \leq c \left\|\hat{\boldsymbol{A}}\right\|_{H(\mathrm{curl},\Omega)} \left\|\tilde{\boldsymbol{A}}\right\|_{H(\mathrm{curl},\Omega)}$$

and therefore

$$|L_2(\tilde{\boldsymbol{A}})| \leq \|\boldsymbol{K}\|_{H^{-\frac{1}{2}}(\mathrm{div},\Gamma)} \left\|\tilde{\boldsymbol{A}}\right\|_{H(\mathrm{curl},\Omega)},$$

as, due to the relation $\gamma_t^*\hat{\boldsymbol{A}} = \boldsymbol{K}$, the functional L_2 is independent of $\hat{\boldsymbol{A}}$. Summing up, for the linear form $\hat{l}$, we obtain the estimate

$$\hat{l}(\tilde{\boldsymbol{A}}) \leq C \left\|\tilde{\boldsymbol{A}}\right\|_{H(\mathrm{curl},\Omega)} \left(\|\boldsymbol{j}_I\|_{\mathbf{0}} + \|\boldsymbol{K}\|_{H^{-\frac{1}{2}}(\mathrm{div},\Gamma)}\right)$$

for a constant $C \in \mathbb{R}$.
For $\kappa_{ij} \in \mathbb{R}^+$ for all $i,j = 1,2,3$, the bilinear form $\hat{b}(\cdot,\cdot)$ is continuous,

$$\hat{b}(\boldsymbol{A}, \tilde{\boldsymbol{A}}) \leq \hat{\beta} \|\boldsymbol{A}\|_{H(\mathrm{curl},\Omega)} \left\|\tilde{\boldsymbol{A}}\right\|_{H(\mathrm{curl},\Omega)},$$

with the constant

$$\hat{\beta} := \max\{\max_{i=1,2,3} \mu_{ii}^{-1}, \max_{i=1,2,3} \kappa_{ii}\},$$

where μ_{ii}^{-1} denote the entries of the matrix $\boldsymbol{\mu}^{-1}$. Furthermore, $\hat{b}(\cdot,\cdot)$ is coercive,

$$\hat{b}(\boldsymbol{A}, \boldsymbol{A}) \geq \hat{\alpha} \|\boldsymbol{A}\|^2_{H(\mathrm{curl},\Omega)},$$

with the constant

$$\hat{\alpha} := \min\{\min_{i=1,2,3} \mu_{ii}^{-1}, \min_{i=1,2,3} \kappa_{ii}\}.$$

Note that we assumed the parameter matrices $\boldsymbol{\mu}$ and $\boldsymbol{\kappa}$ to have a diagonal structure with positive entries. The verification of the above-mentioned properties will be given in Chapter 4 for a material class satisfying this assumption.
The Lax-Milgram lemma now directly yields a unique solution of the weak problem.

The case $\kappa_{ij} \in \mathbb{C}$

In case that the bilinear form $\hat{b}(\cdot,\cdot)$ is not coercive, we can still obtain a unique solution by requiring that

$$\sup_{\boldsymbol{A}\in H_\Gamma(\mathrm{curl},\Omega)} \frac{\hat{b}(\boldsymbol{A},\tilde{\boldsymbol{A}})}{\|\boldsymbol{A}\|_{H(\mathrm{curl},\Omega)}} \geq \gamma \left\|\tilde{\boldsymbol{A}}\right\|_{H(\mathrm{curl},\Omega)} \quad \text{for all } \tilde{\boldsymbol{A}} \in H_\Gamma(\mathrm{curl},\Omega), \tag{2.125}$$

for a constant $\gamma > 0$ according to the generalized Lax-Milgram lemma [4].
This result can be applied to the case $\kappa_{ij} \in \mathbb{C}$ for $i,j = 1,2,3$, i.e.

$$\kappa_{ij} = \mathrm{Re}(\kappa_{ij}) + i\,\mathrm{Im}(\kappa_{ij}),$$

with $\mathrm{Im}(\kappa_{ij}) \neq 0$. Following [101], we split the strong form into its real and imaginary part, by rewriting

$$\begin{aligned} \boldsymbol{A} &= \mathrm{Re}(\boldsymbol{A}) + i\,\mathrm{Im}(\boldsymbol{A}), \\ \boldsymbol{j}_I &= \mathrm{Re}(\boldsymbol{j}_I) + i\,\mathrm{Im}(\boldsymbol{j}_I), \end{aligned}$$

and obtain the real system

$$\begin{aligned} \mathrm{curl}(\boldsymbol{\mu}^{-1}\,\mathrm{curl}\,\mathrm{Re}(\boldsymbol{A})) + \mathrm{Re}(\boldsymbol{\kappa})\,\mathrm{Re}(\boldsymbol{A}) - \mathrm{Im}(\boldsymbol{\kappa})\,\mathrm{Im}(\boldsymbol{A}) &= \mathrm{Re}(\boldsymbol{j}_I), \\ \mathrm{curl}(\boldsymbol{\mu}^{-1}\,\mathrm{curl}\,\mathrm{Im}(\boldsymbol{A})) + \mathrm{Im}(\boldsymbol{\kappa})\,\mathrm{Re}(\boldsymbol{A}) + \mathrm{Re}(\boldsymbol{\kappa})\,\mathrm{Im}(\boldsymbol{A}) &= \mathrm{Im}(\boldsymbol{j}_I), \end{aligned}$$

where $\mathrm{Re}(\boldsymbol{A}) = (\mathrm{Re}(A_i))_i$ and $\mathrm{Im}(\boldsymbol{A}) = (\mathrm{Im}(A_i))_i$, $i = 1,2,3$ are the vectors of the real and imaginary parts of the coefficients of $\boldsymbol{A}$ (the same convention holds for $\boldsymbol{j}_I$). The matrices $\mathrm{Re}(\boldsymbol{\kappa}) = \mathrm{Re}(\kappa_{ij})_{i,j=1,2,3}$ and $\mathrm{Im}(\boldsymbol{\kappa}) = \mathrm{Im}(\kappa_{ij})_{i,j=1,2,3}$ are defined in the same way.
To obtain the weak form of the system, we multiply the equations by $\mathrm{Re}(\tilde{\boldsymbol{A}})$ and $\mathrm{Im}(\tilde{\boldsymbol{A}})$, respectively, perform the usual partial integration and add the two resulting equations to obtain a single weak problem:

Problem $(EM)^w_{\mathbb{C}}$: Find $(\mathrm{Re}(\boldsymbol{A}),\mathrm{Im}(\boldsymbol{A})) \in H_\Gamma(\mathrm{curl},\Omega) \times H_\Gamma(\mathrm{curl},\Omega)$, such that

$$\hat{b}\big((\mathrm{Re}(\boldsymbol{A}),\mathrm{Im}(\boldsymbol{A})),(\mathrm{Re}(\tilde{\boldsymbol{A}}),\mathrm{Im}(\tilde{\boldsymbol{A}}))\big) = \hat{l}\big((\mathrm{Re}(\tilde{\boldsymbol{A}})),\mathrm{Im}(\tilde{\boldsymbol{A}})\big) \tag{2.126}$$

holds for all $(\mathrm{Re}(\tilde{\boldsymbol{A}}),\mathrm{Im}(\tilde{\boldsymbol{A}})) \in H_\Gamma(\mathrm{curl},\Omega) \times H_\Gamma(\mathrm{curl},\Omega)$. Suppressing the arguments for the sake of clarity, $\hat{b}(\cdot,\cdot)$ and $\hat{l}(\cdot)$ can be written as

$$\begin{aligned} \hat{b}(\cdot,\cdot) &= \int_\Omega \boldsymbol{\mu}^{-1}(\mathrm{curl}\,\mathrm{Re}(\boldsymbol{A}))\cdot(\mathrm{curl}\,\mathrm{Re}(\tilde{\boldsymbol{A}}))\,\mathrm{d}x \\ &+ \int_\Omega \boldsymbol{\mu}^{-1}(\mathrm{curl}\,\mathrm{Im}(\boldsymbol{A}))\cdot(\mathrm{curl}\,\mathrm{Im}(\tilde{\boldsymbol{A}}))\,\mathrm{d}x \\ &+ \int_\Omega \mathrm{Re}(\boldsymbol{\kappa})\left[\mathrm{Re}(\boldsymbol{A})\cdot\mathrm{Re}(\tilde{\boldsymbol{A}}) + \mathrm{Im}(\boldsymbol{A})\cdot\mathrm{Im}(\tilde{\boldsymbol{A}})\right]\mathrm{d}x \\ &+ \int_\Omega \mathrm{Im}(\boldsymbol{\kappa})\left[\mathrm{Re}(\boldsymbol{A})\cdot\mathrm{Im}(\tilde{\boldsymbol{A}}) - \mathrm{Im}(\boldsymbol{A})\cdot\mathrm{Re}(\tilde{\boldsymbol{A}})\right]\mathrm{d}x \\ \hat{l}(\cdot) &= \int_\Omega \mathrm{Re}(\boldsymbol{j}_I)\cdot\mathrm{Re}(\tilde{\boldsymbol{A}}) + \mathrm{Im}(\boldsymbol{j}_I)\cdot\mathrm{Im}(\tilde{\boldsymbol{A}})\,\mathrm{d}x \\ &+ \int_{\Gamma_N} \boldsymbol{K}\cdot\big(\mathrm{Re}(\tilde{\boldsymbol{A}}_t) + \mathrm{Im}(\tilde{\boldsymbol{A}}_t)\big)\,\mathrm{d}s. \end{aligned}$$

As in the real case, $\hat{b}(\cdot,\cdot)$ and $\hat{l}(\cdot)$ are continuous and we merely have to verify the condition (2.125). Hence, we have to find $\boldsymbol{A} = (\mathrm{Re}(\boldsymbol{A}), \mathrm{Im}(\boldsymbol{A})) \in H_\Gamma(\mathrm{curl}, \Omega) \times H_\Gamma(\mathrm{curl}, \Omega)$ such that

$$\hat{b}(\cdot,\cdot) \geq \gamma \left\| (\mathrm{Re}(\tilde{\boldsymbol{A}}), \mathrm{Im}(\tilde{\boldsymbol{A}})) \right\|_{H(\mathrm{curl},\Omega)} \| (\mathrm{Re}(\boldsymbol{A}), \mathrm{Im}(\boldsymbol{A})) \|_{H(\mathrm{curl},\Omega)}$$

for all $\tilde{\boldsymbol{A}} = (\mathrm{Re}(\tilde{\boldsymbol{A}}), \mathrm{Im}(\tilde{\boldsymbol{A}})) \in H_\Gamma(\mathrm{curl}, \Omega)$. Choosing

$$\boldsymbol{A} = ((\mathrm{Re}(\boldsymbol{A})), \mathrm{Im}(\boldsymbol{A})) := (\mathrm{Re}(\tilde{\boldsymbol{A}}), \mathrm{Im}(\tilde{\boldsymbol{A}})) + \hat{\gamma}(\mathrm{Im}(\tilde{\boldsymbol{A}}), -\mathrm{Re}(\tilde{\boldsymbol{A}})), \tag{2.127}$$

for a constant $\hat{\gamma} > 0$, inserting (2.127) into the bilinear form $\hat{b}(\cdot,\cdot)$ and assuming that $\boldsymbol{\kappa}$ and $\boldsymbol{\mu}$ are diagonal matrices as required above, we obtain

$$\begin{aligned}
\hat{b}(\cdot,\cdot) &= \int_\Omega (\boldsymbol{\mu}^{-1} \operatorname{curl} \mathrm{Re}(\tilde{\boldsymbol{A}})) \cdot \operatorname{curl} \mathrm{Re}(\tilde{\boldsymbol{A}}) \, \mathrm{d}x + \int_\Omega (\boldsymbol{\mu}^{-1} \operatorname{curl} \mathrm{Im}(\tilde{\boldsymbol{A}})) \cdot \operatorname{curl} \mathrm{Im}(\tilde{\boldsymbol{A}}) \, \mathrm{d}x \\
&+ \int_\Omega \hat{\gamma} \left(\boldsymbol{\mu}^{-1} \operatorname{curl} \mathrm{Im}(\tilde{\boldsymbol{A}}) \cdot \operatorname{curl} \mathrm{Re}(\tilde{\boldsymbol{A}}) - \boldsymbol{\mu}^{-1} \operatorname{curl} \mathrm{Re}(\tilde{\boldsymbol{A}}) \cdot \operatorname{curl} \mathrm{Im}(\tilde{\boldsymbol{A}}) \right) \mathrm{d}x \\
&+ \int_\Omega \mathrm{Re}(\kappa) \left[\mathrm{Re}(\tilde{\boldsymbol{A}}) \, \mathrm{Re}(\tilde{\boldsymbol{A}}) + \mathrm{Im}(\tilde{\boldsymbol{A}}) \, \mathrm{Im}(\tilde{\boldsymbol{A}}) \right] \mathrm{d}x \\
&+ \int_\Omega \hat{\gamma} \, \mathrm{Im}(\kappa) \left[\mathrm{Im}(\tilde{\boldsymbol{A}}) \, \mathrm{Im}(\tilde{\boldsymbol{A}}) + \mathrm{Re}(\tilde{\boldsymbol{A}}) \, \mathrm{Re}(\tilde{\boldsymbol{A}}) \right] \mathrm{d}x \\
&\geq \min_{i=1,2,3} \mu_{ii}^{-1} \left(\left\| \operatorname{curl} \mathrm{Re}(\tilde{\boldsymbol{A}}) \right\|_{\mathbf{0}}^2 + \left\| \operatorname{curl} \mathrm{Im}(\tilde{\boldsymbol{A}}) \right\|_{\mathbf{0}}^2 \right) \\
&+ \min_{i=1,2,3} \mathrm{Re}(\kappa_{ii}) \left(\left\| \mathrm{Re}(\tilde{\boldsymbol{A}}) \right\|_{\mathbf{0}}^2 + \left\| \mathrm{Im}(\tilde{\boldsymbol{A}}) \right\|_{\mathbf{0}}^2 \right) \\
&+ \hat{\gamma} \min_{i=1,2,3} \mathrm{Im}(\kappa_{ii}) \left(\left\| \mathrm{Im}(\tilde{\boldsymbol{A}}) \right\|_{\mathbf{0}}^2 + \left\| \mathrm{Re}(\tilde{\boldsymbol{A}}) \right\|_{\mathbf{0}}^2 \right) \\
&= \min_{i=1,2,3} \mu_{ii}^{-1} \left\| \operatorname{curl} \tilde{\boldsymbol{A}} \right\|_{\mathbf{0}}^2 + \left(\min_{i=1,2,3} \mathrm{Re}(\kappa_{ii}) + \hat{\gamma} \min_{i=1,2,3} \mathrm{Im}(\kappa_{ii}) \right) \left\| \tilde{\boldsymbol{A}} \right\|_{\mathbf{0}}^2 .
\end{aligned}$$

Now setting

$$\hat{\gamma} := \frac{\min\limits_{i=1,2,3} \mu_{ii}^{-1} - \min\limits_{i=1,2,3} \mathrm{Re}(\kappa_{ii})}{\min\limits_{i=1,2,3} \mathrm{Im}(\kappa_{ii})},$$

we obtain the estimate

$$\sup_{\boldsymbol{A} \in H_\Gamma(\mathrm{curl},\Omega)} \hat{b}((\mathrm{Re}(\boldsymbol{A}), \mathrm{Im}(\boldsymbol{A})), (\mathrm{Re}(\tilde{\boldsymbol{A}}), \mathrm{Im}(\tilde{\boldsymbol{A}}))) \geq \gamma \left\| \tilde{\boldsymbol{A}} \right\|_{H(\mathrm{curl},\Omega)},$$

with

$$\gamma := \min_{i=1,2,3} \mu_{ii}^{-1},$$

which implies the existence and uniqueness of the solution to the problem with $\boldsymbol{\kappa} \in \mathbb{C}^{3\times3}$.

The case $\kappa_{ij} = 0$

In a next step, we will consider a magnetostatic problem, which is obtained from setting $\kappa_{ij} = 0$ for all $i, j = 1, 2, 3$. In this case, the bilinear form

$$\hat{b}(\boldsymbol{A}, \boldsymbol{A}) = \int_\Omega \boldsymbol{\mu}^{-1} \operatorname{curl} \boldsymbol{A} \cdot \operatorname{curl} \tilde{\boldsymbol{A}} \, \mathrm{d}x,$$

is not coercive: For $\boldsymbol{A} = \nabla\phi$, where ϕ is a scalar potential function, we have $\hat{b}(\nabla\phi, \nabla\phi) = 0$, whereas the corresponding norm $\|\nabla\phi\|^2_{H(\mathrm{curl},\Omega)} = \|\nabla\phi\|^2_{\mathbf{0}}$ does not vanish. We therefore require

$$\int_\Omega \boldsymbol{j}_I \cdot \nabla\psi \,\mathrm{d}x = -\int_\Omega \mathrm{div}\, \boldsymbol{j}_I \psi \,\mathrm{d}x + \int_{\partial\Omega} (\boldsymbol{j}_I \cdot \boldsymbol{n})\psi \,\mathrm{d}x = 0 \quad \text{for all } \psi \in H^1(\Omega). \tag{2.128}$$

Note that in this case,

$$\int_{\Gamma_N} \boldsymbol{K} \cdot \boldsymbol{A} \,\mathrm{d}s = 0,$$

as $\boldsymbol{K} = \boldsymbol{\mu}^{-1}\,\mathrm{curl}\,\nabla\psi = \boldsymbol{0}$. Partial integration implies that $\mathrm{div}\,\boldsymbol{j}_I = 0$ in Ω and $\boldsymbol{j}_I \cdot \boldsymbol{n} = 0$ on the boundary $\partial\Omega$, i.e. the right-hand side has to be compatible. Since neither the Lax-Milgram lemma nor its generalization can be applied here, the weak problem is reformulated as a saddle point problem.
Adding the condition

$$\int_\Omega \boldsymbol{A} \cdot \nabla\psi \,\mathrm{d}x = 0 \quad \text{for all } \psi \in H^1(\Omega),$$

the weak formulation turns into

Problem $(EM)^w_s$: Find $(\boldsymbol{A}, \phi) \in H_\Gamma(\mathrm{curl},\Omega) \times H^1(\Omega)$, such that

$$\hat{b}(\boldsymbol{A}, \tilde{\boldsymbol{A}}) + \hat{d}(\tilde{\boldsymbol{A}}, \phi) = \hat{l}(\tilde{\boldsymbol{A}}) \quad \text{for all } \tilde{\boldsymbol{A}} \in H_\Gamma(\mathrm{curl},\Omega), \tag{2.129}$$

$$\hat{d}(\boldsymbol{A}, \psi) = 0 \quad \text{for all } \psi \in H^1(\Omega), \tag{2.130}$$

with the definitions

$$\hat{b}(\boldsymbol{A}, \tilde{\boldsymbol{A}}) = \int_\Omega (\boldsymbol{\mu}^{-1}\,\mathrm{curl}\,\boldsymbol{A}) \cdot (\mathrm{curl}\,\tilde{\boldsymbol{A}}) \,\mathrm{d}x \tag{2.131}$$

$$\hat{d}(\boldsymbol{A}, \psi) = \int_\Omega \boldsymbol{A} \cdot \nabla\psi \,\mathrm{d}x, \tag{2.132}$$

$$\hat{l}(\tilde{\boldsymbol{A}}) = \int_\Omega \boldsymbol{j}_I \cdot \tilde{\boldsymbol{A}} \,\mathrm{d}x + \int_{\Gamma_N} \boldsymbol{K} \cdot \boldsymbol{A} \,\mathrm{d}s. \tag{2.133}$$

In fact, the space $H^1(\Omega)$ of the functions ψ can even be replaced by the quotient space $H^1(\Omega)/\mathbb{R}$, as every $\psi + c$, $c \in \mathbb{R}$ is a solution of the above weak system as well.
The existence and uniqueness of this problem is guaranteed by Brezzi's Splitting Theorem [23] (presented in detail in Chapter 3), which states that a saddle point problem of the form $(EM)^w_s$ with continuous bilinear forms and a continuous linear functional has a unique solution if the bilinear form $\hat{b}(\cdot,\cdot)$ is coercive on the kernel

$$\ker(\hat{\mathcal{D}}) := \{\boldsymbol{A} \in H_\Gamma(\mathrm{curl},\Omega) \mid \hat{d}(\boldsymbol{A}, \psi) = 0 \;\forall \psi \in H^1(\Omega)\},$$

and, additionally, the bilinear form $\hat{d}(\cdot,\cdot)$ satisfies the inf-sup condition (also called Ladyshenskaya-Babuška-Brezzi condition or LBB-condition)

$$\inf_{\psi\in H^1(\Omega)} \sup_{\boldsymbol{A}\in H_\Gamma(\mathrm{curl},\Omega)} \frac{\hat{d}(\boldsymbol{A}, \psi)}{\|\psi\|_1 \, \|\boldsymbol{A}\|_{H(\mathrm{curl},\Omega)}} \geq \hat{\beta}, \tag{2.134}$$

for a constant $\hat{\beta} > 0$, where $\|\psi\|_1$ denotes the norm in the Sobolev space $H^1(\Omega)$.
The coercivity of $\hat{b}(\cdot,\cdot)$ on $\ker(\hat{\mathcal{D}})$ can be shown by using the Friedrichs-type inequality

$$c\,\|\mathrm{curl}\,\boldsymbol{A}\|_{\mathbf{0}} \geq \|\boldsymbol{A}\|_{\mathbf{0}} \tag{2.135}$$

with $c > 0$ for all $\boldsymbol{A} \in H(\mathrm{curl}, \Omega)$ satisfying

$$\int_\Omega \boldsymbol{A} \cdot \nabla\psi \, \mathrm{d}x = 0 \quad \text{for all } \psi \in H^1(\Omega), \tag{2.136}$$

which is proven on the basis of a Helmholtz decomposition of $\boldsymbol{A}$ (shown, e.g. in [101]). Inequality (2.135) implies that

$$\begin{aligned}(c+1)\,\|\mathrm{curl}\,\boldsymbol{A}\|_{\mathbf{0}}^2 &\geq \|\boldsymbol{A}\|_{\mathbf{0}}^2\,\|\mathrm{curl}\,\boldsymbol{A}\|_{\mathbf{0}} + \|\mathrm{curl}\,\boldsymbol{A}\|_{\mathbf{0}}^2 \\ &\geq \frac{1}{c}\,\|\boldsymbol{A}\|_{\mathbf{0}}^2 + \|\mathrm{curl}\,\boldsymbol{A}\|_{\mathbf{0}}^2 \\ &\geq \min\left\{1, \frac{1}{c}\right\}(\|\boldsymbol{A}\|_{\mathbf{0}}^2 + \|\mathrm{curl}\,\boldsymbol{A}\|_{\mathbf{0}}^2),\end{aligned}$$

for all $\boldsymbol{A} \in H(\mathrm{curl}, \Omega)$ satisfying condition (2.136). Hence,

$$\begin{aligned}\hat{b}(\boldsymbol{A}, \tilde{\boldsymbol{A}}) &= \int_\Omega (\boldsymbol{\mu}^{-1}\,\mathrm{curl}\,\boldsymbol{A}) \cdot \mathrm{curl}\,\boldsymbol{A}\,\mathrm{d}x = \int_\Omega \min_{i=1,2,3} \mu_{ii}^{-1}\,\|\mathrm{curl}\,\boldsymbol{A}\|_{\mathbf{0}}^2\,\mathrm{d}x \\ &\geq \hat{\alpha}(\|\boldsymbol{A}\|_{\mathbf{0}}^2 + \|\nabla\times\boldsymbol{A}\|_{\mathbf{0}}^2) = \hat{\alpha}\,\|\boldsymbol{A}\|_{H(\mathrm{curl},\Omega)},\end{aligned}$$

where the constant $\hat{\alpha}$ is given by

$$\hat{\alpha} := \frac{\min\limits_{i=1,..,3} \mu_{ii}^{-1}\,\min\{1, \frac{1}{c}\}}{c+1}.$$

Thus, the coercivity requirement is fulfilled.
The LBB-condition (2.134) can be proven by showing the equivalent formulation

$$\sup_{\boldsymbol{A}\in H_\Gamma(\mathrm{curl},\Omega)} \frac{\hat{d}(\boldsymbol{A}, \psi)}{\|\boldsymbol{A}\|_{H(\mathrm{curl},\Omega)}} \geq \bar{\beta}\,\|\nabla\psi\|_{\mathbf{0}} \quad \forall\psi \in H^1(\Omega),$$

with $\bar{\beta} > 0$. Now we can choose $\boldsymbol{A} \in H_\Gamma(\mathrm{curl}, \Omega)$ with $\boldsymbol{A} = \nabla\psi$ and obtain

$$\sup_{\boldsymbol{A}\in H_\Gamma(\mathrm{curl},\Omega)} \frac{\hat{d}(\boldsymbol{A}, \psi)}{\|\boldsymbol{A}\|_{H(\mathrm{curl},\Omega)}} \geq \frac{\|\nabla\psi\|_{\mathbf{0}}^2}{\|\nabla\psi\|_{\mathbf{0}}} = \|\nabla\psi\|_{\mathbf{0}}\,.$$

Finally, we mention that in case $\kappa_{ii} \in \mathbb{R}_-$ for all $i = 1, 2, 3$, the coercivity of the bilinear form $\hat{b}(\cdot,\cdot)$ or the satisfaction of the ellipticity condition on $\ker(\hat{\mathcal{D}})$ are in general not guaranteed. However, one can show that a unique solution of the corresponding weak problem is not obtained only for a discrete set of choices $\kappa_{ij} \in \mathbb{R}_-$ [79, 101]. This case will not be discussed in the thesis.

2.2.9 Influence of perturbations

For the case $\kappa_{ii} \in \mathbb{R}_+$, $i = 1, 2, 3$, the Lax-Milgram lemma yields the stability estimate

$$\|\boldsymbol{A}\|_{H(\mathrm{curl},\Omega)} \leq \frac{1}{\hat{\alpha}}\,\left\|\hat{l}\right\|_{H(\mathrm{curl},\Omega)'} = \frac{1}{\hat{\alpha}}\left(\|\boldsymbol{j}_I\|_0 + \|\boldsymbol{K}\|_{H^{-\frac{1}{2}}(\mathrm{div},\Gamma)}\right) \tag{2.137}$$

where $H(\mathrm{curl}, \Omega)'$ denotes the dual space of $H(\mathrm{curl}, \Omega)$. Thus, the solution depends continuously on the right-hand side data $\boldsymbol{K}$ and $\boldsymbol{j}_I$. For very small values of $\min\limits_{i=1,2,3} \kappa_{ii}$, the stability estimate does not yield satisfactory results any more.

If $\boldsymbol{\kappa} \in \mathbb{C}^{3\times 3}$ with $\mathrm{Im}(\kappa_{ii}) > 0$, the generalized Lax-Milgram lemma yields the stability estimate

$$\|\boldsymbol{A}\|_{H(\mathrm{curl},\Omega)} \leq \frac{1}{\min\limits_{i=1,2,3} \mu_{ii}^{-1}} \left\|\hat{l}\right\|_{H(\mathrm{curl},\Omega)'} \leq \frac{1}{\min\limits_{i=1,2,3} \mu_{ii}^{-1}} \left(\|\boldsymbol{j}_I\|_{\mathbf{0}} + \|\boldsymbol{K}\|_{H^{-\frac{1}{2}}(\mathrm{div},\Gamma)} \right). \tag{2.138}$$

If, however, $\mathrm{Im}(\kappa_{ii}) \to 0$, the stability estimate fails, i.e. the imaginary part of κ_{ii} "stabilizes the problem" in this case [101].
Finally, in the magnetostatic case, Brezzi's theorem yields the stability estimate

$$\|\boldsymbol{A}\|_{H(\mathrm{curl},\Omega)} + \|\Psi\|_1 \leq c \left\|\hat{l}\right\|_{H(\mathrm{curl},\Omega)'}.$$

Chapter 3

The Coupled Model: Magnetic Scalar Potential Formulation

Having introduced the basic modeling and analysis aspects of linear elasticity and electrodynamics, we are finally able to take the next step by coupling the two concepts in a single model. As the title suggests, the model presented in this chapter uses the total scalar potential formulation of Maxwell's equations, which was introduced in Section 2.2.1. Its derivation based on a special case of Hamilton's principle is similar to the derivation of the linear elastic equations of motion presented in Section 2.1.2. In this way, a coupled system of partial differential equations can be obtained for the elastic and magnetic quantities, which serves as a basis for further analysis.
The structure of the chapter follows the development of the model from its physical origin to the discussion of whether or not it is (uniquely) solvable. The derivation of the coupled magnetoelastic model is presented in Section 3.1, leading to the strong and weak forms of the coupled equations. Section 3.2 is concerned with the analysis of the structure of the coupled problem in the continuous case. We show that the resulting system of equations constitutes a saddle point problem with a penalty term. Using appropriate tools from functional analysis, the existence and uniqueness of the solution to this system is shown and the corresponding function spaces are discussed. In particular, we prove a continuous and discrete inf-sup condition for a class of magnetostrictive materials having certain coupling properties. In Section 3.4.2 the general results are specified to a two-dimensional model under the assumption of plane stress.

3.1 Derivation of the coupled model

Consider a magnetostrictive material that is assumed to be homogeneous at the macroscopic level and forms a body whose undeformed state we denote by the domain $\Omega \subset \mathbb{R}^3$. We aim at examining the behavior of the material due to the influence of external magnetic and mechanical fields. On the one hand, the application of the magnetic field will cause a change in the elastic strain of the material. On the other hand, the magnetization of the material will be affected by the mechanical stress. We suppose that the deformation of the body has no effect on the magnetic field outside the material and thus the coupling occurs only in the material itself. Furthermore, we assume that

- only small strains and deviations from the initial magnetization state are considered,
- the material behavior is linear and reversible,

- the process is time-independent,
- the system energy is conservative and that
- no hysteresis effects occur.

In general, magnetostrictive materials show a non-linear material behavior. As explained in Section 1.1.3, the linearity assumption can be satisfied by applying a magnetic bias using a DC voltage or a permanent magnet, as well as a mechanical bias in terms of a prestress, such that for small variations from the initial magnetization and stressed state, the material can be reasonably characterized by a linear model. The biasing can be additionally used to produce so-called "giant" dynamic strains in some applications [39]. In the following, we will retain the notation introduced in Chapter 2 and define the gradient $\nabla \boldsymbol{v}$ of a vector field as the Jacobian

$$\nabla \boldsymbol{v} := \left(\frac{\partial v_i}{\partial x_j} \right)_{i,j=1,2,3}$$

and the divergence $\mathbf{div}\, \boldsymbol{\sigma}$ of a second order tensor $\boldsymbol{\sigma}$ as

$$\mathbf{div}\, \boldsymbol{\sigma} := \nabla^T \cdot \boldsymbol{\sigma}^T = \left(\sum_{j=1}^{3} \frac{\partial \sigma_{ij}}{\partial x_j} \right)_{i=1,2,3}.$$

The deformation of the body is characterized by the displacement field $\boldsymbol{u} : \Omega \to \mathbb{R}^3$ or the strain $\boldsymbol{\epsilon}(\boldsymbol{u}) : \Omega \to \mathbb{R}^{3\times3}$ using the linear relation

$$\boldsymbol{\epsilon}(\boldsymbol{u}) = \frac{\nabla \boldsymbol{u} + \nabla \boldsymbol{u}^T}{2}.$$

The magnetic influence is described by the magnetic field $\boldsymbol{H} : \Omega \to \mathbb{R}^3$ and the magnetic flux density $\boldsymbol{B} : \Omega \to \mathbb{R}^3$. Furthermore, $\boldsymbol{\sigma} : \Omega \to \mathbb{R}^{3\times3}$ denotes the second order Cauchy stress tensor (see Chapter 2).

3.1.1 Constitutive equations

Due to the analogy to piezomagnetic materials, the constitutive equations of biased magnetostrictive materials can be derived using a thermodynamical ansatz and considering the Taylor approximation of the coupled free-energy density function $\Psi(\boldsymbol{\epsilon}, \boldsymbol{H})$ that depends on the elastic strain $\boldsymbol{\epsilon}$ and the magnetic field $\boldsymbol{H}$. Since only a linear approximation is considered, Ψ can be written as [82, 95]

$$\Psi(\boldsymbol{\epsilon}, \boldsymbol{H}) = \frac{1}{2} \boldsymbol{H} \cdot \frac{\partial^2 \Psi}{\partial \boldsymbol{H} \partial \boldsymbol{H}} \cdot \boldsymbol{H} + \boldsymbol{\epsilon} : \frac{\partial^2 \Psi}{\partial \boldsymbol{\epsilon} \partial \boldsymbol{H}} \cdot \boldsymbol{H} - \frac{1}{2} \boldsymbol{\epsilon} : \frac{\partial^2 \Psi}{\partial \boldsymbol{\epsilon} \partial \boldsymbol{\epsilon}} : \boldsymbol{\epsilon}, \tag{3.1}$$

where the first summand describes the stored magnetic energy, the second one represents the magnetomechanical part and the third term the stored mechanical energy. The second order derivatives in Equation (3.1) are assumed to be constant and result in the material tensors

$$\boldsymbol{\mu}^{\boldsymbol{\epsilon}} := \frac{\partial^2 \Psi}{\partial \boldsymbol{H} \partial \boldsymbol{H}}, \qquad \boldsymbol{e} := \frac{\partial^2 \Psi}{\partial \boldsymbol{\epsilon} \partial \boldsymbol{H}}, \qquad \boldsymbol{C}^{\boldsymbol{H}} := \frac{\partial^2 \Psi}{\partial \boldsymbol{\epsilon} \partial \boldsymbol{\epsilon}}. \tag{3.2}$$

The fourth order tensor $\boldsymbol{C}^{\boldsymbol{H}} \in \mathbb{R}^{3\times3\times3\times3}$ is defined as the tensor of linear elasticity for a constant magnetic field. As explained in Chapter 2, it can be reduced to a symmetric,

positive definite matrix. Furthermore, $\boldsymbol{\mu}^{\epsilon} \in \mathbb{R}^{3\times3}$ is the second order magnetic permeability tensor for constant strain. Adopting the piezomagnetic nomenclature, $\boldsymbol{\mu}^{\epsilon}$ can be considered as a diagonal matrix with positive entries $\mu_{ii} > 0$, $i = 1,2,3$. The coupling tensor $\boldsymbol{e} \in \mathbb{R}^{3\times3\times3}$ is of order three but can be reduced to a matrix in $\mathbb{R}^{6\times3}$ for materials with a certain polycrystalline structure. This transformation will be explained in Section 3.4.1
The coupled elastic and magnetic quantities can be determined as derivatives of the energy density function. In the resulting linearized constitutive relations, the bias is included in the constant material tensors. In this manner, a system of coupled constitutive relations is obtained, similar to those of piezoelectric or piezomagnetic materials:

$$\begin{aligned} \boldsymbol{\sigma}(\boldsymbol{\epsilon}, \boldsymbol{H}) &= -\frac{\partial \Psi}{\partial \boldsymbol{\epsilon}} = \boldsymbol{C}^{H} : \boldsymbol{\epsilon} - \boldsymbol{e} \cdot \boldsymbol{H}, \\ \boldsymbol{B}(\boldsymbol{\epsilon}, \boldsymbol{H}) &= \frac{\partial \Psi}{\partial \boldsymbol{H}} = \boldsymbol{e}^{T} : \boldsymbol{\epsilon} + \boldsymbol{\mu}^{\epsilon} \boldsymbol{H}. \end{aligned} \tag{3.3}$$

Note that the elastic strain $\boldsymbol{\epsilon}$ and the magnetic field $\boldsymbol{H}$ are the independent variables in the above system of equations, whereas the stress $\boldsymbol{\sigma}$ and the magnetic flux density $\boldsymbol{B}$ are coupled variables depending on both mechanical and magnetic quantities.
The dot product (single inner product) of the third order tensor $\boldsymbol{e}$ and the vector $\boldsymbol{H}$ can be defined componentwise by

$$(\boldsymbol{e} \cdot \boldsymbol{H})_{ij} := \sum_{k=1}^{3} e_{ijk} H_k.$$

Similarly, the double inner product of $\boldsymbol{e}^{T}$ and the second order tensor $\boldsymbol{\epsilon}$ has the componentwise definition

$$(\boldsymbol{e}^{T} : \boldsymbol{\epsilon})_k := \sum_{j,k=1}^{3} e_{kij} \epsilon_{ji}.$$

The product $\boldsymbol{C}^{H} : \boldsymbol{\epsilon}$ was already defined in Section 2.1 and yields a second order tensor.
Throughout the thesis, we will use the dot notation to refer to the single inner product of a third order tensor and a vector, as defined above, as well as to the scalar product of two vectors. Since only few third order tensors will appear in the presented models, the notation will not cause ambiguity.
Assuming a static curl-free magnetic field, we can use the magnetic scalar potential $\Psi : \Omega \to \mathbb{R}$ with $\boldsymbol{H} = -\nabla\Psi$. Then, the above system can is reformulated as

$$\begin{aligned} \boldsymbol{\sigma}(\boldsymbol{u}, \Psi) &= \boldsymbol{C}^{H} : \boldsymbol{\epsilon}(\boldsymbol{u}) + \boldsymbol{e} \cdot \nabla\Psi, \\ \boldsymbol{B}(\boldsymbol{u}, \Psi) &= \boldsymbol{e}^{T} : \boldsymbol{\epsilon}(\boldsymbol{u}) - \boldsymbol{\mu}^{\epsilon} \nabla\Psi. \end{aligned} \tag{3.4}$$

3.1.2 Strong and weak formulations

Let $\Omega \subset \mathbb{R}^3$ describe the magnetoelastic domain. As in the previous chapters, we suppose that Ω is an open, bounded and simply connected set in $\mathbb{R}^3$ with a Lipschitz continuous boundary $\partial\Omega$. Furthermore, let Γ_D and Γ_N, as well as $\Gamma_{c,D}$ and $\Gamma_{c,N}$ denote the (non-overlapping) elastic and magnetic Dirichlet and Neumann boundaries, respectively, with $\partial\Omega = \overline{\Gamma}_D \cup \overline{\Gamma}_N$ and $\partial\Omega = \overline{\Gamma}_{c,D} \cup \overline{\Gamma}_{c,N}$. Furthermore, we assume that $\Gamma_D \subseteq \Gamma_{c,D}$ and prescribe homogeneous Dirichlet boundary conditions, i.e.

$$\boldsymbol{u} = \boldsymbol{0} \quad \text{on } \Gamma_D \qquad \text{and} \quad \Psi = 0 \qquad \text{on } \Gamma_{c,D}.$$

Moreover, by $\boldsymbol{\tau} = \boldsymbol{\sigma}(\boldsymbol{u}, \Psi) \cdot \boldsymbol{n}$ and $-\tilde{B} = \boldsymbol{B}(\boldsymbol{u}, \Psi) \cdot \boldsymbol{n}$, $\boldsymbol{\tau} \in \mathbb{R}^3$, $\tilde{\boldsymbol{B}} \in \mathbb{R}$, we denote the prescribed values of $\boldsymbol{\sigma}(\boldsymbol{u}, \Psi)$ and $\boldsymbol{B}(\boldsymbol{u}, \Psi)$ on the boundaries Γ_N and $\Gamma_{c,N}$, respectively,

with the outer normal vector $\boldsymbol{n} \in \mathbb{R}^3$. We use a special case of Hamilton's principle applied to the stationary setting using the Lagrangian L of the system,

$$L = W_{mag} - U, \tag{3.5}$$

where W_{mag} is the magnetic energy and U is the potential energy defined as

$$U(\boldsymbol{u}, \Psi) = \frac{1}{2} \int_{\Omega} \boldsymbol{\sigma}(\boldsymbol{u}, \Psi) : \boldsymbol{\epsilon}(\boldsymbol{u}) \, \mathrm{d}x - \int_{\Gamma_N} \boldsymbol{u} \cdot \boldsymbol{\tau} \, \mathrm{d}s, \tag{3.6}$$

$$W_{mag}(\boldsymbol{u}, \Psi) = \frac{1}{2} \int_{\Omega} \boldsymbol{H}(\Psi) \cdot \boldsymbol{B}(\boldsymbol{u}, \Psi) \, \mathrm{d}x - \int_{\Gamma_{c,N}} \Psi \tilde{B} \, \mathrm{d}s. \tag{3.7}$$

The Lagrangian is the difference between the internal mechanical and magnetic energies and does not include terms representing the electric energy or kinetic energy. The potential energy U and the magnetic energy W_{mag} can each be expressed as sum of the strain energy or magnetostatic energy, respectively, and terms defining elastic and magnetic surface forces, as explained in Chapter 2. The idea behind the different signs of the magnetic and mechanical energy terms can be ascribed to the distinction of *energy* and *coenergy*, indicating that the choice of the independent variables in the constitutive equations influences the signs of the magnetic and mechanical terms in (3.5). In the above energy formulation, the magnetic part can be characterized as a *coenergy* term with $\boldsymbol{H}$ as the independent (uncoupled) variable, while the formulation of the mechanical part constitutes an *energy* term with the uncoupled variable $\boldsymbol{\epsilon}$. We will come back to this issue in Chapter 4 with an elaborate discussion of the constitutive equations deriving from different considerations of the system's energy and coenergy.
The functions U and W_{mag} depend on the elastic displacement $\boldsymbol{u}$ and the magnetic scalar potential Ψ since the coupling is implemented by the dependent variables $\boldsymbol{\sigma}$ and $\boldsymbol{B}$ through the constitutive equations (3.4).

To derive the strong and weak formulations of the coupled problem, a variational approach can be used. Consider the variations $\theta\boldsymbol{v}$ for $\boldsymbol{u}$ and $\theta\Phi$ for Ψ with test functions $\boldsymbol{v} : \Omega \to \mathbb{R}^3$ and $\Phi : \Omega \to \mathbb{R}$ and a parameter $\theta \in \mathbb{R}$. The admissible test functions and the perturbed variables $\boldsymbol{u} + \theta\boldsymbol{v}$ and $\Psi + \theta\Phi$ must satisfy the given homogeneous Dirichlet boundary conditions

$$\begin{aligned} \boldsymbol{v}(\boldsymbol{x}) &= \boldsymbol{0}, \qquad \boldsymbol{u} + \theta\boldsymbol{v} = \boldsymbol{0} \quad \text{on } \Gamma_D, \\ \Phi(x) &= 0, \qquad \Psi + \theta\Phi = 0 \quad \text{on } \Gamma_{c,D}. \end{aligned}$$

For the function $J : \mathbb{R} \to \mathbb{R}$ defined as

$$J(\theta) := W_{mag}(\boldsymbol{u}, \Psi + \theta\Phi) - U(\boldsymbol{u} + \theta\boldsymbol{v}, \Psi),$$

the principle states that

$$\left. \frac{dJ(\theta)}{d\theta} \right|_{\theta=0} \stackrel{!}{=} 0.$$

Inserting the constitutive equations (3.4) into the expressions for the magnetic and elastic energies leads to

$$\begin{aligned} J(\theta) = {} & \frac{1}{2} \int_{\Omega} -\nabla(\Psi + \theta\Phi)(\boldsymbol{e}^T : \boldsymbol{\epsilon}(\boldsymbol{u}) - \boldsymbol{\mu}^{\epsilon} \nabla(\Psi + \theta\Phi)) \, \mathrm{d}x - \int_{\Gamma_{c,N}} (\Psi + \theta\Phi)\tilde{B} \, \mathrm{d}s \\ & - \frac{1}{2} \int_{\Omega} (\boldsymbol{C}^H : \boldsymbol{\epsilon}(\boldsymbol{u} + \theta\boldsymbol{v}) + \boldsymbol{e} \cdot \nabla\Psi) : \boldsymbol{\epsilon}(\boldsymbol{u} + \theta\boldsymbol{v}) \, \mathrm{d}x + \int_{\Gamma_N} (\boldsymbol{u} + \theta\boldsymbol{v}) \cdot \boldsymbol{\tau} \, \mathrm{d}s. \end{aligned} \tag{3.8}$$

Differentiation with respect to θ yields

$$\begin{aligned} 0 = \left.\frac{dJ(\theta)}{d\theta}\right|_{\theta=0} &= \frac{1}{2}\int_\Omega 2(\boldsymbol{\mu}^{\boldsymbol{\epsilon}}\nabla\Psi)\nabla\Phi - \nabla\Phi(\boldsymbol{e}^T : \boldsymbol{\epsilon}(\boldsymbol{u}))\,\mathrm{d}x - \int_{\Gamma_{c,N}} \Phi\tilde{B}\,\mathrm{d}s \\ &- \frac{1}{2}\int_\Omega (\boldsymbol{C}^H : \boldsymbol{\epsilon}(\boldsymbol{v})) : \boldsymbol{\epsilon}(\boldsymbol{u}) + \boldsymbol{\sigma}(\boldsymbol{u},\Psi) : \boldsymbol{\epsilon}(\boldsymbol{v})\,\mathrm{d}x + \int_{\Gamma_N} \boldsymbol{v}\cdot\boldsymbol{\tau}\,\mathrm{d}s, \end{aligned} \tag{3.9}$$

where the relation $\nabla\Phi\cdot(\boldsymbol{\mu}^{\boldsymbol{\epsilon}}\nabla\Psi) = \nabla\Psi\cdot(\boldsymbol{\mu}^{\boldsymbol{\epsilon}}\nabla\Phi)$ has been taken into account.
Using the definition of the strain tensor, we can reformulate:

$$\int_\Omega \boldsymbol{\sigma}(\boldsymbol{u},\Psi) : \boldsymbol{\epsilon}(\boldsymbol{v})\,\mathrm{d}x = \int_\Omega \boldsymbol{\sigma}(\boldsymbol{u},\Psi) : \nabla\boldsymbol{v}\,\mathrm{d}x. \tag{3.10}$$

The transformation (3.10) requires the coupled tensor $\boldsymbol{\sigma}(\boldsymbol{u},\Psi)$ to be symmetric. Its elastic part $\boldsymbol{C}^H : \boldsymbol{\epsilon}(\boldsymbol{u})$ is symmetric by definition, whereas the term $\boldsymbol{e}\cdot\boldsymbol{H}$ yields a second order tensor $\boldsymbol{G}$ whose components are defined by the single inner product

$$G_{ij} = \sum_{k=1}^{3} e_{ijk}H_k.$$

Due to the definition

$$e_{ijk} = \frac{\partial^2\Psi}{\partial\epsilon_{ij}H_k}$$

and the symmetry of the strain tensor, the third order tensor $\boldsymbol{e}$ is symmetric in the components i and j, which directly yields the symmetry of $\boldsymbol{G}$. Furthermore, Gauss' theorem implies that

$$\int_{\Gamma_N} \boldsymbol{v}\cdot(\boldsymbol{\sigma}(\boldsymbol{u},\Psi)\boldsymbol{n})\,\mathrm{d}s = \int_\Omega \boldsymbol{\sigma}(\boldsymbol{u},\Psi) : \nabla\boldsymbol{v}\,\mathrm{d}x + \int_\Omega \boldsymbol{v}\cdot\mathbf{div}\,\boldsymbol{\sigma}(\boldsymbol{u},\Psi)\,\mathrm{d}x,$$

and thus

$$\begin{aligned} \int_\Omega \boldsymbol{\sigma}(\boldsymbol{u},\Psi) : \boldsymbol{\epsilon}(\boldsymbol{v})\,\mathrm{d}x &= \int_\Omega \boldsymbol{\sigma}(\boldsymbol{u},\Psi) : \nabla\boldsymbol{v}\,\mathrm{d}x \\ &= \int_{\Gamma_N} \boldsymbol{v}\cdot(\boldsymbol{\sigma}(\boldsymbol{u},\Psi)\boldsymbol{n})\,\mathrm{d}s - \int_\Omega \boldsymbol{v}\cdot\mathbf{div}\,\boldsymbol{\sigma}(\boldsymbol{u},\Psi)\,\mathrm{d}x. \end{aligned} \tag{3.11}$$

Similar computations can be carried out for the magnetic scalar potential Ψ and the elastic strain $\boldsymbol{\epsilon}$,

$$\int_\Omega (\boldsymbol{\mu}^{\epsilon}\nabla\Psi)\cdot\nabla\Phi\,\mathrm{d}x = \int_{\Gamma_{c,N}} \Phi(\boldsymbol{\mu}^{\epsilon}\nabla\Psi)\cdot\boldsymbol{n}\,\mathrm{d}s - \int_\Omega \Phi\,\mathrm{div}(\boldsymbol{\mu}^{\epsilon}\nabla\Psi)\,\mathrm{d}x\,, \tag{3.12}$$

$$\int_\Omega (\boldsymbol{C}^H : \boldsymbol{\epsilon}(\boldsymbol{u})) : \boldsymbol{\epsilon}(\boldsymbol{v})\,\mathrm{d}x = \int_{\Gamma_N} \boldsymbol{v}\cdot(\boldsymbol{C}^{\boldsymbol{H}} : \boldsymbol{\epsilon}(\boldsymbol{u}))\boldsymbol{n}\,\mathrm{d}s - \int_\Omega \boldsymbol{v}\cdot\mathbf{div}(\boldsymbol{C}^H : \boldsymbol{\epsilon}(\boldsymbol{u}))\,\mathrm{d}x\,, \tag{3.13}$$

where $(\boldsymbol{C}^H : \boldsymbol{\epsilon}(\boldsymbol{v})) : \boldsymbol{\epsilon}(\boldsymbol{u}) = (\boldsymbol{C}^H : \boldsymbol{\epsilon}(\boldsymbol{u})) : \boldsymbol{\epsilon}(\boldsymbol{v})$ holds due to the commutativity of the double inner product of second order tensors.
Inserting Equations (3.11)–(3.13) into the expression (3.9) results in

$$\begin{aligned} 0 = &\int_\Omega \boldsymbol{v}\cdot\left(\frac{1}{2}\mathbf{div}\,\boldsymbol{\sigma} + \frac{1}{2}\mathbf{div}(\boldsymbol{C}^H : \boldsymbol{\epsilon}(\boldsymbol{u}))\right)\mathrm{d}x - \int_\Omega \Phi\,\mathrm{div}(\boldsymbol{\mu}^{\epsilon}\nabla\Psi) + \frac{1}{2}\nabla\Phi\cdot(\boldsymbol{e}^T : \boldsymbol{\epsilon}(\boldsymbol{u}))\,\mathrm{d}x \\ &- \int_{\Gamma_N} \boldsymbol{v}\cdot\left(\frac{1}{2}\boldsymbol{\sigma}(\boldsymbol{u},\Psi)\boldsymbol{n} + \frac{1}{2}(\boldsymbol{C}^H : \boldsymbol{\epsilon}(\boldsymbol{u}))\boldsymbol{n} - \boldsymbol{\tau}\right)\mathrm{d}s - \int_{\Gamma_{c,N}} -\Phi\left((\boldsymbol{\mu}^{\epsilon}\nabla\Psi)\cdot\boldsymbol{n} - \tilde{B}\right)\mathrm{d}s. \end{aligned} \tag{3.14}$$

Once again applying Green's formula

$$\int_\Omega \nabla\Phi \cdot (\boldsymbol{e}^T : \boldsymbol{\epsilon}(\boldsymbol{u}))\,\mathrm{d}x = \int_{\Gamma_{c,N}} \Phi(\boldsymbol{e}^T : \boldsymbol{\epsilon}(\boldsymbol{u})) \cdot \boldsymbol{n}\,\mathrm{d}s - \int_\Omega \Phi \operatorname{div}(\boldsymbol{e}^T : \boldsymbol{\epsilon}(\boldsymbol{u}))\,\mathrm{d}x,$$

finally, the variational formulation of the coupled problem can be derived,

$$\begin{aligned}
0 = &\int_\Omega \boldsymbol{v} \cdot \left(\frac{1}{2}\,\mathbf{div}\,\boldsymbol{\sigma}(\boldsymbol{u},\Psi) + \frac{1}{2}\,\mathbf{div}(\boldsymbol{C}^H : \boldsymbol{\epsilon}(\boldsymbol{u}))\right)\mathrm{d}x \\
&+ \int_\Omega \Phi\left(-\operatorname{div}(\boldsymbol{\mu}^\epsilon \nabla\Psi) + \frac{1}{2}\operatorname{div}(\boldsymbol{e}^T : \boldsymbol{\epsilon}(\boldsymbol{u}))\right)\mathrm{d}x \\
&- \int_{\Gamma_N} \boldsymbol{v} \cdot \left(\frac{1}{2}\boldsymbol{\sigma}(\boldsymbol{u},\Psi)\boldsymbol{n} + \frac{1}{2}(\boldsymbol{C}^H : \boldsymbol{\epsilon}(\boldsymbol{u}))\boldsymbol{n} - \boldsymbol{\tau}\right)\mathrm{d}s \\
&- \int_{\Gamma_{c,N}} \Phi\left((-\boldsymbol{\mu}^\epsilon \nabla\Psi)\boldsymbol{n} + \frac{1}{2}(\boldsymbol{e}^T : \boldsymbol{\epsilon}(\boldsymbol{u}))\cdot\boldsymbol{n} + \tilde{B}\right)\mathrm{d}s
\end{aligned} \tag{3.15}$$

for all admissible $\boldsymbol{v}$ and Φ. In particular, if $\boldsymbol{v} = \mathbf{0}$ on Γ_N and $\Phi = 0$ on $\Gamma_{c,N}$, Equation (3.15) reduces to

$$\begin{aligned}
0 \;=\; &\int_\Omega \boldsymbol{v} \cdot \left(\frac{1}{2}\,\mathbf{div}\,\boldsymbol{\sigma}(\boldsymbol{u},\Psi) + \frac{1}{2}\,\mathbf{div}(\boldsymbol{C}^H : \boldsymbol{\epsilon}(\boldsymbol{u}))\right)\mathrm{d}s \\
+ &\int_\Omega \Phi\left(\operatorname{div}(\boldsymbol{\mu}^\epsilon \nabla\Psi) + \frac{1}{2}\operatorname{div}(\boldsymbol{e}^T : \boldsymbol{\epsilon}(\boldsymbol{u}))\right)\mathrm{d}s,
\end{aligned} \tag{3.16}$$

which suggests that both integrals must vanish. Using the fundamental lemma of calculus of variations [44], we can deduce that the integrands of both integrals must vanish, too. In case that $\boldsymbol{v}$ and Φ are not equal to zero on the Neumann boundaries, the above considerations lead to the equation

$$\begin{aligned}
0 \;=\; &\int_{\Gamma_N} \boldsymbol{v} \cdot \left(\frac{1}{2}\boldsymbol{\sigma}(\boldsymbol{u},\Psi)\boldsymbol{n} + \frac{1}{2}(\boldsymbol{C}^{\boldsymbol{H}} : \boldsymbol{\epsilon}(\boldsymbol{u}))\boldsymbol{n} - \boldsymbol{\tau}\right)\mathrm{d}s \\
+ &\int_{\Gamma_{c,N}} \Phi\left((-\boldsymbol{\mu}^\epsilon \nabla\Psi)\cdot\boldsymbol{n} + \frac{1}{2}(\boldsymbol{e}^T : \boldsymbol{\epsilon}(\boldsymbol{u}))\cdot\boldsymbol{n} + \tilde{B}\right)\mathrm{d}s,
\end{aligned} \tag{3.17}$$

yielding the Neumann boundary conditions for the elastic and magnetic boundaries.
With this preliminary work, we can finally state the strong form of the coupled problem:

Problem (CP): Find $(\boldsymbol{u},\Psi) \in C^2(\Omega)^3 \times C^2(\Omega)$, such that

$$\begin{aligned}
\mathbf{div}(\boldsymbol{C}^{\boldsymbol{H}} : \boldsymbol{\epsilon}(\boldsymbol{u})) + \frac{1}{2}\,\mathbf{div}(\boldsymbol{e}\cdot\nabla\Psi) &= \mathbf{0} \quad \text{in } \Omega, \\
\frac{1}{2}\operatorname{div}(\boldsymbol{e}^T : \boldsymbol{\epsilon}(\boldsymbol{u})) - \operatorname{div}(\boldsymbol{\mu}^\epsilon \cdot \nabla\Psi) &= 0 \quad \text{in } \Omega,
\end{aligned}$$

with Dirichlet boundary conditions

$$\begin{aligned}
\boldsymbol{u} &= \mathbf{0} \quad \text{on } \Gamma_D, \\
\Psi &= 0 \quad \text{on } \Gamma_{c,D},
\end{aligned}$$

and Neumann boundary conditions

$$\begin{aligned}\left(\boldsymbol{C}^H : \boldsymbol{\epsilon}(\boldsymbol{u}) + \frac{1}{2}\boldsymbol{e}\cdot\nabla\Psi\right)\boldsymbol{n} &= \boldsymbol{\tau} \quad \text{on } \Gamma_N,\\ \left(\frac{1}{2}\boldsymbol{e}^T : \boldsymbol{\epsilon}(\boldsymbol{u}) - \boldsymbol{\mu}^\epsilon\nabla\Psi\right)\cdot\boldsymbol{n} &= -\tilde{B} \quad \text{on } \Gamma_{c,N},\end{aligned}$$

where the linearity of the divergence operator has been used.
Following back the steps of the above derivation, the weak formulation of (CP) can be deduced. Multiplication of the strong form with test functions $\boldsymbol{v}$, $\boldsymbol{v} = \boldsymbol{0}$ on Γ_D, and Φ with $\Phi = 0$ on $\Gamma_{c,D}$, integration and use of Green's formula yields the system of equations

$$\begin{aligned}0 &= \int_{\Gamma_N} \boldsymbol{v}\cdot(\boldsymbol{C}^H : \boldsymbol{\epsilon}(\boldsymbol{u}))\cdot\boldsymbol{n}\,\mathrm{d}s - \int_\Omega \nabla\boldsymbol{v} : (\boldsymbol{C}^H : \boldsymbol{\epsilon}(\boldsymbol{u}))\,\mathrm{d}x\\ &+ \frac{1}{2}\int_{\Gamma_N} \boldsymbol{v}\cdot(\boldsymbol{e}\cdot\nabla\Psi)\boldsymbol{n}\,\mathrm{d}s - \frac{1}{2}\int_\Omega \nabla\boldsymbol{v} : (\boldsymbol{e}^T\cdot\nabla\Psi)\,\mathrm{d}x,\\ 0 &= \frac{1}{2}\int_{\Gamma_{c,N}} \Phi(\boldsymbol{e} : \boldsymbol{\epsilon}(\boldsymbol{u}))\cdot\boldsymbol{n}\,\mathrm{d}s - \frac{1}{2}\int_\Omega \nabla\Phi\cdot(\boldsymbol{e} : \boldsymbol{\epsilon}(\boldsymbol{u}))\,\mathrm{d}x\\ &- \int_{\Gamma_{c,N}} \Phi(\boldsymbol{\mu}^\epsilon\nabla\Psi)\cdot\boldsymbol{n}\,\mathrm{d}s + \int_\Omega \nabla\Phi\cdot(\boldsymbol{\mu}^\epsilon\nabla\Psi)\,\mathrm{d}x,\end{aligned}$$

which finally results in the following weak formulation:

$$\begin{aligned}0 &= \int_\Omega \nabla\boldsymbol{v} : \left(\boldsymbol{C}^H : \boldsymbol{\epsilon}(\boldsymbol{u}) + \frac{1}{2}\boldsymbol{e}^T\cdot\nabla\Psi\right)\mathrm{d}x - \int_{\Gamma_N} \boldsymbol{v}\cdot\left(\boldsymbol{C}^H : \boldsymbol{\epsilon}(\boldsymbol{u}) + \frac{1}{2}\boldsymbol{e}^T\cdot\nabla\Psi\right)\boldsymbol{n}\,\mathrm{d}s,\\ 0 &= \int_\Omega \nabla\Phi\cdot\left(\frac{1}{2}\boldsymbol{e} : \boldsymbol{\epsilon}(\boldsymbol{u}) - \boldsymbol{\mu}^\epsilon\nabla\Psi\right)\mathrm{d}x - \int_{\Gamma_{c,N}} \Phi\left(\frac{1}{2}\boldsymbol{e} : \boldsymbol{\epsilon}(\boldsymbol{u}) - \boldsymbol{\mu}^\epsilon\nabla\Psi\right)\cdot\boldsymbol{n}\,\mathrm{d}s. \qquad (3.18)\end{aligned}$$

The system (3.18) can be reformulated in terms of bilinear forms and linear functionals. Let the spaces of test functions be defined as

$$\begin{aligned}\mathcal{V} &:= (H^1(\Omega))^3,\\ \mathcal{V}_0 &:= \{\boldsymbol{v}\in\mathcal{V} \mid v_i = 0 \text{ on } \Gamma_D,\ i = 1,2,3\},\\ \mathcal{M} &:= H^1(\Omega),\\ \mathcal{M}_0 &:= \{\Phi\in\mathcal{M} \mid \Phi = 0 \text{ on } \Gamma_{c,D}\}.\end{aligned}$$

The above function spaces are Hilbert spaces with corresponding norms $\|\cdot\|_{\mathcal{V}}$ and $\|\cdot\|_{\mathcal{M}}$. Then, the weak form of the coupled problem reads:

Problem $(CP)^w$: Find $(\boldsymbol{u},\Psi)\in\mathcal{V}_0\times\mathcal{M}_0$, such that

$$\begin{aligned}a(\boldsymbol{u},\boldsymbol{v}) + c(\boldsymbol{v},\Psi) &= l(\boldsymbol{v}) \qquad &\boldsymbol{v}\in\mathcal{V}_0,\\ c(\boldsymbol{u},\Phi) - b(\Psi,\Phi) &= m(\Phi) \qquad &\Phi\in\mathcal{M}_0,\end{aligned}$$

with

$$a(\boldsymbol{u},\boldsymbol{v}) = \int_\Omega \nabla\boldsymbol{v} : (\boldsymbol{C^H} : \boldsymbol{\epsilon}(\boldsymbol{u}))\,\mathrm{d}x = \int_\Omega (\boldsymbol{C^H} : \boldsymbol{\epsilon}(\boldsymbol{u})) : \boldsymbol{\epsilon}(\boldsymbol{v})\,\mathrm{d}x, \tag{3.19}$$

$$b(\Psi,\Phi) = \int_\Omega \nabla\Phi \cdot (\boldsymbol{\mu^\epsilon}\nabla\Psi)\,\mathrm{d}x, \tag{3.20}$$

$$c(\boldsymbol{v},\Psi) = \frac{1}{2}\int_\Omega \boldsymbol{\nabla v} : (\boldsymbol{e}\cdot\nabla\Psi)\,\mathrm{d}x = \frac{1}{2}\int_\Omega \boldsymbol{\epsilon}(\boldsymbol{v}) : (\boldsymbol{e}\nabla\Psi)\,\mathrm{d}x, \tag{3.21}$$

$$l(\boldsymbol{v}) = \int_{\Gamma_N} \boldsymbol{v}\cdot\boldsymbol{\tau}\,\mathrm{d}s, \tag{3.22}$$

$$m(\Phi) = -\int_{\Gamma_{c,N}} \Phi\tilde{B}\,\mathrm{d}s, \tag{3.23}$$

where the bilinear forms $a : \mathcal{V}_0 \times \mathcal{V}_0 \to \mathbb{R}$ and $b : \mathcal{M}_0 \times \mathcal{M}_0 \to \mathbb{R}$ correspond to the purely elastic and purely magnetic influence, respectively, the bilinear form $c : \mathcal{V}_0 \times \mathcal{M}_0 \to \mathbb{R}$ describes the coupling between the two fields and the linear functionals $l : \mathcal{V}_0 \to \mathbb{R}$ and $m : \mathcal{M}_0 \to \mathbb{R}$ represent the magnetic and elastic surface forces.

So far $\boldsymbol{C}^H$, $\boldsymbol{\mu}^\epsilon$ and $\boldsymbol{e}$ only appeared in their general form as tensors. However, exploiting the symmetries of the tensors of linear elasticity and following the Voigt notation (Section 2.1), the above expressions can be simplified. This will be especially useful in the next section, where the examination of the properties of the system and its bilinear forms requires a vivid formulation of the respective expressions.
Instead of using tensors of order three and higher, we can thus restrict ourselves to tensors of order one and two. The stress and strain tensors then have the representation (see Section 2.1),

$$\begin{aligned}\boldsymbol{\sigma} &= (\sigma_1,\sigma_2,\sigma_3,\sigma_4,\sigma_5,\sigma_6)^T := (\sigma_{11},\sigma_{22},\sigma_{33},\sigma_{23},\sigma_{13},\sigma_{12})^T,\\ \boldsymbol{\epsilon} &= (\epsilon_1,\epsilon_2,\epsilon_3,\epsilon_4,\epsilon_5,\epsilon_6)^T := (\epsilon_{11},\epsilon_{22},\epsilon_{33},2\epsilon_{23},2\epsilon_{13},2\epsilon_{12})^T.\end{aligned} \tag{3.24}$$

In a similar manner, the coupling tensor $\boldsymbol{e} \in \mathbb{R}^{3\times3\times3}$ can be turned into a 6×3 - matrix. An examination with respect to the underlying crystallographic structure of the given material allows a further simplification of the matrix [92]. A detailed characterization of the above matrices for a specific material class will be given in Section 3.4.1.

3.2 Existence and uniqueness of the solution

Having derived the strong and weak form of the coupled magnetoelastic problem in the previous section, we will now analyze the structure of the resulting system of partial differential equations and address the question of existence and uniqueness of its solution. To accomplish this, we first need to verify some important properties of the aforementioned bilinear forms. We start with showing the basic property of continuity for all three bilinear forms. For the analysis, we will switch from the general tensor notation to the vector and matrix-notation and assume that $\boldsymbol{C}^H \in \mathbb{R}^{6\times 6}$, $\boldsymbol{e} \in \mathbb{R}^{6\times 3}$ and $\boldsymbol{\epsilon}, \boldsymbol{\sigma} \in \mathbb{R}^6$.

Lemma 3.1. *The bilinear forms $a : \mathcal{V}_0 \times \mathcal{V}_0 \to \mathbb{R}$, $b : \mathcal{M}_0 \times \mathcal{M}_0 \to \mathbb{R}$ and $c : \mathcal{V}_0 \times \mathcal{M}_0 \to \mathbb{R}$ defined in* (3.19) – (3.21) *are continuous.*

Proof. The continuity of the bilinear form of linear elasticity is already known (see e.g. [21]). To prove the continuity of the bilinear form $b(\cdot,\cdot)$, we have to show that there exists a constant $b_0 > 0$, such that

$$|b(\Psi,\Phi)| \le b_0 \|\Psi\|_1 \|\Phi\|_1 \qquad \text{for all} \quad \Psi,\Phi \in \mathcal{M}_0,$$

where $\|\Psi\|_1$ denotes the $H^1(\Omega)$-norm and $|\Psi|_1$ the corresponding seminorm, as defined in the previous chapter. Using Equation (3.20), the following estimate can be made,

$$\begin{aligned} b(\Psi,\Phi) &= \int_\Omega \sum_{i=1}^3 \mu_{ii} \left(\frac{\partial \Psi}{\partial x_i}\right)\left(\frac{\partial \Phi}{\partial x_i}\right) \mathrm{d}x \\ &\le \max_{i=1,2,3} \mu_{ii} \sum_{i=1}^3 \int_\Omega \left|\frac{\partial \Psi}{\partial x_i}\frac{\partial \Phi}{\partial x_i}\right| \mathrm{d}x \\ &\le \mu_M \sum_{i=1}^3 \sqrt{\int_\Omega \left(\frac{\partial \Psi}{\partial x_i}\right)^2 \mathrm{d}x \int_\Omega \left(\frac{\partial \Phi}{\partial x_i}\right)^2 \mathrm{d}x}, \end{aligned}$$

where $\mu_M := \max_{i=1,2,3} \mu_{ii}$, $\mu_{ii} > 0$ and the last step follows from the Cauchy-Schwarz-inequality [85] for the Hilbert space $L^2(\Omega)$. On the other hand,

$$\begin{aligned} \|\Psi\|_1 \|\Phi\|_1 \ge |\Psi|_1 |\Phi|_1 &= \sqrt{\int_\Omega \sum_{i=1}^3 \left(\frac{\partial \Psi}{\partial x_i}\right)^2 \mathrm{d}x} \sqrt{\int_\Omega \sum_{i=1}^3 \left(\frac{\partial \Phi}{\partial x_i}\right)^2 \mathrm{d}x} \\ &= \sqrt{\sum_{i=1}^3 \sum_{j=1}^3 \int_\Omega \left(\frac{\partial \Psi}{\partial x_i}\right)^2 \mathrm{d}x \int_\Omega \left(\frac{\partial \Phi}{\partial x_j}\right)^2 \mathrm{d}x} \\ &\ge \sqrt{\sum_{i=1}^3 \int_\Omega \left(\frac{\partial \Psi}{\partial x_i}\right)^2 \mathrm{d}x \int_\Omega \left(\frac{\partial \Phi}{\partial x_i}\right)^2 \mathrm{d}x}. \end{aligned}$$

Using the concavity of the root function on $\mathbb{R}_0^+$,

$$\sqrt{\frac{1}{2}A + \frac{1}{2}B} > \frac{1}{2}\sqrt{A} + \frac{1}{2}\sqrt{B} \qquad \forall A, B \in \mathbb{R}_0^+, \quad A \ne B$$

we can finally estimate:

$$\begin{aligned}
\sqrt{2}\mu_M \|\Psi\|_1 \|\Phi\|_1 &\geq \sqrt{2}\mu_M \sqrt{\sum_{i=1}^{3} \int_\Omega \left(\frac{\partial \Psi}{\partial x_i}\right)^2 \mathrm{d}x \int_\Omega \left(\frac{\partial \Phi}{\partial x_i}\right)^2 \mathrm{d}x} \\
&> \mu_M \left(\sum_{i=1}^{3} \sqrt{\int_\Omega \left(\frac{\partial \Psi}{\partial x_i}\right)^2 \mathrm{d}x \int_\Omega \left(\frac{\partial \Phi}{\partial x_i}\right)^2 \mathrm{d}x} \right) \\
&\geq b(\Psi, \Phi),
\end{aligned}$$

where the relation

$$\frac{1}{2\sqrt{2}} \sqrt{A + B + C} > \frac{1}{4}\sqrt{A} + \frac{1}{2}(\sqrt{B} + \sqrt{C})$$

has been used. Thus, continuity holds with the constant $b_0 := \sqrt{2}\mu_M$.
The continuity of $c(\cdot,\cdot)$ can be proven in a similar manner. Since $c(\boldsymbol{v}, \Psi)$ has the form

$$\begin{aligned}
c(\boldsymbol{v}, \Psi) &= \frac{1}{2} \int_\Omega \frac{\partial v_1}{\partial x_1} \left(\sum_{i=1}^{3} e_{i1} \frac{\partial \Psi}{\partial x_i} \right) + \frac{\partial v_2}{\partial x_2} \left(\sum_{i=1}^{3} e_{i2} \frac{\partial \Psi}{\partial x_i} \right) + \frac{\partial v_3}{\partial x_3} \left(\sum_{i=1}^{3} e_{i3} \frac{\partial \Psi}{\partial x_i} \right) \\
&+ \left(\frac{\partial v_2}{\partial x_3} + \frac{\partial v_3}{\partial x_2} \right) \left(\sum_{i=1}^{3} e_{i4} \frac{\partial \Psi}{\partial x_i} \right) + \left(\frac{\partial v_1}{\partial x_3} + \frac{\partial v_3}{\partial x_1} \right) \left(\sum_{i=1}^{3} e_{i5} \frac{\partial \Psi}{\partial x_i} \right) \\
&+ \left(\frac{\partial v_1}{\partial x_2} + \frac{\partial v_2}{\partial x_1} \right) \left(\sum_{i=1}^{3} e_{i6} \frac{\partial \Psi}{\partial x_i} \right) \mathrm{d}x,
\end{aligned}$$

with v_i, $i = 1, 2, 3$ denoting the components of $\boldsymbol{v}$, we can use again Cauchy-Schwarz and the concavity of the root function to obtain

$$\begin{aligned}
\frac{1}{2} c(\boldsymbol{v}, \Psi) &\leq \frac{1}{4} \max_{\substack{i=1,2,3, \\ l=1,\ldots,6}} |e_{ij}| \sum_{i,l=1}^{3} \int_\Omega \left| \frac{\partial v_i}{\partial x_l} \left(\sum_{k=1}^{3} \frac{\partial \Psi}{\partial x_k} \right) \right| \mathrm{d}x \\
&\leq \frac{1}{4} e_M \sum_{i,l=1}^{3} \sum_{k=1}^{3} \sqrt{\int_\Omega \left(\frac{\partial v_i}{\partial x_l}\right)^2 \mathrm{d}x \int_\Omega \left(\frac{\partial \Psi}{\partial x_k}\right)^2 \mathrm{d}x} \\
&< e_M \sum_{i,l=1}^{3} \sqrt{\int_\Omega \left(\frac{\partial v_i}{\partial x_l}\right)^2 \mathrm{d}x \sum_{k=1}^{3} \int_\Omega \left(\frac{\partial \Psi}{\partial x_k}\right)^2 \mathrm{d}x} \\
&< e_M \sqrt{\sum_{i,l=1}^{3} \int_\Omega \left(\frac{\partial v_i}{\partial x_l}\right)^2 \mathrm{d}x} \sqrt{\sum_{k=1}^{3} \int_\Omega \left(\frac{\partial \Psi}{\partial x_k}\right)^2 \mathrm{d}x} \\
&= e_M \, \|\boldsymbol{v}\|_{\mathcal{V}} \, \|\boldsymbol{\Psi}\|_{\mathcal{M}},
\end{aligned}$$

with $e_M := \max_{i,j} |e_{ij}|$ for $i = 1, 2, 3$ and $j = 1, \ldots, 6$. □

Moreover, the bilinear forms $a(\cdot,\cdot)$ and $b(\cdot,\cdot)$ are obviously symmetric and non-negative for all $\boldsymbol{v} \in \mathcal{V}_0$ and $\Phi \in \mathcal{M}_0$. Hence, the coupled system can be interpreted as a saddle point problem with the penalty term $b(\Psi, \Phi)$.
For a classical saddle point problem, i.e. in the absence of the bilinear form $b(\cdot,\cdot)$, *Brezzi's Splitting Theorem* [23] the fundamental theorem for saddle point problems, provides criteria for unique solvability.

Theorem 3.1. *(based on Brezzi's Splitting Theorem) A classical saddle point problem of type* $(CP)^w$ *with* $b(\cdot,\cdot) = 0$ *and continuous bilinear forms* $a(\cdot,\cdot)$ *and* $c(\cdot,\cdot)$*, where* $a(\cdot,\cdot)$ *is symmetric and non-negative on* $\mathcal{V}_0$*, has a unique solution, if and only if the following conditions hold:*

(a) The bilinear form $a(\cdot,\cdot)$ is elliptic on the kernel

$$\ker \mathcal{C} := \{\boldsymbol{v} \in \mathcal{V}_0 \mid c(v,\Psi) = 0 \ \ \forall \Psi \in \mathcal{M}_0\},$$

that is,

$$\exists \alpha > 0 \ \ s.t. \ \ a(\boldsymbol{v},\boldsymbol{v}) \geq \alpha \|\boldsymbol{v}\|_{\mathcal{V}}^2 \quad \forall \boldsymbol{v} \in \ker \mathcal{C}. \tag{3.25}$$

(b) The bilinear form $c(\cdot,\cdot)$ satisfies the inf-sup condition (LBB condition)

$$\exists \beta > 0 \ \ s.t. \ \ \inf_{\Psi \in \mathcal{M}_0} \sup_{\boldsymbol{v} \in \mathcal{V}_0} \frac{c(\boldsymbol{v},\Psi)}{\|\boldsymbol{v}\|_{\mathcal{V}} \|\Psi\|_{\mathcal{M}}} \geq \beta. \tag{3.26}$$

In this context, the following definition of stability in the sense of Babuška [6, 7] is of importance.

Definition 3.1. *A saddle point problem is said to be stable or inf-sup stable, iff the LBB condition is fulfilled.*

Braess [20] used the notion of stability to characterize the unique solvability of classical saddle point problems.
For penalized saddle point problems, additional conditions have to be imposed on the bilinear forms. A sufficient condition is the boundedness and non-negativity of the bilinear form $b(\cdot,\cdot)$ defining the penalty term [20, 21]. The penalty term can be regarded as a perturbation that, in most cases, stabilizes the saddle point problem.

Remark 3.1. *Note that in the formal definition of a saddle point problem with a penalty term, the bilinear form characterizing the penalty term is not necessarily defined on the whole Hilbert space $\mathcal{M}_0$, but rather on a dense subset $\mathcal{M}_c \subset \mathcal{M}_0$. However, if the bilinear form is bounded on $\mathcal{M}_c$, it can be continued to a continuous function and we can set $\mathcal{M}_c = \mathcal{M}_0$.*

The next theorem shows that all conditions stated above are satisfied for the coupled magnetoelastic saddle point problem $(CP)^w$. Before stating the theorem, we need to characterize a certain property of the coupling matrix $\boldsymbol{e}$ in the first instance.

Definition 3.2. *(Minimal positivity) Let $\boldsymbol{A}$ be a matrix in $\mathbb{R}^{6\times 3}$. We say that $\boldsymbol{A}$ satisfies the minimal positivity property iff its components a_{ij} fulfill the requirement*

$$\hat{A} := \min_{k=1,\ldots,6} \hat{A}_k > 0, \tag{3.27}$$

with $\hat{A}_k$ defined as

$$\begin{aligned}
\hat{A}_1 &:= \frac{1}{2}(a_{11} + a_{51} + a_{61}),\\
\hat{A}_2 &:= \frac{1}{2}(a_{22} + a_{42} + a_{62}),\\
\hat{A}_3 &:= \frac{1}{2}(a_{33} + a_{43} + a_{53}),\\
\hat{A}_4 &:= \frac{1}{2}(a_{12} + a_{21} + a_{41} + a_{52} + a_{61} + a_{62}),\\
\hat{A}_5 &:= \frac{1}{2}(a_{13} + a_{31} + a_{41} + a_{51} + a_{53} + a_{63}),\\
\hat{A}_6 &:= \frac{1}{2}(a_{23} + a_{32} + a_{42} + a_{43} + a_{52} + a_{63}).
\end{aligned}$$

Theorem 3.2. *The coupled saddle point problem* $(CP)^w$ *with bilinear forms and linear functionals as defined in* (3.19) – (3.23) *has a unique and uniformly bounded solution if the coupling matrix* $\boldsymbol{e}$ *fulfills the minimal positivity requirement* (3.27).

Remark 3.2. *Note that the property of minimal positivity serves as a purely mathematical characteristic of the coupling tensor. So far, no physical interpretation of this property could be found.*

Proof. Lemma 3.1 states that all three bilinear forms are continuous on the corresponding spaces. Moreover, both $a(\cdot,\cdot)$ and $b(\cdot,\cdot)$ are obviously symmetric and non-negative on $\mathcal{V}_0$ and $\mathcal{M}_0$, respectively. Thus, only the conditions (3.25) and (3.26) of Theorem 3.1 need to be verified.
The bilinear form $a(\cdot,\cdot)$ is in fact coercive on the whole space $\mathcal{V}_0$ rather than just on the kernel $\ker \mathcal{C} \subset \mathcal{V}_0$, which follows directly from Korn's inequality. To show the inf-sup condition for the bilinear form $c(\cdot,\cdot)$, we will prove the equivalent formulation:

Show that $\exists \beta > 0$ s.t.

$$\sup_{\boldsymbol{v}\in\mathcal{V}_0} \frac{c(\boldsymbol{v},\Psi)}{\|\boldsymbol{v}\|_{\mathcal{V}}} \geq \beta \|\Psi\|_{\mathcal{M}} \quad \forall \Psi \in \mathcal{M}_0.$$

The coupled bilinear form $c(\boldsymbol{v},\Psi)$ is given by

$$\begin{aligned} c(\boldsymbol{v},\Psi) &= \frac{1}{2}\int_\Omega \frac{\partial v_1}{\partial x_1}\left(\sum_{i=1}^3 e_{1i}\frac{\partial \Psi}{\partial x_i}\right) + \frac{\partial v_2}{\partial x_2}\left(\sum_{i=1}^3 e_{2i}\frac{\partial \Psi}{\partial x_i}\right) + \frac{\partial v_3}{\partial x_3}\left(\sum_{i=1}^3 e_{3i}\frac{\partial \Psi}{\partial x_i}\right) \\ &+ \left(\frac{\partial v_2}{\partial x_3}+\frac{\partial v_3}{\partial x_2}\right)\left(\sum_{i=1}^3 e_{4i}\frac{\partial \Psi}{\partial x_i}\right) + \left(\frac{\partial v_1}{\partial x_3}+\frac{\partial v_3}{\partial x_1}\right)\left(\sum_{i=1}^3 e_{5i}\frac{\partial \Psi}{\partial x_i}\right) \\ &+ \left(\frac{\partial v_1}{\partial x_2}+\frac{\partial v_2}{\partial x_1}\right)\left(\sum_{i=1}^3 e_{6i}\frac{\partial \Psi}{\partial x_i}\right) \mathrm{d}x, \end{aligned}$$

Choosing $v_i = \Psi$ for $i = 1,2,3$, we obtain

$$c(\boldsymbol{v},\Psi) = \frac{1}{2}\int_\Omega 2\sum_{i=1}^3 \left(\frac{\partial \Psi}{\partial x_i}\right)^2 \hat{E}_i + \frac{\partial \Psi}{\partial x_1}\frac{\partial \Psi}{\partial x_2}\hat{E}_4 + \frac{\partial \Psi}{\partial x_1}\frac{\partial \Psi}{\partial x_3}\hat{E}_5 + \frac{\partial \Psi}{\partial x_2}\frac{\partial \Psi}{\partial x_3}\hat{E}_6 \,\mathrm{d}x,$$

with $\hat{E}_i$, $i = 1,..,6$ as given in Definition 3.2. Since $\boldsymbol{e}$ satisfies the minimal positivity property (3.27), i.e.

$$\hat{E} := \min_{i=1,\dots,6} \hat{E}_i > 0,$$

we obtain the estimate

$$\begin{aligned} c(\boldsymbol{v},\Psi) &\geq \frac{1}{4}\hat{E}\int_\Omega 4\sum_{i=1}^3 \left(\frac{\partial \Psi}{\partial x_i}\right)^2 + \sum_{\substack{i,j=1\\ i\neq j}}^3 \frac{\partial \Psi}{\partial x_i}\frac{\partial \Psi}{\partial x_j}\,\mathrm{d}x \\ &= \frac{1}{4}\hat{E}\int_\Omega \sum_{i=1}^3 \left(\frac{\partial \Psi}{\partial x_i}\right)^2 \mathrm{d}x \\ &+ \frac{1}{4}\hat{E}\int_\Omega \sum_{i=1}^3 \left(\frac{\partial \Psi}{\partial x_i}\right)^2 + \left(\frac{\partial \Psi}{\partial x_1}+\frac{\partial \Psi}{\partial x_2}\right)^2 + \left(\frac{\partial \Psi}{\partial x_1}+\frac{\partial \Psi}{\partial x_3}\right)^2 + \left(\frac{\partial \Psi}{\partial x_2}+\frac{\partial \Psi}{\partial x_3}\right)^2 \mathrm{d}x. \end{aligned}$$

Hence,

$$c(\boldsymbol{v},\Psi) \geq \frac{1}{4}\hat{E}|\boldsymbol{v}|_{\mathcal{V}}^2 + \frac{1}{4}\hat{E}\int_\Omega \boldsymbol{\epsilon}(\boldsymbol{v})\cdot\boldsymbol{\epsilon}(\boldsymbol{v})\,\mathrm{d}x,$$

with $|\boldsymbol{v}|_{\mathcal{V}}$ denoting the seminorm in $\mathcal{V} = H^1(\Omega)^3$, and we obtain the estimate

$$c(\boldsymbol{v}, \Psi) \geq \frac{1}{4}\hat{E} \int_{\Omega} \boldsymbol{\epsilon}(\boldsymbol{v}) : \boldsymbol{\epsilon}(\boldsymbol{v}) \, \mathrm{d}x \geq \frac{1}{4}\hat{E}C' \|\boldsymbol{v}\|_{\mathcal{V}}^2,$$

with a constant $C' = C'(\Omega, \Gamma_D)$ from Korn's inequality. For

$$\|\boldsymbol{v}\|_{\mathcal{V}} = \sqrt{\sum_{i=1}^{3} \|v_i\|_1^2},$$

the following estimate holds,

$$\begin{aligned} \|\boldsymbol{v}\|_{\mathcal{V}} &= \sqrt{\sum_{i=1}^{3} (\|v_i\|_0 + |v_i|_1)^2} \geq \sqrt{\sum_{i=1}^{3} |v_i|_1^2} \\ &= \sqrt{\int_{\Omega} \sum_{i,j=1}^{3} \left(\frac{\partial v_i}{\partial x_j}\right)^2 \mathrm{d}x}, \end{aligned}$$

where $\|\cdot\|_0$ and $\|\cdot\|_1$ denote the $L^2(\Omega)$-norm and the $H^1(\Omega)$-norm, respectively. On the other hand,

$$\|\Psi\|_1 = \sqrt{(\|\Psi\|_0 + |\Psi|_1)^2} \leq \sqrt{s^2 + 1}|\Psi|_1,$$

with a constant $s = s(\Omega)$ from the Poincaré-Friedrichs-inequality [21], assuming that Ω can be included in a cube with side length s. Using the above estimates for $\|\boldsymbol{v}\|_{\mathcal{V}}$ and $\|\Psi\|_1$, we derive the following chain of inequalities:

$$\begin{aligned} \sup_{\boldsymbol{v} \in \mathcal{V}_0} \frac{c(\boldsymbol{v}, \Psi)}{\|\boldsymbol{v}\|_{\mathcal{V}}} &\geq \frac{c(\boldsymbol{v}, \Psi)}{\|\boldsymbol{v}\|_{\mathcal{V}}} \\ &\geq \frac{1}{4}\hat{E}C' \|\boldsymbol{v}\|_{\mathcal{V}} \geq \frac{1}{4}\hat{E}C' \sqrt{\int_{\Omega} \sum_{i,j=1}^{3} \left(\frac{\partial v_i}{\partial x_j}\right)^2 \mathrm{d}x} \\ &= \frac{\sqrt{3}}{4}\hat{E}C' \sqrt{\int_{\Omega} \sum_{i=1}^{3} \left(\frac{\partial \Psi}{\partial x_i}\right)^2 \mathrm{d}x} \geq \beta \|\Psi\|_{\mathcal{M}}, \end{aligned}$$

with β defined as

$$\beta := \frac{\sqrt{3}\hat{E}C'}{4\sqrt{s^2 + 1}}.$$

□

Remark 3.3. *Since the constant in the inf-sup estimate depends on the components of the coupling matrix $\boldsymbol{e}$, the estimate in the proof of Theorem 3.2 does not provide a satisfactory bound for weakly magnetostrictive materials, i.e. for $e_{ij} \to 0$. However, as mentioned in Chapter 1, we are focusing on giant magnetostrictive materials used in most industrial applications. Hence, we can assume the constant $\hat{E}$ from the proof of Theorem 3.2 to be "sufficiently large". In Chapter 5 we will provide a set of typical values for the coupling matrix of the giant magnetostrictive material Terfenol-D, for which the minimal positivity assumption from Definition 3.2 is satisfied.*

Note that, to obtain a unique solution, the continuity requirement for the bilinear form $b(\cdot, \cdot)$ in a penalized saddle point problem of type $(CP)^w$ can be dropped if the coercivity of the bilinear form $a(\cdot, \cdot)$ holds on the whole space $\mathcal{V}_0$ (see [20], [67]). This is the case in our model. As the next lemma shows, the coercivity condition is also fulfilled for the bilinear form $b(\cdot, \cdot)$.

Lemma 3.2. *The bilinear form $b(\cdot,\cdot)$ defined in (3.20) is coercive on the space $\mathcal{M}_0$.*

Proof. For $\Psi \in \mathcal{V}_0$, the following estimates hold:

$$\begin{aligned} r\,||\Psi||_1^2 &= r(||\Psi||_0^2 + |\Psi|_1^2) \le r(s^2+1)|\Psi|_1^2 = r(s^2+1)\int_\Omega \sum_{i=1}^{3}\left(\frac{\partial\Psi}{\partial x_i}\right)^2 \mathrm{d}x \\ &\le (s^2+1)\int_\Omega \sum_{i=1}^{3}\mu_{ii}\left(\frac{\partial\Psi}{\partial x_i}\right)^2 \mathrm{d}x = (s^2+1)b(\Psi,\Psi), \end{aligned}$$

where the parameter s stems from the Poincaré-Friedrichs inequality and $r := \min_{i=1,2,3}\mu_{ii}$. Thus, coercivity holds with the constant

$$\gamma := \frac{r}{(s^2+1)}.$$

□

As a consequence, both $a(\cdot,\cdot)$ and $b(\cdot,\cdot)$ are positive definite and define inner products on the corresponding spaces.

Remark 3.4. *Since $b(\cdot,\cdot)$ is coercive, the existence and uniqueness of the problem $(CP)^w$ follows directly from the application of the Lax-Milgram lemma to the composite bilinear form*

$$\mathcal{A} : (\mathcal{V}_0 \times \mathcal{M}_0) \times (\mathcal{V}_0 \times \mathcal{M}_0) \to \mathbb{R}, \quad \mathcal{A}((\boldsymbol{u},\Psi),(\boldsymbol{v},\Phi)) = a(\boldsymbol{u},\boldsymbol{v}) + c(\boldsymbol{v},\Psi) - c(\boldsymbol{u},\Phi) + b(\Psi,\Phi),$$

which transfers the system of two coupled equations to a problem with a single equation:

Problem. *Find $(\boldsymbol{u},\Psi) \in \mathcal{V}_0 \times \mathcal{M}_0$, such that*

$$\mathcal{A}((\boldsymbol{u},\Psi),(\boldsymbol{v},\Phi)) = l(\boldsymbol{v}) - m(\Phi) \quad \forall (\boldsymbol{v},\Phi) \in \mathcal{V}_0 \times M_0. \tag{3.28}$$

Using the coercivity of the bilinear forms $a(\cdot,\cdot)$ and $b(\cdot,\cdot)$ (as well as the continuity of all three bilinear forms), we obtain

$$\begin{aligned} \alpha\,||\boldsymbol{v}||_{\mathcal{V}_0}^2 + \gamma\,||\Phi||_{\mathcal{M}_0}^2 &\le a(\boldsymbol{v},\boldsymbol{v}) + b(\Phi,\Phi) \\ &= a(\boldsymbol{v},\boldsymbol{v}) + b(\Phi,\Phi) + c(\boldsymbol{v},\Phi) - c(\boldsymbol{v},\Phi) = \mathcal{A}((\boldsymbol{v},\Phi),(\boldsymbol{v},\Phi)), \end{aligned}$$

implying that there exists a constant $\delta := \min(\alpha,\gamma)$ such that

$$\mathcal{A}((\boldsymbol{v},\Phi),(\boldsymbol{v},\Phi)) \ge \delta\,||(\boldsymbol{v},\Phi)||_{\mathcal{V}\times\mathcal{M}}^2 \quad \textit{for all} \quad (\boldsymbol{v},\Phi) \in \mathcal{V}_0 \times \mathcal{M}_0,$$

where

$$||(\boldsymbol{v},\Phi)||_{\mathcal{V}\times\mathcal{M}}^2 := ||\boldsymbol{v}||_{\mathcal{V}}^2 + ||\Phi||_{\mathcal{M}}^2.$$

Hence, the composite bilinear form $\mathcal{A}$ is continuous and coercive and the Lax-Milgram lemma yields the existence and uniqueness of the solution $(\boldsymbol{u},\Psi)$ of the above problem. However, exploiting the coercivity of the uncoupled bilinear forms does not necessarily let us avoid showing the inf-sup condition for $c(\cdot,\cdot)$. In fact, the stability estimate that can be obtained by using just the coercivity property as explained above does not yield a satisfactory result for our problem. This aspect will be picked up in the next section.

3.3 Influence of perturbations

As we have seen in the previous section, the main requirement in showing the unique solvability of the problem $(CP)^w$ was the satisfaction of the inf-sup condition (3.26) for the coupled bilinear form $c(\cdot,\cdot)$. Furthermore, in Remark 3.4 we proved that the existence and uniqueness of the solution can also be directly deduced from the Lax-Milgram lemma. Nevertheless, one can show that the stability estimate obtained from the latter approach is not satisfactory.

Let α and γ denote the coercivity constants of the bilinear forms $a(\cdot,\cdot)$ and $b(\cdot,\cdot)$. Equation (3.28) yields

$$\begin{aligned}
\|(\boldsymbol{u},\Psi)\|^2_{\mathcal{V}\times\mathcal{M}} &= \|\boldsymbol{u}\|^2_{\mathcal{V}} + \|\Psi\|^2_{\mathcal{M}} = \frac{1}{\alpha}a(\boldsymbol{u},\boldsymbol{u}) + \frac{1}{\gamma}b(\Psi,\Psi) \leq \max\left\{\frac{1}{\alpha},\frac{1}{\gamma}\right\}(a(\boldsymbol{u},\boldsymbol{u}) + b(\Psi,\Psi)) \\
&= \max\left\{\frac{1}{\alpha},\frac{1}{\gamma}\right\}|l(\boldsymbol{u}) - m(\Psi)| \\
&\leq \max\left\{\frac{1}{\alpha},\frac{1}{\gamma}\right\}\left\|\tilde{l}(\boldsymbol{u},\Psi)\right\|_{(\mathcal{V}\times\mathcal{M})'}\|(\boldsymbol{u},\Psi)\|_{\mathcal{V}\times\mathcal{M}},
\end{aligned}$$

where $\tilde{l}(\boldsymbol{u},\Psi) := l(\boldsymbol{u}) - m(\Psi)$ and

$$\|l\|_{\mathcal{V}'} := \sup_{\boldsymbol{v}\in\mathcal{V}_0}\frac{l(\boldsymbol{v})}{\|\boldsymbol{v}\|_{\mathcal{V}}} \quad \text{and} \quad \|m\|_{\mathcal{M}'} := \sup_{\Psi\in\mathcal{M}_0}\frac{m(\Psi)}{\|\Psi\|_{\mathcal{M}}}$$

are the norms of the dual spaces $\mathcal{V}'$ and $\mathcal{M}'$ of $\mathcal{V}$ and $\mathcal{M}$, respectively. Thus, we obtain

$$\|(\boldsymbol{u},\Psi)\|_{\mathcal{V}\times\mathcal{M}} \leq \max\left\{\frac{1}{\alpha},\frac{1}{\gamma}\right\}\left\|\tilde{l}(\boldsymbol{u},\Psi)\right\|_{(\mathcal{V}\times\mathcal{M})'}.$$

Taking a look at the coercivity constant

$$\gamma = \frac{\min\limits_{i=1,..,3}\mu_{ii}}{(s^2+1)}$$

of the bilinear form $b(\cdot,\cdot)$ we can conclude that $1/\gamma$ has a magnitude of 10^3 and higher due to the very small values of magnetic permeability for magnetostrictive materials. The coercivity constant α of the elastic bilinear form depends on the elasticity matrix C^H whose values usually have a dimension range between 10^{-11} and 10^{-9} (see e.g. the material data of Terfenol-D presented in Chapter 5). Thus, the constants in the above estimate do not provide a proper bound for the norm of the solution.
This problem can be cured by additionally requiring that $c(\cdot,\cdot)$ fulfills the inf-sup condition with a constant β. The inf-sup stability can then be used to obtain better estimates for the norms $\|\boldsymbol{u}\|_{\mathcal{V}}$ and $\|\Psi\|_{\mathcal{M}}$. For certain choices of the bilinear form $c(\cdot,\cdot)$, Boffi et al. [12] have derived stability estimates for the solution of saddle point problems of type $(CP)^w$. Before stating these estimates, we need some introductory definitions.

Let $\mathcal{C} : \mathcal{V}_0 \to \mathcal{M}_0'$ and $\mathcal{C}^T : \mathcal{M}_0 \to \mathcal{V}_0'$ be the linear operators associated with the continuous bilinear form $c(\cdot,\cdot)$. Furthermore, we define $K := \ker\mathcal{C}$ and $H := \ker\mathcal{C}^T$, as well as their orthogonal complements

$$K^\perp := \{\boldsymbol{v}\in\mathcal{V}_0 \mid (\boldsymbol{v},\boldsymbol{w})_{\mathcal{V}} = 0\ \forall\boldsymbol{w}\in K\},$$

and

$$H^\perp := \{\Psi\in\mathcal{M}_0 \mid (\Psi,\Phi)_{\mathcal{M}} = 0\ \forall\Phi\in H\},$$

where $(\cdot,\cdot)_{\mathcal{V}}$ and $(\cdot,\cdot)_{\mathcal{M}}$ denote the scalar products in the Hilbert spaces $\mathcal{V} = H^1(\Omega)^3$ and $\mathcal{M} = H^1(\Omega)$, respectively.
Boffi et al. derive a stability estimate by considering the cases of homogeneous right-hand sides $l = 0$ and $m = 0$ separately, exploiting the symmetry of the problem and using linearity to sum up the estimates for these two cases. Moreover, they suggest the splitting of the functions $\boldsymbol{v}$, Ψ into a part lying in K and H, respectively, and a part lying in the corresponding orthogonal complement. A similar procedure is applied to the functionals $l(\cdot)$ and $m(\cdot)$, i.e.

$$\boldsymbol{v} = \boldsymbol{v}_0 + \bar{\boldsymbol{v}}, \quad \Psi = \Psi_0 + \bar{\Psi}, \quad l = l_0 + \bar{l}, \quad m = m_0 + \bar{m},$$

with $\boldsymbol{v}_0 \in K$, $\bar{\boldsymbol{v}} \in K^\perp$, $\Psi_0 \in H$, $\bar{\Psi} \in H^\perp$, $l_0 \in K'$, $\bar{l} \in (K^\perp)' = K^0$, $m_0 \in H'$, $\bar{m} \in (H^\perp)' = H^0$.
The spaces

$$\begin{aligned} K^0 &:= \{l \in \mathcal{V}_0' \mid l(\boldsymbol{v}) = 0 \ \forall\ \boldsymbol{v} \in K\}, \\ H^0 &:= \{m \in \mathcal{M}_0' \mid m(\Psi) = 0 \ \forall\ \Psi \in H\}, \end{aligned}$$

are the *polar spaces* of K and H, respectively.
Note that, due to linearity,

$$l(\boldsymbol{v}) = l_0(\boldsymbol{v}_0) + \bar{l}(\bar{\boldsymbol{v}}), \quad m(\Psi) = m_0(\Psi_0) + \bar{m}(\bar{\Psi}).$$

Theorem 3.3. *(Stability estimates after Boffi et al.) The problem $(CP)^w$ with continuous and coercive bilinear forms $a(\cdot,\cdot)$ and $b(\cdot,\cdot)$ and a continuous bilinear form $c(\cdot,\cdot)$ as defined in (3.19) – (3.21) fulfilling the inf-sup condition (3.26) has a unique solution $(\boldsymbol{u}, \Psi) \in \mathcal{V}_0 \times \mathcal{M}_0$ that satisfies the stability estimate*

$$\|\boldsymbol{u}\|_{\mathcal{V}} + \|\Psi\|_{\mathcal{M}} \leq C(\alpha, \gamma, a_0, c_0, \delta)(\|l\|_{\mathcal{V}'} + \|m\|_{\mathcal{M}'}),$$

where α and γ, as well as a_0 and c_0 are the coercivity and continuity constants of $a(\cdot,\cdot)$ and $b(\cdot,\cdot)$, respectively, C is a constant and $\delta > 0$ is defined as

$$\delta := \inf_{\Psi \in H^\perp} \sup_{\boldsymbol{v} \in \mathcal{V}_0} \frac{c(\boldsymbol{v}, \Psi)}{\|\boldsymbol{v}\|_{\mathcal{V}} \|\Psi\|_{\mathcal{M}}} = \inf_{\boldsymbol{v} \in K^\perp} \sup_{\Psi \in \mathcal{M}_0} \frac{c(\boldsymbol{v}, \Psi)}{\|\boldsymbol{v}\|_{\mathcal{V}} \|\Psi\|_{\mathcal{M}}}.$$

More precisely,

$$\begin{aligned} \|\boldsymbol{u}\|_{\mathcal{V}} &\leq C_1 \left\|\bar{l}\right\|_{K^0} + C_2 \|l_0\|_{K'} + C_3 \|\bar{m}\|_{H^0} + C_4 \|m_0\|_{H'}, \\ \|\Psi\|_{\mathcal{M}} &\leq \tilde{C}_1 \left\|\bar{l}\right\|_{K^0} + \tilde{C}_2 \|l_0\|_{K'} + \tilde{C}_3 \|\bar{m}\|_{H^0} + \tilde{C}_4 \|m_0\|_{H'}, \end{aligned}$$

where the constants C_i and $\tilde{C}_i$, $i = 1, .., 4$ depend on $\alpha, \gamma, a_0, c_0, \delta$.

We skip the rather technical and extensive proof of the above theorem at this point and refer to [12] for the exact forms of the stability constants.

3.4 Numerical treatment

While in the previous sections we discussed the structure and solvability of the coupled magnetoelastic problem in the continuous case, we now concentrate on its numerical treatment. The first step towards this aim leads us to a thorough analysis of the material tensors for polycrystalline magnetostrictive materials, using a common representative of this material class, the *grain-oriented Terfenol-D*, a material used in many applications [38, 39, 56, 60]. For simplicity, the coupled model will be reduced to the two-dimensional

case, considering a thin magnetostrictive plate in the loading case of plane stress. After introducing the 2D problem, we will transfer the already presented solvability conditions to the discrete case and show that they are valid independent from the chosen discretization. In addition, also an algebraic approach to the solvability of the coupled saddle point problem will be discussed and parallels to the formerly mentioned conditions will be drawn.

3.4.1 Magneto-elastic coupling properties of polycrystals

In general, the magnetic properties of polycrystalline ferromagnetic materials (which are almost all ferromagnets serving industrial purposes, see e.g. [27]) depend on their crystallographic texture, that is, on the size, shape, orientation and arrangement of their microscopic grains, the crystallites. Due to the highly anisotropic nature of magnetostriction, it is strongly influenced by the crystallographic direction of the magnetization and the mechanical (pre-)stress applied on the material. To describe the coupling properties of the material, it is thus essential to characterize the behavior of the body under symmetry operations, which is reflected by the coupling tensor $\boldsymbol{e}$.

Within this framework, we briefly introduce the notions of *polar* vectors (*polar tensors*), that are used to represent translations, mechanical forces, velocity, acceleration or momentum and *axial* vectors or *pseudovectors* (*pseudotensors*), which are usually associated with angular velocity, angular momentum or torque.
To explain these concepts, we consider a coordinate transformation described by a matrix $\boldsymbol{L} = (l_{ij})_{i,j=1,2,3}$ that converts an (orthonormal) basis $\{\boldsymbol{b}_j\}$, $j = 1,2,3$, of $\mathbb{R}^3$ into a new (orthonormal) basis $\{\tilde{\boldsymbol{b}}_i\}$, $i = 1,2,3$. The transformation law of a polar vector

$$\boldsymbol{v} = \sum_{i=1}^{3} v_i \boldsymbol{b}_i,$$

with components v_i, $i = 1,2,3$, is given by

$$\tilde{\boldsymbol{v}} = \sum_{i=1}^{3} \tilde{v}_i \tilde{\boldsymbol{b}}_i,$$

where $\tilde{v}_i = \sum_{j=1}^{3} l_{ij} v_j$. If the transformation is an inversion, i.e. changing a right-handed coordinate system into a left-handed one (or vice versa), then

$$L = \begin{pmatrix} -1 & 0 & 0 \\ 0 & -1 & 0 \\ 0 & 0 & -1 \end{pmatrix},$$

and the basis $\boldsymbol{b}_i$, $i = 1,2,3$, changes its sign under the inversion, i.e. $\tilde{\boldsymbol{b}}_i = -\boldsymbol{b}_i$. The vector $\tilde{\boldsymbol{v}}$ can then be written as

$$\tilde{\boldsymbol{v}} = \sum_{i=1}^{3} \tilde{v}_i \tilde{\boldsymbol{b}}_i = \sum_{i=1}^{3} (-v_i)(-\boldsymbol{b}_i) = \boldsymbol{v},$$

indicating that a polar vector remains unchanged under a transformation of the coordinate system.
Consider now the cross product $\boldsymbol{y} = \boldsymbol{v} \times \boldsymbol{w}$ of $\boldsymbol{v}$ and a polar vector $\boldsymbol{w} \in \mathbb{R}^3$. The resulting vector is an axial vector that transforms to

$$\tilde{\boldsymbol{y}} = \left(\sum_{i=1}^{3} -v_i(-\boldsymbol{b}_i) \right) \times \left(\sum_{j=1}^{3} -w_j(-\boldsymbol{b}_j) \right) = \sum_{i,j=1}^{3} v_j w_j (-\boldsymbol{b}_i \times -\boldsymbol{b}_j).$$

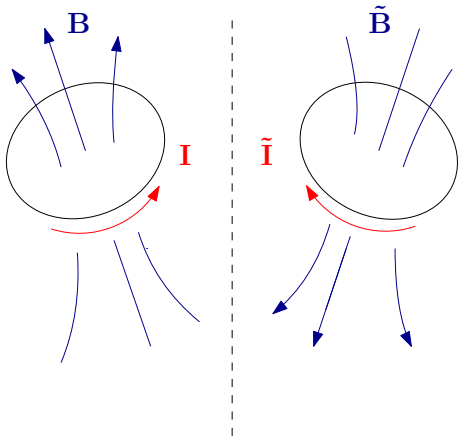

Figure 3.1: Illustration of the axial vector $\boldsymbol{B}$ representing the magnetic flux density and the polar vector $\boldsymbol{I}$ in a reflection across a plane (dashed line).

As the cross product $-\boldsymbol{b}_i \times -\boldsymbol{b}_j$ yields a basis vector $\tilde{\boldsymbol{b}}_k$, the vector $\tilde{\boldsymbol{y}}$ flips its sign with respect to the new coordinate system, i.e.

$$\tilde{\boldsymbol{y}} = \sum_{k=1}^{3} y_k \tilde{\boldsymbol{b}}_k = -\sum_{k=1}^{3} \tilde{y}_k \tilde{\boldsymbol{b}}_k.$$

Summing up, we notice that while the polar vector $\boldsymbol{v} \in \mathbb{R}^3$ transforms according to the relation

$$\tilde{v}_i = \sum_{j=1}^{3} l_{ij} v_j, \quad i = 1, ..., 3,$$

the axial vector $\boldsymbol{y} \in \mathbb{R}^3$ turns into

$$\tilde{y}_i = \det L \sum_{j=1}^{3} l_{ij} y_j, \quad i = 1, ..., 3.$$

The sign of an axial vector therefore depends on the choice of the coordinate system, more precisely, on its "handedness", the associated direction of rotation. Now the idea behind the term *pseudovector* becomes clear: While axial vectors have the same manner of composition as "proper" vectors, their transformation law is different.
The magnetic field and flux density vectors $\boldsymbol{H}$ and $\boldsymbol{B}$ are examples of axial vectors. Figure 3.1 shows the reflection of a loop of a current-carrying wire that creates a magnetic flux density $\boldsymbol{B}$. While the current vector $\boldsymbol{I}$ is just reflected across the plane, the magnetic flux density vector $\boldsymbol{B}$ is additionally reversed.

The concept of polar and axial vectors can also be applied to tensors. A second order polar tensor $\boldsymbol{T} = (t_{ij})_{i,j=1,2,3}$, for example, transforms to the tensor $\tilde{\boldsymbol{T}}$ via

$$\tilde{t}_{ji} = \sum_{k,l=1}^{3} l_{jk} l_{il} t_{kl}, \tag{3.29}$$

an axial tensor $\boldsymbol{S} = (s_{ij})_{i,j=1,2,3}$ turns into the tensor $\tilde{\boldsymbol{S}}$ with coordinates

$$\tilde{s}_{ji} = \det L \sum_{k,l=1}^{3} l_{jk} l_{il} t_{kl}. \tag{3.30}$$

The elasticity tensor $\boldsymbol{C}^H$ and the magnetic permeability tensor $\boldsymbol{\mu}^\epsilon$ are polar tensors, while the magnetoelastic coupling tensor $\boldsymbol{e}$ is an axial tensor [60].

In the following, we will focus on examining the magnetoelastic coupling matrix resulting from the third-order tensor $\boldsymbol{e}$ with respect to the underlying symmetry structure of the crystal. The symmetry group of a crystal includes all operations on the crystal that leave its structure invariant. Such operations can be a translation, a rotation about an axis, an inversion through a point, a reflection through a plane or a combination of these operations. Different types of crystal lattices can be defined according to their symmetry operations, such as lattices having *translation group* symmetries, *point group* symmetries or *space group* symmetries. While the translation group consists of operations $\{I\,|\,T\}$ with an identity rotation I and a translation T, the point group operations have the form $\{\alpha\,|\,0\}$, where α describes a symmetry operation at a point. The operations of the space group, on the other hand, are characterized by the pattern $\{\alpha\,|\,T\}$, combining both point symmetry operations and translations.
According to the *Neumann principle*, a fundamental principle of crystal physics (see. e.g. [92]), a material tensor of a crystal must include the spatial symmetry of the crystal structure, i.e. all symmetry operations of the crystal's point group. For the axial matrix $\boldsymbol{e}$, Neumann's principle suggests that if a transformation L is an element of the point group of the crystal, the components

$$\tilde{e}_{ji} = \det L \sum_{k=1}^{6} \sum_{l=1}^{3} l_{jk} l_{il} e_{kl} \tag{3.31}$$

of the transformed matrix $\tilde{\boldsymbol{e}}$ should coincide with the elements e_{kl}, $k = 1, .., 6$, $l = 1, ..., 3$, of the original matrix. The grain-oriented Terfenol-D, the polycrystalline ferromagnetic material we use in our model, can be categorized in the $6/mm^*m^*$ crystallographic symmetry group[1] [40, 60], meaning that the material shows hexagonal anti-symmetry with respect to one of the spatial axes. Neumann's principle implies that the structure of a material tensor must reflect the anti-symmetries of the crystal structure. An axial tensor, however, should not change its form under anti-symmetry transformations. Fuentes [60] showed that the conditions (3.30) implicate that the *piezomagnetic coupling matrix* $\boldsymbol{d}^T$ of the grain-oriented Terfenol-D has the following structure,

$$\boldsymbol{d}^T = \begin{pmatrix} 0 & 0 & 0 & 0 & d_{51} & 0 \\ 0 & 0 & 0 & d_{51} & 0 & 0 \\ d_{13} & d_{13} & d_{33} & 0 & 0 & 0 \end{pmatrix},$$

assuming anti-symmetry with respect to the x_3-axis. Due to the anti-symmetry operations, certain components d_{ij} of the transformed matrix have to be imposed with a minus sign and vanish according to the requirement of invariance, creating the specific form of the above matrix. The matrix $\boldsymbol{d}^T$ results from a different formulation of the piezomagnetic constitutive equations and can be transformed into the matrix $\boldsymbol{e}^T$ via the relation $\boldsymbol{e}^T = \boldsymbol{d}^T C^H$. As $\boldsymbol{e}^T$ characterizes the magnetic properties of the same material, we can directly transfer the above result to our model. This, of course, has implications for the structure of the elasticity matrix $\boldsymbol{C}^H$ of the material. Requiring that the matrix $\boldsymbol{d}^T\boldsymbol{C}^H$ has the same form as the matrix $\boldsymbol{d}^T$, we obtain the following conditions for the components of the symmetric elasticity matrix $\boldsymbol{C}^H$

$$\begin{aligned} C_{5i} = 0 = C_{i5} \quad & \text{for } i = 1, ..., 6,\ i \neq 5, \\ C_{4i} = 0 = C_{i4} \quad & \text{for } i = 1, ..., 6,\ i \neq 4, \\ C_{i6} = 0 = C_{6i} \quad & \text{for } i = 1, 2, 3, \end{aligned}$$

[1] The asterisk is used to denote anti-symmetries in the crystal structure.

which lead to the block-diagonal form of the elasticity matrix,

$$\boldsymbol{C}^H = \begin{pmatrix} C_{11} & C_{12} & C_{13} & 0 & 0 & 0 \\ C_{21} & C_{22} & C_{23} & 0 & 0 & 0 \\ C_{31} & C_{32} & C_{33} & 0 & 0 & 0 \\ 0 & 0 & 0 & C_{44} & 0 & 0 \\ 0 & 0 & 0 & 0 & C_{55} & 0 \\ 0 & 0 & 0 & 0 & 0 & C_{66} \end{pmatrix}.$$

This special structure of the elasticity matrix suggests a certain material anisotropy. More precisely, elasticity matrices of the above form are ascribed to orthotropic or transversely isotropic material behavior. Indeed, polycrystalline ferromagnetic materials are isotropic in unpolarized (unbiased) condition and gain the features of a transversely isotropic material due to magnetic polarization [39, 56]. In other words, the properties of the polarized material are isotropic in the directions perpendicular to the magnetization direction. The coupling matrix $\boldsymbol{d}^T$ presented above corresponds to a material with magnetic polarization direction x_3, having transversely isotropic material properties with respect to this direction. In the next section, we will present detailed forms of the elasticity matrix $\boldsymbol{C}^H$ and the coupling matrix $\boldsymbol{e}$ for a two-dimensional model in case of plane stress. Additionally, we will slightly change the assumptions on the structure of the coupling matrix $\boldsymbol{e}$ described above and require a magnetic polarization in x_1-direction, obtaining transverse isotropy with respect to this coordinate axis. The matrix $\boldsymbol{e}^T$ is then given by

$$\boldsymbol{e}^T = \begin{pmatrix} e_{11} & e_{21} & e_{31} & 0 & 0 & 0 \\ 0 & 0 & 0 & 0 & 0 & e_{62} \\ 0 & 0 & 0 & 0 & e_{53} & 0 \end{pmatrix}. \tag{3.32}$$

3.4.2 Reduction to 2D

The coupled system of partial differential equations derived in Section 3.2 has been kept rather general. Reducing the model to the two-dimensional case provides a better insight into the structural details of the material matrices and the different bilinear forms.
We focus now on a two-dimensional body, by misuse of notation again denoted by $\Omega \subset \mathbb{R}^2$ for the sake of clarity, characterized by a thin magnetostrictive plate (see Figure 3.2) in the loading state of plane stress. We assume that the plate is made of the grain-oriented Terfenol-D magnetically polarized in x_1-direction, as explained in the previous section.
The plane stress - assumption requires that all internal forces act on the (x_1, x_2) - plane, i.e.

$$\boldsymbol{\sigma} = \boldsymbol{\sigma}(x_1, x_2),\ \boldsymbol{\epsilon} = \boldsymbol{\epsilon}(x_1, x_2),\ \sigma_{33} = \sigma_{13} = \sigma_{23} = 0,\ \epsilon_{13} = \epsilon_{23} = 0$$

Using the Voigt notation, $\boldsymbol{\sigma}$ and $\boldsymbol{\epsilon}$ can be written as,

$$\boldsymbol{\sigma} = (\sigma_1, \sigma_2, \sigma_3)^T := (\sigma_{11}, \sigma_{22}, \sigma_{12})^T, \quad \boldsymbol{\epsilon} = (\epsilon_1, \epsilon_2, \epsilon_3)^T := (\epsilon_{11}, \epsilon_{22}, 2\epsilon_{12})^T.$$

Furthermore,

$$\boldsymbol{u} = \boldsymbol{u}(x_1, x_2),\ \boldsymbol{H} = \boldsymbol{H}(x_1, x_2),\ \boldsymbol{B} = \boldsymbol{B}(x_1, x_2),\ \Phi = \Phi(x_1, x_2).$$

The transversely isotropic elasticity matrix for constant magnetic field takes the form

$$C^H = \frac{1}{E_1 - \nu_{12}^2 E_2} \begin{pmatrix} E_1^2 & \nu_{12} E_1 E_2 & 0 \\ \nu_{12} E_1 E_2 & E_1 E_2 & 0 \\ 0 & 0 & G_{12}(E_1 - \nu_{12}^2 E_2) \end{pmatrix},$$

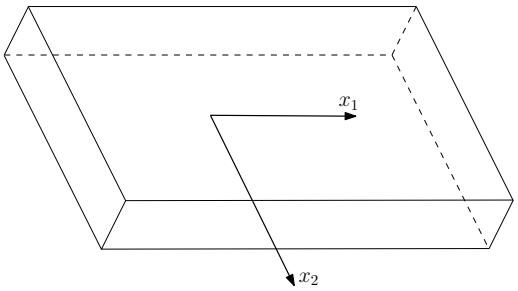

Figure 3.2: Sketch of the magnetostrictive plate with its principle material directions.

with E_i, $i = 1, 2$, denoting Young's modulus in the axial direction i, ν_{12} being Poisson's ratio for the (x_1, x_2) - plane and G_{12} describing the pre-magnetization in x_1-direction. Equation (3.32) together with the plane stress - setting indicate that the magnetic permeability matrix at constant strain, $\boldsymbol{\mu}^{\boldsymbol{\epsilon}}$ and the coupling matrix $\boldsymbol{e}$ must have the form,

$$\boldsymbol{\mu}^{\boldsymbol{\epsilon}} = \begin{pmatrix} \mu_{11} & 0 & 0 \\ 0 & \mu_{22} & 0 \\ 0 & 0 & \mu_{22} \end{pmatrix}, \qquad \boldsymbol{e} = \begin{pmatrix} e_{11} & 0 & 0 \\ e_{21} & 0 & 0 \\ 0 & e_{62} & 0 \end{pmatrix}. \tag{3.33}$$

Considering the above assumptions, the elastic, magnetic and coupled bilinear forms are eventually given by

$$\begin{aligned} \boldsymbol{a}(\boldsymbol{u}, \boldsymbol{v}) &= r \int_\Omega \frac{1}{E_1 - \nu_{12}^2 E_2} \left(E_1^2 \frac{\partial u_1}{\partial x_1} \frac{\partial v_1}{\partial x_1} + \nu_{12} E_2 E_1 \left(\frac{\partial u_1}{\partial x_1} \frac{\partial v_2}{\partial x_2} + \frac{\partial u_2}{\partial x_2} \frac{\partial v_1}{\partial x_1} \right) \right. \\ &+ \left. E_1 E_2 \frac{\partial u_2}{\partial x_2} \frac{\partial v_2}{\partial x_2} + G_{12}(E_1 - \nu_{12}^2 E_2) \left(\frac{\partial u_1}{\partial x_2} + \frac{\partial u_2}{\partial x_1} \right) \left(\frac{\partial v_1}{\partial x_2} + \frac{\partial v_2}{\partial x_1} \right) \right) \mathrm{d}x, \end{aligned} \tag{3.34}$$

$$\boldsymbol{b}(\Psi, \Phi) = r \int_\Omega \mu_{11} \frac{\partial \Psi}{\partial x_1} \frac{\partial \Phi}{\partial x_1} + \mu_{22} \frac{\partial \Psi}{\partial x_2} \frac{\partial \Phi}{\partial x_2} \, \mathrm{d}x, \tag{3.35}$$

$$\boldsymbol{c}(\boldsymbol{v}, \Psi) = r \frac{1}{2} \int_\Omega e_{11} \frac{\partial v_1}{\partial x_1} \frac{\partial \Psi}{\partial x_1} + e_{21} \frac{\partial v_2}{\partial x_2} \frac{\partial \Psi}{\partial x_1} + e_{62} \left(\frac{\partial v_1}{\partial x_2} + \frac{\partial v_2}{\partial x_1} \right) \frac{\partial \Psi}{\partial x_2} \, \mathrm{d}x, \tag{3.36}$$

where r is the (constant) thickness of the plate.

3.4.3 Solvability in the discrete case

Let $\Omega \subset \mathbb{R}^2$ and consider finite dimensional subspaces $V_h \subset \mathcal{V}_0$ and $M_h \subset \mathcal{M}_0$ of the Hilbert spaces defined in Section 3.1.2, where $h > 0$ denotes the mesh parameter. Then, the Galerkin approximation (e.g. in [21] or [22]), of the coupled saddle point problem reads

Problem $(CP)_h^w$: Find $(\boldsymbol{u}_h, \Psi_h) \in V_h \times M_h$, such that

$$\begin{aligned} a(\boldsymbol{u}_h, \boldsymbol{v}_h) + c(\boldsymbol{v}_h, \Psi_h) &= l(\boldsymbol{v}_h) \qquad && \forall \boldsymbol{v}_h \in V_h, \\ c(\boldsymbol{u}_h, \Phi_h) - b(\Psi_h, \Phi_h) &= m(\Phi_h) \qquad && \forall \Phi_h \in M_h. \end{aligned}$$

In contrast to problems with a single bounded, coercive bilinear form, the well-posedness of discrete saddle point problems, in general, cannot be automatically deduced from their continuous counterpart: On the one hand, the coercivity of the bilinear form $a(\cdot, \cdot)$ on the kernel $\ker \boldsymbol{\mathcal{C}}$ does not necessarily imply its coercivity on the kernel

$$(\ker \boldsymbol{\mathcal{C}})_h := \{ \boldsymbol{v}_h \in V_h \mid c(\boldsymbol{v}_h, \Psi_h) = 0 \ \forall \ \Psi_h \in M_h \}.$$

This is the case for the Stokes Problem (e.g. in [21]), for example. On the other hand, the discrete inf-sup condition on $V_h \times M_h$ cannot be directly deduced from the continuous one on $\mathcal{V}_0 \times \mathcal{M}_0$ since the supremum over a set Y is greater than or equal to the supremum over a subset $Y_h \subset Y$.
In the coupled magnetoelastic saddle point problem $(CP)_h^w$, however, the continuity of the bilinear form $c(\cdot,\cdot)$ as well as the coercivity of the bilinear forms $a(\cdot,\cdot)$ and $b(\cdot,\cdot)$ on the corresponding discrete spaces are directly inherited from the continuous case. The discrete inf-sup condition is then the only assumption that needs verification. In this context, special attention has to be paid to the appropriate choice of the discrete spaces V_h and M_h. Difficulties arise again for the Stokes problem, where the discrete inf-sup condition is not fulfilled for certain choices of the discrete spaces (for details refer to [21]). We will return to this issue after presenting the proof of the next theorem. Before stating the theorem, we briefly introduce some notations referring to Lagrangian finite element spaces without going further into the details of the Finite Element Method and refer the reader to the corresponding literature (e.g. [21, 22, 68]).
Let $\mathcal{T}_h = \{T_1, ..., T_M\}$ be a partition of the domain $\Omega \subset \mathbb{R}^2$ into elements T_i,

$$\overline{\Omega} = \bigcup_{i=1}^{M} T_i,$$

having each a maximum diameter $2h$. Moreover, let $\mathcal{P}_k$ denote the space of polynomials of degree $\leq k$. The space

$$S_k(\Omega, \mathcal{T}_h) := \{v_h \in L^2(\Omega) \mid v_h|_T \in \mathcal{P}_k \ \text{ for all } T \in \mathcal{T}\}$$

is called the (conforming) *Lagrangian finite element space* of degree k.
The following theorem shows that by selecting Lagrangian finite elements for the discretization, we can prove that the discrete inf-sup condition for $c(\cdot,\cdot)$ is satisfied with a constant independent of the mesh parameter h.

Theorem 3.4. *For $V_h = S_k(\Omega, \mathcal{T}_h)^2$ and $M_h = S_k(\Omega, \mathcal{T}_h)$, the bilinear form $c(\cdot,\cdot)$ defined in* (3.36) *with a coupling matrix $\boldsymbol{e}$ that fulfills the minimal positivity property* (3.27) *satisfies the discrete inf-sup condition*

$$\exists \hat{\beta} > 0 \quad \textit{such that} \quad \inf_{\Psi_h \in M_h} \sup_{\boldsymbol{v}_h \in V_h} \frac{c(\boldsymbol{v}_h, \Psi_h)}{\|\boldsymbol{v}_h\|_{\mathcal{V}} \|\Psi_h\|_{\mathcal{M}}} \geq \hat{\beta}, \tag{3.37}$$

with a constant $\hat{\beta}$ independent of h.

Proof. Note that the theorem is proven for the reduced bilinear form obtained by the specification of the material class in Section 3.4.2. The proof for the general three-dimensional case is analogous. As in the continuous case, we want to show the equivalent formulation

$$\sup_{\boldsymbol{v}_h \in V_h} \frac{c(\boldsymbol{v}_h, \Psi_h)}{\|\boldsymbol{v}_h\|_{\mathcal{V}} \|\Psi_h\|_{\mathcal{M}}} \geq \hat{\beta}$$

for a $\hat{\beta} > 0$. Using the Finite Element Method, we partition the domain $\Omega \subset \mathbb{R}^2$ into L elements T_l. For $\boldsymbol{v}_h \in V_h$ and $\Psi_h \in M_h$,

$$c(\boldsymbol{v}_h, \Psi_h) = \sum_{l=1}^{L} c(\boldsymbol{v}_h, \Psi_h)^{T_l},$$

where $c(\boldsymbol{v}_h, \Psi_h)^{T_l}$ is the bilinear form of the element T_l. Denoting $n = \dim V_h$ and $m = \dim M_h$, we can use the basis functions $\boldsymbol{w}_i \in V_h$, $i = 1, ..., n$ and $\tilde{\Psi}_j \in M_h$, $j = 1, .., m$, to express $\boldsymbol{v}_h$ and Ψ_h as

$$\boldsymbol{v}_h = \sum_{i=1}^{n} W_i \boldsymbol{w}_i,$$

with coefficients W_i and

$$\Psi_h = \sum_{j=1}^{m} P_j \tilde{\Psi}_j.$$

with coefficients P_j. However, since the components $(\boldsymbol{v}_h)_r$, $r = 1, 2$ belong to the same discretization space as Ψ_h, we can choose them in such a way that

$$(\boldsymbol{v}_h)_r = \Psi_h = \sum_{j=1}^{m} P_j \tilde{\Psi} \in S_k(\Omega, \mathcal{T}_h).$$

As in the proof of the continuous inf-sup condition (Theorem 3.2), we now obtain the estimate

$$\frac{c(\boldsymbol{v}_h, \tilde{\Psi}_h)}{\|\boldsymbol{v}_h\|_{\mathcal{V}}} \geq \frac{1}{4} \hat{E} C' \|\boldsymbol{v}_h\|_{\mathcal{V}} \geq \hat{\beta} \|\Psi_h\|_{\mathcal{M}}$$

with

$$\hat{E} := \min\left\{ \frac{e_{11}}{2}, \frac{e_{62}}{2}, e_{21} + e_{62} \right\} > 0$$

from Definition 3.27. The mesh-independent constant $\hat{\beta}$ is given by

$$\hat{\beta} := \frac{\sqrt{2}}{4\sqrt{s^2 + 1}} \hat{E} C',$$

where C' and s depend on Ω. □

Note that in the proof of the above lemma, the special choice of the elastic and magnetic basis functions as polynomials of the same degree enables the use of Korn's inequality. This is a major difference to the Stokes problem, where the pairs (S_k, S_k), $k \geq 1$ do not satisfy the inf-sup condition, leading to singularities in the resulting system [10, 24].
In case that the basis functions w_i, $i = 1, 2$ and $\tilde{\Psi}$ are polynomials of different degrees, another type of proof has to be considered using the properties of the discretization.

Remark 3.5. *Let $\alpha > 0$ and $\gamma > 0$ denote the coercivity constants of the bilinear forms $a(\cdot,\cdot)$ and $b(\cdot,\cdot)$, respectively (Lemma 3.2). Furthermore, let $a_0, b_0, c_0 \in \mathbb{R}^+$ denote the continuity constants of $a(\cdot,\cdot)$, $b(\cdot,\cdot)$ and $c(\cdot,\cdot)$, respectively (Lemma 3.1). Finally, let $\hat{\beta} > 0$ denote the constant from the discrete inf-sup condition for $c(\cdot,\cdot)$ as defined in the proof of Theorem 3.4.*
Then, using a result from Brezzi and Fortin [24], which can be interpreted as an analogon of Céa's Lemma (e.g. in [22]), we can provide an error bound for the solution $(\boldsymbol{u}_h, \Psi_h) \in V_h \times M_h$ of the discrete problem $(CP)_h^w$ ensuring the convergence of the Galerkin method:

$$\|\boldsymbol{u} - \boldsymbol{u}_h\|_{\mathcal{V}} + \|\Psi - \Psi_h\|_{\mathcal{M}} \leq K\left(a_0, b_0, c_0, \frac{1}{\alpha}, \frac{b_0}{\gamma}, \frac{1}{\beta}\right) \inf_{\boldsymbol{v}_h \in V_h} \|\boldsymbol{u} - \boldsymbol{v}_h\|_{\mathcal{V}} + \inf_{\Psi_h \in M_h} \|\Psi - \Phi_h\|_{\mathcal{M}},$$

where $(\boldsymbol{u}, \Psi) \in \mathcal{V}_0 \times \mathcal{M}_0$ is the solution of the continuous problem $(CP)^w$ and K is a non-linear function that is bounded on bounded subsets.

3.4.4 Algebraic approach

Let us now consider an algebraic approach to the solvability of the discrete coupled saddle point problem $(CP)_h^w$. As in the proof of Theorem 3.4, consider bases $(\boldsymbol{w}_i)_{i=1,..n}$ and $(\tilde{\Psi}_j)_{j=1,..m}$ of V_h and M_h respectively. Then, $\boldsymbol{u}_h \in V_h$ and $\Psi_h \in M_h$ have the following basis represantation,

$$\boldsymbol{u}_h = \sum_{i=1}^{n} W_i \boldsymbol{w}_i, \qquad \Psi_h = \sum_{j=1}^{m} P_j \tilde{\Psi}_j, \tag{3.38}$$

with coefficient vectors $\boldsymbol{W} = (W_i)_{i=1,\dots,n}$ and $\boldsymbol{P} = (P_j)_{j=1,\dots,m}$. Furthermore, by $\boldsymbol{L} \in \mathbb{R}^n$ we denote the vector $(l(w_i))_{i=1,\dots,n}$ and by $\boldsymbol{M} \in \mathbb{R}^m$ the vector $(m(\Psi_j))_{j=1,\dots,m}$. Inserting the expressions (3.38) into the discrete problem $(CP)_h^w$ yields the block linear system

$$\underbrace{\begin{pmatrix} \boldsymbol{A} & \boldsymbol{C} \\ \boldsymbol{C}^T & -\boldsymbol{B} \end{pmatrix}}_{\mathcal{A}} \begin{pmatrix} \boldsymbol{r} \\ \boldsymbol{s} \end{pmatrix} = \begin{pmatrix} \boldsymbol{L} \\ \boldsymbol{M} \end{pmatrix}, \tag{3.39}$$

with

$$\begin{aligned} \boldsymbol{A} &= (a(\boldsymbol{w}_i, \boldsymbol{w}_j))_{i,j} \in \mathbb{R}^{n\times n}, \\ \boldsymbol{B} &= (b(\Psi_i, \Psi_j))_{i,j} \in \mathbb{R}^{m\times m}, \\ \boldsymbol{C} &= (c(\boldsymbol{w}_i, \Psi_j))_{i,j} \in \mathbb{R}^{n\times m} \end{aligned}$$

and the saddle point matrix $\boldsymbol{\mathcal{A}} \in \mathbb{R}^{(n+m)\times(n+m)}$. The matrices $\boldsymbol{A}$ and $\boldsymbol{B}$ are symmetric and positive definite due to the properties of the corresponding bilinear forms. Since the matrix $\boldsymbol{A}$ is non-singular, the saddle point matrix $\boldsymbol{\mathcal{A}}$ can be factorized in the following way [10]:

$$\boldsymbol{\mathcal{A}} = \begin{pmatrix} \boldsymbol{I} & \boldsymbol{0} \\ \boldsymbol{C}^T\boldsymbol{A}^{-1} & \boldsymbol{I} \end{pmatrix} \begin{pmatrix} \boldsymbol{A} & \boldsymbol{0} \\ \boldsymbol{0} & \boldsymbol{S} \end{pmatrix} \begin{pmatrix} \boldsymbol{I} & \boldsymbol{A}^{-1}\boldsymbol{C} \\ \boldsymbol{0} & \boldsymbol{I} \end{pmatrix},$$

where

$$\boldsymbol{S} = -(\boldsymbol{B} + \boldsymbol{C}^T\boldsymbol{A}^{-1}\boldsymbol{C})$$

is the Schur complement of $\boldsymbol{A}$ in $\boldsymbol{\mathcal{A}}$. The block triangular factorization of $\boldsymbol{\mathcal{A}}$ implies that $\boldsymbol{\mathcal{A}}$ is invertible if and only if $\boldsymbol{S}$ is non-singular. The regularity of $\boldsymbol{S}$ is fulfilled since $\boldsymbol{B}$ is positive definite, leading to a symmetric and negative definite matrix $\boldsymbol{S}$.
Obviously, the positive definiteness of the matrix $\boldsymbol{B}$ is a sufficient condition for the regularity of the Schur complement $\boldsymbol{S}$ and thus for the regularity of the saddle point matrix $\boldsymbol{\mathcal{A}}$. If the symmetric matrix $\boldsymbol{B}$ is only positive semidefinite, the Schur complement $\boldsymbol{S}$ is a symmetric negative semidefinite matrix and regularity holds iff

$$\ker(\boldsymbol{B}) \cap \ker(\boldsymbol{C}) = \{0\}.$$

Another sufficient condition for the regularity of $\boldsymbol{S}$ is the full-rank condition for the matrix $\boldsymbol{C}$, indicating that the associated operator $\mathcal{C} : \mathcal{M}_0 \to \mathcal{V}_0'$, with $\mathcal{V}_0'$ being the dual space of $\mathcal{V}_0$, is injective. In fact, with some minor effort we can see that the requirement

$$\ker \boldsymbol{C} = \{0\}$$

is the algebraic analogon of the discrete inf-sup condition (following [61]):
Let $c(\cdot,\cdot)$ satisfy the discrete inf-sup condition (3.37) with a constant $\hat{\beta}_h$ (not necessarily independent of h), i.e.

$$\sup_{\boldsymbol{v}_h \in V_h} \frac{c(\boldsymbol{v}_h, \Psi_h)}{\|\boldsymbol{v}_h\|_{\mathcal{V}}} \geq \hat{\beta}_h \|\Psi_h\|_{\mathcal{M}} \qquad \forall \Psi_h \in M_h \quad \text{and} \quad \hat{\beta}_h > 0.$$

For vectors $\boldsymbol{V} \in \mathbb{R},^n$ $\boldsymbol{W} \in \mathbb{R}^n$ and $\boldsymbol{P} \in \mathbb{R}^m$ representing the coefficients of $\boldsymbol{v}_h$, $\boldsymbol{w}_h \in V_h$ and $\Psi_h \in M_h$ in the basis representation (3.38), define the norms

$$\|\boldsymbol{V}\|_{V_h} := \|\boldsymbol{v}_h\|_{\mathcal{V}}, \qquad \|\boldsymbol{V}\|_* := \sup_{\boldsymbol{W}\in\mathbb{R}^n} \frac{\boldsymbol{V}\cdot\boldsymbol{W}}{\|\boldsymbol{W}\|_{V_h}}, \qquad \|\boldsymbol{P}\|_{M_h} := \|\Psi\|_{\mathcal{M}}. \tag{3.40}$$

Then, replacing $\boldsymbol{v}_h$ and Ψ_h by the vectors $\boldsymbol{V}$ and $\boldsymbol{P}$, the inf-sup condition turns into

$$\sup_{\boldsymbol{V}\in\mathbb{R}^n} \frac{(\boldsymbol{C}^T\boldsymbol{V})\cdot\boldsymbol{P}}{\|\boldsymbol{V}\|_*} \geq \beta^h \|\boldsymbol{P}\|_{M^h} \qquad \forall \boldsymbol{P} \in \mathbb{R}^m \quad \text{and} \quad \beta^h > 0.$$

With the definition of the norm $\|.\|_*$ from Equation 3.40, the condition finally states

$$\|\boldsymbol{C}\boldsymbol{P}\|_* \geq \hat{\beta}_h \|\boldsymbol{P}\|_{M_h} \quad \forall \boldsymbol{P} \in \mathbb{R}^m \text{ and } \hat{\beta}_h > 0,$$

directly implying the injectivity of the operator $\mathcal{C}$ and the full-rank condition for $\boldsymbol{C}$. This relation is of particular importance for the numerical verification of the inf-sup condition for the coupling matrix $\boldsymbol{C}$, further discussed in Chapter 5.

Chapter 4

The Coupled Model: Magnetic Vector Potential Formulation

As we have seen in the previous chapter, the special choice of the constitutive equations and the energy functions in the Lagrangian resulted in a coupled magnetoelastic saddle point problem. In this chapter, we will follow another approach based on the magnetic vector potential $\boldsymbol{A}$ instead of the total magnetic scalar potential Ψ. Under certain conditions, this approach, which uses a reformulation of the coupled constitutive equations, leads to a symmetric system.
Why does the rearrangement of the variables and the use of a vector potential influence the structure and type of the resulting system? This question is closely linked to the concepts of energy and coenergy, which were discussed in the context of electromechanical and piezoelectric systems by Preumont [95]. Bossavit [17] introduced a differential-geometric approach to magnetoelasticity showing that both elasticity and electromagnetism can be treated within the same framework, making it easier to understand the mutual influence of the magnetic and elastic fields. He discussed some possibilities of choosing the coupled magnetoelastic energy functions, stating that the choice of the energy function and the magnetic and elastic quantities it depends on strongly influences the structure of the resulting problem. As we will see in the next section, the different types of energy functions arise from a Legendre-Fenchel transformation that changes the constitutive laws for the magnetic and elastic variables and the signs of certain terms in the coupled energy density function. Bossavit [17] predicted in his work that the choices of the pairings $\boldsymbol{B}$ and $\boldsymbol{\epsilon}$, as well as $\boldsymbol{H}$ and $\boldsymbol{\sigma}$ as variables of the total energy function lead to a standard minimization problem, whereas in the case of the pairings $\boldsymbol{B}$ and $\boldsymbol{\sigma}$ or $\boldsymbol{H}$ and $\boldsymbol{\epsilon}$, a saddle point problem has to be solved. This difference arises from the duality of the formulations based on mechanical stress on the one hand and strain on the other hand (discussed, e.g. by Ciarlet et al. [37]), as well as the magnetic field $\boldsymbol{H}$ on the one hand and the magnetic flux density $\boldsymbol{B}$ on the other hand (see e.g. Hiptmair's work [66]).

After introducing the concepts of energy and coenergy in the first section of this chapter, we will proceed by deriving a model based on the magnetic flux density $\boldsymbol{B}$ and the strain $\boldsymbol{\epsilon}$ as independent variables, in a similar way as presented in Chapter 3. Taking $\boldsymbol{B}$ instead of $\boldsymbol{H}$ implies the usage of the magnetic vector potential $\boldsymbol{A}$ with $\boldsymbol{B} = \operatorname{curl} \boldsymbol{A}$ instead of the formerly-used magnetic scalar potential Ψ with $\boldsymbol{H} = -\nabla\Psi$. The resulting model conforms with Bossavit's predictions, as in this case a fully-symmetric problem is achieved, which, in the first instance, can be regarded as an advantage over the system with saddle point structure. However, in the general three-dimensional case, the analysis of the new coupled system involves some challenges. Since the choice of $\boldsymbol{A}$ with $\boldsymbol{B} = \operatorname{curl} \boldsymbol{A}$ is not unique, it

requires additional gauging, e.g. by the Coulomb gauge $\nu \operatorname{div} \boldsymbol{A} = \mathbf{0}$. Moreover, due to the curl-curl formulation, the standard Sobolev space $H^1(\Omega)$ has to be replaced by appropriate function spaces like the $H(\operatorname{curl}, \Omega)$-space in the ungauged case and $H(\operatorname{curl}, \Omega) \cap H(\operatorname{div}, \Omega)$ in the gauged (mixed) formulation. In the planar case, these problems do not arise as the gauging condition is automatically fulfilled, and the magnetic vector potential has only a single out of plane - component which leads to a reduction of the (coupled) three-dimensional Ampère's law to a single partial differential equation.

In the course of the chapter, we will discuss the solvability of the new problem and its reduction to the 2D case. In this context, the magnetostatic and time-varying cases will be examined separately since they constitute essentially different formulations, as it was already shown in the introductory chapter.

4.1 The energy - coenergy approach

Before introducing the notion of coenergy for coupled magnetoelastic systems, first of all, we illustrate its relevance in Newtonian mechanics (following Preumont [95]). The commonly-used expression for the kinetic energy of a particle traveling with a velocity v and constant mass m is

$$T^*(v) = \frac{1}{2} m v^2.$$

The above energy term was marked with an asterisk for a special reason: It is not the term we obtain straightaway when deriving an expression for the kinetic energy of a Newtonian particle. If we consider a particle traveling with a linear momentum $p(v)$ in a certain direction x, the force acting on the particle is given by Newton's law

$$f = \frac{\mathrm{d}p}{\mathrm{d}t},$$

and the increment work can be computed as

$$f\,dx = \frac{\mathrm{d}p}{\mathrm{d}t} dx = v \mathrm{d}p.$$

Thus, the total work that is required to increase the momentum from state 0 to state p is described by the kinetic energy

$$T(p) = \int_0^p v(\tilde{p})\, \mathrm{d}\tilde{p}.$$

Using now the constitutive equation $p(v) = mv$ of Newtonian mechanics, we obtain

$$T(p) = \frac{p^2}{2m}.$$

The energy can also be expressed in terms of the velocity rather than the momentum. This leads to a complementary energy function

$$T^*(v) = \int_0^v p(\tilde{v})\, \mathrm{d}\tilde{v},$$

called the kinetic *coenergy* function. Figure 4.1(a) illustrates the two complementary

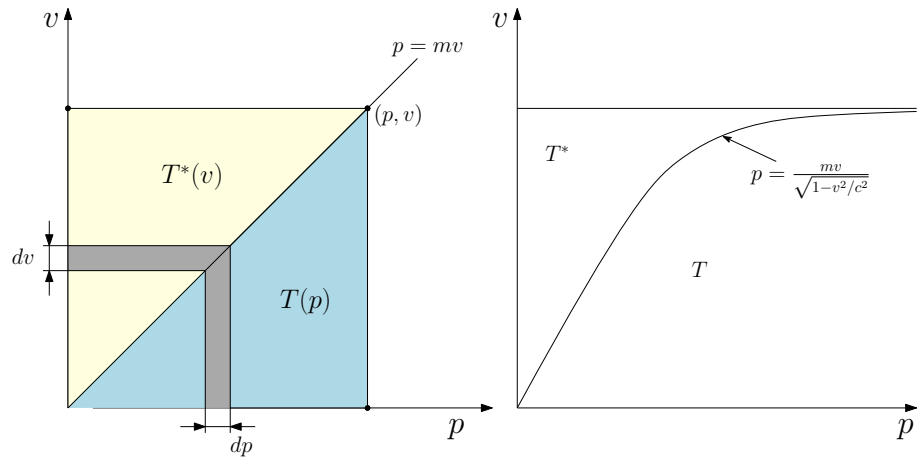

Figure 4.1: Velocity-momentum relation in Newtonian mechanics and special relativity [95].

energy functions for Newtonian mechanics. The coenergy term can be derived from the energy term by a *Legendre transformation*,

$$T^*(v) = pv - T(p). \tag{4.1}$$

The Legendre-transformation is an important tool of convex analysis and is in general used to derive the Hamiltonian formalism out of Lagrangian's or certain thermodynamic principles. We will use the following definition to derive the different coupled magnetoelastic energy functions.

Definition 4.1. *(Legendre transform, [16]) Let X be a Hilbert space with scalar product $(\cdot,\cdot)$ and $\Phi \in X \to \mathbb{R}$ a differentiable function with the gradient $\nabla\Phi(x)$. If the map $x \mapsto \nabla\Phi(x)$ is invertible in the neighborhood of the point x, the function*

$$\Psi(y) = (y, f^{-1}(y)) - \Phi(f^{-1}(y)) \tag{4.2}$$

defined in the neighborhood of $y = f(x)$ is called Legendre transform of the function Φ. Obviously, $\Phi(x)$ can be expressed as

$$\Phi(x) = (f(x), x) - \Psi(f(x))$$

and $\nabla\Psi(y) = x$.

Equation (4.1) follows directly from Equation (4.2) with $(p, v) := pv$ for $p, v \in \mathbb{R}$.
This concept can also be applied to the equations of linear elasticity and electrodynamics: While the elastic energy is a function of the strain $\boldsymbol{\epsilon}$, the elastic coenergy is a function of the stress $\boldsymbol{\sigma}$; while the magnetic energy is based on the magnetic flux density $\boldsymbol{B}$, the magnetic coenergy depends on the magnetic field $\boldsymbol{H}$ [17, 95].
Due to the linear constitutive laws, however, the distinction between kinetic energy and coenergy is usually not necessary in the uncoupled linear elastic or magnetic cases, since the two energy terms coincide, as illustrated for Newtonian mechanics in Figure 4.1(a). This is the reason why the term

$$T^*(v) = \frac{1}{2}mv^2$$

is generally referred to as the *kinetic energy* in the literature. Since in mechanics, the variational principles are mostly based on virtual displacements, this choice seems rather reasonable. When the relation between p and v is not linear any more, which is valid for example for special relativity,

$$p = \frac{mv}{\sqrt{1 - v^2/c^2}},$$

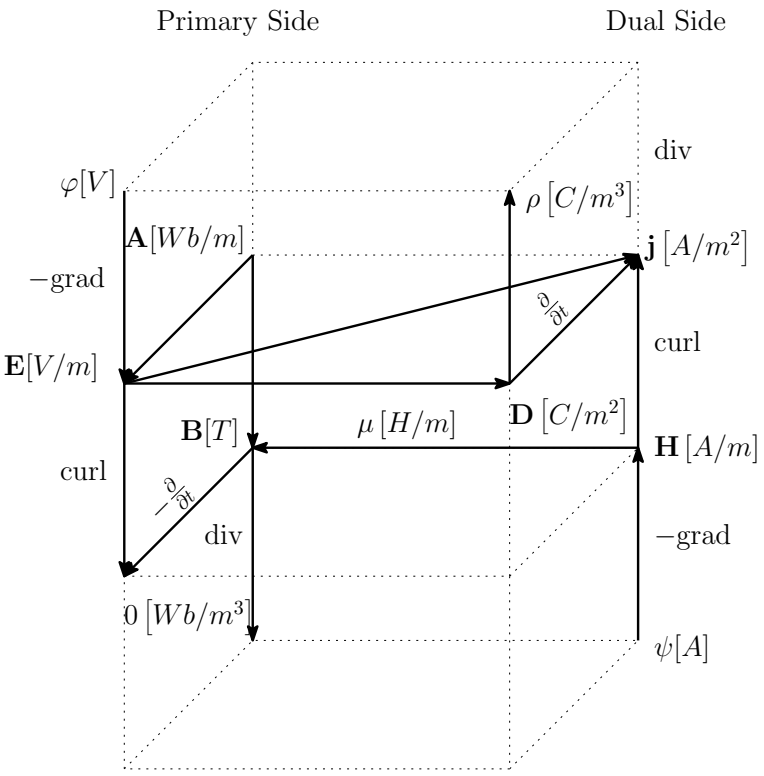

Figure 4.2: Maxwell's house: duality in electromagnetism (after [15, 42]).

with c being the speed of light, then the two energy terms are not equal in case of high velocities v (see Figure 4.1(b)).
The duality between the magnetic flux density $\boldsymbol{B}$ and the magnetic field $\boldsymbol{H}$, as well as the corresponding potentials $\boldsymbol{A}$ and Ψ, is illustrated in Figure 4.2. Electromagnetic quantities such as $\boldsymbol{B}$, $\boldsymbol{H}$ and $\boldsymbol{j}$ build the "floors" of a house, while the operators div, grad and curl connecting them characterize the "pillars". The "building" constructed in such a way was introduced by Bossavit [15] and called *Maxwell's house*.

The distinction between energy and coenergy is also required for coupled systems, since the energy function depends on both elastic and magnetic variables. Preumont [95] discussed this issue for coupled electromechanical systems, listing some possible choices of Lagrangians used in Hamilton's principle for uncoupled mechanical, electromagnetic, as well as for coupled electromagnetic systems. In all cases, the Lagrangian is defined as the difference between the coenergy and energy functions. For mechanical systems, we have

$$L = T^* - U,$$

i.e. the Lagrangian is the difference between the kinetic coenergy and the potential energy. For electromagnetic systems, a possible Lagrangian could be

$$L = W^*_{mag} - W_{el},$$

representing the difference between the magnetic coenergy and the electric energy of the system. For a coupled electromechanical system,

$$L = T^* + W^*_{mag} - U - W_{el} \tag{4.3}$$

could be a possible choice. In order to derive the coupled system based on magnetic scalar potential in Chapter 3, we transferred these results directly to our coupled magnetoelastic model, which seems reasonable as there is a strong analogy between electromechanical and magnetomechanical (e.g. piezoelectric and piezomagnetic) systems. In (3.5), our Lagrangian was similar to (4.3), with T^* and W_{el} being zero. An alternative formulation for

the Lagrangian of the magnetoelastic system is

$$L = T^* + W_{el}^* - U - W_{mag}, \tag{4.4}$$

with W_{el}^* denoting the electrical coenergy and W_{mag} the magnetic energy. Again, T^* and W_{el} are zero for static magnetic and elastic fields. Thus, depending on the type of constitutive equations we are using, we have alternating energy and coenergy terms in the formulation of the Lagrangian. The coupled magnetoelastic energy function depends on $(\boldsymbol{\sigma}, \boldsymbol{H})$ or $(\boldsymbol{B}, \boldsymbol{\epsilon})$, while the pairings $(\boldsymbol{\epsilon}, \boldsymbol{H})$ or $(\boldsymbol{\sigma}, \boldsymbol{B})$ lead to a coupled magnetoelastic coenergy function. In the constitutive equations suggested by the IEEE Standard on Magnetostrictive Materials [70], $\boldsymbol{\sigma}$ and $\boldsymbol{H}$ are considered as independent variables,

$$\begin{aligned} \boldsymbol{\epsilon} &= \boldsymbol{S}^H : \boldsymbol{\sigma} + \boldsymbol{d} \cdot \boldsymbol{H}, \\ \boldsymbol{B} &= \boldsymbol{\mu}^\sigma \boldsymbol{H} + \boldsymbol{d}^T : \boldsymbol{\sigma}, \end{aligned}$$

where $\boldsymbol{S}^H = (\boldsymbol{C}^H)^{-1}$ is the elastic compliance for constant magnetic field, $\boldsymbol{\mu}^\sigma$ is the magnetic permeability for constant stress and $\boldsymbol{b}$ is the magnetoelastic coupling tensor. Changing the independent variables in these equations yields

$$\begin{aligned} \boldsymbol{\sigma} &= \boldsymbol{C}^H : \boldsymbol{\epsilon} - \boldsymbol{e} \cdot \boldsymbol{H}, \\ \boldsymbol{B} &= \boldsymbol{e}^T : \boldsymbol{\epsilon} + \boldsymbol{\mu}^\epsilon \boldsymbol{H}, \end{aligned} \tag{4.5}$$

with the coupling matrix

$$\boldsymbol{e} := \boldsymbol{C}^H : \boldsymbol{d}$$

and the permeability for constant strain,

$$\boldsymbol{\mu}^\epsilon := \boldsymbol{\mu}^\sigma - \boldsymbol{d}^T : \boldsymbol{e}.$$

These are the constitutive equations we used in our model based on the magnetic scalar potential presented in Chapter 3. The free-energy density function corresponding to these constitutive equations is the coenergy function

$$\boldsymbol{\Psi}^*(\boldsymbol{\epsilon}, \boldsymbol{H}) = \frac{1}{2} \boldsymbol{H} \cdot (\boldsymbol{\mu}^\epsilon \boldsymbol{H}) + \boldsymbol{\epsilon} : (\boldsymbol{e} \cdot \boldsymbol{H}) - \frac{1}{2} \boldsymbol{\epsilon} : \boldsymbol{C}^H : \boldsymbol{\epsilon}, \tag{4.6}$$

and $\boldsymbol{\sigma}$ and $\boldsymbol{B}$ can be derived as

$$\begin{aligned} \boldsymbol{\sigma} &= -\frac{\partial \boldsymbol{\Psi}^*(\boldsymbol{\epsilon}, \boldsymbol{H})}{\partial \boldsymbol{\epsilon}} = -\boldsymbol{e} \cdot \boldsymbol{H} + \boldsymbol{C}^H : \boldsymbol{\epsilon} \\ \boldsymbol{B} &= \frac{\partial \boldsymbol{\Psi}^*(\boldsymbol{\epsilon}, \boldsymbol{H})}{\partial \boldsymbol{H}} = \boldsymbol{\mu}^\epsilon \boldsymbol{H} + \boldsymbol{e}^T : \boldsymbol{\epsilon}. \end{aligned}$$

The coupled coenergy function $\boldsymbol{\Psi}^*(\boldsymbol{\epsilon}, \boldsymbol{H})$ is the Legendre-transformation of the coupled energy function

$$\boldsymbol{\Psi}(\boldsymbol{\epsilon}, \boldsymbol{B}) = -\boldsymbol{\Psi}^*(\boldsymbol{\epsilon}, \boldsymbol{H}) + \boldsymbol{H} \cdot \boldsymbol{B} \tag{4.7}$$

with respect to the variable $\boldsymbol{H}$. It is obvious that the use of the coupled coenergy function $\boldsymbol{\Psi}^*(\boldsymbol{\epsilon}, \boldsymbol{H})$ leads to a saddle point problem due to the different signs of the elastic and magnetic terms in (4.6). To avoid this, we can choose constitutive equations based on the coupled energy function $\boldsymbol{\Psi}(\boldsymbol{\epsilon}, \boldsymbol{B})$, rearranging the equations (4.5) in terms of $\boldsymbol{\sigma}$ and $\boldsymbol{H}$:

$$\begin{aligned} \boldsymbol{\sigma} &= \boldsymbol{C}^B : \boldsymbol{\epsilon} - \boldsymbol{f} \cdot \boldsymbol{B}, \\ \boldsymbol{H} &= \boldsymbol{\mu}^{-\epsilon} \boldsymbol{B} - \boldsymbol{f}^T : \boldsymbol{\epsilon}. \end{aligned} \tag{4.8}$$

The tensor

$$\boldsymbol{C}^B := \boldsymbol{C}^H + (\boldsymbol{e} \cdot \boldsymbol{\mu}^{-\epsilon}) \cdot \boldsymbol{e}^T$$

describes the elastic matrix for constant magnetic flux density $\boldsymbol{B}$ and

$$\boldsymbol{f} := \boldsymbol{e} \cdot \boldsymbol{\mu}^{-\epsilon}$$

is the new coupling tensor. The free-energy density function $\boldsymbol{\Psi}(\boldsymbol{\epsilon}, \boldsymbol{B})$ can then be computed using (4.6) and (4.7)

$$\begin{aligned}
\boldsymbol{\Psi}(\boldsymbol{\epsilon}, \boldsymbol{B}) &= \boldsymbol{H} \cdot \boldsymbol{B} - \frac{1}{2}\boldsymbol{H} \cdot (\boldsymbol{\mu}^{\epsilon}\boldsymbol{H}) - \boldsymbol{\epsilon} : (\boldsymbol{e} \cdot \boldsymbol{H}) + \frac{1}{2}\boldsymbol{\epsilon} : \boldsymbol{C}^{H} : \boldsymbol{\epsilon} \\
&= \left(\boldsymbol{\mu}^{-\epsilon}\boldsymbol{B} - \boldsymbol{\mu}^{-\epsilon}(\boldsymbol{e}^{T} : \boldsymbol{\epsilon})\right) \cdot \boldsymbol{B} - \frac{1}{2}\left(\boldsymbol{\mu}^{-\epsilon}\boldsymbol{B} - \boldsymbol{\mu}^{-\epsilon}(\boldsymbol{e}^{T}\,\boldsymbol{\epsilon})\right) \cdot \boldsymbol{\mu}^{\epsilon}\left(\boldsymbol{\mu}^{-\epsilon}\boldsymbol{B} - \boldsymbol{\mu}^{-\epsilon}(\boldsymbol{e}^{T}\,\boldsymbol{\epsilon})\right) \\
&- (\boldsymbol{e}^{T} : \boldsymbol{\epsilon}) \cdot \left(\boldsymbol{\mu}^{-\epsilon}\boldsymbol{B} - \boldsymbol{\mu}^{-\epsilon}(\boldsymbol{e}^{T} : \boldsymbol{\epsilon})\right) + \frac{1}{2}\boldsymbol{\epsilon} : \boldsymbol{C}^{H} : \boldsymbol{\epsilon} \\
&= \frac{1}{2}\boldsymbol{B} \cdot \boldsymbol{\mu}^{-\epsilon}\boldsymbol{B} - \boldsymbol{\epsilon}(\boldsymbol{f} \cdot \boldsymbol{B}) + \frac{1}{2}\boldsymbol{\epsilon} : \boldsymbol{C}^{B} : \boldsymbol{\epsilon}.
\end{aligned}$$

The matrices corresponding to the tensors $\boldsymbol{C}^{B}, \boldsymbol{\mu}^{-\epsilon}$ and $\boldsymbol{f}$ retain the properties of their predecessors, such as positive definiteness and specific features like a diagonal structure. Consider the class of polycrystalline magnetostrictive materials presented in Section 3.4.1. Due to the specific structure of the coupling matrix $\boldsymbol{d}$, the coupling matrix $\boldsymbol{e}$ is given by

$$\begin{aligned}
\boldsymbol{e} = \boldsymbol{C}^{H}\boldsymbol{d} &= \begin{pmatrix} C_{11} & C_{12} & C_{13} & 0 & 0 & 0 \\ C_{12} & C_{22} & C_{23} & 0 & 0 & 0 \\ C_{13} & C_{23} & C_{33} & 0 & 0 & 0 \\ 0 & 0 & 0 & C_{44} & 0 & 0 \\ 0 & 0 & 0 & 0 & C_{55} & 0 \\ 0 & 0 & 0 & 0 & 0 & C_{66} \end{pmatrix} \begin{pmatrix} d_{11} & 0 & 0 \\ d_{21} & 0 & 0 \\ d_{21} & 0 & 0 \\ 0 & 0 & d_{43} \\ 0 & 0 & d_{53} \\ 0 & d_{53} & 0 \end{pmatrix} \\
&= \begin{pmatrix} C_{11}d_{11} + C_{12}d_{21} + C_{13}d_{21} & 0 & 0 \\ C_{12}d_{11} + C_{22}d_{21} + C_{23}d_{21} & 0 & 0 \\ C_{13}d_{11} + C_{23}d_{21} + C_{33}d_{21} & 0 & 0 \\ 0 & 0 & C_{44}d_{43} \\ 0 & 0 & C_{55}d_{53} \\ 0 & C_{66}d_{53} & 0 \end{pmatrix}.
\end{aligned}$$

The matrix $\boldsymbol{d}^{T}\boldsymbol{e} = \boldsymbol{d}^{T}\boldsymbol{C}^{H}\boldsymbol{d}$ is a diagonal matrix with positive entries. Its componentwise expansion yields

$$\boldsymbol{d}^{T}\boldsymbol{e} = \operatorname{diag}\left(d_{11}^{2}C_{11} + 2d_{11}d_{21}(C_{12} + C_{13}) + d_{21}^{2}(C_{22} + 2C_{23} + C_{33}), d_{53}^{2}C_{66}, d_{43}^{2}C_{44} + d_{53}^{2}C_{55}\right).$$

Since C^{H} is symmetric and its components C_{ij} are positive, we have the estimate

$$d_{11}^{2}C_{11} + 2d_{11}d_{21}(C_{12} + C_{13}) + d_{21}^{2}(C_{22} + 2C_{23} + C_{33}) \geq \tilde{C}(d_{11} + d_{21})^{2} \geq 0$$

with

$$\tilde{C} := \min\{C_{11}, (C_{12} + C_{13}), (C_{22} + 2C_{23} + C_{33})\}.$$

Moreover, the reference values for the polycrystalline Terfenol-D used in Section 3.4.2 suggest that the dimension of the components of $\boldsymbol{d}^{T}\boldsymbol{C}^{H}\boldsymbol{d}$ is smaller than the dimension of the entries of $\boldsymbol{\mu}^{\sigma}$, implying that $\boldsymbol{\mu}^{-\epsilon}$ is a diagonal matrix with positive entries as well. Furthermore, if $\boldsymbol{C}^{H}$ is positive definite, then we have

$$\begin{aligned}
\boldsymbol{x}^{T}\boldsymbol{C}^{B}\boldsymbol{x} &= \boldsymbol{x}^{T}\boldsymbol{C}^{H}\boldsymbol{x} + \boldsymbol{x}^{T}\boldsymbol{e}\boldsymbol{\mu}^{-\epsilon}\boldsymbol{e}^{T}\boldsymbol{x} \\
&\geq (\boldsymbol{e}^{T}\boldsymbol{x})^{T}\boldsymbol{\mu}^{-\epsilon}\boldsymbol{e}^{T}\boldsymbol{x} = \boldsymbol{y}^{T}\boldsymbol{\mu}^{-\epsilon}\boldsymbol{y} \geq 0
\end{aligned}$$

for all $\boldsymbol{x} \in \mathbb{R}^{6}$ and $\boldsymbol{y} = \boldsymbol{e}^{T}\boldsymbol{x}$. The last inequality is due to the positive definiteness of a diagonal matrix with positive entries. Finally, the coupling matrix $\boldsymbol{f} = \boldsymbol{e}\boldsymbol{\mu}^{-\epsilon}$ is of the same

form as $\boldsymbol{e}$, since its structure is invariant under the multiplication with the diagonal matrix $\boldsymbol{\mu}^{-\epsilon}$.
After specifying the properties of the system matrices, we can now use the constitutive equations presented above to derive a new coupled system based on the magnetic vector potential.

4.2 The magnetic vector potential model

In analogy to Chapter 3, we will present a derivation of the new coupled model using the example of the magnetostatic case. Furthermore, we will discuss the uniqueness of the magnetic vector potential and present different settings for the coupled problem, stating the strong and weak formulations of the coupled problem for each of the considered cases.

4.2.1 Derivation of the coupled model

Following the same steps as described in Section 3.1, we use the Lagrangian

$$W = -U - W_{mag},$$

as suggested in (4.4). Note that the kinetic coenergy T^* and electrical coenergy W_{el}^* are initially zero, as we deal with a static problem in the first instance. Since we are now considering $\boldsymbol{\epsilon}$ and $\boldsymbol{B}$ as independent variables, we have to introduce several changes to our setting from Chapter 3. Remember that the model presented in Chapter 3 was based on $\boldsymbol{H}$ as an independent variable and we thus assumed that the magnetic field was generated by a permanent magnet, requiring the absence of any currents in the model. This enabled the use of the magnetic scalar potential Ψ with $\boldsymbol{H} = -\nabla\Psi$. In the present model, however, the magnetic flux density $\boldsymbol{B}$ serves as the uncoupled variable, and since $\boldsymbol{B}$ satisfies

$$\operatorname{div} \boldsymbol{B} = 0,$$

it is reasonable to introduce the magnetic vector potential $\boldsymbol{A}$ defined as $\operatorname{curl} \boldsymbol{A} = \boldsymbol{B}$. Obviously, $\operatorname{curl} \boldsymbol{A}$ fulfills the above requirement of a divergence-free magnetic flux density. While in the previous setting, the magnetic field satisfied the homogeneous equation

$$\operatorname{curl} \boldsymbol{H} = \boldsymbol{0},$$

to ensure the existence of a (total) magnetic scalar potential, the new model does not need such a requirement, allowing the magnetic field to be generated by a current-carrying coil. Note that in electromagnetic simulations, coils are commonly not modeled as separate conducting regions but are incorporated into the model by a given current density.
Suppose that the coil is arranged next to the magnetostrictive body and generates a magnetic field in the air region surrounding the material. Hence, we have to distinguish between the material domain $\Omega_c \subset \mathbb{R},^3$ where the subscript refers to the term "conducting" and the total domain $\mathbb{R}^3 \supset \Omega = \Omega_0 \cup \Omega_c$, where Ω_0 describes the surrounding air or vacuum region. We denote by Γ_D and $\Gamma_{c,D}$, the Dirichlet boundaries of the elastic and magnetic field in the conducting region Ω, respectively, and by $\Gamma_{0,D}$ the Dirichlet boundary of the air region. Similarly, Γ_N and $\Gamma_{c,N}$ characterize the corresponding elastic and magnetic Neumann boundaries of the domain Ω_c. The interface between the non-conducting region Ω_0 and the conducting region Ω_c is denoted by Γ_I and assumed to be fixed. Let $\boldsymbol{n}$ denote the outer unit normal vector of the boundaries of Ω_c and of Ω_0, as well as of the interface Γ_I.

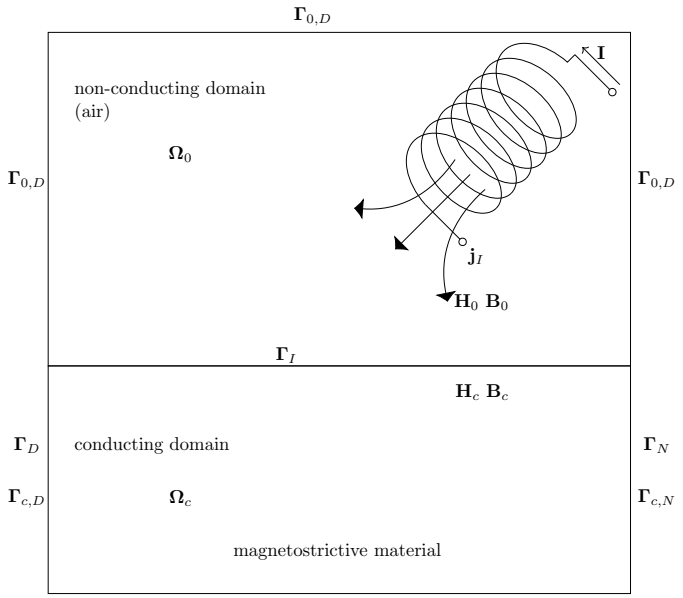

Figure 4.3: 2D sketch of the model geometry with boundaries and interface (based on [81]).

In all models presented in this chapter, we apply the magnetic vector potential on the whole electromagnetic domain Ω. This is the general, though not very economic way of solving a static electromagnetic problem. Another possibility is the combined use of the magnetic vector potential $\boldsymbol{A}$ in the conducting region and a reduced magnetic scalar potential Φ or the total magnetic scalar potential Ψ in the air region, as suggested, e.g. in [81]. This solution method significantly reduces the number of unknowns but has the drawback of imposing additional interface conditions to couple the two different potentials in the model. The use of additional electromagnetic variables might not be beneficial for the coupled magnetoelastic problem as it increases the complexity of the model. Figure 4.3 shows a two-dimensional sketch of the magnetostrictive material placed in a region filled with air. A coil driven with the *impressed current density* $\boldsymbol{j}_I : \Omega_0 \to \mathbb{R}^3$ generates the magnetic flux density $\boldsymbol{B}_0 : \Omega_0 \to \mathbb{R}^3$ and the magnetic field $\boldsymbol{H}_0 : \Omega_0 \to \mathbb{R}^3$ in the air region. The corresponding quantities of the conducting region are $\boldsymbol{B}_c$ and $\boldsymbol{H}_c$. The mechanical displacement $\boldsymbol{u}$ is now defined on the domain Ω_c, i.e. $\boldsymbol{u} : \Omega_c \to \mathbb{R}^3$.
To be able to state the strong form of the coupled system in the whole domain Ω, we have to extend the above definitions and introduce material parameters as discontinuous functions on Ω. This is a common notation used in the literature concerned with electromagnetic problems as it reduces the number of the resulting equations and provides a clearly represented model. Ampere's law is then presented in a single vector-valued equation on Ω involving differential operators applied to quantities with jumping material parameters instead of two vector-valued equations on the domains Ω_0 and Ω_c.
We consider the magnetic vector potential $\boldsymbol{A} : \Omega \to \mathbb{R}^3$ with $\boldsymbol{B} = \operatorname{curl} \boldsymbol{A}$ as the independent variable of the magnetic part of the problem. The total magnetic flux density $\boldsymbol{B} : \Omega \to \mathbb{R}^3$ is defined as

$$\boldsymbol{B}(\boldsymbol{x}) = \begin{cases} \boldsymbol{B}_0 & \boldsymbol{x} \in \Omega_0, \\ \boldsymbol{B}_c & \boldsymbol{x} \in \Omega_c, \end{cases}$$

and the total magnetic field $\boldsymbol{H} : \Omega \to \mathbb{R}^3$ is defined in the same manner.
The normal component of the magnetic flux density is assumed to be vanishing on the boundary $\Gamma_{0,D}$ of the air region. Moreover, a homogeneous condition is also set on the

Dirichlet boundary $\Gamma_{c,D}$ of the material.

$$\boldsymbol{A} \times \boldsymbol{n} = \boldsymbol{0} \text{ on } \Gamma_{0,D} \cup \Gamma_{c,D}.$$

To incorporate the above-mentioned changes into the constitutive equations, we define the magnetic permeability tensor $\boldsymbol{\mu}$ by,

$$\boldsymbol{\mu}(\boldsymbol{x}) := \begin{cases} \boldsymbol{\mu}_0 & \boldsymbol{x} \in \Omega_0, \\ \boldsymbol{\mu}^{\epsilon} & \text{otherwise,} \end{cases}$$

where $\boldsymbol{\mu}_0 := \mu_0 \boldsymbol{I}$ denotes the 3×3 vacuum permeability tensor. The inverse $\boldsymbol{\mu}^{-1}$ is then given by

$$\boldsymbol{\mu}^{-1}(\boldsymbol{x}) := \begin{cases} \boldsymbol{\mu}_0^{-1} & \boldsymbol{x} \in \Omega_0, \\ \boldsymbol{\mu}^{-\epsilon} & \text{otherwise.} \end{cases}$$

The coupling tensor $\boldsymbol{f}$ can be generalized to

$$\hat{\boldsymbol{f}}(\boldsymbol{x}) := \begin{cases} \boldsymbol{0} & \boldsymbol{x} \in \Omega_0 \\ \boldsymbol{f} & \text{otherwise,} \end{cases}$$

which implies that the total magnetic field vector $\boldsymbol{H}$ is given by

$$\boldsymbol{H}(\boldsymbol{x}) := \begin{cases} \boldsymbol{H}_0 = \boldsymbol{\mu}_0^{-1} \operatorname{curl} \boldsymbol{A}(\boldsymbol{x}) & \boldsymbol{x} \in \Omega_0, \\ \boldsymbol{H}_c = \boldsymbol{\mu}^{-\epsilon} \operatorname{curl} \boldsymbol{A}(\boldsymbol{x}) - \boldsymbol{f}^T \cdot \boldsymbol{\epsilon}(\boldsymbol{u}(\boldsymbol{x})) & \text{otherwise.} \end{cases}$$

To avoid confusion, we drop the subscript "f" denoting the free current in Chapter 2 and define the total current density vector

$$\boldsymbol{j}(\boldsymbol{x}) := \begin{cases} \boldsymbol{j}_0 & \boldsymbol{x} \in \Omega_0, \\ \boldsymbol{j}_c & \text{otherwise.} \end{cases}$$

Note that in the magnetostatic setting, there is no current flow in the conductor, i.e. $\boldsymbol{j}_c = \boldsymbol{0}$. The current density in the vacuum or air region is defined by the impressed current density, i.e. $\boldsymbol{j}_0 = \boldsymbol{j}_I$. Ampere's law $\operatorname{curl} \boldsymbol{H} = \boldsymbol{j}$ implies that $\boldsymbol{j}_I$ must be a solenoidal field. Finally, the elastic displacement field can be generalized to Ω by setting $\boldsymbol{u}(\boldsymbol{x}) = \boldsymbol{0}$ for $\boldsymbol{x} \in \Omega_0$.
On the magnetic Neumann boundary of the magnetostrictive material, we impose the condition

$$\boldsymbol{H}_c \times \boldsymbol{n} = \boldsymbol{K},$$

with $\boldsymbol{K}$ denoting the surface current density. Finally, the continuity conditions

$$\begin{aligned} \boldsymbol{H}_c \times \boldsymbol{n} &= \boldsymbol{H}_0 \times \boldsymbol{n}, \\ \boldsymbol{B}_c \cdot \boldsymbol{n} &= \boldsymbol{B}_0 \cdot \boldsymbol{n}, \end{aligned}$$

hold on the interface Γ_I of the material and vacuum/air region.

Summing up, we can state the expression for the total energy of the magnetoelastic system, formulating it in terms of the general tensor-valued notation in the first instance, as done in Chapter 3.

$$\begin{aligned} L &= -U - W_{mag} \\ &= -\frac{1}{2} \int_{\Omega} \boldsymbol{H}(\boldsymbol{u}, \boldsymbol{A}) \cdot \boldsymbol{B}(\boldsymbol{A}) \, \mathrm{d}x + \int_{\Omega} \boldsymbol{A} \cdot \boldsymbol{j} \, \mathrm{d}x + \int_{\Gamma_{c,N}} \boldsymbol{A} \cdot \boldsymbol{K} \, \mathrm{d}s \\ &\quad - \int_{\Omega_c} \boldsymbol{\sigma}(\boldsymbol{u}, \boldsymbol{A}) : \boldsymbol{\epsilon}(\boldsymbol{u}) \, \mathrm{d}x + \int_{\Gamma_N} \boldsymbol{u} \cdot \boldsymbol{\tau} \, \mathrm{d}s, \end{aligned} \tag{4.9}$$

where $\boldsymbol{\tau}$ and $\boldsymbol{K}$ are the elastic and magnetic surface tractions on the corresponding Neumann boundaries. Note that

$$\int_\Omega \boldsymbol{H}\cdot\boldsymbol{B}\,\mathrm{d}x = \int_{\Omega_c} (\boldsymbol{\mu}^{-\epsilon}\operatorname{curl}\boldsymbol{A} - \boldsymbol{f}^T:\boldsymbol{\epsilon})\cdot\operatorname{curl}\boldsymbol{A}\,\mathrm{d}x + \int_{\Omega_0}\boldsymbol{\mu}_0^{-1}\operatorname{curl}\boldsymbol{A}\cdot\operatorname{curl}\boldsymbol{A}\,\mathrm{d}x$$

and

$$\int_\Omega \boldsymbol{A}\cdot\boldsymbol{j}\,\mathrm{d}x = \int_{\Omega_c}\boldsymbol{A}\cdot\boldsymbol{j}_c\,\mathrm{d}x + \int_{\Omega_0}\boldsymbol{A}\cdot\boldsymbol{j}_0\,\mathrm{d}x.$$

Defining the function

$$J(\theta) := -W_{mag}(\boldsymbol{u}, \boldsymbol{A}+\theta\tilde{\boldsymbol{A}}) - U(\boldsymbol{u}+\theta\boldsymbol{v}, \boldsymbol{A}),$$

with admissible test functions

$$\boldsymbol{v}(\boldsymbol{x}) = \boldsymbol{0} \quad \text{on } \Gamma_D \quad \text{and} \quad \tilde{\boldsymbol{A}}(\boldsymbol{x})\times\boldsymbol{n} = \boldsymbol{0} \quad \text{on } \Gamma_{c,D},$$

and inserting the relation $\operatorname{curl}\boldsymbol{A} = \boldsymbol{B}$, as well as the constitutive equations (4.8), we obtain

$$\begin{aligned} J(\theta) &= \frac{d}{d\theta}\Big|_{\theta=0}\Bigg[-\frac{1}{2}\int_\Omega\Big[\boldsymbol{\mu}^{-1}\operatorname{curl}(\boldsymbol{A}+\theta\tilde{\boldsymbol{A}})) - \hat{\boldsymbol{f}}^T:\boldsymbol{\epsilon}(\boldsymbol{u})\Big]\cdot\operatorname{curl}(\boldsymbol{A}+\theta\tilde{\boldsymbol{A}})\,\mathrm{d}x \\ &+ \int_\Omega(\boldsymbol{A}+\theta\tilde{\boldsymbol{A}})\cdot\boldsymbol{j}\,\mathrm{d}x + \int_{\Gamma_{c,N}}(\boldsymbol{A}+\theta\tilde{\boldsymbol{A}})\cdot\boldsymbol{K}\,\mathrm{d}s \\ &- \frac{1}{2}\int_{\Omega_c}\big(\boldsymbol{C}^B:\boldsymbol{\epsilon}(\boldsymbol{u}+\theta\boldsymbol{v}) - \boldsymbol{f}\cdot\operatorname{curl}\boldsymbol{A}\big):\boldsymbol{\epsilon}(\boldsymbol{u}+\theta\boldsymbol{v})\,\mathrm{d}x + \int_{\Gamma_N}(\boldsymbol{u}+\theta\boldsymbol{v})\cdot\boldsymbol{\tau}\,\mathrm{d}s\Bigg]. \end{aligned}$$

Differentiating with respect to θ results in

$$\begin{aligned} 0 &= \frac{1}{2}\int_\Omega 2(\boldsymbol{\mu}^{-1}\operatorname{curl}\boldsymbol{A})\cdot\operatorname{curl}\tilde{\boldsymbol{A}} - (\hat{\boldsymbol{f}}^T:\boldsymbol{\epsilon}(\boldsymbol{u}))\cdot\operatorname{curl}\tilde{\boldsymbol{A}}\,\mathrm{d}x - \int_\Omega\tilde{\boldsymbol{A}}\cdot\boldsymbol{j}\,\mathrm{d}x - \int_{\Gamma_{c,N}}\tilde{\boldsymbol{A}}\cdot\boldsymbol{K}\,\mathrm{d}s \\ &+ \frac{1}{2}\int_{\Omega_c}\big(\boldsymbol{C}^B:\boldsymbol{\epsilon}(\boldsymbol{u})\big):\boldsymbol{\epsilon}(\boldsymbol{v}) + \boldsymbol{\sigma}(\boldsymbol{u},\boldsymbol{A}):\boldsymbol{\epsilon}(\boldsymbol{v}) - \boldsymbol{f}\cdot(\operatorname{curl}\boldsymbol{A}):\boldsymbol{\epsilon}(\boldsymbol{v})\,\mathrm{d}x - \int_{\Gamma_N}\boldsymbol{v}\cdot\boldsymbol{\tau}\,\mathrm{d}s. \end{aligned}$$

Using the same arguments and reformulations as in the derivation of the model based on scalar potential, as well as the relations

$$\begin{aligned} \int_\Omega(\boldsymbol{\mu}^{-1}\operatorname{curl}\boldsymbol{A})\cdot\operatorname{curl}\tilde{\boldsymbol{A}}\,\mathrm{d}x &= \int_\Omega\tilde{\boldsymbol{A}}\cdot\big(\operatorname{curl}(\boldsymbol{\mu}^{-1}\operatorname{curl}\boldsymbol{A})\big)\,\mathrm{d}x \\ &- \int_{\Gamma_{c,N}}(\tilde{\boldsymbol{A}}\times\boldsymbol{n})\cdot(\boldsymbol{\mu}^{-\epsilon}\operatorname{curl}\boldsymbol{A})\,\mathrm{d}s, \\ \int_\Omega(\hat{\boldsymbol{f}}^T:\boldsymbol{\epsilon}(\boldsymbol{u}))\cdot\operatorname{curl}\tilde{\boldsymbol{A}}\,\mathrm{d}x &= \int_\Omega\tilde{\boldsymbol{A}}\cdot\operatorname{curl}(\hat{\boldsymbol{f}}^T:\boldsymbol{\epsilon}(\boldsymbol{u}))\,\mathrm{d}x \\ &- \int_{\Gamma_{c,N}}(\tilde{\boldsymbol{A}}\times\boldsymbol{n})\cdot(\boldsymbol{f}^T:\boldsymbol{\epsilon}(\boldsymbol{u}))\,\mathrm{d}s, \end{aligned}$$

for the coupled magnetic part, we obtain the equation

$$\begin{aligned}
0 &= \int_\Omega \tilde{\boldsymbol{A}} \cdot \left[\operatorname{curl}(\boldsymbol{u}^{-1} \operatorname{curl} \boldsymbol{A}) - \frac{1}{2} \operatorname{curl}\left(\hat{\boldsymbol{f}}^T : \boldsymbol{\epsilon}(\boldsymbol{u}) \right) - \tilde{\boldsymbol{A}} \cdot \boldsymbol{j} \right] \mathrm{d}x \\
&- \int_{\Omega_c} \boldsymbol{v} \cdot \left[\mathbf{div}\left(\boldsymbol{C}^B : \boldsymbol{\epsilon}(\boldsymbol{u}) \right) - \frac{1}{2} \mathbf{div}\left(\boldsymbol{f} \cdot \operatorname{curl} \boldsymbol{A} \right) \right] \mathrm{d}x \\
&+ \int_{\Gamma_{c,N}} \frac{1}{2} (\tilde{\boldsymbol{A}} \times \boldsymbol{n})(\boldsymbol{f}^T : \boldsymbol{\epsilon}(\boldsymbol{u})) \, \mathrm{d}s + \int_{\Gamma_{c,N}} (\tilde{\boldsymbol{A}} \times \boldsymbol{n})(-\boldsymbol{\mu}^{-\epsilon} \cdot \operatorname{curl} \boldsymbol{A}) \, \mathrm{d}s - \int_{\Gamma_{c,N}} \tilde{\boldsymbol{A}} \cdot \boldsymbol{K} \, \mathrm{d}s \\
&+ \int_{\Gamma_N} \boldsymbol{v} \cdot \left[\left(\boldsymbol{C}^B : \boldsymbol{\epsilon}(\boldsymbol{u}) - \frac{1}{2} \boldsymbol{f} \cdot (\operatorname{curl} \boldsymbol{A}) \right) \cdot \boldsymbol{n} - \boldsymbol{\tau} \right] \mathrm{d}s.
\end{aligned}$$

Note that although the differential operators are applied to discontinuous quantities, the integration over the whole domain Ω implies a summation of integrals over its subsets Ω_c and Ω_0. Therefore, the known integral relations over Lipschitz domains are still valid for this setting.
Using the relation

$$(\tilde{\boldsymbol{A}} \times \boldsymbol{n}) \left(\frac{1}{2} \boldsymbol{f}^T : \boldsymbol{\epsilon}(\boldsymbol{u}) - \boldsymbol{\mu}^{-\epsilon} \operatorname{curl} \boldsymbol{A} \right) = \tilde{\boldsymbol{A}} \cdot \left[-\frac{1}{2} \boldsymbol{f}^T : \boldsymbol{\epsilon}(\boldsymbol{u}) + \boldsymbol{\mu}^{-1} \operatorname{curl} \boldsymbol{A} \right] \times \boldsymbol{n},$$

the variational formulation of our new coupled problem can be written as

$$\begin{aligned}
0 &= \int_\Omega \tilde{\boldsymbol{A}} \cdot \left[\operatorname{curl}(\boldsymbol{\mu}^{-1} \operatorname{curl} \times \boldsymbol{A}) - \frac{1}{2} \operatorname{curl}(\hat{\boldsymbol{f}}^T : \boldsymbol{\epsilon}(\boldsymbol{u})) - \boldsymbol{j} \right] \mathrm{d}x \\
&+ \int_{\Omega_c} \boldsymbol{v} \cdot \left[- \mathbf{div}(\boldsymbol{C}^B : \boldsymbol{\epsilon}(\boldsymbol{u})) + \frac{1}{2} \mathbf{div}(\boldsymbol{f} \cdot \operatorname{curl} \boldsymbol{A}) \right] \mathrm{d}x \\
&+ \int_{\Gamma_{c,N}} \tilde{\boldsymbol{A}} \cdot \left[\left(\boldsymbol{\mu}^{-\epsilon} \operatorname{curl} \boldsymbol{A} - \frac{1}{2} (\boldsymbol{f}^T : \boldsymbol{\epsilon}(\boldsymbol{u})) \right) \times \boldsymbol{n} - \boldsymbol{K} \right] \mathrm{d}s \\
&+ \int_{\Gamma_N} \boldsymbol{v} \cdot \left[\left(\boldsymbol{C}^B : \boldsymbol{\epsilon}(\boldsymbol{u}) - \frac{1}{2} \boldsymbol{f} \cdot \operatorname{curl} \boldsymbol{A} \right) \boldsymbol{n} - \boldsymbol{\tau} \right] \mathrm{d}s,
\end{aligned} \tag{4.10}$$

for all admissible $\boldsymbol{v}$ and $\tilde{\boldsymbol{A}}$. Considering the cases $\boldsymbol{v} = \boldsymbol{0}$ on Γ_N and $\tilde{\boldsymbol{A}} \times \boldsymbol{n} = \boldsymbol{0}$ on $\Gamma_{c,N}$, as well as $\boldsymbol{v} \neq \boldsymbol{0}$ on Γ_N and $\tilde{\boldsymbol{A}} \times \boldsymbol{n} \neq \boldsymbol{0}$ on $\Gamma_{c,N}$ separately and making use of the fundamental lemma of calculus of variations as we did for the previous model, we can state the strong form of the new coupled problem for sufficiently smooth $\boldsymbol{u}$ and $\boldsymbol{A}$,

Problem $(CP)^{A^*}$: Find $(\boldsymbol{u}, \boldsymbol{A})$, such that

$$\begin{aligned}
\mathbf{div}(\boldsymbol{C}^B : \boldsymbol{\epsilon}(\boldsymbol{u})) - \frac{1}{2} \mathbf{div}(\boldsymbol{f} \cdot \operatorname{curl} \boldsymbol{A}) &= \boldsymbol{0} \quad \text{in } \Omega_c, \\
\operatorname{curl}(\boldsymbol{\mu}^{-1} \operatorname{curl} \boldsymbol{A}) - \frac{1}{2} \operatorname{curl}(\hat{\boldsymbol{f}}^T : \boldsymbol{\epsilon}(\boldsymbol{u})) &= \boldsymbol{j} \quad \text{in } \Omega,
\end{aligned}$$

with Dirichlet boundary conditions

$$\begin{aligned}
\boldsymbol{u} &= \boldsymbol{0} \quad \text{on } \Gamma_D, \\
\boldsymbol{A} \times \boldsymbol{n} &= \boldsymbol{0} \quad \text{on } \Gamma_{c,D} \cup \Gamma_{0,D}
\end{aligned}$$

and Neumann boundary conditions

$$\begin{aligned}
\left(\boldsymbol{C}^B : \boldsymbol{\epsilon}(\boldsymbol{u}) - \frac{1}{2} \boldsymbol{f} \cdot (\operatorname{curl} \boldsymbol{A}) \right) \cdot \boldsymbol{n} &= \boldsymbol{\tau} \quad \text{on } \Gamma_N, \\
\left(\boldsymbol{\mu}^{-\epsilon} \operatorname{curl} \boldsymbol{A} - \frac{1}{2} \boldsymbol{f}^T : \boldsymbol{\epsilon}(\boldsymbol{u}) \right) \times \boldsymbol{n} &= \boldsymbol{K} \quad \text{on } \Gamma_{c,N}.
\end{aligned}$$

4.2.2 The uniqueness issue

The uniqueness of the vector potential has not been assumed so far. As mentioned before, uniqueness can be ensured by an additional gauging condition. The most commonly used gauge is the Coulomb gauge (e.g. in [2])

$$\operatorname{div} \boldsymbol{A} = 0,$$

valid in the considered domain, with the boundary condition

$$\boldsymbol{A} \cdot \boldsymbol{n} = 0,$$

which stems from Gauss' integral law.

Remark 4.1. *Remember that in a general geometrical setting, the above conditions do not necessarily guarantee the uniqueness of a function in a region Ω. The elements of the finite-dimensional space of harmonic functions defined as*

$$\mathcal{H}(m,\Omega) := \{\boldsymbol{w} \in L^2(\Omega)^3 \mid \operatorname{curl} \boldsymbol{w} = \boldsymbol{0},\ \operatorname{div} \boldsymbol{w} = 0 \ \text{ in } \Omega,\ \boldsymbol{w} \cdot \boldsymbol{n} = 0 \text{ on } \partial\Omega\},$$

with $\partial\Omega$ denoting the boundary of Ω and $\boldsymbol{n}$ the corresponding normal vector, are irrotational, solenoidal and tangential and are thus examples of non-trivial vector fields satisfying the above-mentioned uniqueness assumptions. In this case, additional conditions have to be imposed (for a detailed insight, refer to [2]). If, however, Ω is a simply connected region, which is the case in most engineering applications, no additional uniqueness conditions are required.

At the discrete level, the construction of a suitable finite element space with divergence-free functions is not straightforward. A way out is to impose the divergence-free condition by introducing Lagrange multipliers or by adding a penalization term (see e.g. Coulomb [43], Bíró and Preis [32] or Preis et al. [93]).
In the following, we will consider three different settings for Maxwell's equations. As explained in Chapter 2, assuming that the electric field can be expressed as $\boldsymbol{E} = -\frac{\partial \boldsymbol{A}}{\partial t}$, Ampere's law takes the form

$$\operatorname{curl}(\boldsymbol{\mu}^{-1} \operatorname{curl} \boldsymbol{A}) - \boldsymbol{\sigma} \frac{\partial \boldsymbol{A}}{\partial t} + \hat{\boldsymbol{\epsilon}} \frac{\partial^2 \boldsymbol{A}}{\partial t^2} = \boldsymbol{j}_I. \tag{4.11}$$

Here, $\boldsymbol{\sigma}$ and $\hat{\boldsymbol{\epsilon}}$ are the total magnetic conductivity and permittivity tensors, defined as

$$\boldsymbol{\sigma}(\boldsymbol{x}) = \begin{cases} \boldsymbol{0} & \boldsymbol{x} \in \Omega_0, \\ \boldsymbol{\sigma}_c & \text{otherwise}, \end{cases}$$

with $\boldsymbol{\sigma}_c$ being the conductivity of the material and

$$\hat{\boldsymbol{\epsilon}}(\boldsymbol{x}) = \begin{cases} \epsilon_0 \boldsymbol{I} & \boldsymbol{x} \in \Omega_0, \\ \boldsymbol{\epsilon}_c & \text{otherwise}, \end{cases}$$

where ϵ_0 is the vacuum permittivity, $\boldsymbol{I} \in \mathbb{R}^{3\times 3}$ denotes the identity tensor and $\boldsymbol{\epsilon}_c$ is the permittivity of the material. Note that all of the above-defined tensors are of order two and, as in the case of the magnetic permeability, can be assumed to have a diagonal structure for the considered material class of polycrystalline magnetostrictive materials.
In terms of the parameter tensor $\boldsymbol{\kappa}$, the above equation reads

$$\operatorname{curl}(\boldsymbol{\mu}^{-1} \operatorname{curl} \boldsymbol{A}) + \boldsymbol{\kappa} \boldsymbol{A} = \boldsymbol{j}_I. \tag{4.12}$$

In the magnetostatic case, $\boldsymbol{\kappa} = \mathbf{0}$ in Ω and $\operatorname{supp}(\boldsymbol{j}_I) = \Omega_0$. Therefore, as in the previous section, we introduce a total current density vector $\boldsymbol{j}$ with

$$\boldsymbol{j}(\boldsymbol{x}) = \begin{cases} \boldsymbol{j}_I & \boldsymbol{x} \in \Omega_0, \\ \mathbf{0} & \text{otherwise}, \end{cases}$$

and express the magnetostatic Ampere law in Ω as

$$\operatorname{curl}(\boldsymbol{\mu}^{-1} \operatorname{curl} \boldsymbol{A}) = \boldsymbol{j}. \tag{4.13}$$

In this case, the magnetic vector potential is not uniquely defined and additional gauging is required.
In the time-harmonic case, assuming that the time-harmonic current density and magnetic vector potential can be expressed as

$$\begin{aligned} \tilde{\boldsymbol{j}}_I(\boldsymbol{x}, t) &= \operatorname{Re}(\boldsymbol{j}_I(\boldsymbol{x}) e^{i\omega t}), \\ \tilde{\boldsymbol{A}}(\boldsymbol{x}, t) &= \operatorname{Re}(\boldsymbol{A}(\boldsymbol{x}) e^{i\omega t}), \end{aligned}$$

where $\boldsymbol{A} : \Omega \to \mathbb{C}^3$ and $\boldsymbol{j}_I : \Omega \to \mathbb{C}^3$ are complex-valued functions and ω denotes the frequency, we obtain the full Maxwell system in the frequency domain with

$$\boldsymbol{\kappa} = i\omega\boldsymbol{\sigma} - \omega^2 \hat{\boldsymbol{\epsilon}}.$$

Note that the time-harmonic Maxwell system is satisfied by the field $\boldsymbol{A} : \Omega \to \mathbb{C}^3$, as well as by its real and imaginary parts.
Since $\boldsymbol{\kappa} \neq \mathbf{0}$ on the whole domain Ω, the vector potential $\boldsymbol{A}$ is uniquely defined and no gauging is needed. In the eddy current approximation of Maxwell's equations in the frequency domain, $\boldsymbol{\kappa}$ vanishes in Ω_0 and gauging is required only for the air region. Finally, in case that $\boldsymbol{\kappa} \in \mathbb{R}^{3\times3}_+$, the vector potential is again uniquely defined on the whole domain. Note that the impressed current density is present in the differential equation for the material domain in all cases except the magnetostatic case, where there is no current flow in the conductor.
The derivation of the coupled models with $\boldsymbol{\kappa} \in \mathbb{C}^{3\times3}$ follows the same steps as presented in Section 4.2.1 by additionally including the term

$$\frac{1}{2} \int_\Omega (\boldsymbol{\kappa}\boldsymbol{A}) \cdot \boldsymbol{A} \, \mathrm{d}x$$

into the magnetic energy functional and will therefore be omitted in this work. We will directly present and discuss the strong and weak forms of the coupled models for the above-mentioned settings in the following sections.

4.2.3 The coupled problem in the magnetostatic case

In the magnetostatic case, we obtain uniqueness by enforcing the Coulomb gauge on the whole domain Ω through an additional condition. Then, the strong form of the coupled problem for sufficiently smooth $\boldsymbol{u}$ and $\boldsymbol{A}$ reads

Problem $(CP)^A$: Find $(\boldsymbol{u}, \boldsymbol{A})$ such that

$$\begin{aligned} \mathbf{div}(\boldsymbol{C}^B : \boldsymbol{\epsilon}(\boldsymbol{u})) - \frac{1}{2} \mathbf{div}(\boldsymbol{f} \cdot \operatorname{curl} \boldsymbol{A}) &= \mathbf{0} \quad \text{in } \Omega, \\ \operatorname{curl}(\boldsymbol{\mu}^{-1} \operatorname{curl} \boldsymbol{A}) - \frac{1}{2} \operatorname{curl}(\boldsymbol{f}^T : \boldsymbol{\epsilon}(\boldsymbol{u})) &= \boldsymbol{j} \quad \text{in } \Omega, \\ \operatorname{div} \boldsymbol{A} &= 0 \quad \text{in } \Omega. \end{aligned}$$

In addition to the boundary and interface conditions defined in Section 4.2.1, the gauging entails the boundary conditions

$$\begin{aligned} \boldsymbol{A}\cdot\boldsymbol{n} &= 0 \quad \text{on } \Gamma_{0,D}\cup\Gamma_{c,D},\\ \operatorname{div}\boldsymbol{A} &= 0 \quad \text{on } \Gamma_{c,N}. \end{aligned}$$

To obtain the weak form of the coupled gauged magnetostatic problem $(CP)^A$, we reformulate it as a saddle point problem, following the procedure explained in Chapter 2. Since $\boldsymbol{A}$ is only defined up to a gradient of a scalar function $\psi \in H^1(\Omega)$, we require that

$$\int_\Omega \boldsymbol{A}\cdot\nabla\psi \,\mathrm{d}x = 0,$$

for all $\psi \in H^1(\Omega)$. Moreover, we use the function spaces

$$\begin{aligned} \mathcal{V} &:= H^1(\Omega_c)^3,\\ \mathcal{V}_0 &:= \{\boldsymbol{v}\in\mathcal{V} \mid \boldsymbol{v}=\boldsymbol{0} \text{ on } \Gamma_D\}, \end{aligned}$$

for the elastic displacement and the space

$$H_\Gamma(\operatorname{curl},\Omega) := \{\boldsymbol{w}\in H(\operatorname{curl},\Omega) \mid \boldsymbol{w}\times\boldsymbol{n}=\boldsymbol{0} \text{ on } \Gamma_{c,D}\cup\Gamma_{0,D}\},$$

for the magnetic vector potential. Note that the current density $\boldsymbol{j}_I$ is an element of the space $L^2(\Omega)^3$, while the Neumann boundary value $\boldsymbol{K}$ belongs to the trace space $H^{-\frac{1}{2}}(\operatorname{div},\Gamma_{c,N})$ (see Chapter 2).
With the above definitions, we obtain the following weak problem:

Problem $(CP)^{A,w}$: Find $(\boldsymbol{u},\boldsymbol{A},\phi)\in\mathcal{V}_0\times H_\Gamma(\operatorname{curl},\Omega)\times H^1(\Omega)$, such that

$$\begin{aligned} a(\boldsymbol{u},\boldsymbol{v}) - \tilde{c}(\boldsymbol{A},\boldsymbol{v}) &= l(\boldsymbol{v}) && \text{for } \boldsymbol{v}\in\mathcal{V}_0,\\ -\tilde{c}(\tilde{\boldsymbol{A}},\boldsymbol{u}) + \bar{b}(\boldsymbol{A},\tilde{\boldsymbol{A}}) + d(\tilde{\boldsymbol{A}},\phi) &= \tilde{m}(\boldsymbol{A}) && \text{for } \tilde{\boldsymbol{A}}\in H_\Gamma(\operatorname{curl},\Omega),\\ d(\boldsymbol{A},\psi) &= 0 && \text{for } \psi\in H^1(\Omega), \end{aligned}$$

with bilinear forms and linear functionals defined as

$$a(\boldsymbol{u},\boldsymbol{v}) = \int_{\Omega_c} \nabla\boldsymbol{v} : (\boldsymbol{C}^{\boldsymbol{H}} : \boldsymbol{\epsilon}(\boldsymbol{u}))\,\mathrm{d}x = \int_{\Omega_c} (\boldsymbol{C}^{\boldsymbol{H}} : \boldsymbol{\epsilon}(\boldsymbol{u})) : \boldsymbol{\epsilon}(\boldsymbol{v})\,\mathrm{d}x, \tag{4.14}$$

$$\bar{b}(\boldsymbol{A},\tilde{\boldsymbol{A}}) = \int_\Omega (\boldsymbol{\mu}^{-1}\operatorname{curl}\boldsymbol{A})\cdot\operatorname{curl}\tilde{\boldsymbol{A}}\,\mathrm{d}x, \tag{4.15}$$

$$\tilde{c}(\boldsymbol{v},\boldsymbol{A}) = \frac{1}{2}\int_{\Omega_c} \operatorname{curl}\boldsymbol{A}\cdot(\boldsymbol{f}^T : \boldsymbol{\epsilon}(\boldsymbol{v}))\,\mathrm{d}x, \tag{4.16}$$

$$d(\boldsymbol{A},\psi) = \int_\Omega \boldsymbol{A}\cdot\nabla\psi\,\mathrm{d}x, \tag{4.17}$$

$$l(\boldsymbol{v}) = \int_{\Gamma_N} \boldsymbol{v}\boldsymbol{\tau}\,\mathrm{d}s, \tag{4.18}$$

$$\tilde{m}(\boldsymbol{A}) = \int_{\Gamma_{c,N}} \boldsymbol{K}\cdot\tilde{\boldsymbol{A}}\,\mathrm{d}s + \int_\Omega \boldsymbol{j}_I\cdot\tilde{\boldsymbol{A}}\,\mathrm{d}x. \tag{4.19}$$

4.2.4 The coupled problem for the eddy current setting

To obtain uniqueness of the solution in the magnetoquasistatic case, we adopt the technique of adding a penalization term to Ampere's law, which is a common approach for eddy current models based on the vector potential (see e.g. Biró and Preis [32], Rodriguez and Valli [2]). It suggests the modification of Ampère's law in the non-conducting domain (where gauging is required) by adding the term $\nabla(\nu \operatorname{div} \boldsymbol{A})$, where ν is a suitable average of the entries of $\boldsymbol{\mu}_c^{-1}$. According to Rodriguez and Valli [2], ν is used as an auxiliary constant and does not necessarily have to be equal to the magnetic reluctivity (the inverse of the magnetic permeability). However, it can be physically interpreted as an equivalent to a reluctivity. In case that the magnetic permeability is a constant, i.e. for isotropic materials, $\nu = 1/\mu$ is a reasonable choice [43].
For convenience, we adopt the approach suggested by Rodriguez and Valli [2] and require the magnetic vector potential as well as the current density $\boldsymbol{j}_I$ to be solenoidal on the whole domain Ω, although this method yields only a modified solution to the (coupled) magnetoquasistatic Maxwell's equations in frequency domain. Instead of the original Maxwell's equations, we thus solve

$$\operatorname{curl}(\boldsymbol{\mu}^{-1} \operatorname{curl} \boldsymbol{A}) - \nabla(\nu \operatorname{div} \boldsymbol{A}) + i\omega\boldsymbol{\sigma}\boldsymbol{A} - \frac{1}{2} \operatorname{curl}(\hat{\boldsymbol{f}}^T : \boldsymbol{\epsilon}(\boldsymbol{u})) = \boldsymbol{j}_I, \tag{4.20}$$

with

$$\nu = \begin{cases} \nu_0 & \boldsymbol{x} \in \Omega_0, \\ \nu_c & \text{otherwise}, \end{cases}$$

under the assumptions $\nu \operatorname{div} \boldsymbol{A} = 0$ and $\operatorname{div} \boldsymbol{j}_I = 0$ on Ω.
In addition to the above modification, we have to require that $\boldsymbol{A}\cdot\boldsymbol{n}$ vanishes on the Dirichlet boundaries of the model and that $\operatorname{div} \boldsymbol{A} = 0$ on the Neumann boundary of the material. Summing up, the full set of boundary conditions for the magnetic vector potential is given by

$$\boldsymbol{\mu}_c^{-1} \operatorname{curl} \boldsymbol{A} \times \boldsymbol{n} = \boldsymbol{K} \quad \text{on } \Gamma_{c,N}, \tag{4.21}$$
$$\nu_c \operatorname{div} \boldsymbol{A} = 0 \quad \text{on } \Gamma_{c,N}, \tag{4.22}$$
$$\boldsymbol{A} \cdot \boldsymbol{n} = 0 \quad \text{on } \Gamma_{c,D}, \tag{4.23}$$
$$\boldsymbol{A} \times \boldsymbol{n} = \boldsymbol{0} \quad \text{on } \Gamma_{c,D}, \tag{4.24}$$
$$\boldsymbol{A} \cdot \boldsymbol{n} = 0 \quad \text{on } \Gamma_{0,D}, \tag{4.25}$$
$$\boldsymbol{A} \times \boldsymbol{n} = \boldsymbol{0} \quad \text{on } \Gamma_{0,D}. \tag{4.26}$$

The constant ν_c is usually kept in the Neumann boundary condition (4.22) as $\nu_c \operatorname{div} \boldsymbol{A}$ can be physically interpreted as a magnetic flux through the surface $\Gamma_{c,N}$.
The new boundary conditions can be reproduced by the following consideration: Taking the divergence on both sides of (4.20), we obtain

$$-\operatorname{div}\left(\nabla(\nu \operatorname{div} \boldsymbol{A})\right) + \operatorname{div}(i\omega\boldsymbol{\sigma}\boldsymbol{A}) = \operatorname{div} \boldsymbol{j}_I,$$

which, due to the assumption $\operatorname{div} \boldsymbol{j}_I = 0$ and the condition $\operatorname{div}(i\omega\boldsymbol{\sigma}\boldsymbol{A}) = 0$ from the ungauged formulation results in

$$-\operatorname{div} \nabla(\nu \operatorname{div} \boldsymbol{A}) = 0,$$

a Laplace equation in the scalar variable $\nu \operatorname{div} \boldsymbol{A}$ for the domain Ω. In the domain Ω_0, this equation has the solution $\operatorname{div} \boldsymbol{A} \equiv 0$ if the boundary conditions (4.25) and (4.26) hold. The conditions (4.22)–(4.24), on the other hand, ensure that $\operatorname{div} \boldsymbol{A} = 0$ on the boundary of the domain Ω_c.

Remark 4.2. *Due to the transformation*

$$\operatorname{curl}(\operatorname{curl} \boldsymbol{A}) - \nabla(\operatorname{div} \boldsymbol{A}) = -\Delta \boldsymbol{A},$$

the penalization leads to a Poisson equation for the vector potential $\boldsymbol{A}$ *in the magnetically linear, homogeneous and isotropic case. For anisotropic materials, the transformation can be interpreted as a general vector-valued Laplacian. From the variational point of view, one does not gain much from the transformation, since the boundary conditions still remain in the curl-curl and div-div form. The gauging thus turns a parabolic-semi-elliptic equation to a parabolic-elliptic equation.*

Based on the above transformations, the strong form of the gauged coupled problem for sufficiently smooth $\boldsymbol{u} : \Omega \to \mathbb{R}^3$ and $\boldsymbol{A} : \Omega \to \mathbb{C}^3$ reads

Problem $(CP)^{A}_{eddy,\mathbb{C}}$: Find $(\boldsymbol{u}, \boldsymbol{A})$, such that

$$\begin{aligned} \mathbf{div}(\boldsymbol{C}^B : \boldsymbol{\epsilon}(\boldsymbol{u})) - \frac{1}{2}\mathbf{div}(\boldsymbol{f} \cdot \operatorname{curl} \boldsymbol{A}) &= \mathbf{0} \quad \text{in } \Omega_c, \\ \operatorname{curl}(\boldsymbol{\mu}^{-1} \operatorname{curl} \boldsymbol{A}) + i\omega\boldsymbol{\sigma}\boldsymbol{A} - \nabla(\nu \operatorname{div} \boldsymbol{A}) - \frac{1}{2}\operatorname{curl}(\hat{\boldsymbol{f}}^T : \boldsymbol{\epsilon}(\boldsymbol{u})) &= \boldsymbol{j}_I \quad \text{in } \Omega, \end{aligned}$$

with Dirichlet boundary conditions,

$$\begin{aligned} \boldsymbol{u} &= \mathbf{0} \quad \text{on } \Gamma_D, \\ \boldsymbol{A} &= \mathbf{0} \quad \text{on } \Gamma_{c,D} \cup \Gamma_{0,D}, \end{aligned}$$

Neumann boundary conditions

$$\begin{aligned} \left(\boldsymbol{C}^B : \boldsymbol{\epsilon}(\boldsymbol{u}) - \frac{1}{2}\boldsymbol{f} : \operatorname{curl} \boldsymbol{A}\right) \cdot \boldsymbol{n} &= \boldsymbol{\tau} \quad \text{on } \Gamma_N, \\ \left(\boldsymbol{\mu}^{-\epsilon} \operatorname{curl} \boldsymbol{A} - \frac{1}{2}\boldsymbol{f}^T : \boldsymbol{\epsilon}\right) \times \boldsymbol{n} &= \boldsymbol{K} \quad \text{on } \Gamma_{c,N}, \\ \nu \operatorname{div} \boldsymbol{A} &= 0 \quad \text{on } \Gamma_{c,N}, \end{aligned}$$

and interface conditions

$$\begin{aligned} \boldsymbol{H}_c \times \boldsymbol{n} &= \boldsymbol{H}_0 \times \boldsymbol{n} \quad \text{on } \Gamma_I, \\ \boldsymbol{B}_c \cdot \boldsymbol{n} &= \boldsymbol{B}_0 \cdot \boldsymbol{n} \quad \text{on } \Gamma_I. \end{aligned}$$

Remark 4.3. *The above modified strong system can be derived from the variational principle in the same manner as the unmodified one by adding the term*

$$\frac{1}{2}\int_{\Omega} \nu(\operatorname{div} \boldsymbol{A})^2 \, \mathrm{d}x$$

to the magnetic energy functional and carrying out the same transformation steps.

Before stating the weak formulation, we note that due to the additional boundary conditions, the function space for the magnetic vector potential is given by

$$\mathcal{V}_0^{\mathbb{C}} := H_\Gamma(\operatorname{curl}, \Omega) \cap H_\Gamma(\operatorname{div}, \Omega),$$

with spaces $H_\Gamma(\operatorname{curl}, \Omega)$ and $H_\Gamma(\operatorname{div}, \Omega)$ as defined in Chapter 2.

Problem $(CP)^{A,w}_{eddy,\mathbb{C}}$: Find $(\boldsymbol{u},\boldsymbol{A}) \in \mathcal{V}_0 \times \mathcal{V}_0^{\mathbb{C}}$, such that

$$\begin{aligned} a(\boldsymbol{u},\boldsymbol{v}) - \tilde{c}(\boldsymbol{A},\boldsymbol{v}) &= l(\boldsymbol{v}) \qquad \text{for } \boldsymbol{v} \in \mathcal{V}_0, \\ -\tilde{c}(\tilde{\boldsymbol{A}},\boldsymbol{u}) + \tilde{b}(\boldsymbol{A},\tilde{\boldsymbol{A}}) &= \tilde{m}(\boldsymbol{A}) \qquad \text{for } \tilde{\boldsymbol{A}} \in \mathcal{V}_0^{\mathbb{C}}, \end{aligned}$$

with real and complex-valued bilinear forms and linear functionals defined as

$$a(\boldsymbol{u},\boldsymbol{v}) = \int_{\Omega_c} \nabla\boldsymbol{v} : (\boldsymbol{C}^{\boldsymbol{H}} : \boldsymbol{\epsilon}(\boldsymbol{u}))\,\mathrm{d}x = \int_{\Omega} (\boldsymbol{C}^{\boldsymbol{H}} : \boldsymbol{\epsilon}(\boldsymbol{u})) : \boldsymbol{\epsilon}(\boldsymbol{v})\,\mathrm{d}x, \tag{4.27}$$

$$\hat{b}(\boldsymbol{A},\tilde{\boldsymbol{A}}) = \int_{\Omega} (\boldsymbol{\mu}^{-1}\operatorname{curl}\boldsymbol{A})\cdot(\operatorname{curl}\tilde{\boldsymbol{A}}) + (\nu \operatorname{div}\boldsymbol{A})\operatorname{div}\tilde{\boldsymbol{A}} + (i\omega\boldsymbol{\sigma}\boldsymbol{A})\cdot\tilde{\boldsymbol{A}}\,\mathrm{d}x, \tag{4.28}$$

$$\tilde{c}(\boldsymbol{v},\boldsymbol{A}) = \frac{1}{2}\int_{\Omega_c} (\operatorname{curl}\boldsymbol{A})\cdot(\boldsymbol{f}^T : \boldsymbol{\epsilon}(\boldsymbol{v}))\,\mathrm{d}x, \tag{4.29}$$

$$\tag{4.30}$$

$$l(\boldsymbol{v}) = \int_{\Gamma_N} \boldsymbol{v}\cdot\boldsymbol{\tau}\,\mathrm{d}s, \tag{4.31}$$

$$\tilde{m}(\boldsymbol{A}) = \int_{\Gamma_{c,N}} \boldsymbol{K}\cdot\tilde{\boldsymbol{A}}\,\mathrm{d}s + \int_{\Omega} \boldsymbol{j}_I\cdot\tilde{\boldsymbol{A}}\,\mathrm{d}x. \tag{4.32}$$

4.2.5 The coupled problem for the full Maxwell system

The strong form of the coupled problem for the full Maxwell system in the frequency domain with $\boldsymbol{\kappa} = i\omega\boldsymbol{\sigma} - \omega^2\hat{\boldsymbol{\epsilon}}$ for sufficiently smooth $\boldsymbol{u} : \Omega \to \mathbb{R}^3$ and $\boldsymbol{A} : \Omega \to \mathbb{C}^3$ is given by

Problem $(CP)^{A}_{t,\mathbb{C}}$: Find $(\boldsymbol{u},\boldsymbol{A})$, such that

$$\begin{aligned} \mathbf{div}(\boldsymbol{C}^B : \boldsymbol{\epsilon}(\boldsymbol{u})) - \frac{1}{2}\mathbf{div}(\boldsymbol{f}\cdot\operatorname{curl}\boldsymbol{A}) &= \boldsymbol{0} \quad \text{in } \Omega_c, \\ \operatorname{curl}(\boldsymbol{\mu}^{-1}\operatorname{curl}\boldsymbol{A}) + \boldsymbol{\kappa}\cdot\boldsymbol{A} - \frac{1}{2}\operatorname{curl}(\hat{\boldsymbol{f}}^T : \boldsymbol{\epsilon}(\boldsymbol{u})) &= \boldsymbol{j}_I \quad \text{in } \Omega, \end{aligned}$$

with Dirichlet boundary conditions,

$$\begin{aligned} \boldsymbol{u} &= \boldsymbol{0} \quad \text{on } \Gamma_D, \\ \boldsymbol{A}\times\boldsymbol{n} &= \boldsymbol{0} \quad \text{on } \Gamma_{c,D}\cup\Gamma_{0,D}, \end{aligned}$$

Neumann boundary conditions

$$\begin{aligned} \left(\boldsymbol{C}^B : \boldsymbol{\epsilon}(\boldsymbol{u}) - \frac{1}{2}\boldsymbol{f} : \operatorname{curl}\boldsymbol{A}\right)\cdot\boldsymbol{n} &= \boldsymbol{\tau} \quad \text{on } \Gamma_N, \\ \left(\boldsymbol{\mu}^{-\epsilon}\operatorname{curl}\boldsymbol{A} - \frac{1}{2}\boldsymbol{f}^T : \boldsymbol{\epsilon}\right)\times\boldsymbol{n} &= \boldsymbol{K} \quad \text{on } \Gamma_{c,N}, \end{aligned}$$

and interface conditions

$$\begin{aligned} \boldsymbol{H}_c\times\boldsymbol{n} &= \boldsymbol{H}_0\times\boldsymbol{n} \quad \text{on } \Gamma_I, \\ \boldsymbol{B}_c\cdot\boldsymbol{n} &= \boldsymbol{B}_0\cdot\boldsymbol{n} \quad \text{on } \Gamma_I. \end{aligned}$$

The corresponding weak form is

Problem $(CP)^{A,w}_{t,\mathbb{C}}$: Find $(\boldsymbol{u}, \boldsymbol{A}) \in \mathcal{V}_0 \times H_\Gamma(\mathrm{curl}, \Omega)$, such that

$$\begin{aligned} a(\boldsymbol{u}, \boldsymbol{v}) - \tilde{c}(\boldsymbol{A}, \boldsymbol{v}) &= l(\boldsymbol{v}) \qquad \text{for } \boldsymbol{v} \in \mathcal{V}_0, \\ -\tilde{c}(\tilde{\boldsymbol{A}}, \boldsymbol{u}) + \tilde{b}(\boldsymbol{A}, \tilde{\boldsymbol{A}}) &= \tilde{m}(\boldsymbol{A}) \qquad \text{for } \tilde{\boldsymbol{A}} \in H_\Gamma(\mathrm{curl}, \Omega), \end{aligned}$$

with real and complex - valued bilinear forms and linear functionals

$$a(\boldsymbol{u}, \boldsymbol{v}) = \int_{\Omega_c} \nabla \boldsymbol{v} : (\boldsymbol{C}^{\boldsymbol{H}} : \boldsymbol{\epsilon}(\boldsymbol{u}))\, \mathrm{d}x = \int_{\Omega} (\boldsymbol{C}^{\boldsymbol{H}} : \boldsymbol{\epsilon}(\boldsymbol{u})) : \boldsymbol{\epsilon}(\boldsymbol{v})\, \mathrm{d}x, \tag{4.33}$$

$$\tilde{b}(\boldsymbol{A}, \tilde{\boldsymbol{A}}) = \int_{\Omega} (\boldsymbol{\mu}^{-1} \,\mathrm{curl}\, \boldsymbol{A}) \cdot \mathrm{curl}\, \tilde{\boldsymbol{A}} + \boldsymbol{\kappa} \boldsymbol{A} \cdot \tilde{\boldsymbol{A}}\, \mathrm{d}x, \tag{4.34}$$

$$\tilde{c}(\boldsymbol{v}, \boldsymbol{A}) = \frac{1}{2} \int_{\Omega_c} \mathrm{curl}\, \boldsymbol{A} \cdot (\boldsymbol{f}^T : \boldsymbol{\epsilon}(\boldsymbol{v}))\, \mathrm{d}x, \tag{4.35}$$

$$l(\boldsymbol{v}) = \int_{\Gamma_N} \boldsymbol{v} \cdot \boldsymbol{\tau}\, \mathrm{d}s, \tag{4.36}$$

$$\tilde{m}(\boldsymbol{A}) = \int_{\Gamma_{c,N}} \boldsymbol{K} \cdot \tilde{\boldsymbol{A}}\, \mathrm{d}s + \int_{\Omega} \boldsymbol{j}_I \cdot \tilde{\boldsymbol{A}}\, \mathrm{d}x. \tag{4.37}$$

4.3 Existence and uniqueness of the solution

As we have seen in Chapter 2, the approach for proving the existence and uniqueness of the weak solution to Ampère's law is strongly dependent on the value of the parameter matrix $\boldsymbol{\kappa}$. For $\kappa_{ij} \in \mathbb{R}_+$, $i, j = 1, 2, 3$, the bilinear form $\tilde{b}(\boldsymbol{A}, \tilde{\boldsymbol{A}})$ is coercive, which enables the application of Lax-Milgram. In the magnetostatic case, $\kappa_{ij} = 0$ for $i, j = 1, ..., 3$ and the requirement of coercivity is not fulfilled any more, so the problem is cast into a saddle point framework. In this section, we will discuss the existence and uniqueness of the weak solution to the coupled problem for these two cases. For the proofs, we return from the general tensor notation to the more specific vector and matrix notation, as done in Chapter 3, with material parameter matrices as defined at the outset of this chapter.

4.3.1 The coupled problem for $\kappa_{ij} \in \mathbb{R}_+$

In analogy to the previous models, we denote the coupled problem with $\kappa_{ij} \in \mathbb{R}_+$ by $(CP)^{A,w}_{t,\mathbb{R}}$. In contrast to the full Maxwell system in the frequency domain, the bilinear forms and linear functionals in the weak formulation of this problem are real-valued and $\boldsymbol{A}, \tilde{\boldsymbol{A}} \in H_\Gamma(\mathrm{curl}, \Omega)$. The matrix $\boldsymbol{\kappa}$ defined as

$$\boldsymbol{\kappa}(\boldsymbol{x}) := \begin{cases} \boldsymbol{\kappa}^0 & \boldsymbol{x} \in \Omega_0, \\ \boldsymbol{\kappa}^c & \text{otherwise}, \end{cases}$$

is the linear combination of the diagonal matrices $\boldsymbol{\sigma}$ and $\hat{\boldsymbol{\epsilon}}$ and has therefore a diagonal structure for the underlying material class. To show the existence and uniqueness of the solution, we would like to apply the Lax-Milgram lemma to the composite bilinear form

$$\tilde{\mathcal{A}}((\boldsymbol{u}, \boldsymbol{A}), (\boldsymbol{v}, \tilde{\boldsymbol{A}})) := a(\boldsymbol{u}, \boldsymbol{v}) + \tilde{b}(\boldsymbol{A}, \tilde{\boldsymbol{A}}) - \tilde{c}(\boldsymbol{v}, \boldsymbol{A}) - \tilde{c}(\boldsymbol{u}, \tilde{\boldsymbol{A}}) \tag{4.38}$$

for all $(\boldsymbol{u}, \boldsymbol{A}), (\boldsymbol{v}, \tilde{\boldsymbol{A}}) \in \mathcal{V}_0 \times H_\Gamma(\mathrm{curl}, \Omega)$, as done for the scalar potential model (see Remark 3.4). The coupled system hence reduces to the single equation

$$\tilde{\mathcal{A}}((\boldsymbol{u}, \boldsymbol{A}), (\boldsymbol{v}, \tilde{\boldsymbol{A}})) = l(\boldsymbol{v}) + \tilde{m}(\tilde{\boldsymbol{A}}) \quad \forall (\boldsymbol{v}, \tilde{\boldsymbol{A}}) \in \mathcal{V}_0 \times H_\Gamma(\mathrm{curl}, \Omega).$$

Although the coupled part $\tilde{c}(\cdot,\cdot)$ is obviously not symmetric, the composite bilinear form is symmetric in $(\boldsymbol{u}, \boldsymbol{A})$,

$$\begin{aligned}\tilde{\mathcal{A}}((\boldsymbol{u},\boldsymbol{A}),(\boldsymbol{v},\tilde{\boldsymbol{A}})) &= a(\boldsymbol{u},\boldsymbol{v}) + \tilde{b}(\boldsymbol{A},\tilde{\boldsymbol{A}}) - \tilde{c}(\boldsymbol{u},\tilde{\boldsymbol{A}}) - \tilde{c}(\boldsymbol{v},\boldsymbol{A}) \\ &= a(\boldsymbol{v},\boldsymbol{u}) + \tilde{b}(\tilde{\boldsymbol{A}},\boldsymbol{A}) - \tilde{c}(\boldsymbol{v},\boldsymbol{A}) - \tilde{c}(\boldsymbol{u},\tilde{\boldsymbol{A}}) = \tilde{\mathcal{A}}((\boldsymbol{v},\tilde{\boldsymbol{A}}),(\boldsymbol{u},\boldsymbol{A})).\end{aligned}$$

The continuity of the bilinear forms $a(\cdot,\cdot)$ and $\tilde{b}(\cdot,\cdot)$ is inherited from the uncoupled problem in Chapter 2. As the next lemma proves, continuity also holds for the coupled bilinear form $\tilde{c}(\cdot,\cdot)$.

Lemma 4.1. *The coupled bilinear form $\tilde{c} : \mathcal{V}_0 \times H_\Gamma(\mathrm{curl},\Omega) \to \mathbb{R}$ defined in (4.35) is continuous.*

Proof. The bilinear form $\tilde{c}(\boldsymbol{v},\boldsymbol{A})$ can be written as

$$\begin{aligned}\tilde{c}(\boldsymbol{v},\boldsymbol{A}) &= \frac{1}{2}\int_{\Omega_c} \boldsymbol{\epsilon}(\boldsymbol{v}) \cdot (\boldsymbol{f}\,\mathrm{curl}\,\boldsymbol{A})\,\mathrm{d}x \\ &= \frac{1}{2}\int_{\Omega_c} \sum_{k=1}^{3} \frac{\partial v_k}{\partial x_k}\left(\sum_{i=1}^{3} f_{ki}(\mathrm{curl}\,\boldsymbol{A})_i\right)\mathrm{d}x + \frac{1}{2}\int_{\Omega}\left(\frac{\partial v_2}{\partial x_3} + \frac{\partial v_3}{x_2}\right)\sum_{i=1}^{3} f_{4i}(\mathrm{curl}\,\boldsymbol{A})_i \\ &+ \left(\frac{\partial v_1}{\partial x_3} + \frac{\partial v_3}{\partial x_1}\right)\sum_{i=1}^{3} f_{5i}(\mathrm{curl}\,\boldsymbol{A})_i) + \left(\frac{\partial v_1}{\partial x_2} + \frac{\partial v_2}{\partial x_1}\right)\sum_{i=1}^{3} f_{6i}(\mathrm{curl}\,\boldsymbol{A})_i)\,\mathrm{d}x \\ &\le \frac{\tilde{f}}{2}\int_{\Omega}\left|\sum_{i=1}^{3}(\mathrm{curl}\,\boldsymbol{A})_i)\left(\sum_{i=1}^{3}\frac{\partial v_i}{\partial x_i} + \left(\frac{\partial v_2}{\partial x_3} + \frac{\partial v_3}{\partial x_2}\right) + \left(\frac{\partial v_1}{\partial x_3} + \frac{\partial v_3}{\partial x_1}\right) + \left(\frac{\partial v_1}{\partial x_2} + \frac{\partial v_2}{\partial x_1}\right)\right)\right|\,\mathrm{d}x,\end{aligned}$$

where $(\mathrm{curl}\,\boldsymbol{A})_i$ denotes the i-th component of the vector $\mathrm{curl}\,\boldsymbol{A}$ and

$$\tilde{f} := \max_{i,j=1,\dots,6} |f_{ij}|.$$

Componentwise application of the Cauchy-Schwarz inequality and the use of the triangle inequality yields the estimate

$$c(\boldsymbol{v},\boldsymbol{A}) \le \tilde{f}\sum_{i=1}^{3}\left(\int_{\Omega_c}(\mathrm{curl}\,\boldsymbol{A})_i^2\,\mathrm{d}x\right)^{\frac{1}{2}}\sum_{j=1}^{3}\sum_{k=1}^{3}\left(\int_{\Omega_c}\left(\frac{\partial v_k}{\partial x_j}\right)^2\,\mathrm{d}x\right)^2.$$

Eventually, exploiting the (strict) concavity property of the square root function,

$$\frac{1}{4}(\sum_{i=1}^{3}\sqrt{y_i}) \le \frac{1}{2}(\frac{1}{2}\sqrt{y_1} + \frac{1}{2}\sqrt{y_2}) + \frac{1}{2}\sqrt{y_3} \le \frac{1}{\sqrt{2}}\sqrt{\frac{1}{2}(y_1+y_2)} + \sqrt{y_3} \le \frac{1}{\sqrt{2}}\sqrt{\sum_{i=1}^{3} y_i}$$

for all $y_i \ge 0$, $i = 1,2,3$, which implies that

$$\frac{1}{4^2}\left(\sum_{i=1}^{9}\sqrt{y_i}\right) \le \frac{1}{2}\sqrt{\sum_{i=1}^{9} y_i},$$

we obtain

$$\begin{aligned}
\tilde{c}(\boldsymbol{v},\boldsymbol{A}) &\leq \tilde{f}\sum_{i=1}^{3}\left(\int_{\Omega_c}(\operatorname{curl}\boldsymbol{A})_i^2\,\mathrm{d}x\right)^{\frac{1}{2}}\sum_{k=1}^{3}\sum_{j=1}^{3}\left(\int_{\Omega}\left(\frac{\partial v_k}{\partial x_j}\right)^2\mathrm{d}x\right)^{\frac{1}{2}}\\
&\leq \frac{4^2}{2}\tilde{f}\sum_{i=1}^{3}\left(\int_{\Omega}(\operatorname{curl}\boldsymbol{A})_i^2\,\mathrm{d}x\right)^{\frac{1}{2}}\left(\sum_{k=1}^{3}\sum_{j=1}^{3}\int_{\Omega_c}\left(\frac{\partial v_k}{\partial x_j}\right)^2\mathrm{d}x\right)^{\frac{1}{2}}\\
&\leq \frac{4^3}{2\sqrt{2}}\tilde{f}\left(\sum_{i=1}^{3}\int_{\Omega}(\operatorname{curl}\boldsymbol{A})_i^2\,\mathrm{d}x\right)^{\frac{1}{2}}\left(\sum_{k=1}^{3}\sum_{j=1}^{3}\int_{\Omega}\left(\frac{\partial v_k}{\partial x_j}\right)^2\mathrm{d}x\right)^{\frac{1}{2}}\\
&\leq 4^2\sqrt{2}\tilde{f}\,\|\boldsymbol{A}\|_{H(\operatorname{curl},\Omega)}\,\|\boldsymbol{v}\|_{\mathcal{V}_0}.
\end{aligned}$$

Continuity is thus satisfied with the constant

$$\tilde{c}_0 := 4^2\sqrt{2}\tilde{f}.$$

□

Lemma 4.2 uses this result to prove the continuity of the composite bilinear form $\tilde{\mathcal{A}}(\cdot,\cdot)$.

Lemma 4.2. *The composite bilinear form* $\tilde{\mathcal{A}}(\cdot,\cdot):(\mathcal{V}_0\times H_\Gamma(\operatorname{curl},\Omega))\times(\mathcal{V}_0\times H_\Gamma(\operatorname{curl},\Omega))\to\mathbb{R}$ *defined in* (4.38) *is continuous.*

Proof. We have to show that the bilinear form satisfies

$$\begin{aligned}
\tilde{\mathcal{A}}((\boldsymbol{u},\boldsymbol{A}),(\boldsymbol{v},\tilde{\boldsymbol{A}})) &\leq \tilde{a}\left\|\begin{pmatrix}\boldsymbol{u}\\ \boldsymbol{A}\end{pmatrix}\right\|_{\mathcal{V}_0\times H(\operatorname{curl},\Omega)}\left\|\begin{pmatrix}\boldsymbol{v}\\ \tilde{\boldsymbol{A}}\end{pmatrix}\right\|_{\mathcal{V}_0\times H(\operatorname{curl},\Omega)}\\
&= \tilde{a}\sqrt{(\|\boldsymbol{u}\|_{\mathcal{V}_0}^2+\|\boldsymbol{A}\|_{H(\operatorname{curl},\Omega)}^2)(\|\boldsymbol{v}\|_{\mathcal{V}_0}^2+\|\tilde{\boldsymbol{A}}\|_{H(\operatorname{curl},\Omega)}^2)}
\end{aligned}$$

for a constant $\tilde{\alpha}\geq 0$. Exploiting the continuity properties of the bilinear forms $a(\cdot,\cdot)$, $\tilde{b}(\cdot,\cdot)$ and $\tilde{c}(\cdot,\cdot)$, where a_0, $\tilde{b}_0$ and $\tilde{c}_0$ denote the corresponding continuity constants, and using the concavity of the root function as shown in the proof of Lemma 4.1, we obtain

$$\begin{aligned}
&\frac{1}{2}\tilde{\mathcal{A}}((\boldsymbol{u},\boldsymbol{A}),(\boldsymbol{v},\tilde{\boldsymbol{A}})) = \frac{1}{2}\left(a(\boldsymbol{u},\boldsymbol{v})+\tilde{b}(\boldsymbol{A},\tilde{\boldsymbol{A}})-\tilde{c}(\boldsymbol{v},\boldsymbol{A})-\tilde{c}(\boldsymbol{u},\tilde{\boldsymbol{A}})\right)\\
\leq\ & \frac{1}{2}\Big(a_0\|\boldsymbol{u}\|_{\mathcal{V}_0}\|\boldsymbol{v}\|_{\mathcal{V}_0}+\tilde{b}_0\|\boldsymbol{A}\|_{H(\operatorname{curl},\Omega)}\|\tilde{\boldsymbol{A}}\|_{H(\operatorname{curl},\Omega)}\\
-\ & \tilde{c}_0\|\boldsymbol{v}\|_{\mathcal{V}_0}\|\boldsymbol{A}\|_{H(\operatorname{curl},\Omega)}-\tilde{c}_0\|\boldsymbol{u}\|_{\mathcal{V}_0}\|\tilde{\boldsymbol{A}}\|_{H(\operatorname{curl},\Omega)}\Big)\\
=\ & \frac{1}{2}\Bigg[\left(\left(a_0\|\boldsymbol{u}\|_{\mathcal{V}_0}\|\boldsymbol{v}\|_{\mathcal{V}_0}-\tilde{c}_0\|\boldsymbol{v}\|_{\mathcal{V}_0}\|\boldsymbol{A}\|_{H(\operatorname{curl},\Omega)}\right)^2\right)^{\frac{1}{2}}\\
+\ & \left(\left(\tilde{b}_0\|\boldsymbol{A}\|_{H(\operatorname{curl},\Omega)}\|\tilde{\boldsymbol{A}}\|_{H(\operatorname{curl},\Omega)}-\tilde{c}_0\|\boldsymbol{u}\|_{\mathcal{V}_0}\|\tilde{\boldsymbol{A}}\|_{H(\operatorname{curl},\Omega)}\right)^2\right)^{\frac{1}{2}}\Bigg]\\
\leq\ & \Bigg[\frac{1}{2}\left(a_0\|\boldsymbol{u}\|_{\mathcal{V}_0}\|\boldsymbol{v}\|_{\mathcal{V}_0}-\tilde{c}_0\|\boldsymbol{v}\|_{\mathcal{V}_0}\|\boldsymbol{A}\|_{H(\operatorname{curl},\Omega)}\right)^2\\
+\ & \frac{1}{2}\left(\tilde{b}_0\|\boldsymbol{A}\|_{H(\operatorname{curl},\omega)}\|\tilde{\boldsymbol{A}}\|_{H(\operatorname{curl},\Omega)}-\tilde{c}_0\|\boldsymbol{u}\|_{\mathcal{V}_0}\|\tilde{\boldsymbol{A}}_{H(\operatorname{curl},\Omega)}\|\right)^2\Bigg]^{\frac{1}{2}}\\
=\ & \Big[\frac{1}{2}\left(a_0^2\|\boldsymbol{u}\|_{\mathcal{V}_0}^2\|\boldsymbol{v}\|_{\mathcal{V}_0}^2-2\tilde{a}_0\tilde{c}_0\|\boldsymbol{v}\|_{\mathcal{V}_0}^2\|\boldsymbol{u}\|_{\mathcal{V}_0}\|\boldsymbol{A}\|_{H(\operatorname{curl},\Omega)}+\tilde{c}_0^2\|\boldsymbol{v}\|_{\mathcal{V}_0}^2\|\boldsymbol{A}\|_{H(\operatorname{curl},\Omega)}^2\right)
\end{aligned}$$

$$
\begin{aligned}
&+ \quad \frac{1}{2}\Big(\tilde{b}_0^2 \|\boldsymbol{A}\|^2_{H(\mathrm{curl},\Omega)} \big\|\tilde{\boldsymbol{A}}\big\|^2_{H(\mathrm{curl},\Omega)} - 2\tilde{b}_0\tilde{c}_0 \|\boldsymbol{u}\|_{\mathcal{V}_0} \|\boldsymbol{A}\|_{H(\mathrm{curl},\Omega)} \big\|\tilde{\boldsymbol{A}}\big\|^2_{H(\mathrm{curl},\Omega)} \\
&+ \quad \tilde{c}_0^2 \big\|\tilde{\boldsymbol{A}}\big\|^2_{H(\mathrm{curl},\Omega)} \|\boldsymbol{u}\|^2_{\mathcal{V}_0}\Big)\Big]^{\frac{1}{2}} \\
&\leq \quad \Big[\max\{a_0^2, \tilde{b}_0^2, \tilde{c}_0^2\}\frac{1}{2}\Big(\|\boldsymbol{u}\|^2_{\mathcal{V}_0} \|\boldsymbol{v}\|^2_{\mathcal{V}_0} + \|\boldsymbol{v}\|^2_{\mathcal{V}_0} \|\boldsymbol{A}\|^2_{H(\mathrm{curl},\Omega)} \\
&+ \quad \|\boldsymbol{A}\|^2_{H(\mathrm{curl},\Omega)} \big\|\tilde{\boldsymbol{A}}\big\|^2_{H(\mathrm{curl},\Omega)} + \big\|\tilde{\boldsymbol{A}}\big\|^2_{H(\mathrm{curl},\Omega)} \|\boldsymbol{u}\|^2_{\mathcal{V}_0}\Big) \\
&- \quad \tilde{c}_0 \|\boldsymbol{u}\|_{\mathcal{V}_0} \|\boldsymbol{A}\|_{H(\mathrm{curl},\Omega)} \left(a_0 \|\boldsymbol{v}\|^2_{\mathcal{V}_0} + \tilde{b}_0 \big\|\tilde{\boldsymbol{A}}\big\|^2_{H(\mathrm{curl},\Omega)}\right)\Big]^{\frac{1}{2}} \\
&\leq \quad \frac{\max\{a_0, \tilde{b}_0, \tilde{c}_0\}}{\sqrt{2}} \left\|\begin{pmatrix}\boldsymbol{u}\\ \boldsymbol{A}\end{pmatrix}\right\|_{\mathcal{V}_0 \times H(\mathrm{curl},\Omega)} \left\|\begin{pmatrix}\boldsymbol{v}\\ \tilde{\boldsymbol{A}}\end{pmatrix}\right\|_{\mathcal{V}_0 \times H(\mathrm{curl},\Omega)}.
\end{aligned}
$$

Hence, continuity is satisfied with the constant

$$
\tilde{a} := \frac{2\max\{a_0, \tilde{b}_0, \tilde{c}_0\}}{\sqrt{2}}.
$$

□

The next lemma guarantees the coercivity of the bilinear form $b(\cdot,\cdot)$ in $H_\Gamma(\mathrm{curl},\Omega)$.

Lemma 4.3. *The bilinear form $\tilde{b} : H_\Gamma(\mathrm{curl},\Omega) \to H_\Gamma(\mathrm{curl},\Omega)$ defined in (4.34) is coercive.*

Proof.

$$
\begin{aligned}
\tilde{b}(\boldsymbol{A},\boldsymbol{A}) &= \int_\Omega (\boldsymbol{\mu}^{-1}\,\mathrm{curl}\,\boldsymbol{A})\cdot\mathrm{curl}\,\boldsymbol{A} + (\boldsymbol{\kappa}\boldsymbol{A})\cdot\boldsymbol{A}\,\mathrm{d}x \\
&= \int_{\Omega_c} (\boldsymbol{\mu}^{-\epsilon}\,\mathrm{curl}\,\boldsymbol{A})\cdot\mathrm{curl}\,\boldsymbol{A} + (\boldsymbol{\kappa}_c\boldsymbol{A})\cdot\boldsymbol{A}\,\mathrm{d}x + \int_{\Omega_0} (\boldsymbol{\mu}_0^{-1}\,\mathrm{curl}\,\boldsymbol{A})\cdot\mathrm{curl}\,\boldsymbol{A} + (\boldsymbol{\kappa}_0\boldsymbol{A})\cdot\boldsymbol{A}\,\mathrm{d}x \\
&= \sum_{i=1}^3 \int_{\Omega_c} \mu_{ij}^{-\epsilon}(\mathrm{curl}\,\boldsymbol{A})_i^2\,\mathrm{d}x + \sum_{i=1}^3 \int_{\Omega_c} \kappa_{ii}^c A_i^2\,\mathrm{d}x \\
&\geq \min_{i=1,..,3}\{\mu_{ii}^{-\epsilon}, \mu_{0,ii}^{-1}\} \sum_{i=1}^3 \int_\Omega (\mathrm{curl}\,\boldsymbol{A})_i^2\,\mathrm{d}x + \min_{i=1,..,3}\{\kappa_{ii}^c, \kappa_{ii}^0\} \sum_{i=1}^3 \int_\Omega A_i^2\,\mathrm{d}x \\
&\geq \min_{i=1,..,3}\{\mu_{ii}^{-\epsilon}, \mu_{0,ii}^{-1}, \kappa_{ii}^c, \kappa_{ii}^0\} \|\boldsymbol{A}\|^2_{H(\mathrm{curl},\Omega)},
\end{aligned}
$$

where κ_{ii}^0 and κ_{ii}^c, as well as $\mu_{ii}^{-\epsilon}$ and $\mu_{0,ii}^{-1}$ denote the components of the matrices $\boldsymbol{\kappa}$ and $\boldsymbol{\mu}^{-1}$ in the air region and the conducting domain, respectively. As in the proof of the previous lemma, $(\mathrm{curl}\,\boldsymbol{A})_i$ denotes the i-th component of the vector $\mathrm{curl}\,\boldsymbol{A}$. Thus, coercivity holds with the constant

$$
\tilde{\gamma} := \min\{\min_{i=1,..,3}\{\mu_{ii}^{-\epsilon}, \mu_{0,ii}^{-1}\}, \min_{i=1,..,3}\{\kappa_{ii}^c, \kappa_{ii}^0\}\}.
$$

□

To show the coercivity of the composite bilinear form $\tilde{\mathcal{A}}((\cdot,\cdot),(\cdot,\cdot))$, we need to find a suitable estimate for the part $-2\tilde{c}(\boldsymbol{u},\boldsymbol{A})$. Such an estimate will be derived in the proof of the next theorem.

Theorem 4.1. *The coupled magnetoelastic problem $(CP)^{A,w}_{t,\mathbb{R}}$ has a unique solution $(\boldsymbol{u},\boldsymbol{A}) \in \mathcal{V}_0 \times H_\Gamma(\mathrm{curl},\Omega)$ if the underlying material satisfies the property*

$$
\frac{\max\limits_{i=1,\ldots,6} \sum_{j=1}^3 \mu_{jj}^{-\epsilon} e_{ij}^2}{\min\limits_{i=1,\ldots,6}\left(C_{ii}^H + \sum_{j=1}^3 \mu_{jj}^{-\epsilon} e_{ij}^2\right)} \leq 1, \tag{4.39}
$$

where the indices denote the scalar components of the respective tensors.

Proof. We want to apply the Lax-Milgram lemma to the problem

Find $((\boldsymbol{u},\boldsymbol{A}),(\boldsymbol{v},\tilde{\boldsymbol{A}})) \in \mathcal{V}_0 \times H_\Gamma(\mathrm{curl},\Omega)$, such that

$$\tilde{\mathcal{A}}((\boldsymbol{u},\boldsymbol{A}),(\boldsymbol{u},\boldsymbol{A})) = l(\boldsymbol{u}) + \tilde{m}(\boldsymbol{A}),$$

with $\tilde{\mathcal{A}}((\cdot,\cdot),(\cdot,\cdot))$ defined in (4.38). The coercivity of $\tilde{\mathcal{A}}((\cdot,\cdot),(\cdot,\cdot))$ in Ω_0 follows directly from the coercivity of $\tilde{b}(\cdot,\cdot)$, as the bilinear forms $a(\cdot,\cdot)$ and $\tilde{c}(\cdot,\cdot)$ vanish in Ω_0. To show the coercivity in Ω_c, we are seeking for an estimate for the coupled bilinear form $\tilde{c}(\cdot,\cdot)$ in terms of the bilinear forms $a(\cdot,\cdot)$ and $\tilde{b}(\cdot,\cdot)$. Componentwise expansion of the expression for $\tilde{c}(\cdot,\cdot)$ yields

$$\begin{aligned}\tilde{c}(\boldsymbol{u},\boldsymbol{A}) &= \frac{1}{2}\int_{\Omega_c}(\mathrm{curl}\,\boldsymbol{A})\cdot(\boldsymbol{f}^T\boldsymbol{\epsilon}(\boldsymbol{u}))\,\mathrm{d}x = \frac{1}{2}\int_{\Omega}\sum_{j=1}^{3}(\mathrm{curl}\,\boldsymbol{A})_j\sum_{i=1}^{6}f_{ij}\epsilon_i\,\mathrm{d}x\\ &= \frac{1}{2}\sum_{j=1}^{3}\mu_{jj}^{-\epsilon}\int_{\Omega}(\mathrm{curl}\,\boldsymbol{A})_j\sum_{i=1}^{6}e_{ij}\epsilon_i\,\mathrm{d}x,\end{aligned}$$

where ϵ_i denotes the i-th component of the strain $\boldsymbol{\epsilon}$ and $\mu_{jj}^{-\epsilon}$ denotes the j-th diagonal entry of $\boldsymbol{\mu}^{-\epsilon}$. The product $\boldsymbol{f}^T\boldsymbol{\epsilon}$ is given componentwise by

$$(\boldsymbol{f}^T\boldsymbol{\epsilon})_j = \sum_{i=1}^{6}\mu_{jj}^{-\epsilon}e_{ij}\epsilon_i, \quad j=1,2,3.$$

Making use of the Hölder and the triangle inequalities, as well as the estimate

$$2xy \le x^2+y^2 \text{ for } x,y\in\mathbb{R},$$

we obtain the inequality chain

$$\begin{aligned}\tilde{c}(\boldsymbol{u},\boldsymbol{A}) &\le \frac{1}{4}\sum_{j=1}^{3}\mu_{jj}^{-\epsilon}\left(2\,\|(\mathrm{curl}\,\boldsymbol{A})_j\|_0\left\|\sum_{i=1}^{6}e_{ij}\epsilon_i\right\|_0\right)\\ &\le \frac{1}{4}\sum_{j=1}^{3}\mu_{jj}^{-\epsilon}\left(\|(\mathrm{curl}\,\boldsymbol{A})_j\|_0^2+\left\|\sum_{i=1}^{6}e_{ij}\epsilon_i\right\|_0^2\right)\\ &\le \frac{1}{4}\sum_{j=1}^{3}\mu_{jj}^{-\epsilon}\,\|(\mathrm{curl}\,\boldsymbol{A})\|_0^2+\frac{1}{4}\sum_{j=1}^{3}\mu_{jj}^{-\epsilon}\sum_{i=1}^{6}e_{ij}^2\,\|\epsilon_i\|_0^2\\ &= \frac{1}{4}\sum_{j=1}^{3}\mu_{jj}^{-\epsilon}\int_{\Omega}(\mathrm{curl}\,\boldsymbol{A})_j^2\,\mathrm{d}x+\frac{1}{4}\sum_{i=1}^{6}\left(\sum_{j=1}^{3}\mu_{jj}^{-\epsilon}e_{ij}^2\right)\int_{\Omega}\epsilon_i^2\,\mathrm{d}x\\ &\le \frac{1}{4}\tilde{b}(\boldsymbol{A},\boldsymbol{A})+\frac{1}{4}\max_{i=1,\dots,6}\left(\sum_{j=1}^{3}\mu_{jj}^{-\epsilon}e_{ij}^2\right)\sum_{i=1}^{6}\int_{\Omega}\epsilon_i^2\,\mathrm{d}x.\end{aligned}$$

The next step consists of showing that the second term in the last expression of the inequality chain can be estimated from above by a multiple of the bilinear form $a(\cdot,\cdot)$. Due to the positive definiteness of the matrix $\boldsymbol{C}^B = \boldsymbol{C}^H + \boldsymbol{e}\boldsymbol{\mu}^{-\epsilon}\boldsymbol{e}^T$, we can estimate $a(\cdot,\cdot)$ via

$$a(\boldsymbol{u},\boldsymbol{u}) = \sum_{i=1}^{6}\int_{\Omega}C_{ii}^B\epsilon_i^2\,\mathrm{d}x+\sum_{\substack{i,j=1,\\ i\neq j}}^{6}C_{ij}^B\epsilon_i\epsilon_j\,\mathrm{d}x \ge \sum_{i=1}^{6}C_{ii}^B\int_{\Omega}\epsilon_i^2\,\mathrm{d}x \ge \min_{i=1,\dots,6}C_{ii}^B\sum_{i=1}^{6}\int_{\Omega}\epsilon_i^2\,\mathrm{d}x,$$

where C_{ii}^B denotes the ii-th component of the matrix $\boldsymbol{C}^B$. Each diagonal component C_{ii}^B is given by

$$C_{ii}^B = C_{ii}^H + \sum_{j=1}^{3} \mu_{jj}^{-\epsilon} e_{ij}^2.$$

Since (4.39) holds, we obtain

$$\tilde{c}(\boldsymbol{u}, \boldsymbol{A}) \leq \frac{1}{4}\left(\tilde{b}(\boldsymbol{A}, \boldsymbol{A}) + \max_{i=1,\ldots,6} \sum_{j=1}^{3} \mu_{jj}^{-\epsilon} e_{ij}^2 \frac{a(\boldsymbol{u}, \boldsymbol{u})}{\min\limits_{i=1,\ldots,6} C_{ii}^B}\right) \leq \frac{1}{4}(a(\boldsymbol{u}, \boldsymbol{u}) + \tilde{b}(\boldsymbol{A}, \boldsymbol{A}),$$

and, consequently,

$$a(\boldsymbol{u}, \boldsymbol{u}) + \tilde{b}(\boldsymbol{A}, \boldsymbol{A}) - 2\tilde{c}(\boldsymbol{u}, \boldsymbol{A}) \geq \frac{1}{2}(a(\boldsymbol{u}, \boldsymbol{u}) + \tilde{b}(\boldsymbol{A}, \boldsymbol{A})) \geq \frac{1}{2}(\alpha \|\boldsymbol{u}\|_{\mathcal{V}}^2 + \tilde{\gamma} \|\boldsymbol{A}\|_{H(\mathrm{curl},\Omega)}^2),$$

with α and $\tilde{\gamma}$ denoting the coercivity constants of $a(\cdot,\cdot)$ and $\tilde{b}(\cdot,\cdot)$. The Lax-Milgram lemma now immediately yields the existence and uniqueness of a solution $(\boldsymbol{u}, \boldsymbol{A}) \in \mathcal{V}_0 \times H_\Gamma(\mathrm{curl}, \Omega)$ to the coupled weak problem $(CP)_{t,\mathbb{R}}^A$.
Note that for the polycrystalline Terfenol-D (see Tables 5.1 and 5.2 for material data), assumption 4.39 is satisfied since the dimensions of the components of C_{ii}^H are between 10^{10} and 10^{11}, whereas the values of

$$\sum_{j=1}^{3} \mu_{jj}^{-\epsilon} e_{ij}^2$$

have a dimension range between 10^9 and 10^{11}. □

4.3.2 The coupled problem in the magnetostatic case

Consider the coupled saddle point problem $(CP)^{A,w}$ from Section 4.2.3. The continuity of the bilinear form $\tilde{c}(\cdot,\cdot)$ was already proven in the previous section. The continuity of $d(\cdot,\cdot)$ is straightforward:

Lemma 4.4. *The bilinear form $d : H_\Gamma(\mathrm{curl}, \Omega) \times H^1(\Omega) \to \mathbb{R}$ defined in (4.17) is continuous.*

Proof.

$$\begin{aligned} d(\boldsymbol{A}, \Psi) &= \int_\Omega \boldsymbol{A} \nabla\psi \,\mathrm{d}x \leq \left(\int_\Omega \boldsymbol{A}\boldsymbol{A} \,\mathrm{d}x\right)^{\frac{1}{2}} \left(\int_\Omega \nabla\psi\nabla\psi \,\mathrm{d}x\right)^{\frac{1}{2}} \\ &= \|\boldsymbol{A}\|_0 \, |\psi|_1 \leq \|\boldsymbol{A}\|_{H(\mathrm{curl},\Omega} \, \|\psi\|_{H^1(\Omega)}, \end{aligned}$$

where we again used the Hölder inequality. □

The structure of the problem becomes more vivid if we consider its algebraic form, as done in Section 3.4. The system has a symmetric matrix with the block structure

$$\mathbb{E} = \begin{pmatrix} \boldsymbol{\mathcal{A}} & -\tilde{\boldsymbol{\mathcal{C}}} & \boldsymbol{0} \\ -\tilde{\boldsymbol{\mathcal{C}}}^T & \bar{\boldsymbol{\mathcal{B}}} & \boldsymbol{\mathcal{D}} \\ \boldsymbol{0} & \boldsymbol{\mathcal{D}}^T & \boldsymbol{0} \end{pmatrix},$$

with matrices $\boldsymbol{\mathcal{A}} \in \mathbb{R}^{n\times n}$, $\bar{\boldsymbol{\mathcal{C}}} \in \mathbb{R}^{n\times m}$ and $\boldsymbol{\mathcal{D}} \in \mathbb{R}^{m\times k}$ for some $m, n, k \in \mathbb{N}$. Setting

$$\mathbb{A} := \begin{pmatrix} \boldsymbol{\mathcal{A}} & -\tilde{\boldsymbol{\mathcal{C}}} \\ -\tilde{\boldsymbol{\mathcal{C}}}^T & \bar{\boldsymbol{\mathcal{B}}} \end{pmatrix} \in \mathbb{R}^{(n+m)\times(n+m)} \quad \text{and} \quad \mathbb{B} := \begin{pmatrix} \mathbf{0} & \boldsymbol{\mathcal{D}}^{\boldsymbol{T}} \end{pmatrix} \in \mathbb{R}^{k\times(n+m)},$$

the composite system matrix can be rewritten to

$$\mathbb{O} = \begin{pmatrix} \mathbb{A} & \mathbb{B}^T \\ \mathbb{B} & \mathbf{0} \end{pmatrix},$$

which, itself, has a structure of a block-saddle point problem.
The sufficient conditions for showing the non-singularity of the above composite system matrix have already been discussed in Section 3.4. The matrix $\mathbb{O}$ is non-singular if the operator $\mathbb{B} : \mathbb{R}^k \to \mathbb{R}^{n+m}$ corresponding to the matrix $\mathbb{B}$ is surjective (or, equivalently, if $\mathbb{B}^T$ is injective) and the matrix $\mathbb{A} \in \mathbb{R}^{n+m\times n+m}$ is positive definite on the kernel of $\mathbb{B}$ [24].
In the infinite-dimensional case, these conditions translate to the conditions given by Brezzi's Splitting theorem (see Chapter 3). On the one hand, we require the coercivity of the composite bilinear form $\bar{\mathcal{A}} : \mathcal{V}_0 \times H_\Gamma(\mathrm{curl}, \Omega) \to \mathbb{R}$, defined as

$$\bar{\mathcal{A}}((\boldsymbol{u}, \boldsymbol{A}), (\boldsymbol{v}, \tilde{\boldsymbol{A}})) := a(\boldsymbol{u}, \boldsymbol{v}) - \tilde{c}(\boldsymbol{v}, \boldsymbol{A}) - \tilde{c}(\boldsymbol{u}, \tilde{\boldsymbol{A}}) + \bar{b}(\boldsymbol{A}, \tilde{\boldsymbol{A}})$$

on the kernel

$$K := \{(\boldsymbol{u}, \tilde{\boldsymbol{A}}) \in \mathcal{V}_0 \times H_\Gamma(\mathrm{curl}, \Omega)\} \mid \tilde{d}((\boldsymbol{u}, \tilde{\boldsymbol{A}}), \phi) = 0 \ \ \forall\ \phi \in H^1(\Omega)\},$$

where $\tilde{d} : \mathcal{V}_0 \times H_\Gamma(\mathrm{curl}, \Omega) \times H^1(\Omega)$ is defined as

$$\tilde{d}((\boldsymbol{u}, \tilde{A}), \phi) = d(\tilde{A}, \phi).$$

The above coercivity requirement implies that $a(\cdot, \cdot)$ must be elliptic on the whole space $\mathcal{V}_0$, $\bar{b}(\cdot, \cdot)$ must be coercive on the kernel

$$\tilde{K} := \{\tilde{\boldsymbol{A}} \in H_\Gamma(\mathrm{curl}, \Omega) \mid d(\tilde{\boldsymbol{A}}, \phi) = 0 \forall \phi \in H^1(\Omega)\},$$

and the remaining term $-2\tilde{c}(\boldsymbol{u}, \tilde{\boldsymbol{A}})$ has to be estimated in terms of $a(\cdot, \cdot)$ and $\bar{b}(\cdot, \cdot)$, as shown in the proof of Theorem 4.1. The first two conditions are fulfilled for the uncoupled elastic and magnetic bilinear forms.
On the other hand, an inf-sup condition for $\tilde{d}((\boldsymbol{u}, \tilde{A}), \phi)$ has to be satisfied, which, however, directly follows from the corresponding inf-sup condition for $d(\cdot, \cdot)$, presented in Chapter 2.
Finally, the estimate

$$\tilde{c}(\boldsymbol{u}, \boldsymbol{A}) \leq \frac{1}{4}(a(\boldsymbol{u}, \boldsymbol{u}) + \tilde{b}(\boldsymbol{A}, \boldsymbol{A})),$$

obtained in the proof of Theorem 4.1 holds for all $\tilde{\boldsymbol{A}} \in H_\Gamma(\mathrm{curl}, \Omega)$ and thus also for all $\tilde{\boldsymbol{A}}$ satisfying

$$\int_\Omega \tilde{\boldsymbol{A}} \nabla \phi \, \mathrm{d}x = 0 \quad \forall \phi \in H^1(\Omega).$$

completing the requirements for the existence and uniqueness of the solution to the coupled magnetostatic saddle point problem.

For the sake of completeness, we note that the estimates for the continuous dependence of the solution on the data can be obtained in the same manner as discussed in the Chapters 2 and 3 and will therefore not be presented in this chapter. Instead, we will briefly introduce the special case of a two-dimensional setting, which significantly reduces the complexity of the problem.

4.4 Reduction to 2D

The uniqueness of the magnetic vector potential is always valid in the two-dimensional case, as the magnetic vector potential has only one out-of-plane component $A_3(x_1, x_2)$, implying that the Coulomb gauge $\operatorname{div} \boldsymbol{A} = 0$ is automatically satisfied. In the uncoupled magnetostatic case, Maxwell's three-dimensional system of equations thus reduces to

$$\operatorname{curl}(\boldsymbol{\mu}^{-1} \operatorname{curl} \boldsymbol{A}) = \begin{pmatrix} 0 \\ 0 \\ -\frac{1}{\mu_{22}} \left(\frac{\partial^2 A_3}{\partial x_1^2} \right) - \frac{1}{\mu_{11}} \left(\frac{\partial^2 A_3}{\partial x_2^2} \right) \end{pmatrix} = \begin{pmatrix} 0 \\ 0 \\ j_3 \end{pmatrix},$$

resulting in the single equation

$$-\operatorname{div}(\boldsymbol{\mu}^{-1} \nabla A_3) = j_3,$$

where A_i and j_i, $i = 1, .., 3$, denote the spatial components of the magnetic vector potential and the current density, respectively.
In the coupled magnetoelastic model, however, the additional term $-\frac{1}{2} \operatorname{curl}(\boldsymbol{f}^T : \boldsymbol{\epsilon}(\boldsymbol{v}))$ leads to non-zero components j_1 and j_2 of the current density if the coupling matrix $\boldsymbol{f}$ is dense:

$$\begin{aligned} &\operatorname{curl}(\boldsymbol{f}^T : \boldsymbol{\epsilon}(\boldsymbol{v})) \\ = &\begin{pmatrix} f_{13} \frac{\partial^2 v_1}{\partial x_2 \partial x_1} + f_{23} \frac{\partial^2 v_2}{\partial x_2 \partial x_2} + f_{63} \left(\frac{\partial^2 v_1}{\partial x_2 \partial x_2} + \frac{\partial^2 v_2}{\partial x_2 \partial x_1} \right) \\ -f_{13} \frac{\partial^2 v_1}{\partial x_1^2} - f_{23} \frac{\partial^2 v_2}{\partial x_1 \partial x_2} - f_{63} \left(\frac{\partial^2 v_1}{\partial x_2^2} + \frac{\partial^2 v_2}{\partial x_2 \partial x_1} \right) \\ f_{12} \frac{\partial^2 v_1}{\partial x_1^2} + f_{22} \frac{\partial^2 v_2}{\partial x_1 \partial x_2} + f_{62} \left(\frac{\partial^2 v_1}{\partial x_1 \partial x_2} + \frac{\partial^2 v_2}{\partial x_1^2} \right) - f_{11} \frac{\partial^2 v_1}{\partial x_2 \partial x_1} - f_{21} \frac{\partial^2 v_2}{\partial x_2^2} - f_{61} \left(\frac{\partial^2 v_1}{\partial x_2^2} + \frac{\partial^2 v_2}{\partial x_2 \partial x_1} \right) \end{pmatrix}. \end{aligned}$$

Taking the transversely-isotropic plane stress-plate model from Section 3.4.2 as a basis, we can reduce the number of non-zero components of the coupling matrix $\boldsymbol{f}$, since

$$\boldsymbol{f} = \boldsymbol{e}\boldsymbol{\mu}^{-\epsilon} = \begin{pmatrix} \frac{e_{11}}{\mu_{11}^{\epsilon}} & 0 & 0 \\ \frac{e_{21}}{\mu_{11}} & 0 & 0 \\ 0 & \frac{e_{62}}{\mu_{22}^{\epsilon}} & 0 \end{pmatrix}.$$

Setting all but the components f_{11}, f_{21} and f_{62} to zero, we obtain the single scalar coupled equation

$$-\left(\frac{1}{\mu_{22}^{\epsilon}} \frac{\partial^2 A_3}{\partial x_1^2} + \frac{1}{\mu_{11}^{\epsilon}} \frac{\partial^2 A_3}{\partial x_2^2} \right) - \frac{1}{2} \left(f_{11} \frac{\partial^2 v_1}{\partial x_2 \partial x_1} + f_{21} \frac{\partial^2 v_2}{\partial x_2^2} - f_{62} \left(\frac{\partial^2 v_1}{\partial x_1 \partial x_2} + \frac{\partial^2 v_2}{\partial x_1^2} \right) \right) = j_3.$$

On the other hand, the relation

$$\operatorname{div}(\boldsymbol{C}^H : \boldsymbol{\epsilon}(\boldsymbol{u})) - \frac{1}{2} \operatorname{div}(\boldsymbol{f} \operatorname{curl} \boldsymbol{A}) = 0$$

yields a scalar equation with the coupling term

$$\operatorname{div}(\boldsymbol{f} \operatorname{curl} \boldsymbol{A}) = f_{11} \frac{\partial^2 A_3}{\partial x_1 \partial x_2} + f_{21} \frac{\partial^2 A_3}{\partial x_2^2}.$$

With these considerations, we can write the bilinear forms $\bar{b}(\cdot,\cdot)$ and $\tilde{c}(\cdot,\cdot)$ in their new form as

$$\begin{aligned}
\bar{b}(\boldsymbol{A},\tilde{\boldsymbol{A}}) &= \int_\Omega (\boldsymbol{\mu}^{-\epsilon}\operatorname{curl}\boldsymbol{A})\cdot\operatorname{curl}\tilde{\boldsymbol{A}}\,\mathrm{d}x = \int_\Omega \frac{1}{\mu^\epsilon_{22}}\frac{\partial A_3}{\partial x_1}\frac{\partial \tilde{A}_3}{\partial x_1} + \frac{1}{\mu^\epsilon_{11}}\frac{\partial A_3}{\partial x_2}\frac{\partial \tilde{A}_3}{\partial x_2}\,\mathrm{d}x \\
&=: \bar{b}(A_3,\tilde{A}_3) \\
\tilde{c}(\boldsymbol{v},\boldsymbol{A}) &= \frac{1}{2}\int_{\Omega_c} \operatorname{curl}\boldsymbol{A}\cdot(\boldsymbol{f}^T\boldsymbol{\epsilon}(\boldsymbol{v}))\,\mathrm{d}x \\
&= \frac{1}{2}\int_\Omega \frac{\partial A_3}{\partial x_2}\left(f_{11}\frac{\partial v_1}{\partial x_1} + f_{21}\frac{\partial v_2}{\partial x_2}\right) - \frac{\partial A_3}{\partial x_1} f_{62}\left(\frac{\partial v_1}{\partial x_2} + \frac{\partial v_2}{\partial x_1}\right)\mathrm{d}x \\
&=: \tilde{c}(\boldsymbol{v},A_3)
\end{aligned}$$

The bilinear form $\bar{b}(A_3,\tilde{A}_3)$ for the scalar component A_3 is almost identical to the bilinear form $b(\Psi,\Phi)$ for the magnetic scalar potential from Chapter 3 with interchanged components μ^ϵ_{ii}, $i = 1,2$. Analogously, the coupled bilinear form $\tilde{c}(\boldsymbol{v},\boldsymbol{A})$ has a similar structure as the bilinear form $c(\boldsymbol{v},\Psi)$ with minor differences due to the usage of the curl instead of the gradient.
Since the magnetic part of the coupled problem is now based on the single variable A_3, the space $H_\Gamma(\operatorname{curl},\Omega)$ used for the functions $\boldsymbol{A}$ in the three-dimensional model becomes superfluous: Instead, we simply require $A_3 \in H^1(\Omega)$. The coercivity of $\bar{b}(\cdot,\cdot)$ in $H^1(\Omega)^3$ is automatically satisfied and the bilinear form $\tilde{c}(\cdot,\cdot)$ fulfills the estimate from Theorem 4.1 for all $\boldsymbol{A} \in H^1(\Omega)^3$.

Chapter 5

Numerical Simulations

After an extensive theoretical treatment of the coupled magnetoelastic saddle point problem and its discrete counterpart, we now focus on the numerical analysis and simulations of specific 1D and 2D problems. Within this framework, we will present two different models:
In an initial, one-dimensional quasi-static model of a magnetostrictive Euler-Bernoulli beam [64], attention will be drawn only on the weak coupling, that is, on the impact of an external magnetic field on the strain and displacement of the beam. The model is slightly different from the general model presented in Chapter 3 as it examines the bending of the beam and includes time-dependency. However, it follows the same steps of derivation using Hamilton's principle and, thanks to its vivid and comprehensible structure, offers a possibility of demonstrating the coupling effect by showing the deformation of the body at different time steps as a consequence of the applied magnetic field.
The second model, which serves as a basis for the numerical verification of the two-way-coupled model from Chapter 3, is the two-dimensional model of the magnetostrictive plate in the state of plane stress already introduced in Subsection 3.4.2.
After defining the exact model geometries, material parameters and the loading, as well as the appropriate Finite Element spaces, the results of the numerical simulations carried out with the software MATLAB will be illustrated for both models. The second model will be additionally analyzed with respect to the properties of the dicretized system. Aspects such as the course of the energy norm of the coupled model, as well as the full-rank condition mentioned in Section 3.4.3 will be discussed and used as a verification of the theoretical results.

5.1 1D model: the Euler-Bernoulli beam

The one-dimensional model of a beam in a magnetic field can be regarded as a reduced form of an actuator. A giant magnetostrictive actuator generally consists of a magnetostrictive rod, typically made of a giant magnetostrictive material such as Terfenol-D, surrounded by an excitation coil that is provided by a time-dependent current generating a varying magnetic field in the rod. Moreover, it contains permanent magnets which produce the steady magnetic bias field and a prestress spring washer that applies a compressive load to the rod. Figure **??** shows a two-dimensional sketch of the geometry of such an actuator. In our model, we will adopt the basic structure of the actuator, yet making several simplifying assumptions in order to neglect the parts that have no significant effect on the mathematical model. Suppose the rod is represented by an Euler-Bernoulli beam. It is

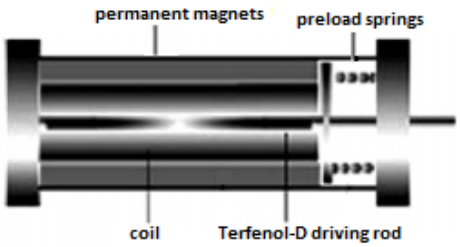

Figure 5.1: Sketch of the cross-section of a giant magnetostrictive actuator (based on [115]).

clamped at the left end and free to move at the right end. The spring washer providing the compressive force is left out of the geometry as we are merely interested in the influence of the magnetic field on the body. Since our model is based on the total magnetic scalar potential defined only in current-free regions, the coil as the source of the magnetic field has to be replaced by permanent magnets. For convenience, only the biasing magnets will be considered. As in the general model from the previous section, the air domain surrounding the body is neglected. This is a plausible simplification in our case, as we focus on small deformations of the body within the framework of linear theory. Consider a planar Euler-Bernoulli beam with rectangular cross-section and length l, which is placed into the magnetic field and undergoes deformations in the (x_1, x_2) - plane, with x_1 denoting the longitudinal axis of the beam. Due to the assumptions of the Euler-Bernoulli beam theory, the behavior of the body is fully determined by the longitudinal and lateral displacements of the neutral fiber, denoted by w_1 and w_2, respectively, depending on the longitudinal coordinate x_1. Considering only small displacements and slopes, the displacement field of the beam can be written as (see, e.g. [102]),

$$\begin{aligned} u_1(x_1,t) &= w_1(x_1,t) - x_2 w_2'(x_1,t), \\ u_2(x_1,t) &= w_2(x_1,t), \\ u_3(x_1,t) &= 0, \end{aligned}$$

where the derivative refers to differentiation with respect to x_1.
Furthermore, the following boundary conditions are chosen: The left end of the beam is clamped, i.e.

$$w_1(0,t) = 0, \quad w_2(0,t) = 0, \quad w_2'(0,t) = 0,$$

and the right end is left free. In addition, we assume that the magnetic influence is described by a given constant magnetic flux density vector $\boldsymbol{B} \in \mathbb{R}^2$.
As in the general model from the previous section, we extend the constitutive relation of linear elasticity by an expression including the magnetic influence,

$$\boldsymbol{\sigma} = \boldsymbol{C}^H \boldsymbol{\epsilon} - \tilde{\boldsymbol{e}} \boldsymbol{B},$$

with the coupling matrix $\tilde{\boldsymbol{e}} := \boldsymbol{e}\boldsymbol{\mu}^{-1}$ and $\boldsymbol{C}^H$ and $\boldsymbol{e}$ as defined in Section 3.1. Using this equation along with the expression for linearized strain of the beam, the strain energy reads

$$\begin{aligned} W(\boldsymbol{u}, \boldsymbol{B}) = \frac{1}{2} \int_\Omega \boldsymbol{\sigma}(\boldsymbol{u}) : \boldsymbol{\epsilon}(\boldsymbol{u}) \, \mathrm{d}x &= \frac{1}{2} E b^2 \int_0^l w_1'(x_1)^2 \, \mathrm{d}x_1 + \frac{1}{2} EI \int_0^l (w_2''(x_1))^2 \, \mathrm{d}x_1 \\ &- \left(\sum_{k=1}^n \tilde{e}_{1k} B_k \right) \left(A \int_0^l w_1'(x_1) \, \mathrm{d}x_1 - \frac{b^3}{2} \int_0^l w_2''(x_1) \, \mathrm{d}x_1 \right) \end{aligned}$$

with $A = b^2$ denoting the cross-sectional area of the beam, E the modulus of elasticity and $I = b^3/12$ the axial moment of inertia. Notice that the magnetic influence is characterized by a volume force term on the right-hand side.
Inserting the above equation into Hamilton's principle, neglecting additional volume and surface force terms like gravity and mechanical traction and using the same variational approach as described in Section 3.1, we end up with the following time-dependent variational problem:

Problem: For all t find $\boldsymbol{w}(.,t) \in V^B$ with

$$V^B := \{\tilde{\boldsymbol{w}} \in H^1((0,l)) \times H^2((0,l))|\ \tilde{w_1}(0,t) = \tilde{w_2}(0,t) = \tilde{w_2}'(0,t) = 0\},$$

such that

$$\langle \rho \ddot{\boldsymbol{w}}, \boldsymbol{v} \rangle + a(\boldsymbol{w}, \boldsymbol{v}) = l(\boldsymbol{v}) \quad \text{for all } \boldsymbol{v} \in V^B,$$

where

$$\begin{aligned}
\langle \rho \ddot{\boldsymbol{w}}, \boldsymbol{v} \rangle &= b^2 \int_0^l \rho \boldsymbol{v} \cdot \ddot{\boldsymbol{w}} \, \mathrm{d}x_1, \\
a(\boldsymbol{w}, \boldsymbol{v}) &= \frac{1}{2} EA \int_0^l w_1'(x_1) v_1'(x_1) \, \mathrm{d}x_1 + \frac{1}{2} EI \int_0^l w_2''(x_1) v_2''(x_1) \, \mathrm{d}x_1, \\
\langle l, \boldsymbol{v} \rangle &= \left(\sum_{k=1}^{n} D_{1k} B_k \right) \left(A \int_0^l v_1'(x_1) \, \mathrm{d}x_1 - \frac{b^3}{2} \int_0^l v_2''(x_1) \, \mathrm{d}x_1 \right),
\end{aligned}$$

with ρ denoting the density of the material.

To discretize w_1 and w_2 with the Finite Element Method, we choose quadratic and cubic finite elements, i.e. functions $w_h^1 \in V_{2,h}^B := S_2(\Omega, \mathcal{T}_h)$ for w_1 and $w_h^2 \in V_{3,h}^B := S_3(\Omega, \mathcal{T}_h)$ for w_2. To maintain the simple structure of the model, the whole beam is discretized as a single element.
Including the boundary conditions, we thus obtain

$$\begin{aligned}
w_1(x,t) &= x^2 \left(-4c_3(t) + 2c_4(t)\right) + x \left(4c_3(t) - c_4(t)\right), \\
w_2(x,t) &= x^3(-2c_1(t) + c_2(t)) + x^2(3c_1(t) - c_2(t)),
\end{aligned}$$

where the coefficients c_1 and c_2 are linked with the lateral displacement and its derivative at the right end of the beam, whereas the coefficients c_3 and c_4 yield the longitudinal displacement in the middle and the right end of the beam, respectively.

For the numerical simulations, the values $l = 0.3m$, $b = 0.008m$ for the dimensions of the beam have been taken, as well as the material parameters $E = 25GPa$ and $\rho = 9250kg/m^3$ of Terfenol-D [89]. All simulations presented in this work have been carried out with the MATLAB version R2012a.

Figure 5.2 shows the results for the stationary loading case as well as for a sequence of static simulations. In both cases, the value of the magnetic field has been set to $B = 1T$. In the latter case, the (quasi-static) time-dependence was characterized by choosing a magnetic field that is exponential in time. It can be seen that the beam experiences a longitudinal extension and vertical deflection under the pure influence of the magnetic field. Due to the clamped boundary condition at the left end, the deformed shape of the beam is nonlinear (see Fig. 5.2(a) and (b)).

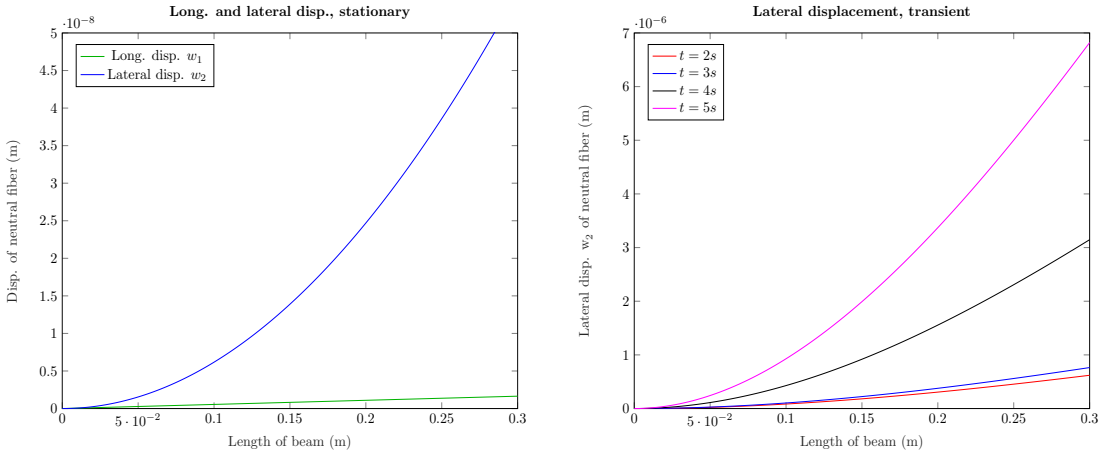

Figure 5.2: Displacements w_1 and w_2 of neutral fiber for stationar and quasi-static loading

5.2 2D model: the plane stress - plate

The one-dimensional beam model from the last subsection showed the impact of the magnetic field on the mechanical deformation of the body. In this section, we will take a step further and numerically simulate the inverse effect as well, additionally extending the model to 2D.
Consider again the thin magnetoelastic plate from Section 3.4.2. Zero Dirichlet boundary conditions for the displacement $\boldsymbol{u}$ imposed on one side of the plate describe the fixed bearings that restrict the translational movement of the plate in its plane, while Neumann boundary conditions on the opposite side specify the uniaxial tension applied to the plate in x_1-direction. Analogously, the magnetic scalar potential Ψ is set to zero on the Dirichlet boundary, while the specification of the normal component of the magnetic flux density $\boldsymbol{B}$ on the Neumann boundary defines a "magnetic surface traction". Note that, as mentioned in Section 3.4.3, the mechanical and magnetic boundaries coincide.
For the simulations with MATLAB, material parameters of a polycrystalline Terfenol-D were taken from the work of Claeyssen et al. [39] and adapted to the model of a transversely isotropic two-dimensional body stressed in x_1 direction (see Table 5.1). However, since the constitutive relations used in [39] are based on $\boldsymbol{\sigma}$ and $\boldsymbol{H}$ as independent variables rather than on $\boldsymbol{\epsilon}$ and $\boldsymbol{H}$ as in Equation (3.3),

$$\begin{aligned} \boldsymbol{\epsilon} &= \boldsymbol{S}^H \boldsymbol{\sigma} + \boldsymbol{d}\boldsymbol{H}, \\ \boldsymbol{B} &= \boldsymbol{d}^T \boldsymbol{\sigma} + \boldsymbol{\mu}^\sigma \boldsymbol{H}, \end{aligned}$$

where $\boldsymbol{d}$ is a suitable magnetoelastic coupling matrix, $\boldsymbol{S}^H$ is the elastic compliance matrix for constant $\boldsymbol{H}$ and $\boldsymbol{\mu}^\sigma$ is the magnetic permeability matrix for constant $\boldsymbol{\sigma}$, we make use of the modifications presented in Section 4.1 in order to adapt the parameters to our model. Solving the above equations for $\boldsymbol{\sigma}$ and $\boldsymbol{B}$, we obtain

$$\begin{aligned} \boldsymbol{\sigma} &= \boldsymbol{C}^H \boldsymbol{\epsilon} - (\boldsymbol{C}^H \boldsymbol{d})\boldsymbol{H}, \\ \boldsymbol{B} &= \boldsymbol{d}^T (\boldsymbol{C}^H \boldsymbol{\epsilon}) - \boldsymbol{d}^T (\boldsymbol{C}^H \boldsymbol{d}^T \boldsymbol{H}) + \boldsymbol{\mu}^\sigma \boldsymbol{H}. \end{aligned}$$

The matrices $\boldsymbol{e}$ and $\boldsymbol{\mu}^\epsilon$ are given by

$$\boldsymbol{e} = \boldsymbol{C}^H \boldsymbol{d}, \qquad \boldsymbol{\mu}^\epsilon = \boldsymbol{\mu}^\sigma - \boldsymbol{d}^T \boldsymbol{e}.$$

Furthermore, $\boldsymbol{\tau}$ and $\tilde{B}$, the prescribed values of the mechanical and magnetic quantities on the Neumann boundary, are computed by inserting the values of the mechanical and mag-

Magnetic permeabilities	$\mu_{11} = 3.77 \cdot 10^{-6}$, $\mu_{22} = 1.012 \cdot 10^{-5}$
Compliance components	$S_{11}^H = 3.8 \cdot 10^{-11}$, $S_{22}^H = 4.4 \cdot 10^{-11}$
	$S_{12} = -1.65 \cdot 10^{-11}$, $S_{66} = 11 \cdot 10^{-11}$
Magnetoelastic coupling coefficients	$d_{11} = 8.5 \cdot 10^{-9}$, $d_{12} = -4.3 \cdot 10^{-9}$
	$d_{26} = 16.5 \cdot 10^{-9}$
Initial bias	$\sigma_1 = 30 \cdot 10^6$, $H_1 = 100 \cdot 10^3$

Table 5.1: Material parameters of polycrystalline Terfenol-D, taken from [39] (without measurement units).

Young's moduli	$E_1 = 2.6 \cdot 10^{10}$, $E_2 = 2.27 \cdot 10^{10}$
Poisson's ratio	$\nu_{12} = 0.429$
Shear modulus	$G_{12} = 1/11 \cdot 10^{11}$
Magnetoelastic coupling coefficients	$e_{11} = 213.30$, $e_{12} = -17.66$, $e_{26} = 150$
Mechanical and magnetic surface forces	$\tau_1 = 8.67 \cdot 10^6$, $\tilde{B} = 0.434$

Table 5.2: Material parameters for the magnetostrictive plate (without measurement units).

netic bias given in Table 5.1 into the above constitutive equations. Using these relations, the quantities from Table 5.1 can be adapted to our model (see Table 5.2).

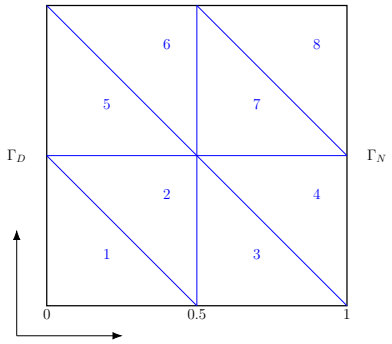

Figure 5.3: 2D sketch of geometry with boundaries and an example of a coarse discretization (mesh parameter $h = 1/\sqrt{2}$)

For the sake of simplicity, $\Omega = [0,1] \times [0,1]$ has been chosen as domain of integration with the thickness $r = 0.1$. Both the displacement $\boldsymbol{u}$ and the magnetic scalar potential Ψ have been discretized with linear 2D finite elements using a triangular mesh. A sketch of the geometry and its boundaries with a coarse mesh are presented in Figure 5.3.
Figure 5.4 shows the results of the numerical simulations, which are in accordance with the theoretical considerations: Due to the joint influence of the mechanical and magnetic tractions, the body experiences longitudinal displacement that is zero at the side fixed by the Dirichlet conditions and increases over the length of the plate to find its maximum at the opposite side, where the Neumann boundary conditions are prescribed (Figure 5.4a). Similarly, the distribution of lateral displacement shown in Figure 5.4b corresponds to the contraction in consequence of a tensile force, which is increased because of the coupling. Note that the origin of the Cartesian coordinate system was set to the midpoint of the left side of the square domain, which induces the symmetrical distribution of the lateral

displacement over the length of the plate.

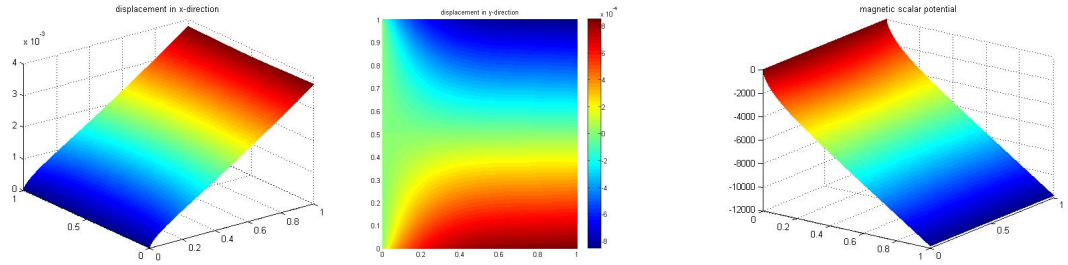

(a) u_1, side view [m] (b) u_2, top view [m] (c) Ψ, side view [A/m]

Figure 5.4: Distributions of the coupled mechanical and magnetic quantities: (a) longitudinal and (b) lateral displacements, (c) scalar potential. The color distribution shows the course of the plotted quantities from the (absolute) lowest value (blue) to the (absolute) highest one (red).

Due to the special form of the elastic coupling tensor in (3.33), the magnetic field mainly affects the longitudinal direction, acting as a magnetic tensile force. Finally, Figure 5.4c depicts the distribution of the (coupled) magnetic scalar potential, which is similar to the distribution in Figure 5.4a, but has a negative incline and negative values due to the definition of the potential.

A common way to demonstrate the validity of the numerical method is the computation of the energy norms of the considered quantities. In the uncoupled case, e.g. in linear elasticity, the energy norm of the solution is always greater than or equal to the energy norm of its numerical approximation:

If $\boldsymbol{u} \in \mathcal{V}$ fulfills the equation

$$a(\boldsymbol{u}, \boldsymbol{v}) = l(\boldsymbol{v}) \quad \text{for all} \quad \boldsymbol{v} \in \mathcal{V}$$

and $\boldsymbol{u}_h \in V_h$ fulfills

$$a(\boldsymbol{u}_h, \boldsymbol{v}_h) = l(\boldsymbol{v}_h) \quad \text{for all} \quad \boldsymbol{v}_h \in V_h,$$

then, defining the error $\boldsymbol{e}^{rr} := \boldsymbol{u}_h - \boldsymbol{u}$, we get

$$a(\boldsymbol{e}^{rr}, \boldsymbol{u}_h) = a(\boldsymbol{u}_h, \boldsymbol{u}_h) - a(\boldsymbol{u}, \boldsymbol{u}_h) = l(\boldsymbol{u}_h) - l(\boldsymbol{u}_h) = 0,$$

since $\boldsymbol{u}_h \in \mathcal{V}$. Consequently, exploiting the symmetry of the bilinear form $a(\cdot, \cdot)$, we obtain

$$a(\boldsymbol{u}, \boldsymbol{u}) = a(\boldsymbol{u}_h - \boldsymbol{e}^{rr}, \boldsymbol{u}_h - \boldsymbol{e}^{rr}) = a(\boldsymbol{u}_h, \boldsymbol{u}_h) - 2a(\boldsymbol{e}^{rr}, \boldsymbol{u}_h) + a(\boldsymbol{e}^{rr}, \boldsymbol{e}^{rr}) = a(\boldsymbol{u}_h, \boldsymbol{u}_h) + a(\boldsymbol{e}^{rr}, \boldsymbol{e}^{rr}),$$

which yields the inequality $a(\boldsymbol{u}, \boldsymbol{u}) \geq a(\boldsymbol{u}_h, \boldsymbol{u}_h)$ due to the positive definiteness of $a(\cdot, \cdot)$. In the coupled case, however, the term $a(\boldsymbol{u}_h, \boldsymbol{e}^{rr})$ does not vanish,

$$a(\boldsymbol{u}_h, \boldsymbol{e}^{rr}) = c(\boldsymbol{u}_h, \Psi) - c(\boldsymbol{u}_h, \Psi_h),$$

which implies that

$$a(\boldsymbol{u}, \boldsymbol{u}) = a(\boldsymbol{u}_h, \boldsymbol{u}_h) + 2c(\boldsymbol{u}_h, e^{rr}_{\text{mag}}) + a(\boldsymbol{e}^{rr}, \boldsymbol{e}^{rr}),$$

with $e^{rr}_{\text{mag}} := \Psi_h - \Psi$. Analogously,

$$b(\Psi, \Psi) = b(\Psi_h, \Psi_h) - 2c(\boldsymbol{e}^{rr}, \Psi) + b(e^{rr}_{\text{mag}}, e^{rr}_{\text{mag}}).$$

Hence, depending on the values of the components of the magnetoelastic coupling tensor $\boldsymbol{e}$, the energy norms $(\boldsymbol{U}^T A\boldsymbol{U})^{\frac{1}{2}}$ and $(\tilde{\boldsymbol{\Psi}}^{\boldsymbol{T}} \boldsymbol{B}\tilde{\boldsymbol{\Psi}})^{\frac{1}{2}}$ of the numerical solutions $\boldsymbol{U}$ and $\tilde{\boldsymbol{\Psi}}$ converge to an upper or lower bound with growing mesh refinement. For the values given in Table 5.2, the energy norms converge to a lower bound, as shown in Figure 5.5a.

The last step of the numerical analysis of our model is the numerical verification of the inf-sup condition from Section 3.4.3. For this purpose, the singular value decomposition (SVD) of the coupling matrix $\boldsymbol{C}$ has been computed. In Section 3.4.3 we showed that the inf-sup condition was equivalent to the algebraic full rank - condition for the matrix $\boldsymbol{C}$. The SVD provides a possibility to check this condition by computing the smallest singular value of the coupling matrix $\boldsymbol{C}$:

Let $\sigma_1 \geq \sigma_2 \geq ... \geq \sigma_p \geq 0$ be the singular values of the matrix $\boldsymbol{C}$ in descending order. If we define t as the index of the smallest non-zero singular value in the above ordering, i.e.

$$\sigma_1 \geq ... \geq \sigma_t > \sigma_{t+1} = ... = \sigma_p = 0,$$

then, $\text{rank}(\boldsymbol{C}) = t$. Hence, we can conclude that $\boldsymbol{C} \in \mathbb{R}^{n \times m}$ has full rank iff $t = n$. We therefore need to check if all singular values of the matrix $\boldsymbol{C}$ resulting from our discretization are positive.
Furthermore, one can show that if equality holds in the (discrete) inf-sup condition with the constant $\bar{\beta} > 0$, then $\bar{\beta}$ coincides with the least singular value of the matrix $\boldsymbol{C}$ (refer e.g. to [12]). Consequently, to show the inf-sup stability of our numerical method, we have to verify that $\bar{\beta}$ is bounded from below by a constant $\hat{\beta}$ that is independent from the discretization h.
In Figure 5.5b, the least singular value σ_p of C is plotted over $1/h$, showing that σ_p converges with increasing h to a fixed value, which is in the limit independent from the discretization. Again, as in the case of the energy norms, the least singular value does not necessarily have to be decreasing with increasing geometry refinement. This result verifies that inf-sup condition for the coupled magnetoelastic saddle point problem numerically, yielding the unique solvability of the discrete problem.

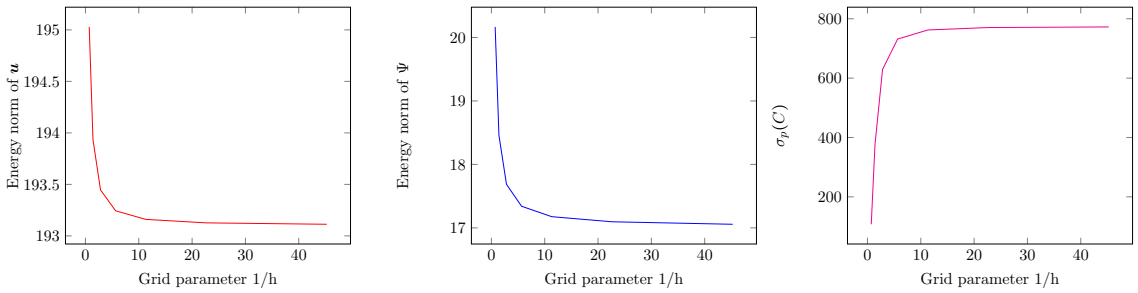

(a) (b) (c)

Figure 5.5: Energy norms of the (a) elastic and (b) magnetic solutions and (c) smallest singular value σ_{min} of coupling matrix C.

Chapter 6

Summary and Outlook

In this thesis, we derived and analyzed coupled magnetoelastic models to describe the behavior of polycrystalline magnetostrictive materials using the linearized constitutive equations of piezomagnetic materials and a special formulation of Hamilton's principle for the coupled system. The linearity assumption was satisfied by considering biased magnetostrictive materials and small deviations of the external electromagnetic and mechanical fields from the initial biased state. Two different approaches were used in this context, a formulation based on the *total magnetic scalar potential* Ψ, the negative gradient of the magnetic field, and a formulation using the *magnetic vector potential* $\boldsymbol{A}$, whose curl is defined to be the magnetic flux density. In the framework of the scalar potential formulation, the influence of the external static magnetic field was incorporated by permanent magnets, while the vector potential approach was formulated in current-carrying regions including both static magnetic and transient electromagnetic fields. The elastic (displacement) field was assumed to be static for all of the introduced models.

On the one hand, the distinctive feature of this work was the analysis of the coupled magnetoelastic problem resulting from these two formulations with regard to its structure, strong and weak formulations, the corresponding function spaces and the existence and uniqueness of the solutions. We showed that the model based on the magnetic scalar potential and elastic displacement field as independent variables can be interpreted a saddle point problem with a penalty term. The main focus in proving the unique solvability of this saddle point problem lay on the verification of an inf-sup condition (LBB-condition) from Brezzi's theorem for the class of polycrystalline magnetostrictive materials. The inf-sup condition also yielded a valuable stability estimate, an evaluation of the influence of perturbations of the given data on the solution of the coupled problem. After dealing with the continuous setting, we proved that the inf-sup condition is also satisfied for its discrete counterpart, showing that the constant in the inf-sup estimate does not depend on the discretization parameter but solely on the geometry.

Furthermore, the strong and weak formulation of models using the magnetic vector potential and the elastic displacement as independent variables were presented for the magnetostatic and -quasistatic settings, as well as for the full Maxwell system in the frequency domain. In the time-varying case, the existence and uniqueness of the solutions to the weak formulations was shown by adding the two mutually coupled partial differential equations and applying the Lax-Milgram lemma on the resulting composite bilinear form. To prove the coercivity of this bilinear form, suitable estimates for the coupled elasto-magnetic bilinear form were derived. In the magnetostatic case, the coupled system represents a block-saddle point problem whose solvability could be directly deduced from the uncoupled case using the previously mentioned estimates for the coupled bilinear form

and applying Brezzi's theorem.

On the other hand, we discussed the impact of a reformulation of the constitutive equations in terms of the dual magnetic variables on the structure of the resulting coupled system. We showed that by choosing constitutive equations that depend on the elastic strain and magnetic field and making use of the corresponding coenergy function in the Lagrangian, we obtain a coupled problem with a saddle point structure, whereas taking the magnetic flux density instead of the magnetic field and using the corresponding energy function leads to a symmetric problem in the time-varying case. In the magnetostatic case, we enforce the mixed structure of the coupled problem through an additional condition to cure the lack of uniqueness of the magnetic vector potential. These results are in accordance with Bossavit's predictions [17] and Preumont's work [95] for piezoelectric systems.

So far, we have only dealt with linear material behavior. In a next step, these models can be enhanced by considering non-linearity. One way to incorporate this behavior is to derive the corresponding constitutive relations by using Taylor approximations of higher order for the coupled free-energy density function. The Standard Square constitutive model suggested by Carman and Mitrovic [33], for example, characterizes a quadratic dependence of the coupled quantities on the mechanical stress and the magnetic field.
Another possibility of extending the linear setting is to decompose the elastic and magnetic quantities into a reversible and an irreversible part, as discussed in the introductory chapter and as seen, e.g. in the paper of Kaltenbacher et al. [76]. They suggest to describe the irreversible magnetic flux density by a Preisach hysteresis operator and to model the irreversible part of the strain as a polynomial function of the magnetic hysteresis operator.
Finally, a third idea is to change the constitutive equations by assuming non-constant material parameters such as the magnetic permeability and the elasticity tensor. Following this assumption, we would obtain a model similar to the one developed by Poutala et al. [91]. The authors suggest a model for the weak coupling in a magnetostrictive material, that is, they only consider the influence of the magnetic mechanical strain on the magnetic field by requiring a dependence of the magnetic permeability on the strain. The corresponding function is then obtained by measurements and corresponding numerical simulations.
Moreover, the models presented in this thesis can be extended by including the time-dependence of the mechanical displacement field: While the systems based on the magnetic vector potential considered time-varying magnetic fields, the mechanical displacement was assumed to be stationary. In case of the scalar potential formulation, one would have to deal with a transient saddle point problem with a penalty term and go back to suitable techniques for the analysis of mixed problems developed by Brezzi et al. (e.g. in [24]) to prove the existence and uniqueness of the solution. As the transient problem of elasticity represents a hyperbolic system of partial differential equations, referring to the theory of Duvaut and Lions [54] might be helpful for proving the unique solvability of the coupled system resulting from the vector potential formulation.

The numerical simulations of the models can be supplemented with suitable three-dimensional examples. In the case of the magnetic vector potential, a three-dimensional numerical treatment involves the use of curl-conforming edge elements (*Nédelec elements*) for the discretization of the magnetic vector potential in the ungauged formulation and nodal finite elements in the gauged one, as depicted, for example, in [2].

Bibliography

[1] Adly, A., Mayergoyz, I., and Bergqvist, A. Preisach modeling of magnetostrictive hysteresis. *Journal of Applied Physics 69* (1991), 5777 – 5779.

[2] Alonso Rodriguez, A., and Valli, A. *Eddy Current Approximation of Maxwell Equations: Theory, algorithms and applications*. Springer Italia, Milan, 2010.

[3] Ammari, H., Buffa, A., and Nédélec, J.-C. A justification of eddy currents model for the Maxwell equations. *SIAM Journal on Applied Mathematics 60/5* (2000), 1805–1823.

[4] Atkinson, K., and Weimin, H. *Theoretical Numerical Analysis: A Functional Analysis Framework*. Springer, New York, 2001.

[5] Auld, B. A. Magnetoelastic phenomena. In *Magnetism and Magnetic Materials: 1965 Digest*, R. L. White and K. A. Wickersheim, Eds. Academic Press, New York-London, 1965.

[6] Babuska, I., and Aziz, A. Survey lectures on the mathematical foundations of the finite element method. In *The Mathematical Foundation of the Finite Element Method with Applications to Partial Differential Equations*, A. Aziz, Ed. Academic Press, New York-London, 1972, pp. 3–363.

[7] Babuška, I. Error bounds for finite element method. *Numer. Math. 16* (1971), 322–333.

[8] Barham, M., Steigmann, D., McElfresh, M., and Rudd, R. Finite deformation of a pressurized magnetoelastic membrane in a stationary dipole field. *Acta Mechanica 191* (2007), 1–19.

[9] Bedford, A. Hamilton's principle in continuum mechanics. In *Research Notes in Mathematics*, vol. 139. Pitman Advanced Publishing Program, Boston, 1985.

[10] Benzi, M., Golub, G., and Liesen, J. Numerical solution of saddle point problems. *Acta Numerica* (2005), 1–137.

[11] Biró, O., Preis, K., and Paul, C. The use of a reduced vector potential A_r formulation for the calculation of iron induced field errors. *Proceedings of the First International ROXIE User's Meeting and Workshop (CERN)* (1999), 31–46.

[12] Boffi, D., Brezzi, F., and Fortin, M. *Mixed Finite Element Methods and Applications*. Springer, Berlin-Heidelberg, 2013.

[13] Borcea, L., and Bruno, O. On the magneto-elastic properties of elastomer-ferromagnet composites. *Journal of the Mechanics and Physics of Solids 49* (2001), 2877 – 2919.

[14] Borthwick, D. *Introduction to Partial Differential Equations.* Springer International Publishing, 2017.

[15] Bossavit, A. *Computational Electromagnetism. Variational Formulations, Complementarity, Edge Elements.* Academic Press, San Diego, 1998.

[16] Bossavit, A. *A course in Convex Analysis. Lecture notes.* ICM, Warsaw, 2003.

[17] Bossavit, A. Discrete Magnetoelasticity: A Geometrical Approach. *IEEE Transactions on Magnetics 46* (2010), 3485–3491.

[18] Bower, A. F. *Applied Mechanics of Solids.* CRC Press, New York, 2009.

[19] Bozorth, R. M. *Ferromagnetism.* Wiley-IEEE Press, New Jersey, 1993.

[20] Braess, D. Stability of saddle point problems with penalty. *Rairo - Modélisation mathémathique et analyse numérique 30* (1996), 731–742.

[21] Braess, D. *Finite Elements: Theory, Fast Solvers, and Applications.* Cambridge University Press, Cambridge, 2007.

[22] Brenner, S., and Ridgway Scott, L. *The Mathematical Theory of Finite Element Methods.* Springer, New York, 1994.

[23] Brezzi, F. On the existence, uniqueness and approximation of saddle-point problems arising from Lagrangian multipliers. *ESAIM: Mathematical Modelling and Numerical Analysis - Modélisation Mathématique et Analyse Numérique 8* (1974), 129–151.

[24] Brezzi, F., and Fortin, M. *Mixed and Hybrid Finite Element Methods.* Springer, New York, 1991.

[25] Brown, W. Magnetoelastic interactions. In *Springer Tracts in Natural Philosophy*, C. Truesdell, Ed., vol. 529. Springer, Berlin-Heidelberg, 1966.

[26] Buffa, A. Trace Theorems on Non-Smooth Boundaries for Functional Spaces Related to Maxwell Equations: an Overview. In *Computational Electromagnetics* (Berlin, 2003), P. Monk, C. Carstensen, S. Funken, W. Hackbusch, and R. H. W. Hoppe, Eds., vol. 28 of *Lectue Notes in Computational Science and Engineering*, Springer, pp. 23–34.

[27] Bunge, H. Texture and magnetic properties. *Textures and Microstructures 11* (1989), 75–91.

[28] Bustamanate, R., Dorfmann, A., and Ogden, R. A nonlinear magnetoelastic tube under extension and inflation in an axial magnetic field: numerical solution. *Journal of Engineering Mathematics 59* (2007), 139–153.

[29] Bustamante, R., Dorfmann, A., and Ogden, R. Nonlinear electroelastostatics: a variational framework. *Zeitschrift für Angewandte Mathematik und Physik 60* (2009), 154–177.

[30] Bustamante, R., Dorfmann, A., and Ogden, R. Numerical solution of finite geometry boundary-value problems in nonlinear magnetoelasticity. *International Journal of Solids and Structures 48* (2011), 843–883.

[31] Bíró, O. Edge element formulations of eddy current problems. *Comput. Methods Appl. Mech. Engrg 169* (1999), 391–405.

[32] Bíró, O., and Preis, K. On the use of the magnetic vector potential in the finite element analysis of three-dimensional eddy currents. *IEEE Transactions on Magnetics 25* (1989), 3145–3159.

[33] Carman, G. P., and Mitrovic, M. Nonlinear Constitutive Relations for Magnetostrictive Materials with Applications to 1-D Problems. *Journal of Intelligent Material Systems and Structures 6* (1995), 673–683.

[34] Ciarlet, P. *The Finite Element Method for Elliptic Problems.* North-Holland, Amsterdam, 1978.

[35] Ciarlet, P. *Mathematical Elasticity I.* North Holland, New York, 1988.

[36] Ciarlet, P. *Linear and Nonlinear Functional Analysis with Applications.* Society for Industrial and Applied Mathematics, Philadelphia, PA, 2013.

[37] Ciarlet, P., Geymonat, G., and Krasucki, F. Legendre-Fenchel duality in elasticity. *Comptes rendus de l'Académie des sciences 1* (2011), 597–602.

[38] Claeyssen, F. *Design and building of low-frequency sonar transducers based on rare-earth iron magnetostrictive alloys.* Doctoral thesis, Lyon, 1989.

[39] Claeyssen, F., Lhermet, N., Barillot, F., and Le Letty, R. Giant dynamic strains in magnetostrictive actuators and transducers. Paper presented at ISAGMM 2006 Conference, China, 2006.

[40] Claeyssen, F., Lhermet, N., Le Letty, R., and Bouchilloux, P. Actuators, transducers and motors based on giant magnetostrictive materials. *Journal of alloys and compounds 258 (1-2)* (1997), 61–73.

[41] Clark, A. E., and Belson, H. Giant room-temperature magnetostrictions in $tbfe_2$ and $dyfe_2$. *Physical Review B 5* (1972), 3642 – 3644.

[42] Clemens, M. Large systems of equations in a discrete electromagnetism: formulations and numerical algorithms. *IEE Proceedings - Science, Measurement and Technology 152* (2005), 50–72.

[43] Coulomb, J.-L. Finite element three dimensional magnetic field computation. *IEEE Transactions on Magnetics MAG-17* (1981), 3241 – 3246.

[44] Courant, R., and Hilbert, D. *Methoden der mathematischen Physik I.* Springer, Heidelberg, 1968.

[45] Dapino, M. On magnetostrictive materials and their use in smart material transducer. *Structural Engineering and Mechanics Journal 17* (2002), 1–28.

[46] Dapino, M. On magnetostrictive materials and their use in adaptive structures. *Structural Engineering and Mechanics 17* (2004), 303–329.

[47] Dorfmanm, L., and Ogden, R. Some problems in nonlinear magnetoelasticity. *Zeitschrift für Angewandte Mathematik und Physik 56* (2005), 718–745.

[48] Dorfmann, A., and Ogden, R. Nonlinear magnetoelastic deformations of elastomers. *Acta Mechanica 167*, 13–28.

[49] Dorfmann, A., and Ogden, R. Magnetoelastic modelling of elastomers. *European J. Mech. A/Solids 22* (2003), 497–507.

[50] Dorfmann, A., and Ogden, R. Nonlinear magnetoelastic deformations. *Quarterly Journal of Mechanics and Applied Mathematics 57* (2004), 599–622.

[51] Dorfmann, A., and Ogden, R. Nonlinear magnetoelastic deformations of elastomers. *Acta Mechanica 167* (2004), 13–28.

[52] Dorfmann, L., and Ogden, R. Nonlinear magnetoelastic deformations. *The Quarterly Journal of Mechanics and Applied Mathematics 57* (2004), 599–622.

[53] Dorfmann, L., and Ogden, R. Magnetomechanical interactions in magnetosensitive elastomers. In *Proceedings of the Third European Conference on Constitutive Models for Rubber* (2005), P. Austrell and L. Kari, Eds., pp. 531–543.

[54] Duvaut, B., and Lions, J. *Inequalities in Mechanics and Physics.* Springer, New York, 1975.

[55] Emson, C., and Trowbridge, C. Transient 3d eddy currentsusing modified vector potentials and magnetic scalar potentials. *IEEE Transactions on Magnetics 24* (1988), 86–89.

[56] Engdahl, G., Ed. *Handbook of Giant Magnetostrictive Materials.* Academic Press, San Diego, 2000.

[57] Farshad, M., and Le Roux, M. A new active noise abatement barrier system. *Polymer Testing 23* (2004), 855–860.

[58] Fichera, G. Existence theorems in elasticity - boundary value problems of elasticity with unilateral constraints. In *Encyclopedia of Physics*, S. Flügge, Ed., vol. VIa/2 of *Mechanics of Solids II,* (C. Truedell, Series Editor). Springer, Berlin, 1972, pp. 347 – 424.

[59] Franklin, J. *Classical Electromagnetism.* Dover Publications, Inc., Mineola, New York, 2017.

[60] Fuentes-Cobas, L. Magnetic-coupling properties in polycrystals. *Textures and Microstructures 30* (1998), 167–189.

[61] Gerbeau, J.-F., and Farhat, C. The finite element method for fluid mechanics. Lecture notes CME 358, Stanford University, Spring 2009.

[62] Griffiths, D. *Introduction to Electrodynamics.* Prentice Hall, New Jersey, 2008.

[63] Hamilton, W. Second essay on a general method in dynamics. *Philosophical Transactions of the Royal Society of London 1* (1835), 95–144.

[64] Harutyunyan, M., and Simeon, B. Mathematical Modeling and Numerical Simulation of a Magnetostrictive Euler-Bernoulli Beam. *Proceedings in Applied Mathematics and Mechanics 14* (1), 517–518.

[65] Herzer, G. Magnetic materials for electronic article surveillance. *Journal of Magnetism and Magnetic Materials 254-255* (2003), 598 – 602.

[66] Hiptmair, R. Finite elements in computational electromagnetism. *Acta Numerica 11* (2002), 237–339.

[67] Huang, Z. A multi-grid algorithm for mixed problems with penalty. *Numer. Math. 57* (1990), 227–247.

[68] Hughes, T. *The Finite Element Method: Linear Static and Dynamic Finite Element Analysis.* Dover, Minneola, New York, 2000.

[69] Hutter, K., and Van den Veen, A. *Field Matter Interactions in Thermoelastic Solids.* Springer, Berlin, 1978.

[70] IEEE. Standard on Magnetostrictive Materials: Piezomagnetic Nomenclature. Tech. rep., 1990.

[71] Jackson, J. *Classical Electrodynamics.* John Wiley & Sons, Inc., New York, 1962.

[72] Jiles, D. *Introduction to magnetism and magnetic materials.* Chapman and Hall, London, 1991.

[73] Jiles, D., and Atherton, D. Theory of ferromagnetic hysteresis. *Journal of Magnetism and Magnetic Materials 61* (1986), 48 – 60.

[74] Jolly, M.R. and Carlson, J.D. and Muñoz, B.C. A model of the behaviour of magnetorheological materials. *Smart Mater. Struct. 5* (2000), 555–569.

[75] Joule, J. On a new class of magnetic forces. *Sturgeon's Annals of Electricity 8* (1842), 219.

[76] Kaltenbacher, M., Meiler, M., and Ertl, M. Physical modeling and numerical computation of magnetostriction. *The International Journal for Computation and Mathematics in Electrical and Electronic Engineering 28* (2009), 819 – 832.

[77] Kamila, S. Introduction, Classification and Applications of Smart Materials: An Overview. *American Journal of Applied Sciences 10* (2013), 876–880.

[78] Kankanala, S., and Triantafyllidis, N. On finitey strained magnetorheological elastomers. *J. Mech. Phys. Solids 52* (2004), 2869–2908.

[79] Kirsch, A., and Hettlich, F. *The Mathematical Theory of Time-Harmonic Maxwell Equations.* Springer, Berlin, 2015.

[80] Kovetz, A. *Electromagnetic Theory.* University Press, Oxford, 2000.

[81] Kuczmann, M. *Potential formulations in magnetics applying the finite element method. Lecture notes.* Labaratory of Electromagnetic Fields, Szechenyi Istvan University, Gyor, Hungary, 2009.

[82] Linnemann, K. *Magnetostriktive und piezoelektrische Materialien - konstitutive Modellerung und Finite Elemente Formulierung.* PhD thesis, Univeristät Fridericiana zu Karlsruhe, 2008.

[83] Maugin, G., and Eringen, A. Deformable magnetically saturated media i. field equations. *Journal of Mathematical Physics 13* (1972), 143 – 155.

[84] Maxwell, J. A dynamical theory of the electromagnetic field. *Royal Society Transactions 155* (1865), 459–512.

[85] McCluer, B. *Elementary Functional Analysis.* Springer, New York, 2009.

[86] McLean, W. *Strongly Elliptic Systems and Boundary Integral Equations.* Cambridge University Press, Cambridge, 2000.

[87] Monk, P. *Finite Element Methods for Maxwell's Equations.* Oxford University Press, New York, 2003.

[88] Morisue, T. Gauging of the magnetic vector potential. *Electrical Engineering in Japan 111* (1991), 11–21.

[89] Olabi, A. G., and Grunwald, A. Design and application of magnetostrictive materials. *Materials and Design 29* (2008), 469 – 483.

[90] Pao, Y. Electromagnetic forces in deformable continua. In *Mechanics Today (4)*, S. Nemat-Nasser, Ed. Pergamon Press, Oxford, 1978, pp. 209–306.

[91] Poutala, A., Kovanen, T., and Kettunen, L. Essential measurements for finite element simulations of magnetostrictive materials. *IEEE Transactions on Magnetics PP* (2017), 1–7.

[92] Powell, R. *Symmetry, Group Theory, and the Physical Properties of Crystals.* Springer, New York, 2010.

[93] Preis, K., Bardl, I., Biro, O., Magele, C., Renhart, W., Richter, K., and Vrisk, G. Numerical analysis of 3D magnetostatic fields. *IEEE Transactions on Magnetics 27* (1991), 3798–3803.

[94] Preisach, F. Über die magnetische Nachwirkung. *Zeitschrift für Physik A Hadrons and Nuclei 94* (1935), 277 – 302.

[95] Preumont, A. Mechatronics: Dynamics of electromechanical and piezoelectric systems. In *Solid Mechanics and Its Applications (136)*, G. Gladwell, Ed. Springer Netherlands, Dordrecht, 2006.

[96] Pucci, E., and Saccomandi, G. Potential symmetries and solutions by reduction of partial differential equations. *Journal of Physics A: Mathematical and General 26* (1993), 681–690.

[97] Reddy, B. *Introductory Functional Analysis.With Applications to Boundary Value Problems and Finite Elements.* Springer, New York, 1998.

[98] Ren, Z., and Ida, N. Solving 3d eddy current problems using second order nodal and edge elements. *IEEE Transactions on Magnetics 36* (2000), 746–750.

[99] Salas, E., and Bustamante, R. Numerical solution of some boundary value problems in nonlinear magneto-elasticity. *Journal of Intelligent Material Systems and Structures 26* (2015), 156 – 171.

[100] Schmidt, K., Sterz, O., and Hiptmair, R. *IEEE transactions on Magnetics 44* (2008), 686 – 689.

[101] Schoeberl, J. Numerical Methods for Maxwell Equations, April 2009. [Lecture notes. Institute of Analysis and Scientific Computing, Technische Universität Wien].

[102] Simeon, B. *Computational Flexible Multibody Dynamics: A Differential-Algebraic Approach.* Springer, Berlin-Heidelberg, 2013.

[103] Spaldin, N. A. *Magnetic Materials. Fundamentals and Applications.* Cambridge University Press, Cambridge, 2003.

[104] Steigmann, D. Equilibrium theory for magnetic elastomers amd magnetoelastic membranes. *International Journal of Non-Linear Mechanics 39* (2004), 1193 – 1216.

[105] Tan, X., and Baras, J. Modeling and control of hysteresis in magnetostrictive actuators. *Automatica 40* (2004), 1469 – 1480.

[106] Tiersten, H. Coupled magnetomechanical equations for magnetically saturated insulators. *Journal of Mathematical Physics 5* (1964), 1298–1318.

[107] Tiersten, H. Variatonal principle for saturated magnetoelastic insulators. *Journal of Mathematical Physics 6* (1965), 779 – 787.

[108] Trémolet de Lacheisserie, E. *Magnetostriction - Theory and Applications of Magnetoelasticity.* CRC Press, Boca Raton, 1993.

[109] Truesdell, C., and Taupin, R. The classical field theories. In *Handbuch der Physik 2/3/1*, S. Flügge, Ed. Springer, Berlin, 1960, pp. 126–868.

[110] Vanderlinde, J. *Classical Electromagnetic Theory.* Kluwer Academic Publishers, Dordrecht, 2005.

[111] Villari, E. Über die Änderungen des magnetischen Moments, welche der Zug und das Hindurchleiten eines galvanischen Stroms in einem Stabe von Stahl oder Eisen hervorbringen. *Annalen der Physik 126* (1865), 87 – 122.

[112] Voigt, W. Über Pyro- und Piezomagnetismus der Kristalle. *Nachrichten der Gesellschaft der Wissenschaft zu Göttingen, Mathematisch-Physikalische Klasse* (1901), 1–19.

[113] Voigt, W. *Lehrbuch der Kristallphysik: mit Ausschluß der Kristalloptik.* Vieweg + Teubner, Leipzig, 1910.

[114] Wan, Y., Fang, D., and Hwang, K. Non-linear constitutive relations for magnetostrictive materials. *International Journal of Non-Linear Mechanics 38* (2003), 1053 – 1065.

[115] Zhang, T., Jiang, C., and Xu, H. Giant magnetostrictive actuators for active vibration control. *Smart Materials and Structures 13* (2004), 473–477.

[116] Zheng, X., and Liu, X. E. A nonlinear constitutive model for Terfenol-D rods. *Journal of Applied Physics 97* (2005), 053901.

[117] Zheng, X., and Sun, L. A one-dimension coupled hysteresis model for giant magnetostrictive materials. *Journal of Magnetism and Magnetic Materials 309* (2007), 263–271.

Academic Curriciulum Vitae

School Education

1994–2001 **Yeghishé Charents School**, in Yerevan, Armenia.

2001–2007 **Albert-Schweizer-Gymnasium**, in Kaiserslautern, Germany.

2007 **Abitur**, with distinction.

Academic Eductaion

2007–2012 **Studies of Mathematics**, *Minor subject: Mechanical Engineering*, Technische Universität Kaiserslautern.

2012 **Diploma in Mathematics**, *Major field of study: Modeling und Scientific Computing*, Diploma thesis: "Mathematical Modeling and Numerical Simulation of Fiber-Reinforced Materials".
Advisor: Prof. Dr. Bernd Simeon

2012–2018 **Doctoral Studies in Mathematics**, Title: "Mathematical Modeling and Numerical Simulation of Magnetoelastic Coupling".
Thesis Advisor: Prof. Dr. Bernd Simeon, Defence: 18. May 2018

.

Awards and Scholarships

2007 Award of the principal of the Albert-Schweizer-Gymnasium for excellent achievements in high school

2007 Membership of the German Physical Society as award for outstanding performance in the subject Physics

2007 Award of the member of the Bundestag Anita Schäfer for the excellent Abitur

2007 Award of the Albert-Schweizer-Gymnasium für outstanding achievements in the subject English

2007 Award of the mayor of the city Kaiserslautern, Bernhard J. Deubig for the excellent Abitur

2007/2008 Scholarship of the TU Kaiserslautern for female beginners

2009/2010 Award of the Student Council of the Department of Computer Science for the best teaching assistance in Mathematics

2012 Graduation Scholarship of the TU Kaiserslautern

2017 Award of the TU Kaiserslautern for the scientific report "Magnetostriktive Materialien. Wie intelligente Werkstoffe unsere Zukunft beeinflussen." ("Magnetostrictive Materials. How smart materials affect our future.")